Genetic Risk Factors and Immunopathogenesis of Antimicrobial-Induced Severe Cutaneous Adverse Reactions

By

Katherine Chanel Konvinse

Dissertation
Submitted to the Faculty of the
Graduate School of Vanderbilt University
in partial fulfillment of the requirements
for the degree of

DOCTOR OF PHILOSOPHY
in

Microbiology and Immunology
May 31, 2019
Nashville, Tennessee

Approved:

David M. Aronoff, MD, Chair
Elizabeth Jane Phillips, MD, Thesis Advisor
Justin M. Balko, PharmD, PhD
Dawn C. Newcomb, PhD
Ray Stokes Peebles, Jr., MD
Dan M. Roden, MD

Copyright © 2019 by Katherine Chanel Konvinse
All Rights Reserved

To my husband, Ananth, and the ~508,600 miles we have traveled to make this dream possible.

ACKNOWLEDGEMENTS

My heartfelt thanks and sincere gratitude to the many people and resources that made this work possible. This journey truly took a village! This research and my training would not have been possible without the financial support of Public Health Services grants NIH F30 AI131780, P50 GM115305 and T32 GM7347 from the National Institutes of Health as well as institutional funding from the Vanderbilt Medical Scientist Training Program (MSTP) and the Vanderbilt Department of Medicine, Division of Infectious Diseases.

My interest in biomedical sciences started early in life as a middle school student in a school where the entire district was housed in one building pre-Kindergarten through 12th grade in a village with fewer than 300 residents. I am immensely grateful to the teachers of Letchworth Central School for encouraging me to learn and explore beyond the school walls. I would like to extend a particularly special thank you to Mr. Ernie Lawrence for handing me an application for a summer internship at Roswell Park Cancer Institute and encouraging me to apply and an additional thank you to Harry Slocum, PhD in the laboratory of Youcef Rustum, PhD at Roswell for dedicating time to training high school students. I learned so much that summer about what it meant to be a scientist and what it felt like to be part of a community that understood my aspirations. That summer, I found ‘my people.’

I am indebted to my undergraduate mentors, Volker Vogt, PhD at Cornell University and Simon Hayward, PhD at Vanderbilt University Medical Center for opening your labs and frequently your homes to an idealistic undergraduate. Volker, thank you for sharing with me your love of viruses and for teaching me the importance of patience, integrity, repetition and the value of negative data.

To my graduate student mentor at the time, Rob Dick, PhD, thank you for teaching me to delight in every successful experiment. Simon H., in your lab, I not only found a dedicated group of researchers including Doug Strand, PhD and Omar Franco, MD, PhD who took me under their wings, but in you, I also found a mentor, a father figure and a friend. I will be eternally grateful for every career chat over lunch, the dozens of cups of Suzie's coffee and the years of guidance.

My graduate training at Vanderbilt was possible due to the extensive support of mentors, friends and co-workers. First and foremost, I thank my PhD advisor, Elizabeth Phillips, MD. Thank you for reading almost every word I have written in the last four years including a few truly horrendous first drafts, for trusting me with important science, and for fostering innovative solutions to challenging questions. Elizabeth gave me ample time to learn the art of grant and manuscript writing, supported my attendance at numerous conferences, took time out of her busy schedule to nominate me for accolades, and helped me build my own international network of colleagues and collaborators. She negotiated my authorship on book chapters and reviews that discouraged the participation of student authors. When I was frustrated by the protracted progress of my project, Elizabeth encouraged me to fly to South Africa and collect data from the source. It was truly an honor to train under such an accomplished and dedicated physician-scientist. I know her mentorship will continue to be instrumental in shaping my career.

I extend deep gratitude to the members of my thesis committee, David Aronoff, MD, Dan Roden, MD, Dawn Newcomb, PhD, Stokes Peebles, MD and Justin Balko, PharmD, PhD, for asking critical questions, for keeping me focused, and for their investment in my professional development. I thank the Microbiology and Immunology graduate program, including the Director

of Graduate Studies, Chris Aiken, PhD, for welcoming me and providing me with a scientific home for my research and training over the last four years. Thank you to Nora Gilgallon-Keele in the Division of Infectious Diseases for looking after me like I was one of your fellows and for the endless gum, chocolate and encouragement.

To the MSTP leadership, both past and present, especially the former director, Terry Dermody, MD and current director, Chris Williams, MD, PhD, thank you for your commitment to training the next generation of physician-scientists. I would like to express my particular appreciation for the MSTP's former Assistant Director, Melissa Krasnove. Melissa, thank you for being the program's always accessible mentor, therapist, and motherly older sister. Thank you for every text, email, hug, and for your endless supply of tissues. Your constant reassurance is the reason I have made it this far. You have nurtured an entire generation of Vanderbilt physician-scientists. Know that any of our future discoveries are in part also yours.

While I was the only graduate student in the Phillips Lab during my training, I was never alone. Within the Phillips Lab, I would like to extend my gratitude to Katie White, MD, PhD for her help and mentorship and to Kristina Williams, RN, BSN, CRRP for her dedication and camaraderie. I am fortunate to have worked alongside excellent researchers in our shared infectious diseases laboratory space including Simon Mallal, MBBS, Spyros Kalams, MD and John Koethe, MD and members of their laboratories, Celestine Wanjalla, MD, PhD, Mark Pilkinton, MD, PhD, Katie Nicholas Vowell, PhD, Chike Abana, PhD, and Wyatt McDonnell, MS. A special thank you to Celly for the frequent hugs, for calling me just to check in when I'm out of town and you're on your way to clinic, and for our Friday evening career chats. You always know how to lift my

spirits. To the research specialists and research assistants with whom I worked closely, particularly Dana King, Cindy Crawford Nochowicz, Rita Smith, MBA, Rama Gangula, MS, Lilanka Fernando, MS, Patricia Correia, MS, Louise Barnett, Joshua Simmons and Amondrea Blackman, thank you all for your experimental design expertise, technical support and companionship. Dana, I am exceptionally grateful for your friendship. When you saw me hand-labeling pathology slides on a Friday evening, instead of wishing me a good night, you picked up a marker and pulled up a chair to join me. I cannot thank you enough for the spontaneous hugs in the hallway, lunches at Kay Bob's, the stash of ice cream in the freezer for particularly tough days, and the time you took to review my posters and presentations.

Stevens-Johnson syndrome and toxic epidermal necrolysis (SJS/TEN) and drug reaction with eosinophilia and systemic symptoms (DRESS) are two relatively uncommon, but life-threatening diseases with significant acute mortality. Anyone who has studied these and similar disease knows that the work is not possible without a legion of collaborators. At Vanderbilt, this work was made possible in part to due to the dedication, technical expertise, availability and responsiveness of individuals in the Vanderbilt Institute for Clinical and Translational Research (VICTR) (BioVU and the Synthetic Derivative), Vanderbilt Technologies for Advanced Genomics (VANTAGE), the Translational Pathology Share Resource, the Digital Histology Shared Resource, and the Flow Cytometry Shared Resource. Thank you to the Vanderbilt Department of Dermatology and Burn Center for their help with patient recruitment, to the physicians of the Dermatopathology Resource at Vanderbilt, Alan Boyd, MD and Jeffrey Zwerner, MD, PhD for scoring slides, to David Haas, MD for access to CYP2B6 SNP panels he developed, and to Christian Shaffer and Adi Bejan, PhD for tolerating my frequent BioVU queries. Also, special thanks to P50 and PGRN collaborators

Josh Denny, MD, MS and Dan Roden, MD. Josh Denny, MD, MS, in particular, was responsible for setting up the electronic alerts in KnowledgeMap that gave us an early heads-up about SJS/TEN and DRESS sample collection and has been integral to the success of our program.

Outside of Vanderbilt, I must start by acknowledging our collaborators at the University of Cape Town for their clinical expertise, their access to patients that made studying nevirapine-induced Stevens-Johnson syndrome possible, and their hospitality during my visit. In particular, I would like to thank Jonny Peter, MBBS, PhD, for opening his lab to me, Rannakoe Lehloenya, MBBS, and Lauren Knight, MBBS for their help with case validation and patient recruitment, and Sarah Pedretti, PhD and Julie Esterhuizen for making me feel at home in Cape Town and for their tireless work tracking patients and processing samples. I am profoundly grateful to Jason Trubiano, MBBS, PhD, of Austin Health and the Peter MacCallum Cancer Centre in Melbourne, VIC, Australia, for being my long-distance scientific partner in writing and drug hypersensitivity ELISpot pipetting and my occasional "conference husband." When review deadlines loomed or we were testing out new drug concentrations, it was always comforting to know that one of us was working on the task 24-hours a day.

I thank our colleagues at the Institute for Immunology and Infectious Diseases in Perth, WA, Australia particularly Ian James, PhD for your patience analyzing a continuous evolving patient population, Silvana Gaudieri, PhD for the endless Tim Tam supply, impromptu whiteboard lessons on evolution and being my dinner companion, Abha Chopra, PhD and Francois Rawandamuriye for spearheading the next step of the vancomycin DRESS project, and Alec Redwood, PhD, Rebecca Pavlos, PhD, Shay Leary, Ramesh Ram, PhD, Mark Watson PhD, Jennifer Currenti, and

Linda Choo for their help with genotyping, single cell analyses tools and technical expertise. Thank you to Misha Rosenbach, MD from the University of Pennsylvania and to Jack Bourke, MBBS and Patricia Martinez, MBBS, PhD from Fiona Stanley and Royal Perth Hospital in Western Australia for their clinical expertise and help with patient recruitment, to Ryan Schutte, PhD and David Ostrov, PhD from the University of Florida for modeling vancomycin and HLA-A*32:01, and to Wen-Hung Chung, MD, PhD and Chuang-Wei Wang from Chang Gung Memorial Hospital for granulysin concentration measurements in acute blister fluid and plasma samples. I would be remiss if I did not take the time to express my heartfelt gratitude to the patients and healthy donors for donating not only their time, but also their blood, saliva, skin and blisters to this research. Thank you for trusting me with your donation and for believing in the good research can do for society. I truly appreciate and respect your contributions to advancement of biomedical science.

Finally, I thank those who matter most, my family and friends. While training, the MSTP has become my second family. I am profoundly grateful to my class, Gabriela DiCarlo, Alex Sundermann, Stephanie Dudzinski, Eileen Shiuan, Shawn Barton, Kevin Graepel, Sumeeth Jonathan, Josh Thompson, John Snow and Joey Elsakr for keeping me pipetting while our incoming medical school class is busy doctoring. I am also quite appreciative of my fellow Microbiology and Immunology PhD students, especially Rhonda Caston, for making me feel welcome when I joined the department. Rhonda, our weekend breakfasts, down-to-earth chats and hallway hugs gave me the resilience I needed to keep going when experiments failed and papers were rejected.

To my parents, thank you for raising me in a home full of unconditional love, laughter and books. Your "free-range chicken" approach to child-rearing instilled in me the curiosity I needed to become a scientist. From The Da, I acquired my appreciation for list making and organizational skills and learned the importance of being a "helper." To my mom, I owe my idealism and my ability to tell a story. Thank you for teaching me to stand tall on my soapbox. Thank you both for dedicating your careers to empowering young minds, for encouraging me to dream big and for affording me with the opportunities I needed to make my dreams a reality. To my husband, Ananth, thank you for your sacrifice, support and wisdom. Thank you for enduring 6+ years of long-distance love and 4+ years of long-distance marriage and never once asking me to compromise on my aspirations. Thank you for believing in me when I doubted myself. I could not have asked for a better partner with whom to share this journey.

TABLE OF CONTENTS

LIST OF TABLES

LIST OF FIGURES

CHAPTER I

INTRODUCTION

OVERVIEW OF ADVERSE DRUG REACTIONS

An adverse drug reaction (ADR) is any unintended, uncomfortable or deleterious effect that a drug may have. All medications have the potential to cause an adverse reaction. Consequently, ADRs are a continuing threat to patient safety and a source of tremendous economic burden. In the United States, ADRs are estimated to be the 4-6th leading cause of death, cause 3-7% of inpatient admissions, occur in 10-20% of hospital admissions, and cost up to $136 billion annually[1-4]. In addition to the significant rate of mortality associated with ADRs, patients who survive these reactions frequently suffer from long-term associated morbidities, fear of taking new medications, and restricted therapeutic options for future treatments. Despite their documented burden to patients and to society, research efforts in the United States focused on accurately predicting and preventing severe ADRs or on understanding their mechanistic basis to fuel earlier diagnosis and more targeted therapies have been limited.

CLASSIFICATION OF ADVERSE DRUG REACTIONS

Adverse drug reactions are divided into on-target and off-target reactions (Figure 1.1). On-target reactions comprise over 80% of adverse drug reactions. They are typically dose-dependent and can be caused by overdose, side effects, secondary effects or drug-drug interactions. They are characterized as being predictable based on their known target of pharmacological action but may

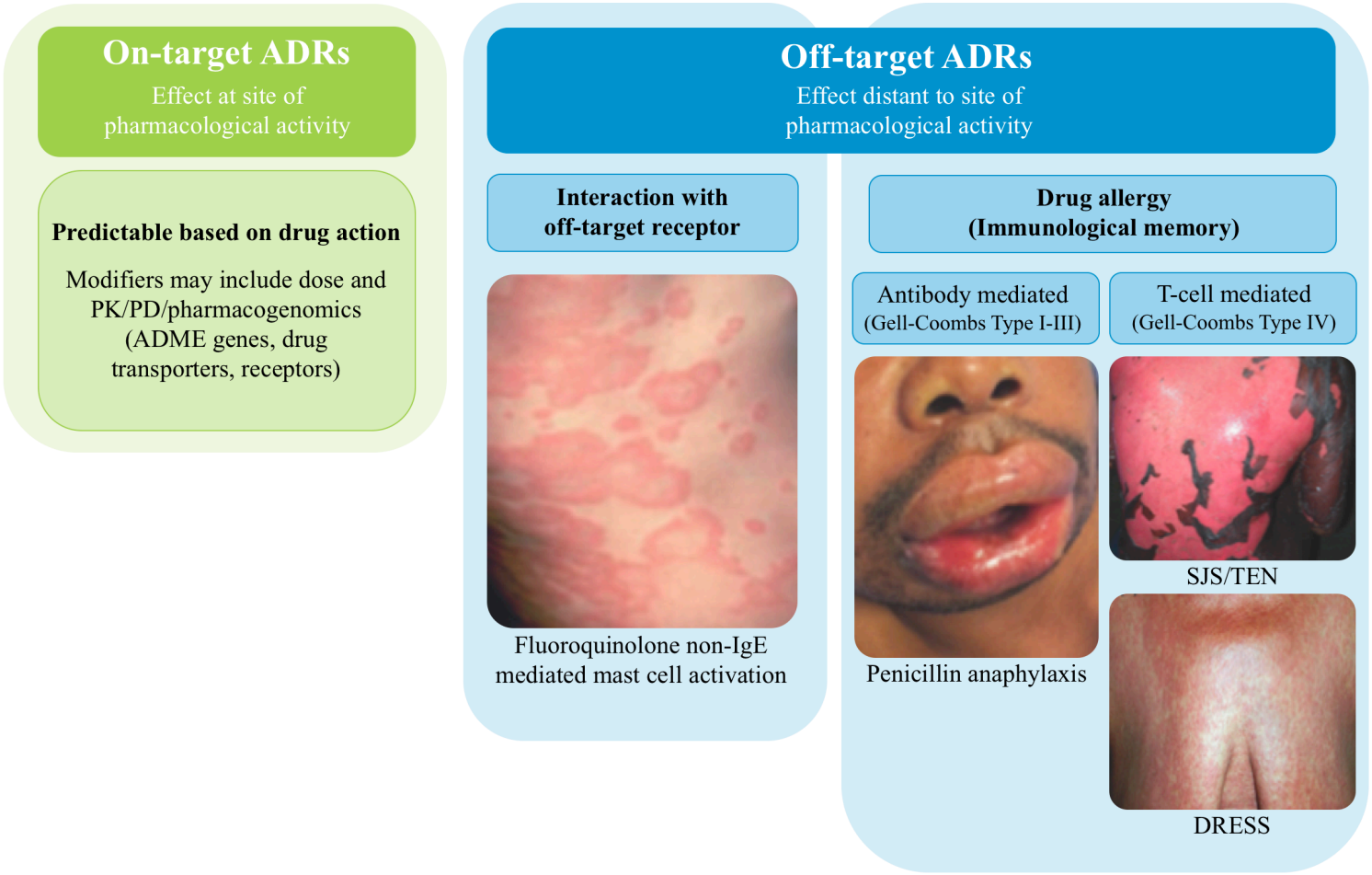

Figure 1.1. Adverse drug reactions can be classified as on-target and off-target reactions. Reactions mediated by the immune system are considered off-target reactions. **Legend:** ADR, adverse drug reaction; PK, pharmacokinetic; PD, pharmacodynamic; ADME, absorption, distribution, metabolism and elimination; SJS/TEN, Stevens-Johnson syndrome/toxic epidermal necrolysis; DRESS, drug reaction with eosinophilia and systemic symptoms. Adapted from Peter, Lehloenya, Dlamini, Risma, White, Konvinse, *et al*, *JACI: In Practice* (2017)[5].

also be subject to genetic variation. One example of an on-target reaction is the development of pseudomembranous colitis from clindamycin use. Off-target reactions result in an unfavorable effect distant to the site of pharmacologic activity and are subject to host genetic variation. Contrary to previous belief, the risk for vast majority of off-target reactions including non-IgE mediated mast cell activation, T-cell mediated reactions and drug intolerance increases with increasing drug dose similar to on-target reactions. However, a minority of off-target reactions are dose-independent (antibody and IgE-mediated reactions)[6-9]. An example of a common off-target reaction is "red man syndrome" which is due to a non-IgE mediated mast cell activation secondary to vancomycin administration.

CLASSIFICATION OF DRUG HYPERSENSITIVITIES

Drug allergies comprise less than 15% of all ADRs. However, patients and physicians often erroneously refer to all ADRs as allergic[10-12]. According to the schema developed by Gell and Coombs in 1963, drug hypersensitivity reactions are classified into four types based on the immune mediators of disease (Figure 1.1)[13]. This mechanism-based classification system is still widely used today. The majority of immune-mediated drug hypersensitivity reactions relevant to clinical practice are mediated by IgE antibodies or T cells. The timing of occurrence of these reactions is critical with most true IgE mediated reactions occurring <1 hour after dosing and most T-cell mediated reactions occurring >6 hours after dosing. By convention, immediate reactions occur within 1 hour of dosing and delayed reactions occur >6 hours after dosing.

Type I, also known as immediate, hypersensitivity reactions typically occur within 30 minutes, but can occur within seconds, of drug exposure. Upon first exposure to the implicated drug, IgE

antibodies bind to Fcε receptors on the surface of mast cells and basophils. These cells are now "sensitized." Later exposure to the same drug results in cross-linking of cell bound antibodies on the mast cells and basophils leading to the cells' degranulation and release of histamine, leukotrienes B4, C4, D4 and E4, prostaglandin D2 and a variety of other immune mediators. The principal effects of these products are vasodilation, increased vessel permeability, smooth muscle contraction and leukocyte extravasation leading to clinical features that range from irritating (pruritis) to life-threatening (anaphylaxis). Urticarial rash, flushing, angioedema and gastrointestinal symptoms are also typical symptoms of type I hypersensitivity reactions. Antimicrobials well known for causing type I hypersensitivity reactions include penicillins, cephalosporins, chlorhexidine, trimethoprim and sulfamethoxazole. Other drugs commonly associated with Type I reactions include NSAIDS, proton pump inhibitors, heparin, insulin, chemotherapeutic agents, etanercept and chimeric monoclonal antibodies. Skin testing is common for IgE-mediated reactions. Typically, the allergen is introduced by skin prick or intradermal injection. In a positive test, a wheal-and-flare reaction occurs within 15 minutes at the site of allergen introduction. The term pseudoallergic or anaphylactoid is used to describe reactions which appear clinically similar to type I hypersensitivity reactions, but are not mediated by cross-linking of IgE antibodies. These reactions may be triggered by small molecules such as fluoroquinolones, neuromuscular blockers, opioids and vancomycin signaling through a G-protein coupled receptor on mast cells[14].

Type II and III hypersensitivities are IgG or IgM (non-IgE) antibody-mediated reactions, which typically occur minutes to several hours after drug exposure. In drug allergy, type II, also known as cytotoxic or antibody-dependent, hypersensitivity reactions occur when IgG or IgM antibodies

are directed against a drug or drug metabolite on the surface of the patient's cells. These antibody-coated cells are recognized and killed by innate immune cells (e.g. natural killer cells, monocytes and macrophages), which bind to the target cells via the Fc region of the antibody. Clinically, type II hypersensitivities may present as drug-induced hemolytic anemia, thrombocytopenia or granulocytopenia. Drugs commonly implicated in hemolytic anemias with IgG antibodies include penicillins, quinidine, α-methyldopa and some cephalosporins. Drug-induced thrombocytopenia has been documented with quinine, quinidine, propylthiouracil, gold salts, acetaminophen, vancomycin and sulfonamides. IgG antibodies against anticonvulsants, pyrazolone drugs, thiouracil, sulfonamides and phenothiazines can produce granulocytopenia by the destruction of peripheral neutrophils.

Type III, also known as immune complex, hypersensitivity reactions occur when antibody (IgG>IgM) binds to soluble antigen (often drug or drug metabolite) forming a circulating immune complex, which can deposit into small vessels, joints and glomeruli. These small immune complexes fix complement and unlike larger immune complexes, they are not cleared from the circulation by macrophages. Examples of antibiotic-induced type III hypersensitivity reactions include serum sickness-like reactions most commonly caused by amoxicillin and cefaclor. Clinically, serum sickness-like reactions must be differentiated from true serum sickness reactions caused by foreign proteins. Serum sickness-like reactions are characterized by fever, lymphadenopathy, urticaria or exanthem with joint pain occurring 7-10 days following initiation of drug dosing in the absence of proteinuria or organ involvement while prominent features of true serum sickness reactions include proteinuria and acute kidney failure due to glomerulonephritis. Other drugs known to cause type III hypersensitivity reactions include penicillins, cephalosporins,

sulfonamides, ciprofloxacin, trimethoprim-sulfamethoxazole, tetracycline, lincomycin, NSAIDS and carbamazepine.

Type IV, also known as delayed, hypersensitivities are T cell-mediated reactions, which as the name implies, occur days to weeks after drug initiation. Drugs implicated in these reactions include antibiotics, antiretrovirals, anticonvulsants, antimalarials, local anesthetics and barbiturates. Type IV hypersensitivities are classified into subtypes based on the specific class of T cells and cytokines mediating each reaction (Table 1.1). In general, all of these reactions occur when an antigen-presenting cell expressing a human leukocyte antigen (HLA)-bound to a peptide interacts with a T-cell receptor (TCR) in the presence of drug or drug metabolite[15].

The specific immune mechanisms underlying type IV hypersensitivities are the subject of intense research. Multiple, non-mutually exclusive models have been proposed to explain how small molecule drugs stimulate immune activation including the hapten/prohapten model, the pharmacological interaction of drugs with immune receptors, or (p-i) model, and the altered peptide repertoire model (Figure 1.2). To elicit a classic immune response, a human leukocyte antigen (HLA)-bound peptide interacts with a T-cell receptor (TCR), along with co-stimulatory molecules. In the hapten/prohapten model, a haptenated protein undergoes intracellular processing to generate modified peptides that are incorporated onto HLA proteins for presentation to T cells. A hapten is a small molecule, often a drug or drug metabolite, that covalently binds to larger protein[6,15]. Since the haptenated protein undergoes all of the steps of antigen processing, HLA loading and traffic to the cell surface, a time delay occurs between ingestion of the causative drug

ADR Subtype	Cellular mediators	Cytokine mediators	Phenotype	Specific immunological parameters for phenotype
IVa	*Primary:* Th1 *Secondary:* Macrophages	IFN-γ TNF-α IL-18	Contact dermatitis Tuberculin reactions	**Contact dermatitis** – Primarily CD8+ T cell infiltrate. ↑ IFN-γ, TNF-α, IL-18. Also noted ↑ lL-31, IL-6 in serum and IL-33 IL-9, IL-4 in skin [17-21].
IVb	*Primary:* Th2 *Secondary:* B-cells, IgE, IgG4, mast cells, eosinophils	IL-4 IL-5 IL-13	MPE HSS DRESS	**MPE** – CD4 > CD8+ T cells. Acute episodes Th1 predominate, ↑ IL-12, IFN-γ/TNF-β in blood, CXCL9/CXCL10 skin. ↓ IL-17 compared with SJS/TEN. ↑ Th2/IL-5 later explains pruritis [22-27]. **DRESS** - ↑ TNF-α, IFN-γ and IL-2 production, production correlates with disease severity. Activation-regulated chemokine (TARC/CCL17) drive Th2 responses, higher than observed in SJS/TEN. Skin biopsies noted eosinophils in 20%; while CD8+ T cells and granzyme B+ lymphocytes ↑ in severe disease [28-30].
IVc	*Primary:* Cytotoxic T cells	Granzyme B Perforin Fas ligand Granulysin	SJS TEN Linear IgA disease DILI FDE EM	**SJS/TEN** – CD8+ T-cells and NK cells lead to keratinocyte apoptosis. Granulysin specific to SJS/TEN. ↑ IL-10 and T_{reg} associated with resolution of SJS/TEN. T_{reg} function often impaired. ↑ IL-2, IL5, IL6, IL-17 and CCL27 in plasma/blister fluid. Th17 cells also have a role [26,31-38]. **Linear IgA disease** – Often mistaken for TEN, however characteristic linear IgA deposits are evident on direct immunofluorescence studies. ↑ CD4+ T-cell, neutrophils and eosinophils. Mixed Th1/Th2 cytokine response. ↑ IL-2, IL-4, IL-5 and IL-8 noted [39-44]. **FDE** – ↑ Intraepidermal CD8+ T-cells, ↑ IFN-γ, cytotoxic granules, granzyme B and perforin. ↑ CD8+ T-cells, CD4+ T-cells and neutrophils cause tissue damage. Late - ↑ IL-10 & T_{reg} (CD4+CD25+Foxp3+) control immune reaction, however IL-15 secreted by keratinocytes continue to propagate CD8+ T-cell mediated injury [45,46]. **EM** – ↑ IL2, IL6, IL8, IL17A, IFN-γ, TNF-α. ↑ Th1/CD4+ T-cell infiltrate with IL-17 expression. ↓ IL10, noted. At skin level, ↑ CD4+ T cell with IL-17 (Th2) expressing cells. CD8+ T cells noted within epidermis, and CD4+ T cells are noted in dermis. [47-49].
IVd	*Primary:* Th1/Th17 *Secondary:* Neutrophils	GM-CSF IL-8 CXCL8	AGEP	**AGEP** – ↑ CD4+ T cells infiltrate, CD8+ T cells and ↑↑ CXCL8 and GM-CSF. CXCL8 is involved in the chemotaxis of neutrophils; Th17 cells involved [50-53].

Table 1.1. T-cell-mediated hypersensitivity reactions classification, pathogenesis and phenotype guide. Legend: Th1, Type 1 T helper cells; Th2, Type 2 T helper cells; Th17, Type 17 T helper cells; IL, interleukin; DHR, Drug hypersensitivity reaction; SJS, Stevens-Johnson syndrome; TEN, toxic epidermal necrolysis; MPE, maculopapular exanthema; DRESS, drug reaction with eosinophilia and systemic symptoms; HSS, hypersensitivity syndrome; FDE, fixed drug eruption; EM, erythema multiforme; DILI, drug induced liver injury; AGEP, acute generalized exanthematous pustolosis; GM-CSF, granulocyte monocyte colony-stimulating factor; PMN, polymorphonuclear cell. Adapted from Konvinse, *et al.*, *Curr Opin in Infect Dis* (2016)[54].

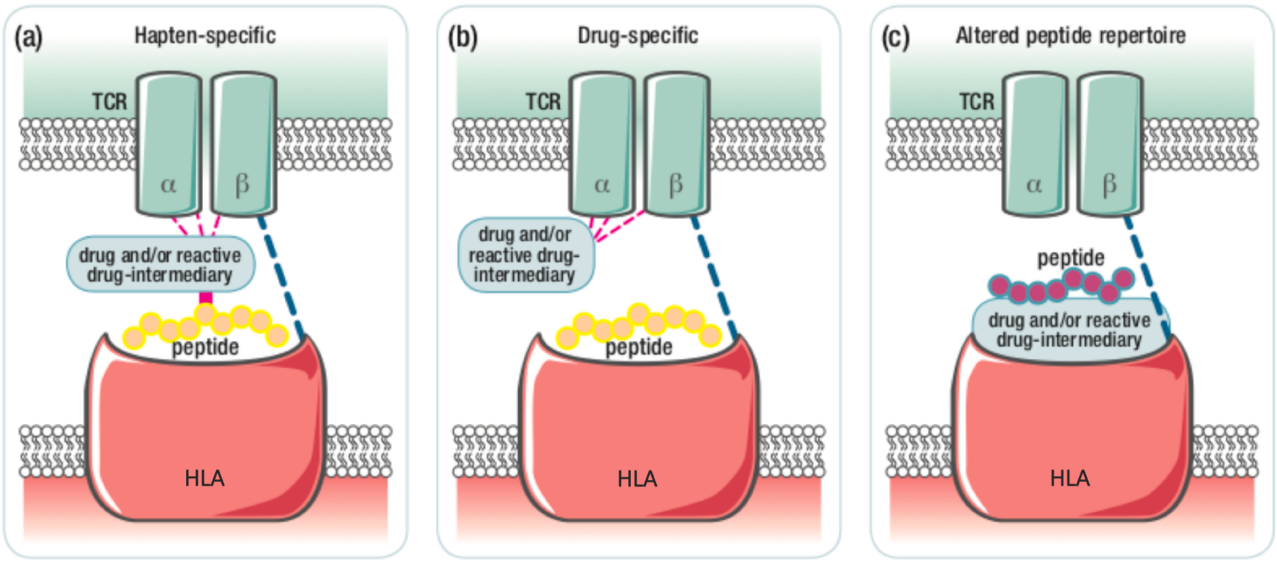

Figure 1.2. Proposed models of drug hypersensitivity. A. In the hapten/prohapten model, drug-modified peptides are processed by antigen-presenting cells and presented on the HLA molecule, resulting in a T-cell response. **B.** The drug-specific pharmacological-interaction (p-i) model proposes that drug binds noncovalently directly to immune receptors without the need for peptide. **C.** The altered peptide repertoire model proposed that the drug forms noncovalent bonds within the binding pocket(s) of the HLA to alter the chemistry of the binding cleft and repertoire of self-peptides able to bind to the HLA molecule in question. Dashed lines represent noncovalent bonds. **Legend:** TCR, T-cell receptor; HLA, human leukocyte antigen. Adapted from Peter, Lehloenya, Dlamini, Risma, White, Konvinse, *et al*, *JACI: In Practice* (2017)[5].

and onset of symptoms of a hypersensitivity syndrome. The best-known hypersensitivity syndrome associated with this model involves the binding of penicillin derivatives to serum albumin[16].

In the p-i model, a chemically inert drug, unable to covalently bind to proteins, binds non-covalently to the TCR or HLA proteins, in the absence of a specific peptide ligand, and directly activates T cells[55]. This theory is supported by evidence that with some drugs, T-cell responses are elicited on the first encounter with that drug and in some cases, within seconds of drug exposure, much more rapidly than would be expected if antigen processing were required[56,57].

The altered peptide repertoire model proposes that the drug occupies sites within the peptide-binding groove of the HLA proteins and thereby changes the chemistry and shape of the binding cleft. This model explains the associations between drug hypersensitivity syndromes and specific HLA alleles, which are often only separated from closely related alleles by polymorphisms in the binding cleft (see *HLA-Associated Antimicrobial Hypersensitivity* below). This model has been best elucidated for hypersensitivity to the antiretroviral, abacavir, and the known risk allele HLA-B*57:01[56,58-60].

T-CELL-MEDIATIED DRUG HYPERSENSITIVITY SYNDROMES

Predominant clinical findings in type IV hypersensitivity reactions involve the skin. Examples of disease states include allergic contact dermatitis, maculopapular exanthema, acute generalized exanthematous pustulosis (AGEP), fixed drug eruption (FDE), erythema multiforme (EM), drug reaction with eosinophilia and systemic symptoms (DRESS) and Stevens-Johnson syndrome/toxic epidermal necrolysis (SJS/TEN) (Table 1.2).

Type of Reaction	Timing	Cutaneous Symptoms	Systemic Symptoms	Possible Laboratories in Acute Setting	Commonly Involved Drugs	Testing	Management
Delayed rash	7-10 days	Maculopapular exanthema Urticaria	Low-grade fever Pruritus	Eosinophilia (mild)	Beta-lactam antibiotics Antiretrovirals Anticonvulsants	Skin testing Oral Challenge	Treat through or avoidance of implicated drug and cross-reacting drugs
SJS/TEN	4–28 days	Painful erythematous macules with purpuric or dusky centers Superficial sloughing Erosive mucositis	Prodrome High fever Malaise Occasional pneumonitis	Anemia Lymphopenia	Sulfonamides antibiotics Antiretrovirals Allopurinol Anticonvulsants	*LTT* *ELISpot* HLA screening	Avoidance of implicated drug and cross-reacting drugs
DRESS	2–8 weeks	Morbilliform eruption (>50% BSA) Nonerosive mucositis Facial edema, infiltrated lesions, scaling, and purpura	Fever Lymphadenopathy	Eosinophilia Atypical lymphocytes Hepatitis Renal impairment	Vancomycin Sulfonamide antibiotics Antiretrovirals Anti-tuberculous drugs Allopurinol Anticonvulsants	Skin testing *LTT* *ELISpot* HLA screening	Avoidance of implicated drug and cross-reacting drugs
FDE	1–14 days[a]	1 or more well-demarcated, round, dusky-to-violaceous macules or plaques Blistering may occur Mucosal predilection but limited mucositis Post-inflammatory hyperpigmentation	None	None	NSAIDS Barbiturates Sulfonamide antibiotics Tetracyclines Fluconazole	Skin testing at site of reaction	Drug provocation testing[b] Avoidance of drug and cross-reacting drugs
AGEP	24–48 hours	Dozens to hundreds of pustules on erythematous background Flexural accentuation	High fever Edema	Neutrophilia > Eosinophilia	Aminopenicillins Clindamycin Hydroxychloroquine	Patch testing	Avoidance of drug and cross-reacting drugs

Table 1.2. Severe cutaneous adverse reactions: clinical features and management. These delayed reactions are all examples of Gell and Coombs Type IV hypersensitivities. **Legend:** SJS/TEN, Stevens-Johnson syndrome/toxic epidermal necrolysis; LTT, lymphocyte transformation test; ELISpot, Enyzme-linked ImmunoSpot Assay; HLA, human leukocyte antigen; DRESS, drug reaction with eosinophilia and systemic symptoms; BSA, body surface area; FDE, fixed drug eruption; AGEP, acute generalized exanthematous pustulosis. [a]Rapid recurrence on drug re-exposure; [b]Contraindicated on generalized FDE. Adopted from Norton, Konvinse, *et al., Pediatrics* (2018) and Phillips, *et al.*, *J Allergy Clin Immunol* (2019)[61,62].

SJS/TEN and DRESS are two of the severest cutaneous adverse reactions. Clinical symptoms of SJS/TEN typically occur between 4 days and 2 weeks after starting a new medication and include a painful, blistering skin rash that results in epidermal necrosis and detachment as well as less specific symptoms including fever and sepsis (Figures 1.1 and 1.3). SJS/TEN is associated with a mortality of up to 50% as well as significant long-term morbidity including permanent corneal scarring, vision loss, prolonged pain and weakness, posttraumatic stress disorder, and fear of drugs. The disease process in SJS/TEN occurs in the epidermis. In SJS/TEN, the drug likely interacts with the HLA protein on keratinocytes that act as antigen-presenting cells to activate drug-specific CD8+ cytotoxic T cells (Figure 1.4). This interaction causes drug-specific CD8+ T cells to accumulate within epidermal blisters and release perforin and granzyme B that can kill keratinocytes. Drugs also trigger the activation of CD8+ T cells, NK cells, and NKT cells to secrete granulysin, which appears to be one of the most important cytotoxic mediators in SJS/TEN and can induce keratinocyte death without the need for cell contact (Figure 1.5). In contrast, DRESS, also known as drug-induced hypersensitivity syndrome typically develops between two and eight weeks after drug initiation and presents with fever, a widespread rash of varying severity without skin separation or blistering, facial edema, white cell abnormalities, most commonly eosinophilia and atypical lymphocytosis, and internal organ involvement frequently affecting the liver, kidneys, heart and lungs (Figure 1.3). Compared to SJS/TEN, DRESS carries a lower, but still notable, overall mortality rate of approximately 10%. Additionally, DRESS is associated with a slow recovery process which frequently includes prolonged treatment with high-dose systemic steroids and long-term autoimmune morbidities. The dermis is the primary skin compartment involved in the immunopathogenesis of DRESS. Both CD8+ and CD4+ T cells are pathogenic mediators (Figures 1.6 and 1.7).

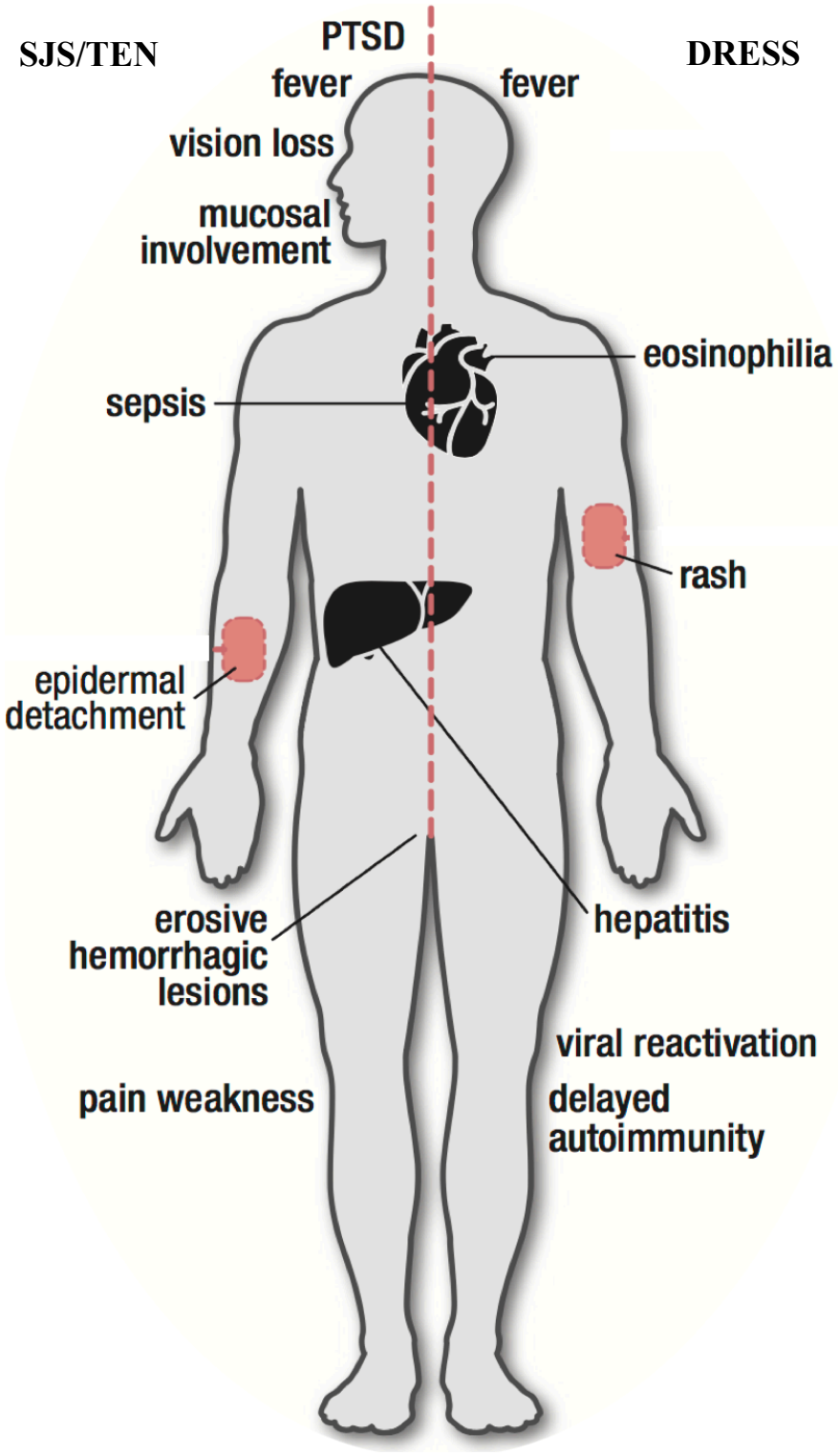

Figure 1.3. Clinical symptoms of SJS/TEN and DRESS. Legend: SJS/TEN, Stevens-Johnson syndrome/toxic epidermal necrolysis; DRESS, drug reaction with eosinophilia and systemic symptoms; PTSD, posttraumatic stress disorder. Adapted from Peter, Lehloenya, Dlamini, Risma, White, Konvinse, *et al*, *JACI: In Practice* (2017)[5].

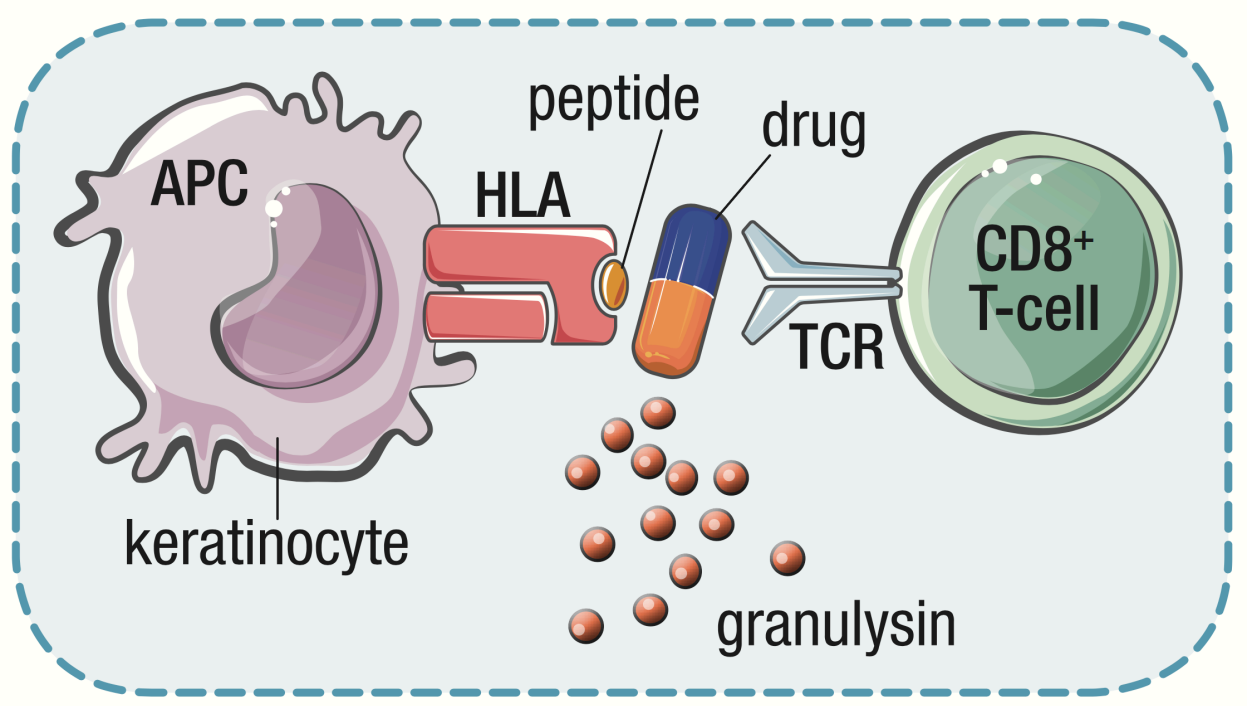

Figure 1.4. Proposed pathogenic mechanisms in drug-induced SJS/TEN. The drug likely interacts with the human leukocyte antigen protein on keratinocytes that act as antigen-presenting cells to activate drug-specific CD8+ cytotoxic T cells. **Legend:** APC, antigen-presenting cell; HLA, human leukocyte antigen; TCR, T-cell receptor. Adapted from Peter, Lehloenya, Dlamini, Risma, White, Konvinse, *et al*, *JACI: In Practice* (2017)[5].

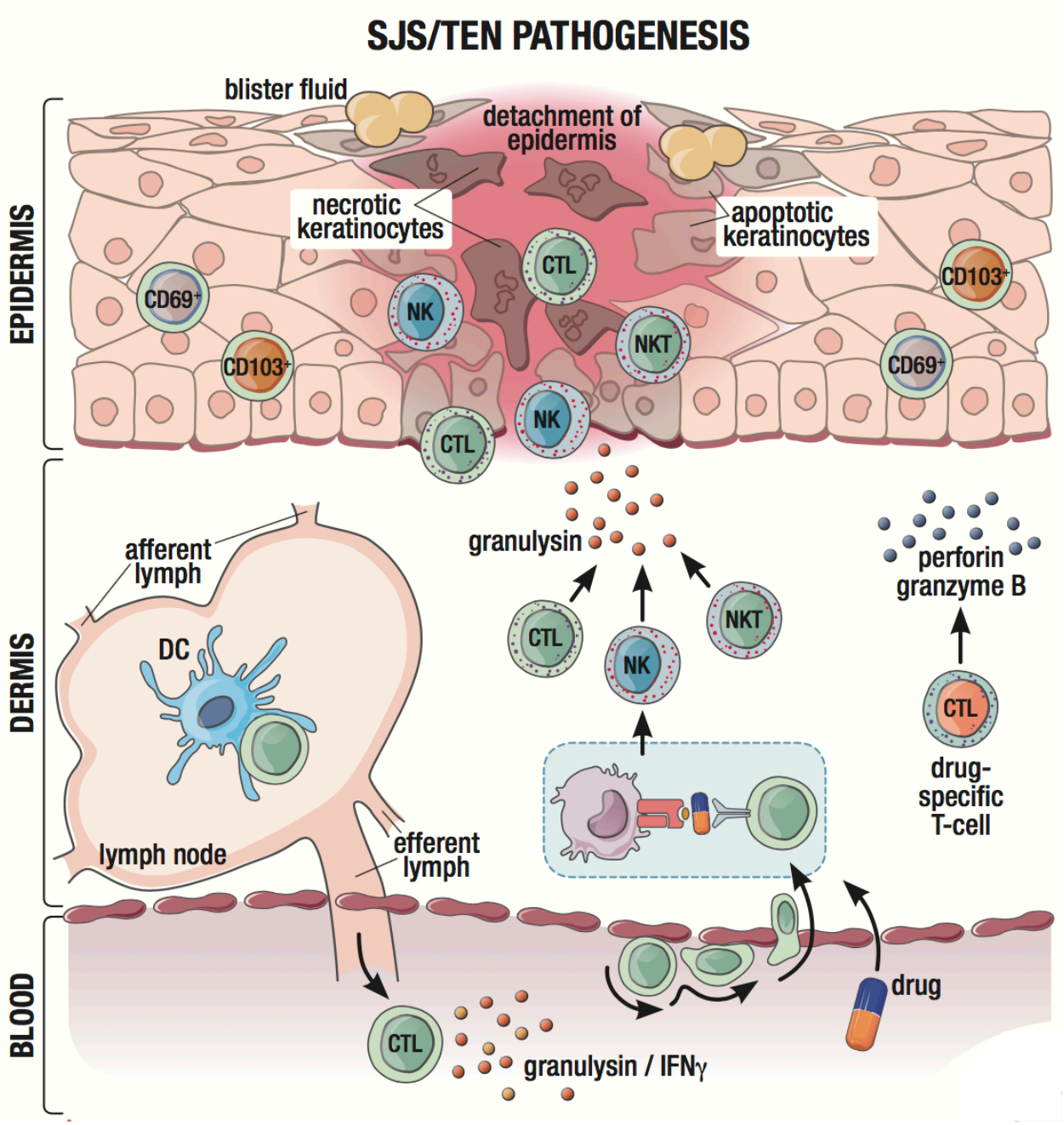

Figure 1.5. The disease process in SJS/TEN occurs in the epidermis. In SJS/TEN, the interaction between the drug, antigen-presenting cells and drug-specific T cell causes CD8+ T cells to accumulate within epidermal blisters and release perforin and granzyme B that can kill keratinocytes. Drugs also trigger the activation of CD8+ T cells, natural killer cells, and natural killer T cells which secrete granulysin. Granulysin appears to be one of the most important cytotoxic mediators in SJS/TEN and can induce keratinocyte death without the need for cell contact. **Legend:** SJS/TEN, Stevens-Johnson syndrome/toxic epidermal necrolysis; CTL, cytotoxic lymphocyte; DC, dendritic cell; NK, natural killer cell; NKT, natural killer T cell. Adapted from Peter, Lehloenya, Dlamini, Risma, White, Konvinse, *et al*, *JACI: In Practice* (2017)[5].

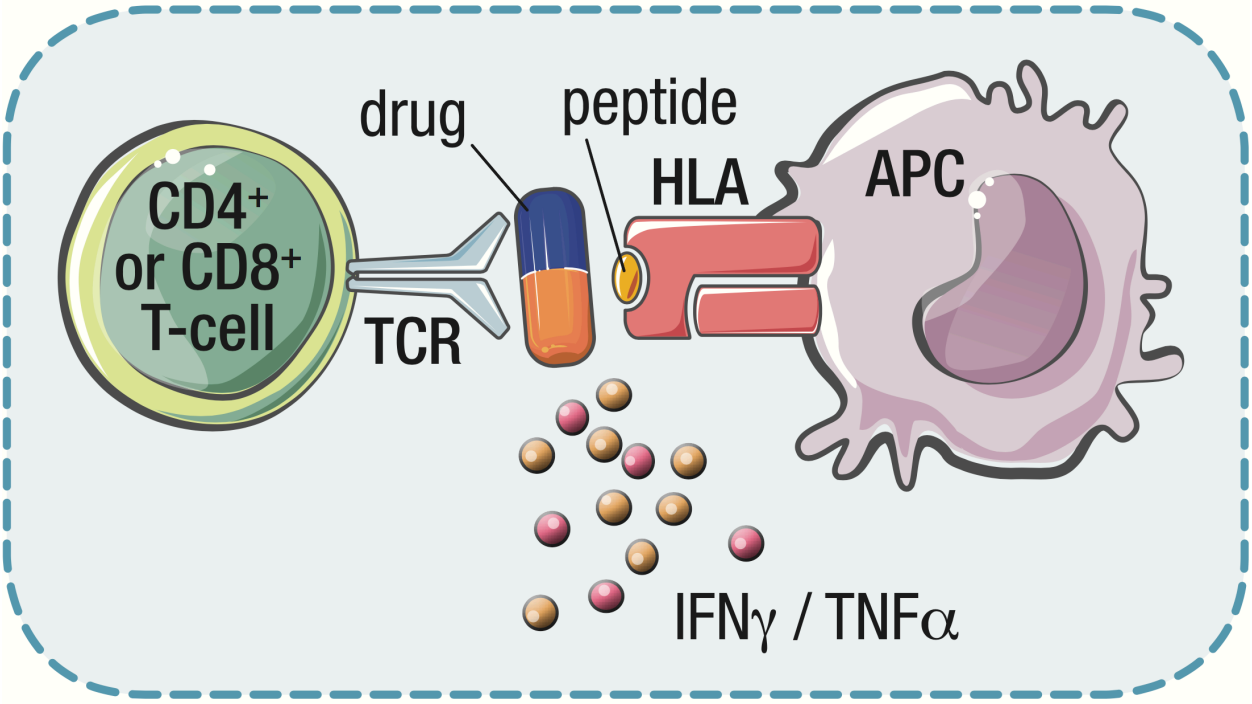

Figure 1.6. Proposed pathogenic mechanisms in drug-induced DRESS. The drug likely interacts with the human leukocyte antigen protein on antigen-presenting cells which then activates drug-specific T cells. The specific type of cells that act as antigen presenting cells in DRESS is currently unknown. Both CD4+ and CD8+ T cells are pathogenic mediators in DRESS. **Legend:** TCR, T-cell receptor; HLA, human leukocyte antigen; APC, Antigen-presenting cell. Adapted from Peter, Lehloenya, Dlamini, Risma, White, Konvinse, *et al*, *JACI: In Practice* (2017)[5].

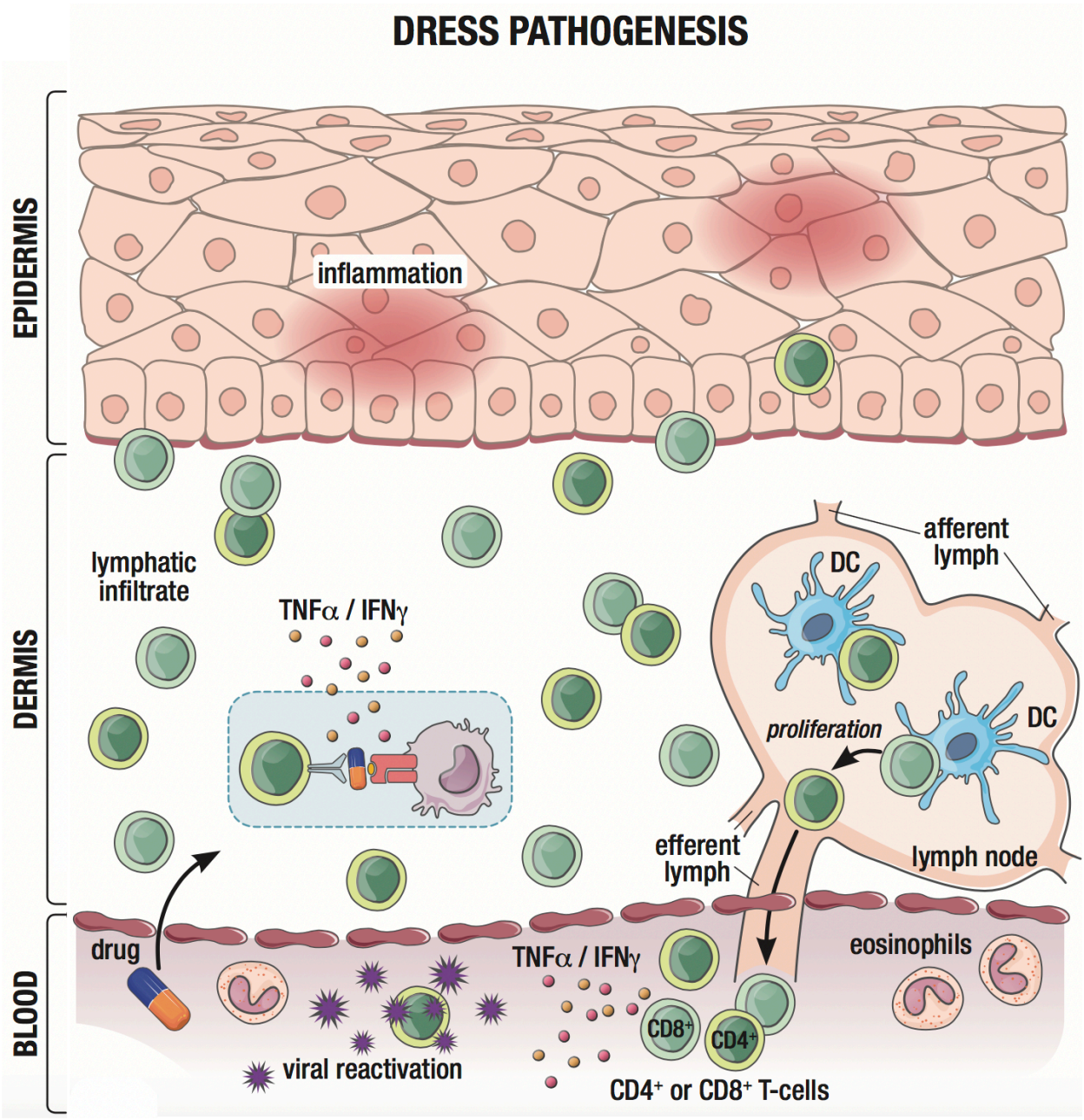

Figure 1.7. The dermis is the primary skin compartment involved in DRESS. DRESS is characterized by a lymphatic infiltrate of T cells into the dermis and increased release of TNF-α and IFN-γ. DRESS is also associated with viral reactivation of human herpesviruses although the role of viral reactivation in DRESS pathogenesis is currently unclear. Delayed autoimmune disease can occur as a sequela of DRESS. **Legend:** DRESS, drug reaction with eosinophilia and systemic symptoms; DC, dendritic cell. Adapted from Peter, Lehloenya, Dlamini, Risma, White, Konvinse, *et al*, *JACI: In Practice* (2017)[5].

DRESS is characterized by a lymphatic infiltrate of T cells into the dermis and increased release of TNF-α and IFN-γ. DRESS is also associated with viral reactivation of human herpesviruses although the role of viral reactivation in DRESS pathogenesis is currently unclear.

ANTIMICROBIAL ADVERSE DRUG REACTIONS

The epidemiology of serious T-cell-mediated reactions varies according to the region studied and is driven by genetic predisposition to these reactions. In general, given the high prevalence of antibiotic use, >50% of severe cutaneous adverse reactions (SCAR) globally are associated with antimicrobials, including antibiotics, antiretrovirals and antimycobacterial drugs used to treat infectious diseases[63-65]. Antimicrobial-associated ADRs have an extensive history with descriptions dating back to the 1930's and the use of the first sulfa antimicrobials[66] and then almost a decade later to early preparations of penicillins[67,68]. Despite the long-time recognition of antimicrobial-associated ADRs in the literature, allergies to these medications remain poorly understood and frequently misdiagnosed.

The overlabeling of antimicrobial allergy is a tremendous burden on society. For example, approximately 10% of the US population is labeled as allergic to penicillin. However, the true rate of penicillin allergy is estimated to be <1% of the general population[69]. Antibiotic allergy labels are usually acquired as a result of parent-reported rashes in young children. However, most benign cutaneous symptoms in small children that are interpreted as drug allergy are actually virus-induced or drug-virus interactions[61]. These symptoms would be unlikely to reoccur after subsequent administration of the same medication. However, very few children undergo a formal allergy evaluation to address the diagnosis. As a result, a high proportion of children carry their

antibiotic allergy labels into adulthood. This results in restricted antibiotic choices in the future and increased cost since alternative antibiotic choices are often more expensive, less efficacious and associated with more toxicities. Patients with reported drug allergies who require alternative therapies are more likely to suffer from complications such as *Clostridium difficile* and antibiotic-resistant infections than those without allergy labels[70]. On the other hand, in true cases of severe allergic reactions such as anaphylaxis, SJS/TEN or DRESS accidental rechallenge with the implicated medication could be life-threatening. Additionally, certain groups of patients such as individuals who are HIV positive or those with cystic fibrosis are disproportionately affected by true ADRs. This is due both to an altered immune profile and the disproportionate use of drugs that cause ADRs in those living with HIV[71-74]. Therefore, in an era of increasing antimicrobial resistance and frequent use of broad-spectrum antimicrobial therapy, ensuring patients are assigned the correct "allergy label" is essential. In this vein, improving diagnostic testing for drug allergy is the subject of considerable ongoing research.

IN VIVO DIAGNOSTIC TESTING

Clinically, multiple *in vivo* tests have been employed to confirm T-cell-mediated hypersensitivities including patch testing, skin prick testing, delayed intradermal testing and direct oral challenge. *In vivo* testing has a high specificity for most T-cell-mediated ADRs. However, skin testing suffers from a low diagnostic sensitivity and is complicated by the fact that the ideal concentration to test for most drugs is unknown because the highest non-irritating concentrations in the skin have not been validated. Due to risk of recurrent reaction, oral challenge with implicated drugs is contraindicated for severe reactions such as SJS/TEN and DRESS[6].

GENETIC SCREENING

Since the HLA genes are the most polymorphic region in the human genome, there is a tremendous amount of diversity in HLA proteins (Figure 1.8). An HLA naming system exists to systematically convey the differences among the thousands of different HLA genes. All alleles start with "HLA" followed by a letter which denotes the HLA class loci. Major HLA Class I genes include HLA-A, HLA-B and HLA-C while major HLA Class II genes include HLA-DP, HLA-DQ and HLA-DR. The letter donating HLA class is then followed by numbers, which distinguish different alleles. The first two numbers denote the supertype, which typically corresponds with the serological antigen that is present. The third and fourth digits specify a nonsynonymous allele.

Recently, an increasing number of antimicrobial immune-mediated adverse drug reactions (IM-ADRs) have been associated with various HLA alleles (Table 1.3). In general, due to varying HLA allele frequencies, different ancestral populations have different genetic associations. Additionally, treatment and prevalence of certain infectious diseases vary by widely geography. Therefore, the regional burden of IM-ADRs due to a particular drug is also dependent use of the drug in that particular area. To date, hypersensitivity syndrome to the antiretroviral abacavir is the best characterized antimicrobial-induced, HLA-associated IM-ADR that also generalizes across all ethnicities. The association between abacavir hypersensitivity syndrome and HLA-B*57:01 resulted in the widespread implementation of a routine screening test that is widely employed in developed countries before abacavir treatment. Before widespread acceptance, the HLA-B*57:01 genetic association with abacavir was established in a large population with a diverse genetic background. This screening test has a positive predictive value (PPV) of 55% and a negative

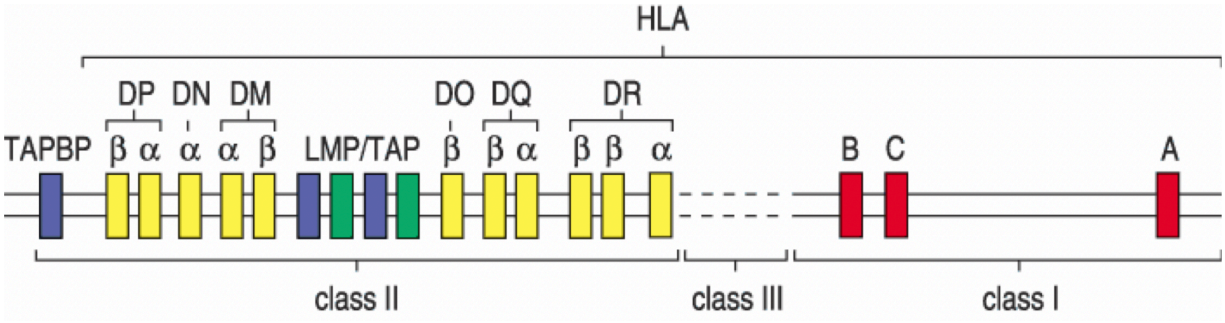

Figure 1.8. Gene structure of the human leukocyte antigen (HLA) region on chromosome 6. Adapted from Murphy K (2011) Janeway's ImmunoBiology, Eighth Edition.

Antimicrobial	Clinical Presentation	Associated HLA Allele(s)	Population	NPV (%)	PPV (%)	NNT
Abacavir[75-77]	Hypersensitivity syndrome	B*57:01	European, African	100	55	13
Efavirenz[78]	Rash	DRB1*01	French			
Nevirapine[78-87]	Rash	B*35:05 Cw4	Thai African, Asian, European, Thai	97	16	
	DRESS	B*14/Cw8 Cw8 Cw*4 and DRB1*15 B*3505 B*3501 and B*15/DRB1*15	Italian Japanese Han Chinese Asian Australian			
	Hepatitis	DRB1*01:01 DRB1*01:02	Australian, European South African	96	18	
	SJS/TEN	C*04:01	Malawian			
Raltegravir[88]	DRESS	B*53:01	African			
Flucloxacillin[89-91]	Hepatitis (DILI)	B*57:01 B*57:03 DRB1*0107-DQB1*0103	European	99.99	0.12	13,819
Dapsone[92]	Rash, hepatitis	B*13:01	Chinese	99.8	7.8	84
Amoxicillin-clavulanate[93-96]	Hepatitis (cholestatic)	A*02:01 DQB1*0602 and rs3135388, a tag SNP of DRB*15:01-DQB1*06:02	European			
Sulfamethoxazole[97,98]	SJS/TEN FDE	B*38 A*30-B*14-Cw*6	European Turkish			
Aminopenicillins[99]	Rash	A*2 DR*52	Italian			
Sulphonamides[100]	SJS/TEN	A*29 B12 (B*44) DR7	European			
Isoniazid[101,102]	DILI	NAT2 slow acetylator, CYP2E1*5 and *1B	European			
	DILE	DR*4	Italian			
Levamisole[103]	Agranulocytosis	B*27	South American			
Minocycline[104]	DILI	B*35:02	European			
Terbinafine[105]	DILI	A*33:01	European			

Table 1.3. Human leukocyte antigen associations for antimicrobial associated T-cell-mediated hypersensitivity syndromes. Legend: DILI, drug-induced liver injury; DILE, drug-induced lupus erythematosus; DRESS, drug reaction with eosinophilia and systemic symptoms; FDE, fixed drug eruption; HLA, human leukocyte antigen; NNT, number needed to treat; NPV, negative predictive value; PPV, positive predictive value; SJS/TEN, Stevens-Johnson syndrome/ toxic epidermal necrolysis. Adapted from Konvinse, *et al.*, *Curr Opin in Infect Dis* (2016)[54].

predictive value (NPV) of 100%, which is crucial for drug safety[75-77]. Less than 100% NPVs and very low PPVs of other antimicrobial drug hypersensitivity HLA associations have limited their translation into routine clinical practice as screening tests. For example, although only 13 individuals would need to be screened for HLA-B*57:01 to prevent a single case of clinically-diagnosed abacavir hypersensitivity syndrome, over 13,000 individuals would have to be tested for this same allele to prevent a single case of flucloxacillin-associated hepatitis.

The story of nevirapine-induced IM-ADRs is quite complex. Nevirapine-induced IM-ADRs have been associated with different HLA alleles across different ethnic populations. These HLA associations appear to be phenotype specific and involve both Class I and Class II HLA alleles. An association between nevirapine-induced hepatitis and HLA-DRB1*01:01 was first reported in a Western Australian population[85] and has since been reported in other Caucasian populations[78]. The closely related allele HLA-DRB1*01:02 was associated with nevirapine-induced hepatitis in a South African cohort[86]. Nevirapine DRESS has been associated with the HLA-Cw*8 or Cw*8-B*14 haplotype in Japanese and Italian populations and also with HLA-Cw*4 and HLA–DRB1*15 in Han Chinese, HLA-B*35:05 in Asians and HLA-B*35:01 and HLA-B*15/DRB1*15 in an Australian cohort[81,82,84,87,106]. Many of these alleles including HLA-DRB*01, HLA-Cw*04 and HLA-B*35:05 are also associated with nevirapine-induced rash[78-80,83,87].

Other HLA associations have been described for IM-ADRs to efavirenz, raltegravir, dapsone, flucloxacillin, amoxicillin-clavulanate, sulfamethoxazole, aminopenicillins, sulfonamides, isoniazid, levamisole, minocycline and terbinafine (Table1.3)[78,88-105]. Many of these antimicrobials such as flucoxacillin and amoxicillin-clavulanate are specifically associated with drug-induced

liver injury (DILI), which can be associated with fulminant hepatic failure[77]. Although few HLA screening tests have advanced to the level of routine clinical practice, HLA associations have significantly advanced our understanding of the immunopathogenesis of IM-ADRs.

EX VIVO TESTING

Intradermal tests are painful and oral challenge may be poorly tolerated in certain populations such as children and is contraindicated in severe hypersensitivity[107]. Therefore, the use of *in vitro* testing for drug hypersensitivity reactions is particularly attractive. Currently, these tests, as a group, have lacked specificity and sensitivity and have not undergone largescale validation. As a result, they cannot be used as the sole basis for drug rechallenge. The basophil activation test (BAT) is an *in vitro* test for type I (immediate) hypersensitivities which measures activation of a patient's basophils in a test tube containing Interleukin-3 and the drug which is to be tested. Although, the symptoms of type I hypersensitivities are due to both tissue-resident mast cell and basophil degranulation, basophils are more easily accessible in the peripheral blood and are therefore favored for *in vitro* testing. BAT uses flow cytometry to detect basophil surface (CD63, CD203c) and intracellular (P-p38MAPK) activation markers after exposure to the expected allergen[108,109]. BAT has been used for causality assessments in beta-lactam antibiotics, quinolones and clavulanic acid as a beta-lactamase inhibitor[107,108,110-112]. For beta-lactam antibiotics, the BAT has a reported sensitivity and specificity of ranging from 33-67% and 79-100%, respectively[108,109].

The lymphocyte transformation test (LTT) is used for the diagnosis of drug-induced type IV (delayed) hypersensitivities. The LTT measures the proliferation of T cells to a drug *in vitro*. LTT is a technically demanding test and is hindered by prolonged testing time and the requirement for

radioactive materials. LTT has been used in the diagnosis of T cell-mediated hypersensitivities to ceftriaxone, ampicillin/sulbactam, metronidazole, penicillins and cephalosporins including ceftazidine and anti-tuberculosis therapies[113-117]. LTT has a reported sensitivity of 27-70% and specificity of 72.7-100%[118-121].

Enzyme-Linked ImmunoSpot (ELISpot) assays are used to analyze low-frequency antigen-specific, cytokine-producing cells in the peripheral blood of patients with a type IV hypersensitivity reaction following stimulation with pharmacological drug concentrations[113]. The limit of detection typically achieved can be 1 in 100,000 cells. Each "spot" that develops in the assay represents a single cytokine-producing cell. ELISpot can be used to measure a variety of cytokine responses including IL-13, IFN-γ, IL-10, IL-5, granzyme B, granulysin and TNFα. The production of different cytokines is measured based on the type of T cell suspected to be involved in the specific hypersensitivity reaction. Multiple studies have demonstrated ELISpot to be an effective test for the diagnosis of delayed hypersensitivity reactions to amoxicillin, ticarcillin, piperacillin, cephalosporins, amikacin and sulfasalazine. ELISpot has been reported to have a better sensitivity than LTT in detecting drug-specific T-cell responses and a specificity ranging from 95-100%[107,122-129].

Similar to ELISpot, intracellular cytokine staining (ICS) is used to measure the production of targeted cytokines by T cells from a patient with a suspect type IV hypersensitivity in response to drug stimulation[119]. In this assay, patient cells are incubated with a range of known pharmacological concentrations of drug. An inhibitor of protein transport is added to retain the cytokines within the cells. After washing, antibodies to surface markers are added. The cells are

then fixed and permeabilized followed by the addition of anti-cytokine antibodies. The cells are analyzed by a flow cytometer. The benefit of ICS in comparison to ELISpot is that a single assay can look at a variety of cytokine outputs (e.g. IFN-γ, IL-2, TNFα) and surface proteins of interest including activation markers (e.g. CD137, CD69) on multiple cell populations. Currently, all of the *in vitro* tests highlighted in this section are predominantly applied only in research settings for the diagnostic management of drug allergy. Additional clinical studies are needed before their entrance into routine clinical care.

MANAGEMENT AND TREATMENT OF SEVERE CUTANEOUS ADVERSE REACTIONS

Management and treatment of SCARs varies depending on the specific type of reaction. In all cases, prompt diagnosis and cessation of the offending drug is imperative[130,131]. There are no established targeted therapies for SJS/TEN although several immunosuppressive and immunomodulating therapies have been used in clinical practice with mixed results[5]. Acutely ill patients with SJS/TEN should receive supportive care in an intensive care or burn unit from a multidisciplinary team including pain management specialists for pain, infectious diseases physicians for sepsis concerns and treatment of underlying infections, dermatologists and burn surgeons for skin treatment, and nutritionists, ophthalmologists and for female patients, gynecologists for treatment of affected mucosal surfaces. Patients with acute DRESS should also be hospitalized. Most cases of suspected DRESS with significant internal organ involvement such as hepatitis and acute kidney injury should be treated with high dose systemic steroids that are weaned slowly over the course of several weeks to months. However, in milder cases limited to cutaneous involvement in patients with severe co-morbidities such as advanced acquired immune

deficiency syndrome (AIDS) or active tuberculosis, topical steroids may be preferable. Follow up is necessary to monitor and manage skin, autoimmune, psychiatric and other long-term sequelae in both SJS/TEN and DRESS. The offending drug and all potential cross-reacting drugs should be listed in the medical record as a severe allergy and patients must be instructed to avoid that medication in the future.

RESEARCH OBJECTIVES AND DISSERTATION OVERVIEW

Because the mechanisms behind most ADRs are not well understood, there continues to be significant unmet need with regard to prevention strategies, earlier diagnoses, and targeted therapeutic options. Thus, the focus of this dissertation is to gain a better understanding of the genetic risk factors and immunopathogenesis of severe cutaneous adverse reactions due to antibiotics and antiretroviral medications. The majority of my dissertation research is focused on two drug-induced hypersensitivity syndromes. Chapter 2 details my research on nevirapine-induced hypersensitivity syndromes, with a focus on nevirapine-induced SJS/TEN, in a South African population. As reviewed in preceding sections, SJS/TEN is a blistering skin disease that causes skin necrosis and detachment resulting in wounds similar to extensive third-degree burns. This process leaves the patient susceptible to infections and fluid loss. The HIV medication nevirapine is a common cause of SJS/TEN in South Africa. Chapter 3 focuses on vancomycin-induced DRESS. Similar to SJS/TEN, patients with DRESS also develop fever and a widespread rash. However, the real danger of DRESS is the risk of internal organ failure. The liver, kidneys, heart and lungs are commonly affected organs. Vancomycin, a regularly prescribed antibiotic to treat life-threatening infections, is the most prevalent cause of antibiotic-induced DRESS. Chapter 4 provides an in-depth case report on one patient with vancomycin-induced SJS. The general

overall aims of this work are to define the clinical and demographic characteristics of patients with severe antimicrobial allergies, to define the genetic risk factors contributing to these reactions in genetically diverse patient populations from around the world, and to identify specific receptors or protein signatures in immune cells that help explain how these reactions occur and help predict who is at risk of developing a severe drug reaction in the future. Chapter 5 details potential future directions of this work.

OVERIVEW OF EXPERIMENTAL APPROACH

I actively recruited patients for this research under Institutional Review Board (IRB)-approved protocols. Patients were enrolled via my mentor's drug allergy clinic and by our collaborators in the United States, Australia and South Africa. In addition to direct referrals, we were able to identify acutely ill, hospitalized patients potentially eligible for our studies by an electronic alert system that was originally designed by Dr. Josh Denny when he was a medical student. This alert system was customized using key words and terms designed to identify cases of severe immunologically-mediated adverse drug reactions. Members of our "on call research team" were then automatically notified every time these key words were entered in the electronic health record by house staff to indicate that an inpatient or outpatient with potential SJS/TEN or DRESS was being assessed at Vanderbilt University Medical Center. I validated all medical records of patients in this dissertation to ensure every patient met study inclusion criteria. Drug tolerant controls were enrolled by participating research centers or detected via Vanderbilt's BioVU repository, a deidentified electronic health record database linked to a DNA biobank. For individuals who met clinical inclusion criteria that suggested a true immunologically-mediated adverse drugs reaction, with the patients' consent, we collected their saliva, blood, affected skin and blister fluid as

appropriate and available. Blister fluid is a valuable source of T cells and other cells relevant to the acute skin necrosis and inflammatory infiltrate seen in SJS/TEN. With sometimes rapidly advancing skin necrosis, blisters can be a transient feature of the disease. Thankfully, the electronic alert system helped us identify patients who may qualify for our studies as soon as they were admitted so we could enroll them shortly after disease onset.

All samples were processed immediately and then used in experiments (Figure 1.9). In general, DNA extracted from blood or saliva is used for HLA, killer-cell immunoglobulin-like receptor (KIR) and endoplasmic reticulum aminopeptidase (ERAP) typing and in the case of nevirapine IM-ADRs, CYP2B6 typing to identify genetic risk factors in the patients' immune system or in their ability to metabolize the drug that place them at an increased risk for a severe reaction. Peripheral blood mononuclear cells (PBMCs) were evaluated for drug-specific responses via IFNγ ELISpot assays. When available, skin and blister fluid samples were used to study the T cells at the sites of disease. Formalin-fixed, paraffin-embedded skin was stained with antibodies against SJS/TEN biomarker granulysin as well as general T cell (CD3, CD4, CD8), skin homing (CCR4, cutaneous lymphocyte-associated antigen (CLA)), natural killer cell (CD56), regulatory T cell (FoxP3), and tissue-resident (CD103) markers. These slides were analyzed blindly by Vanderbilt dermatopathologists. Granulysin levels were measured in acute nevirapine SJS/TEN plasma and blister fluid supernatant via ELISA. Single cell TCR sequencing (sc-TCRseq) paired with whole transcriptome sc-RNAseq was performed on T cells from acute SJS/TEN blister fluid and skin.

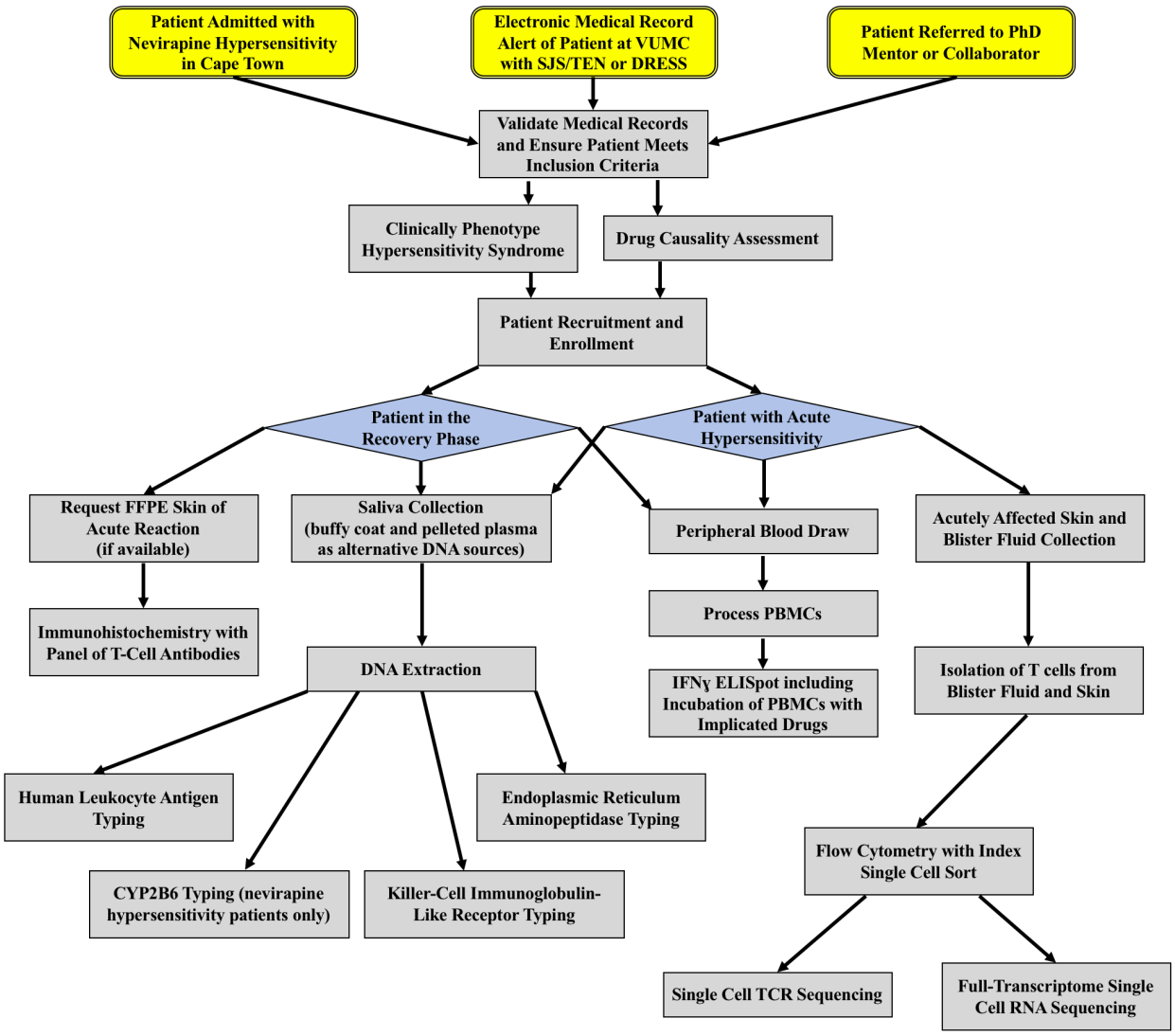

Figure 1.9. Overview of the experimental approach. Legend: SJS/TEN, Stevens-Johnson syndrome/toxic epidermal necrolysis; DRESS; drug reaction with eosinophilia and systemic symptoms; FFPE, formalin-fixed, paraffin-embedded; DNA, deoxyribonucleic acid; ELISpot, Enzyme-linked ImmunoSpot; PBMCs, peripheral blood mononuclear cells; CYP2B6, cytochrome P450 2B6; TCR, T-cell receptor; RNA, ribonucleic acid.

SYNOPSIS OF THE DATA AND SIGNIFICANCE OF THE RESEARCH

Nevirapine is a common cause of SJS/TEN in countries with a high prevalence of HIV. In my cohort of South African patients, 100% of nevirapine SJS/TEN cases (n=20) carried HLA-C*04:01 compared to 21.7% of unrelated individuals tolerating nevirapine (n=10/46) ($p=7.4x10^{-10}$). The strong association of HLA-C*04:01 with nevirapine SJS/TEN in a South African population indicates that this allele is necessary but not sufficient for SJS/TEN development. This risk allele could be used as a screening test to identify patients at risk for developing a reaction before nevirapine is prescribed. With a positive predictive value of 2.4%, this would translate into a number needed to test for HLA-C*04:01 to prevent one case of SJS/TEN of ~200. CYP2B6 genotyping revealed that SJS/TEN patients had slower nevirapine metabolizing phenotypes than tolerant controls. An *ERAP1* SNP rs27044 was independently associated with nevirapine SJS/TEN susceptibility ($p=3.2x10^{-6}$) and was overrepresented in HLA-C*04:01 carriers tolerant of nevirapine suggesting that the peptide repertoire presented to T cells in the presence of nevirapine may contribute to hypersensitivity development. Immunohistochemistry of skin revealed a predominantly CD8+, dense lymphocytic infiltrate with high CLA expression. Granulysin levels in acute nevirapine SJS/TEN plasma and blister fluid supernatant were several-fold higher than in healthy donor plasma and blister fluid supernatant from thermal burns, which supports previous literature proposing elevated granulysin levels as an SJS/TEN biomarker[35]. Single-cell TCR sequencing and single-cell RNA sequencing data helped identify the most likely candidate drug-specific T cells.

Vancomycin is the most common cause of antibiotic-associated DRESS, but most patients are prescribed multiple antibiotics concurrently, which can make definitive ascertainment of the

implicated drug difficult. My research identified HLA-A*32:01 as a risk allele for the development of vancomycin DRESS in a population of predominately European ancestry. In a cohort of 23 individuals diagnosed with vancomycin DRESS, 19/23 (82.6%) cases carried HLA-A*32:01 compared to 0/46 (0%) of the matched vancomycin tolerant controls ($p=1x10^{-8}$) and 6.3% of the BioVU population (n=54,249) ($p=2x10^{-16}$). In a time-to-event analysis of DRESS development during vancomycin treatment in 274 individuals, 50% with and 50% without the risk allele, 13 individuals developed definite or possible DRESS, and all 13 were HLA-A*32:01 positive. Therefore, HLA-A*32:01 testing could improve antibiotic safety, help implicate vancomycin as the causal drug and preserve future treatment options with co-administered antibiotics.

These HLA risk allele findings are readily translatable to clinical practice and will make these medications safer for patients. Additionally, the research in this dissertation provides insights into why not all patients with a genetic risk allele develop a reaction and a roadmap for future work studying severe, delayed allergic reactions to other medications.

CHAPTER II

GENETIC RISK AND IMMUNOPATHOGENESIS OF SEVERE CUTANEOUS ADVERSE REACTIONS ASSOCIATED WITH NEVIRAPINE

INTRODUCTION

Nevirapine is a non-nucleoside reverse transcriptase inhibitor used extensively in pregnant women and infants born to HIV+ mothers in both the developing and developed world to treat HIV and AIDS. The current use of nevirapine in first line therapy is limited only by severe immune-mediated adverse drug reactions (IM-ADRs), which occur in ~5% of patients after the initiation of therapy. Nevirapine has an established long-term safety profile. It is safe in pregnancy and in children. Additionally, due to concerns of decreased bedaquiline exposure in patients also being treated with efavirenz-based combination antiretroviral therapy, nevirapine is commonly used instead of efavirenz in HIV+ patients with multidrug-resistant tuberculosis on bedaquiline-based treatments.

Nevirapine is one of a handful of drugs strongly associated with both Stevens-Johnson syndrome/toxic epidermal necrolysis (SJS/TEN) and Drug Reaction with Eosinophilia and Systemic Symptoms (DRESS). SJS/TEN is the severest IM-ADR associated with nevirapine use. Nevirapine SJS/TEN initially presents with non-specific symptoms such as a fever and sore mouth, but within 48 hours, symptoms progress to include a painful, blistering skin rash that results in epidermal necrosis and detachment. For drugs with long half-lives such as nevirapine, and in populations infected with HIV, SJS/TEN is associated with a mortality of up to 50%. In patients

who survive the acute reaction, nevirapine SJS/TEN has significant associated long-term morbidity predominately due to the involvement of multiple mucosal surfaces. Common morbidities include vision loss and reproductive, digestive and respiratory difficulties. Patients are also likely to suffer from post-traumatic stress disorder, fear of taking new medications, contracted therapeutic options and a shortened life span.

In contrast, nevirapine DRESS presents as a widespread rash of varying severity without skin separation or blistering, but with fever, internal organ involvement and atypical white blood cell counts, most commonly eosinophilia. Due to this variability in presentation that can mimic other clinical syndromes and late onset of symptoms, clinicians are often slow to diagnose nevirapine DRESS and in the meantime, the patient may remain on the offending drug. This syndrome may be particularly difficult to diagnose in an HIV-positive individual who is more prone to common viral and opportunistic infections.

SJS/TEN is considered to be an HLA Class I restricted, CD8+ T-cell dependent delayed hypersensitivity syndrome with long-lasting memory T-cell responses. In contrast, DRESS requires both CD4+ and CD8+ T cells[106]. The mechanism by which nevirapine causes SJS/TEN is unknown. However, several dominant HLA Class I and II risk alleles have been associated with nevirapine IM-ADRs in patients from multiple ethnicities (Chapter 1, Table 1.3). Notably, HLA-C*04:01 has been associated with nevirapine SJS/TEN in a Malawian population and HLA-DRB1*01:02 has been associated with nevirapine-induced hepatitis in South Africans[86,132].

In addition to the carriage of risk HLA alleles, other factors such as drug metabolism also influence the possible development of cutaneous nevirapine IM-ADR. Hepatic metabolism of nevirapine is predominantly through cytochrome P450 enzymes CYP2B6 and CYP3A4 (Figure 2.1). Slow metabolizer genotypes for CYP2B6 alleles (516G→T and 983T→C) correlate with increased plasma levels of nevirapine and greater risk for nevirapine IM-ADR[87,133,134]. This suggests that the development of some nevirapine IM-ADRs is dependent on HLA carriage as well as accumulation of the parent drug.

The endoplasmic reticulum aminopeptidase (ERAP)1 and ERAP2 enzymes are responsible for the N terminal trimming of peptides before they are loaded onto HLA molecules for presentation to the immune system (Figure 2.2). The *ERAP1* and *ERAP2* genes are extremely polymorphic and several common polymorphisms encode variant amino acids which affect enzyme function. Variants in *ERAP* genes have been associated with autoimmune conditions including ankylosing spondylitis, psoriasis and Behçhet's disease[135-139]. In HLA-restricted autoimmune diseases, variants in *ERAP* have been shown to interact in an epistatic manner with disease-associated HLA class I alleles to influence disease risk. In a previously studied cohort of HIV-infected individuals from sub-Saharan Africa, variation in *ERAP1* was not found to modulate risk of nevirapine SJS/TEN in HLA-C*04:01 individuals, but variation in *ERAP2* had a potentially protective effect[140]. Therefore, due to the known HLA class I restriction of nevirapine hypersensitivity reactions, we genotyped 17 key *ERAP* SNPs (Figure 2.3) to see if carriage of specific *ERAP* alleles influenced nevirapine SJS/TEN and DRESS risk in our patient cohort.

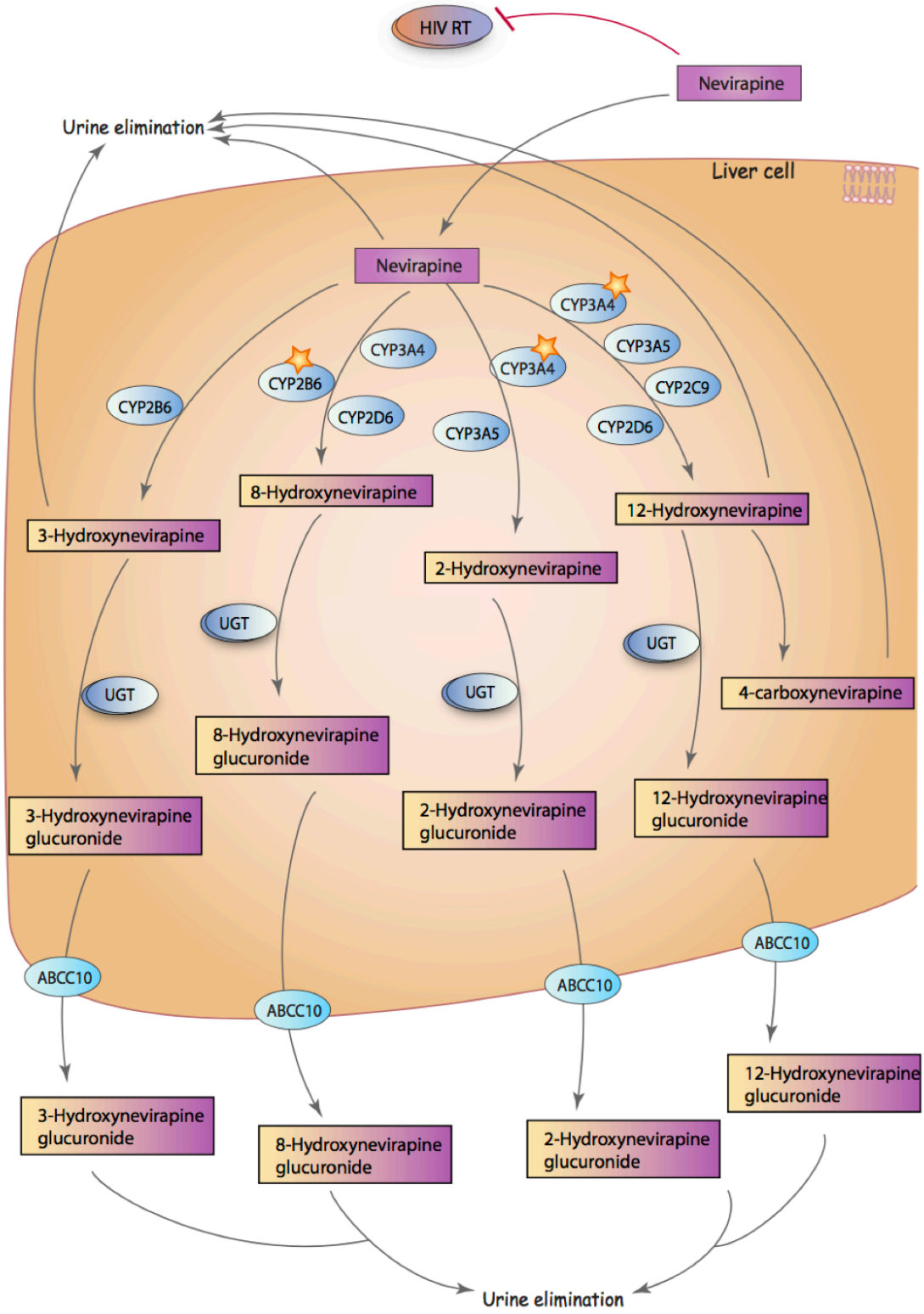

Figure 2.1 Metabolism of nevirapine. Adapted from Whirl-Carrillo, *et al. Clinical Pharmacology and Therapeutics* (2012)[141]. The stars denote enzymes that play a major role in nevirapine metabolism.

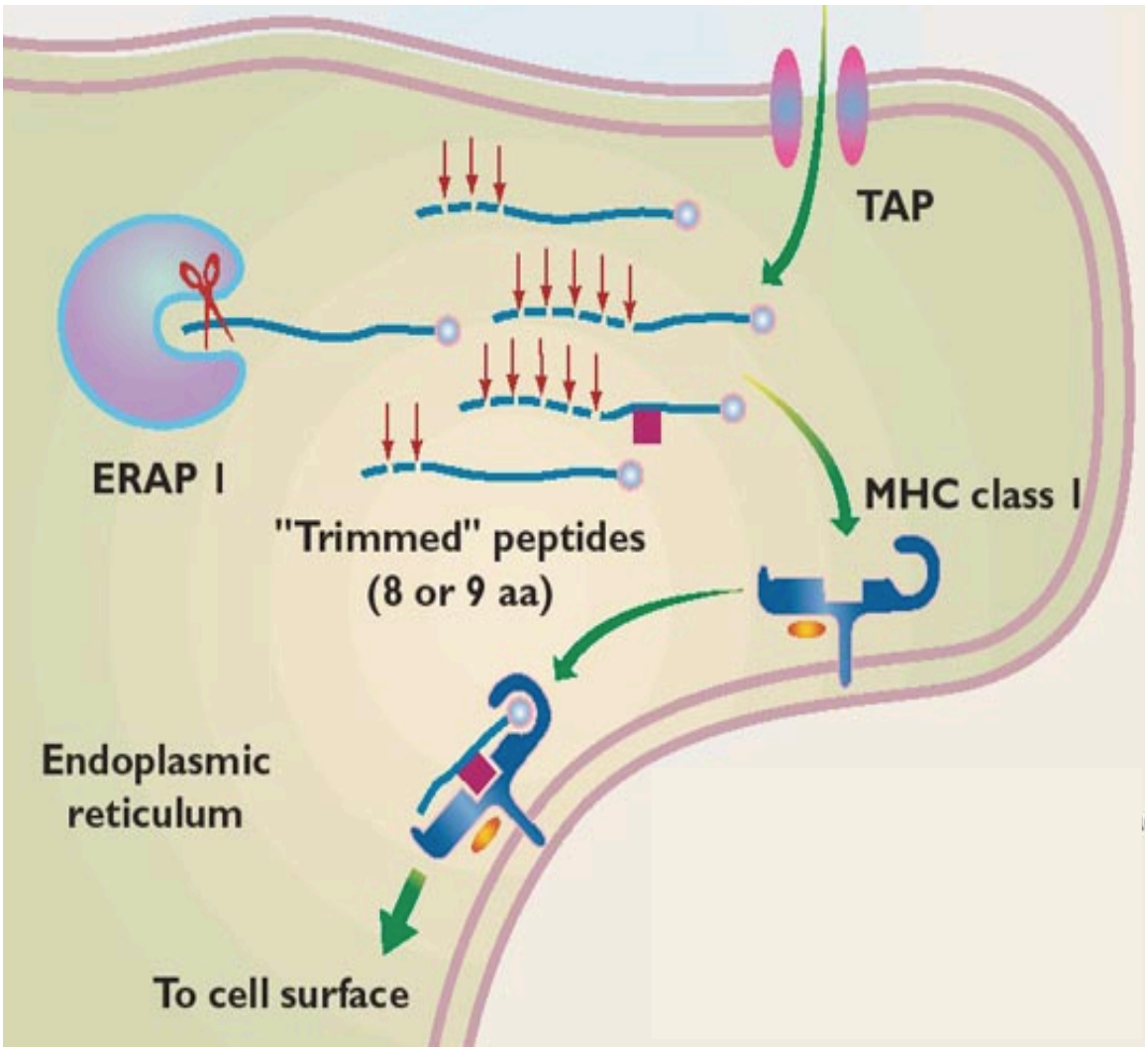

Figure 2.2. Endoplasmic reticulum aminopeptidase 1 (ERAP 1) trims peptides to be loaded onto HLA Class I. Adapted from Falk and Rotzschke, *Nature Immunol* (2002)[142]. **Legend:** ERAP I, endoplasmic reticulum aminopeptidase I; MHC, major histocompatibility complex; TAP, transporter associated with antigen processing.

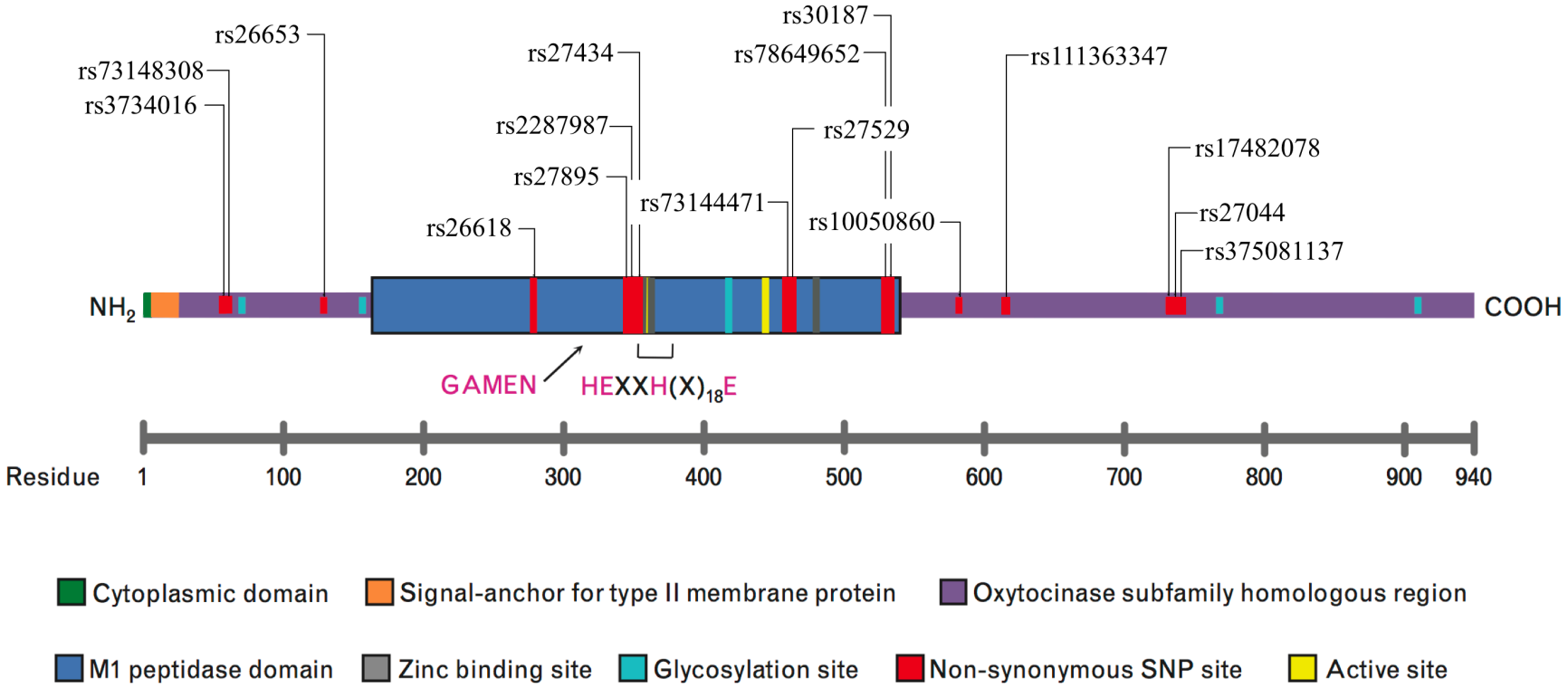

Figure 2.3. Schematic diagram of ERAP1. The locations of non-synonymous SNP sites that were genotyped in the South African nevirapine hypersensitivity cohort are shown. Note that the map is the ERAP1 protein while the reference SNP cluster ID (rs) numbers refer to positions in the *ERAP1* gene. rs numbers are used to keep the terminology consistent with the results section. Adapted from Tran and Colbert, *Curr Opin Rheumatol* (2015)[143].

Since in addition to its role as a T-cell restriction element, HLA-C also acts as a ligand for killer immunoglobulin receptors (KIRs) on natural killer (NK) cells, we also performed KIR genotyping on all patient samples. Killer immunoglobulin-like receptors (KIRs) are cell surface receptors expressed on NK cells. These molecules act as activating or inhibitory receptors regulating the function of NK cells by interacting with Class I HLA ligands. At the genetic level, KIRs are encoded by a highly polymorphic family of 16 genes. The number and type of KIR genes vary among individuals and interactions between polymorphic HLA and KIR have been shown to be associated with susceptibility to or protection from infectious, autoimmune, and malignant disorders.

A key unanswered question central to the mechanism of HLA-associated IM-ADRs is why hypersensitivity generally occurs in only a small proportion of those carrying an HLA-risk allele. In addition to potential contributions from the genetic factors discussed above, we hypothesized that the immunophenotypic characterization and T-cell receptor (TCR) specificities of the T cells in the hypersensitive patients will help answer this question. Previous drug hypersensitivity studies have predominantly focused on T-cell responses in the peripheral blood. Here, we developed methods to study T cells at the sites of disease in affected skin and blister fluid to help identify and characterize candidate drug-specific T cells.

METHODS

Nevirapine Hypersensitivity Cases

Patients ≥12 years of age at the time of study enrollment who developed a severe cutaneous reaction with at least one systemic symptom such as fever, liver enzyme elevation greater than two

times the upper limit of the normal range, or atypical lymphocytes including eosinophilia within eight weeks of initiation nevirapine therapy, with a corresponding Naranjo adverse drug reaction score of ≥5 (probable adverse drug reaction), and with nevirapine identified as the primary implicated drug as determined by the ALDEN algorithm were included in the study.

Naranjo scores calculate the probability that the patient's symptoms are due to an adverse drug reaction and include factors such as whether there are previous conclusive reports of this drug being associated with this particular reaction, whether the adverse event appeared after the suspected drug was administered, whether the reaction improved when the drug was discontinued, whether there are other causes including other drugs that could have caused the reaction, whether this was a rechallenge reaction and whether the adverse event was confirmed by objective evidence such as a biopsy[144].

The ALDEN algorithm was used to determine the likelihood nevirapine was the causative drug in a patient with SJS/TEN and includes parameters such as the delay from initial drug intake to symptom onset, whether the drug was present in the body on the index day, whether this is a rechallenge reaction, whether the drug has been associated with other definite cases of SJS/TEN and whether there are other potential causes for the reaction[145]. A score of equal to or greater than four indicates that the implicated drug was "probably" the cause of the reaction.

Retrospective and prospective patients were recruited between 2016 and 2018 through outpatient clinics and inpatient facilities at participating institutions in Cape Town, South Africa (Groote Schuur Hospital affiliated with the University of Cape Town, Tygerberg Hospital, and DP Marais

Hospital). Peripheral blood and saliva were routinely collected from both retrospective and prospective cases. When possible, blister fluid and skin were collected from hospitalized patients with acute nevirapine SJS. Institutional review board (IRB) approvals were in place for all sites contributing to the study. All aspects of the study including the collection and storage of DNA, plasma, buffy coat, peripheral blood mononuclear cells (PBMCs), blister fluid and skin were IRB-approved and all patients provided written informed consent.

Nevirapine Tolerant Controls

Patients ≥12 years of age who tolerated nevirapine for >12 weeks were enrolled as drug tolerant controls at participating facilities in Cape Town, South Africa (Groote Schuur Hospital, Khayelitsha Community Health Centre, and DP Marais Hospital). IRB approvals were in place for the collection of peripheral blood and saliva from nevirapine tolerant individuals for all sites contributing to the study and all patients provided written informed consent. Blood from nevirapine tolerant relatives of hypersensitive cases was collected when available.

Peripheral Blood Mononuclear Cell (PBMC) and Blister Fluid Preparation

Heparinized blood was drawn for the preservation of PBMCs from both retrospective and prospective patients with nevirapine-induced cutaneous hypersensitivities. PBMCs were isolated by Ficoll separation. When available, blister fluid was collected from intact, fluid-filled bullae by an 18-gauge needle attached to a syringe during acute SJS/TEN. The needle was inserted in the base of each bulla, fluid contents were aspirated and inserted into ethylenediaminetetraacetic acid (EDTA) tubes for processing. Similar to standard PBMC processing, blister fluid cells and supernatant are separated by centrifugation. Vials of blister fluid supernatant were frozen in 500μL

aliquots and cells were stored in standard freezing media (90% FBS, 10% DMSO). Cryopreserved PBMCs and blister fluid were shipped frozen from South Africa to Vanderbilt with dry ice.

Skin Collection and Processing

Four-millimeter punch biopsies were frozen intact in 80% FBS, 20% DMSO and shipped on dry ice from South Africa to Vanderbilt. Two biopsies were taken from each patient with acute SJS, one of skin affected by the disease and one of unaffected skin for comparison. Within one month of sample collection, the skin cells were processed, stained and sorted. For processing, the skin was first placed into a small bubble of media in a petri dish and chopped into fine pieces. The skin was then digested by gentle agitation with 1mg/mL of Collagenase P (Sigma) and 200 units/mL of DNAse I (Sigma) at 37°C for 90 minutes. To create a single cell suspension, the cells were passed through at 70-micron strainer, incubated with ACK lysing buffer (Thermo Fisher Scientific) to lyse the red blood cells, centrifuged, resuspended and washed with PBS. The cells were then immediately stained for flow cytometry and cell sorting.

DNA Extraction

High quality DNA was extracted from saliva collected in DNA Oragene kits using the prepIT protocol (DNA Genotek), or buffy coat or PBMCs using a QIAprep Miniprep kit (Qiagen).

Human Leukocyte Antigen (HLA) Typing

High resolution four-digit HLA A B C DP DR DQ typing was performed using sequence-based typing on the Illumina Miseq as previously described by our collaborators at the Institute for Immunology and Infectious Diseases (IIID)[75,146]. The HLA typing process at IIID in Perth,

Western Australia is accredited by the American Society for Histocompatibility and Immunogenetics (ASHI) and the National Association of Testing Authorities (NATA). Briefly, specific HLA Loci were polymerase chain reaction (PCR)-amplified using sample-specific multiplex identifier (MID)-tagged primers that amplify polymorphic exons from Class I (A, B, C Exons 2 and 3) and Class II (DQ, Exons 2 and 3; DRB and DPB1, Exon 1) HLA genes. MID tagged primers have been optimized to minimize allele dropouts and primer bias. Amplified DNA products from unique MID tagged products (up to 48 MIDs) were pooled in equimolar ratios and subjected to library preparation using Kapa Hyper prep kit (Kapa Biosystems). Libraries were quantified using the KAPA library quantitation kit (Kapa Biosystems) and High sensitivity D1000 ScreenTape on an Agilent 2200 TapeStation (Agilent) for concentration and size distribution. Normalized libraries were then sequenced on the Illumina MiSeq platform using the MiSeq V3 600-cycle kit (2X300bp reads). Sequences were separated by MID tags and the alleles were called using an in-house accredited HLA allele caller software pipeline that minimizes the influence of sequencing errors. Alleles were called using the latest IMGT HLA allele database as the allele reference library. Sample to report integrity was tracked and checked using proprietary and accredited Laboratory Information and Management System (LIMS) and HLA analyze reporting software that performs comprehensive allele balance and contamination checks on the final dataset.

Cytochrome P450 2B6 (CYP2B6) Genotyping

Three CYP2B6 single nucleotide polymorphisms (SNPs) known to be important for metabolism through CYP2B6 (516G→T (rs3745274), 983T→C (rs28399499), 15582C→T (rs4803419)) were genotyped using TaqMan SNP genotyping assays (Applied Biosystems, Foster City, CA) at the

Vanderbilt Technologies for Advanced Genomics (VANTAGE) core facility[87,147]. Carriage of the minor alleles for rs3745274 (516(T)) and rs28399499 (983(C)) has been shown to increase nevirapine plasma levels[133,134]. To a lesser effect than the other two SNPs, carriage of the minor allele for rs4803419 15582(T) has shown to increase plasma concentrations of efavirenz, another non-nucleoside reverse transcriptase inhibitor metabolized through CYP2B6, particularly in individuals who are homozygous for the rs3745274 (516GG) and rs28399499 (983TT) major alleles[147].

Endoplasmic Reticulum Aminopeptidase (ERAP) Genotyping

High resolution *ERAP1* and *ERAP2* genotyping was performed using sequence-based typing on the Illumina Miseq by our collaborators at IIID. PCR primers were utilized to amplify amplicons which contain 15 SNPs for *ERAP1* and 2 SNPs for *ERAP2*. The following SNPs were included: rs3734016, rs73148308, rs26653, rs27895, rs2287987, rs27434, rs73144471, rs27529, rs78649652, rs30187, rs10050860, rs111363347, rs17482078, rs27044, rs375081137, rs2248374 and rs2549782. A minimum sample quantity of 30 μL of good quality DNA (260/280 ratio of >1.7) at a concentration of 30 ng/uL was aliquoted for *ERAP* genotyping. DNA from C1R or K562 cell lines (ATCC) with known *ERAP* typing results were used as positive controls. Sterile water was used as a negative control. Sequencing of the amplicons was followed by identification of the specific SNP variants using IIID's Visual Genome Analysis Studio (VGAS), which was designed for high performance next generation sequencing analysis[148]. African Americans with available genotyping in Vanderbilt's BioVU repository, a deidentified electronic health record (EHR) database linked to a DNA biobank, were used as a source of population data. ERAP population

genotyping was imputed from SNP data using the Expanded Multi-Ethnic Genotyping Array (MEGAEX, Illumina).

Killer Immunoglobulin-like Receptor (KIR) Genotyping

KIR genotyping was performed at IIID using a similar assay to those previously described[149,150]. Real-Time qPCR using an SYBR™ Green master mix was used to detect the presence/absence and haplotyping of KIR genes. 15 KIR genes were amplified using primers designed specific to each gene. The melt curves generated after the real-time PCR reaction gave a gene specific melting temperature that allowed detection of presence or absence of KIR genes. The assay is setup to detect the following KIR genes: 2DL1, 2DL2, 2DL3, 2DL4, 2DL5, 2DP1, 2DS1, 2DS2, 2DS3, 2DS4, 2DS5, 3DL1, 3DL2, 3DL3 and 3DS1. A minimum sample quantity of 30 µL of good quality DNA (260/280 ratio of >1.7) at a concentration of 30 ng/uL was aliquoted for *ERAP* genotyping. The highly conserved housekeeping gene galactosylceramidase (GALC) was used as a positive internal control. GALC has a different melting temperature which allows easy discrimination between the KIR and GALC peak. PCR master mix without sample was used as a negative control to ensure reagents and equipment were free of contamination.

Statistical Analyses of Genotyping Data

Associations of individual factors with cases/controls were assessed via Fisher exact tests. Multivariable joint associations were assessed using case/control logistic regressions and based on likelihood ratio tests for models and sub-models. Analyses were carried out in R version 3.4.3. (R Core Team (2017). R: A language and environment for statistical computing. R Foundation for Statistical Computing, Vienna, Austria. URL https://www.R-project.org/).

Immunohistochemistry of Skin Biopsy

Formalin-fixed, paraffin-embedded punch biopsies of affected skin collected during acute SJS/TEN were sectioned at 5 μm intervals. Slides were placed on the Leica Bond Max IHC stainer. All steps besides dehydration, clearing and coverslipping were performed on the Bond Max. Slides were deparaffinized. Heat induced antigen retrieval was performed on the Bond Max using their Epitope Retrieval 2 solution for 20 minutes. Slides were incubated with anti-CD3 (Cat# NCL-CD3-PS1, Leica, Newcastle, United Kingdom) for one hour at 1:100 dilution, Ready-To-Use anti-CD4 (PA0427, Leica, Buffalo Grove, IL) for one hour or Ready-To-Use anti-CD8 (MM39-10, McKinney, TX) for 15mins. For the anti-CLA stained sections, slides were placed in a Protein Block (Ref# x0909, DAKO, Carpinteria, CA) for 10 minutes and then incubated with anti-CLA (Cat.NB100-78039, Novus, Littleton, CO) for 1 hour at a 1:100 dilution followed by a biotinylated anti-rat (Cat. BA-5000, Vector Laboratories, Inc.) for 15 minutes at a 1:200 dilution. The Bond Polymer Refine detection system was used for visualization. Slides were the dehydrated, cleared and coverslipped. Sections of formalin-fixed, paraffin-embedded normal skin were stained as controls. The slides were scored by Alan Boyd, MD, a Vanderbilt dermatopathologist.

Granulysin Enzyme-linked Immunosorbent Assays (ELISAs)

Granulysin concentrations in blister fluid and plasma from patients with acute nevirapine SJS/TEN were measured with a granulysin-specific ELISA assay by our collaborators at Chang Gung Memorial Hospital in Taipei, Taiwan as previously described[35].

Flow Cytometry Staining

Cryopreserved blister fluid cells were thawed and washed with PBS. Blister fluid and skin cells were incubated with Live/DEAD Fixable Aqua (ThermoFisher) and then surface stained with antibodies at room temperature except for the CCR7 marker, which was stained separately at 37°C. Total blister fluid cells were stained with a targeted T-cell antibody panel including basic T-cell markers (CD3, CD4, CD8), activation markers (CD69, CD137), memory markers (CCR7, CD45RO), an NK cell marker (CD56), and a marker of skin homing (CLA). Skin cells were stained with a similar antibody panel except CD56 and CLA were replaced with skin markers (CD103 and CCR10).

Specific antibodies used for staining were CD3-A700 (UCHT1, BD Pharmingen), CD4-PerCPCy5.5 (RPA-T4, BD Pharmingen), CD8-APC-AF750 (Invitrogen), CD137-PE (BD Pharmingen), CD69-APC (FN50, BD Pharmingen), CD14-V500 (M5E2, BD Horizon), CD19-V500 (H1B19, BD Horizon), CD45RO-CF594 (Invitrogen, UCHL1), CLA-PE/Cy7 (HECA-452, Biolegend) (blister fluid only), CCR7-BB515 (3D12, BD Horizon) (blister fluid only), CD56-BV421 (HCD56, Biolegend) (blister fluid only), CD103-PE/Cy7 (Ber-ACT8, Biolegend) (skin only), CCR7-BV421 (BD Horizon) (skin only) and CCR10-BB515 (BD Horizon) (skin only).

Cell Sorting

All fluorescence-activated cell sorting (FACS) experiments were perform on an ARIA III flow cytometer (Becton Dickinson) at the Vanderbilt University Medical Center Flow Cytometry Shared Resource. All cells were sorted within one hour of staining completion and immediately placed into 4μL of a cDNA-conversion compatible lysis buffer containing a ribonuclease inhibitor

that blocks RNA degradation and stabilizes the RNA. Plates containing the sorted single cells were kept on dry ice during collection and then temporarily stored at -80°C until processing. The gating strategies for single-cell sorting of blister fluid and skin cells are shown in Figures 2.4 and 2.5, respectively. PBMCs from healthy donors were used as biological controls for gating. Data were analyzed using FACSDiva (BD Biosciences) and FlowJo software (Tree Star).

Single-cell TCR and Single-cell RNA Sequencing

The single-cell TCR and single-cell RNA sequencing was done with the help of our scientific partners at IIID in Perth, Western Australia. Using our novel TCR/RNA sequencing platform, the single blister fluid and skin cells underwent oligo (dT)-primed reverse transcription during which the cDNA products of individual wells are barcoded and generically tagged with both 3' oligo (dT) and 5' biotin labelled template switching oligonucleotides (TSO). Subsequent amplification of the cDNA derived from a single cell was amplified using the generic tags. Specific transcripts were targeted with a combination of nested generic tags and gene specific primers including TCRα and TCRβ conserved regions. The transcriptome was analyzed using a modified Nextera transposon-mediated tagging-and-fragmentation ("tagmentation") assay with subsequent amplification of the 5' and 3' ends of the transcripts between the introduced Nextera-tag and the generic tags from cDNA conversion. Samples were multiplexed for next generation library preparation and sequencing. Single cell sequences were bioinformatically separated.

Single-cell TCR Sequencing Analyses

The TCR sequencing data were analyzed using IIID's Visual Genome Analysis Studio (VGAS), which was designed for high performance next generation sequencing analysis[148].

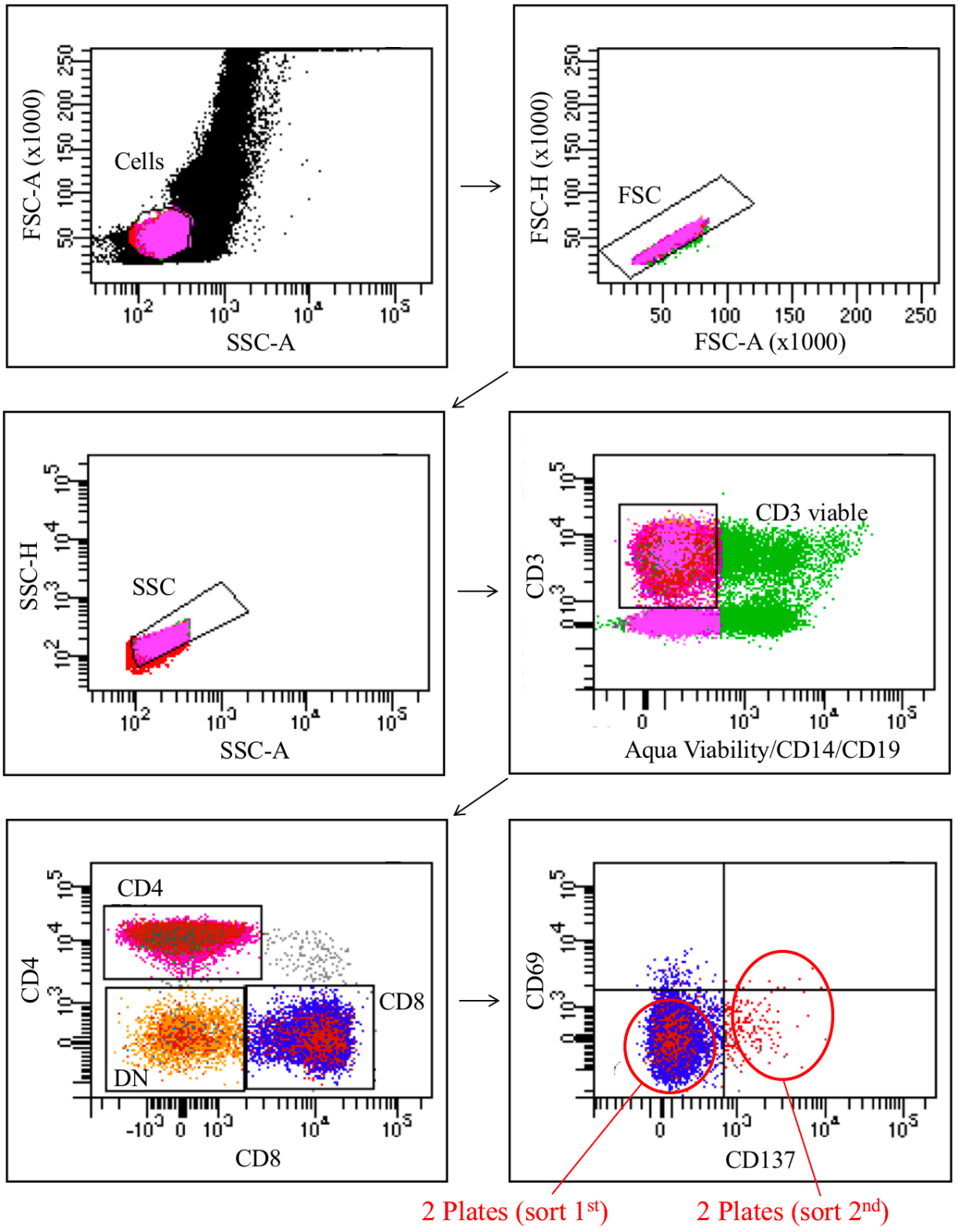

Figure 2.4. Gating strategy for single-cell blister fluid sort. Gating shown on peripheral blood mononuclear cells from a healthy donor. **Legend:** FSC, forward scatter; SSC, side scatter; H, height; A, area; DN, double negative.

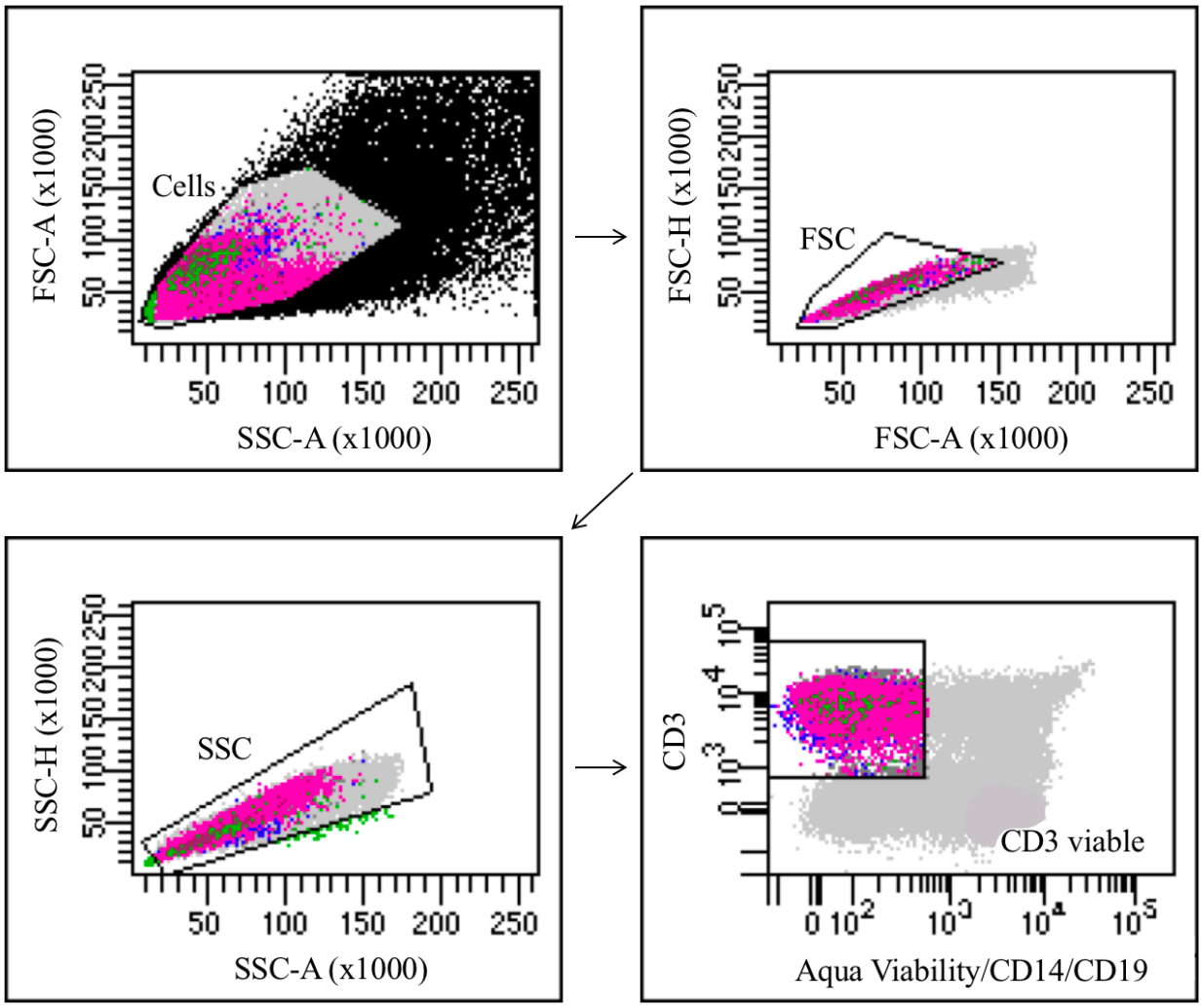

Figure 2.5. Gating strategy for single-cell sort on skin punch biopsies from patients with acute nevirapine SJS/TEN. Gating shown on peripheral blood mononuclear cells from a healthy donor. Due to limited cell numbers in the skin, all CD3+ T cells are sorted instead of T-cell subsets. However, all cells are index sorted so phenotypic data are preserved. **Legend:** FSC, forward scatter; SSC, side scatter; H, height; A, area; DN, double negative.

Single-cell RNA Sequencing Analyses

The single-cell RNA sequencing was performed at the VANTAGE genetics core at Vanderbilt and analyzed with the help of the Vanderbilt University Medical Center, Center for Translational Immunology and Infectious Diseases and our scientific partner IIID using their automated pipeline for working with single-cell RNA sequencing data. First, deconvolved reads in FASTQ format were trimmed to eliminate a) poor quality bases near the ends of reads, and poor-quality reads, and b) Illumina adapters from all Illumina kits. The retained reads were then aligned to the human transcriptome (hg38) using Bowtie2, and quantified using the RSEM software package[151,152]. Count matrixes from Bowtie2/RSEM were automatically fed into the SCONE software package for quality control, evaluation and selection of the most appropriate normalization method, and identification of highly variant genes and other co-variates[153]. The processed count matrices from SCONE were then delivered into FastProject for multidimensional analysis, identification of statistically significant gene signatures that underlie the structure of the data, and differential expression[154]. Both the raw and processed count matrices were also fed into the Seurat software package, which utilizes a different statistical distribution to model variation and abundance of reads in single-cell RNA sequencing data[155]. In a separate environment, the TRAPeS program was used in conjunction with TopHat2 to align, reconstruct, validate, and assemble TCRs that were present in single-cell RNA sequencing data[156,157]. Normalized data were then analyzed in VGAS.

RESULTS

Clinical and Demographic Characteristics of South Africans with Nevirapine Hypersensitivity

Thirty-one HIV+ patients with potential nevirapine hypersensitivity reactions were identified. I reviewed the medical records of each patient to ensure all patients met study criteria and

documented clinical details of hypersensitivity syndromes including pictures of cutaneous symptoms when available (Figure 2.6). After review of the medical records, four patients were excluded because they did not meet study criteria. One patient had drug-induced liver injury with no cutaneous symptoms and two had non-blistering rashes with no associated systemic symptoms. One patient had tolerated nevirapine for 11 weeks and a drug causality assessment showed that his adverse drug reaction was more likely due to fluconazole which was prescribed only two weeks prior to his reaction. Additionally, one potential case of SJS/TEN was excluded because the patient's medical records could not be found. Therefore, in total, 20 cases of nevirapine SJS/TEN and 6 cases of nevirapine DRESS were identified that met study criteria (Tables 2.1, 2.2 and 2.3).

The nevirapine SJS/TEN cases included 12 retrospective cases diagnosed from 2004 to 2016 and 8 prospective cases enrolled during hospitalization for acute SJS/TEN diagnosed from 2017 to 2018. All patients identified with nevirapine SJS/TEN were enrolled at Groote Schuur Hospital. Although there was some mixed ancestry, the cohort was predominantly of African ancestry and included 17 women and 3 men who developed nevirapine SJS/TEN from 11 to 44 years of age. All patients had Naranjo adverse drug reaction scores of 8 (probable adverse drug reaction) and ALDEN scores of 4 to 6 (nevirapine was "probably" or "very probably" the cause of the reaction). While the patients were on a variety of therapies, the only shared medication among all patients with SJS/TEN was nevirapine. The median latency between drug initiation and development of first SJS/TEN symptoms was 18 days. Patients developed SJS/TEN with a wide range of CD4+ T cell counts from 40 to 988 cells/μL with a median of 258 cells/μL (Tables 2.1 and 2.2).

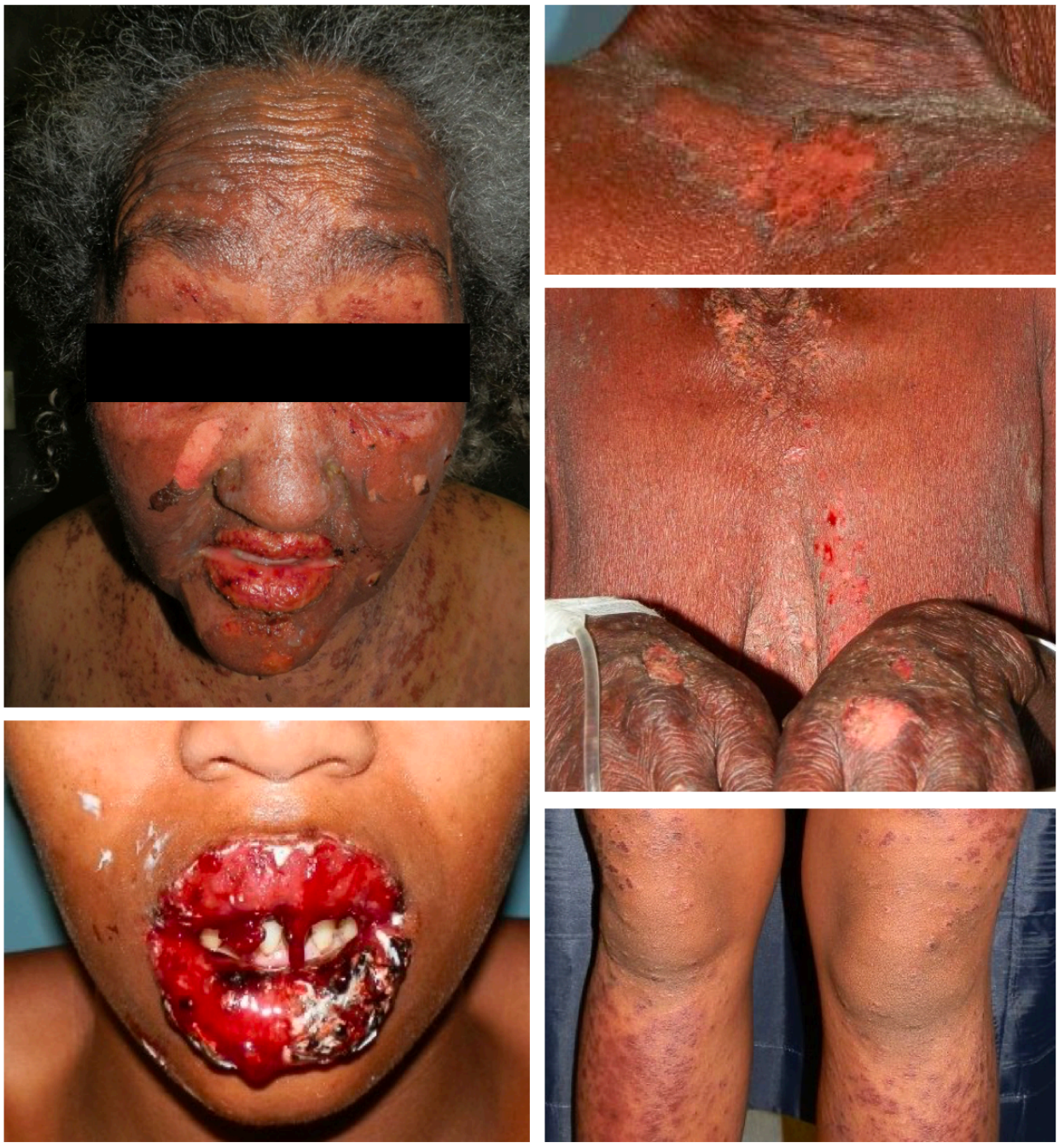

Figure 2.6. Representative photographs of patients with nevirapine-induced SJS/TEN. Photographs demonstrate skin sloughing, skin necrosis and mucosal ulcerations.

	SJS/TEN (n=20)	Nevirapine tolerant (n=46)	p-value
Sex	17 Females 3 Males	21 Females 25 Males	0.0032
Race	18 African 2 Mixed	38 African 6 Mixed 2 White	>0.99
Age (y/o) at nevirapine exposure	11 – 44 (30.5) n = 20	18 – 57 (33) n = 46	0.091
Date of HIV diagnosis	2001 – 2016 (2009) n = 8	1998 – 2016 (2008/9) n = 24	0.83
Date of exposure	2004 – 2018 (2011/2) n = 20	2003 – 2018 (2014/5) n = 46	0.42
Latency period	2 – 44 days (18) n = 19	N/A	
CD4 T cell count at nevirapine exposure	40 – 988 (258) n = 20	4 – 484 (103) n = 29	0.0001

Table 2.1. Aggregated overview of demographics and pertinent medical history of nevirapine SJS/TEN cases and tolerant controls. Sex and race are reported with the number of patients self-identifying in each category. Data for age at nevirapine exposure, date of HIV diagnosis, date of nevirapine exposure, latency period and CD4 T cell count at nevirapine exposure are represented with the range and median (in parenthesis) followed by the number of patients for whom the data were available. CD4 T cell count is reported in cells/μL. **Legend:** SJS/TEN, Stevens-Johnson syndrome/toxic epidermal necrolysis; y/o, years old; HIV, human immunodeficiency virus.

ID	Age	Sex	Race	CD4 Count	Latency (Days)	ALDEN	Naranjo	Concurrent Medications
1	36	F	African	40	16	6	8	lamivudine, stavudine, trimethoprim/sulfamethoxazole
2	29	F	African	622	22	6	8	lamivudine, stavudine
3	35	F	African	98	N/A	N/A	8	N/A
4	32	F	African	234	28	6	8	lamivudine, zidovudine
5	27	F	African	234	18	6	8	lamivudine, tenofovir
6	11	F	African	597	11	6	8	lamivudine, abacavir, imipramine, trimethoprim/sulfamethoxazole
7	35	F	African	427	14	6	8	lamivudine, tenofovir
8	23	F	African	224	17	6	8	lamivudine, tenofovir
9	29	F	African	280	7	6	8	lamivudine, tenofovir
10	17	F	African	211	16	6	8	lamivudine, tenofovir
11	37	F	African	360	15	6	8	lamivudine, tenofovir
12	15	M	African	988	39	5	8	lamivudine, abacavir
13	27	F	Mixed	385	23	6	8	lamivudine, tenofovir, olanzapine, lorazepam, valproate
14	37	M	African	290	2	4	8	lamivudine, abacavir, bedaquiline, terizidone, pyrazinamide, ethambutol, isoniazid, levofloxacin, trimethoprim/sulfamethoxazole
15	44	F	African	505	18	6	8	lamivudine, zidovudine
16	36	M	African	496	28	6	8	emtricitabine, tenofovir
17	33	F	African	221	22	6	8	emtricitabine, tenofovir, ethambutol, isoniazid, pyrazinamide, rifampin
18	26	F	Mixed	236	3	4	8	emtricitabine, tenofovir
19	28	F	African	136	44	5	8	emtricitabine, tenofovir
20	44	F	African	196	18	6	8	emtricitabine, tenofovir

Table 2.2. Nevirapine SJS/TEN case basic demographics, clinical characteristics and concurrent medications. Legend: ID, patient identification; Age, age at time of nevirapine treatment; CD4 Count, CD4 T cell count in cells/μL at time of nevirapine exposure; Latency, days between nevirapine initiation and symptoms development; F, female; M, male; N/A, medical records not available; SJS/TEN, Stevens-Johnson syndrome/toxic epidermal necrolysis.

ID	Age	Sex	Race	CD4 Count	Latency (Days)	Naranjo	Concurrent Medications	Other Medical History
22	32	M	African	411	25	8	zidovudine, atazanavir, ritonavir, levetiracetam	psychosis and epilepsy
23	41	F	African	546	30	8	emtricitabine, tenofovir, olanzapine	delirium, HIV neuropathy and encephalopathy
24	43	F	Mixed	342	36	8	emtricitabine, tenofovir, lithium, risperidone	psychosis
25	30	F	African	287	28	8	emtricitabine, tenofovir, trimethoprim/sulfamethoxazole	none documented
26	48	F	African	495	29	8	emtricitabine, tenofovir, risperidone, citalopram	MDD with psychosis
27	49	F	African	265	24	8	emtricitabine, tenofovir	psychosis

Table 2.3. Summary of nevirapine DRESS case basic demographics, medical history and concurrent medications. Legend: ID, patient identification; Age, age at time of nevirapine treatment; CD4 Count, CD4 T cell count in cells/μL at time of nevirapine exposure; Latency, days between nevirapine initiation and symptoms development; F, female; M, male; HIV, human immunodeficiency virus; MDD, major depressive disorder.

The cases of nevirapine DRESS included 3 retrospective cases diagnosed from 2010 to 2016 (1 from Tygerberg Hospital and 2 from Groote Schuur Hospital) and 3 prospective cases enrolled during hospitalization for the acute reaction diagnosed from 2016 to 2017 (all from Groote Schuur Hospital). The patients with nevirapine DRESS were predominantly of African ancestry with one patient of mixed ancestry and included 1 man and 5 women who developed nevirapine DRESS from 30 to 49 years of age with a median of 42 years. All patients had Naranjo adverse drug reaction scores of 8 (probable adverse drug reaction). While the patients were on a variety of therapies for HIV and other co-morbidities, the only shared medication among all patients with DRESS was nevirapine. The median latency between drug initiation and development of first DRESS symptoms was 28.5 days with a range of 24 to 36 days. Compared to the patients with nevirapine SJS, those with DRESS had higher CD4+ T cell counts ranging from 265 to 546 cells/μL with a median of 377 cells/μL. Notably, 5/6 patients identified with nevirapine DRESS also carried a previous history of neuropsychiatric co-morbidities. In one of the five patients, and the only one with normal CYP2B6 nevirapine metabolism (see CYP2B6 genotyping results below), an episode of psychosis prompted the change from antiretroviral therapy containing efavirenz to a nevirapine-based regimen one month prior to DRESS development. None of the others were exposed to efavirenz before developing DRESS on nevirapine.

Demographics of Unrelated Nevirapine Tolerant Controls

Fifty-one HIV+ individuals were identified as potential nevirapine tolerant controls. Of those, 2 patients were excluded because there was an inadequate amount of DNA extracted for the proposed genotyping studies and 3 were excluded because the patients' medical records could not be found to verify tolerance. In total, 46 patients were enrolled as controls (Table 2.4).

ID	Age	Sex	Race	CD4 Count	Concurrent ART
C1	28	F	African	N/A	lamivudine, zidovudine
C2	48	M	White	20	stavudine, lamivudine
C3	36	F	Mixed	11	stavudine, lamivudine
C4	55	F	African	N/A	emtricitabine, tenofovir
C5	29	M	African	7	lamivudine, zidovudine
C6	36	M	African	N/A	stavudine, lamivudine
C7	57	M	White	293	lamivudine, tenofovir
C8	30	F	African	N/A	stavudine, lamivudine
C9	27	F	African	192	emtricitabine, tenofovir
C10	28	F	African	N/A	stavudine, lamivudine
C11	36	F	Mixed	N/A	stavudine, lamivudine
C12	33	F	African	N/A	emtricitabine, tenofovir
C13	66	M	African	N/A	emtricitabine, tenofovir
C14	20	F	African	N/A	stavudine, lamivudine
C15	32	M	African	N/A	lamivudine, tenofovir
C16	30	M	African	115	abacavir, lamivudine
C17	41	M	Mixed	52	stavudine, lamivudine
C18	57	F	African	4	emtricitabine, tenofovir
C19	18	M	African	N/A	stavudine, lamivudine
C20	39	M	African	484	abacavir, lamivudine
C21	40	M	African	9	emtricitabine, tenofovir
C22	24	M	African	34	emtricitabine, tenofovir
C23	45	M	African	152	abacavir, lamivudine
C24	43	M	African	133	abacavir, lamivudine
C25	33	M	African	44	emtricitabine, tenofovir
C26	27	M	African	38	emtricitabine, tenofovir
C27	40	M	African	163	emtricitabine, tenofovir
C28	24	F	African	N/A	lamivudine, tenofovir
C29	47	F	African	N/A	stavudine, lamivudine
C30	31	M	African	26	abacavir, lamivudine
C31	38	M	African	49	emtricitabine, tenofovir
C32	30	M	African	45	abacavir, lamivudine
C33	38	M	Mixed	70	emtricitabine, tenofovir
C34	36	M	African	108	abacavir, lamivudine
C35	33	M	Mixed	16	emtricitabine, tenofovir
C36	33	M	Mixed	238	abacavir, lamivudine
C37	28	F	African	469	emtricitabine, tenofovir
C38	52	F	African	372	zidovudine, lamivudine
C39	20	F	African	152	emtricitabine, tenofovir
C40	28	F	African	170	emtricitabine, tenofovir
C41	38	F	African	N/A	zidovudine, lamivudine
C42	25	F	African	N/A	zidovudine, lamivudine
C43	33	M	African	272	emtricitabine, tenofovir
C44	28	F	African	N/A	emtricitabine, tenofovir
C45	34	F	African	N/A	emtricitabine, tenofovir
C46	41	F	African	103	emtricitabine, tenofovir

Table 2.4. Nevirapine tolerant controls basic demographics, clinical characteristics and concurrent medications. Legend: ID, patient identification; Age, age at time of nevirapine treatment; CD4 Count, CD4 T cell count in cells/μL at time of nevirapine exposure; F, female; M, male; N/A, medical records not available.

Similar to the nevirapine hypersensitivity cases, these patients were predominantly of African ancestry. The nevirapine tolerant patients included 21 women and 25 men who were between 18 and 57 years of age at the time of initial nevirapine exposure. CD4+ T cell counts were not available for all nevirapine tolerant individuals at the time of nevirapine exposure, but for the 29 controls who did have that data available, their CD4+ T cell counts ranged from 4 to 484 cells/μL with a median of 103 cells/μL (Tables 2.1 and 2.4). The only shared antiretroviral drug among all controls was nevirapine (Table 2.4).

HLA Typing Results

The HLA-C*04:01 allele was carried by 100% (20/20) of the nevirapine SJS/TEN cases compared with 21.7% (10/46) of the nevirapine tolerant controls ($p=7.4x10^{-10}$) (Figure 2.7 and Tables 2.5 and 2.6). HLA-C*04:01 carriage in tolerant controls was similar to the expected prevalence for South African populations (Figure 2.7)[158]. HLA-C*04:01 was the only HLA allele shared by all individuals with nevirapine SJS/TEN. When each HLA allele was analyzed individually, HLA-B*53:01 was also associated with nevirapine SJS/TEN development (p=0.02) as 30% (6/20) of the cases carry HLA-B*53:01 compared to 6.7% (3/45) of the tolerant controls. However, HLA-B*53:01 is known to be haplotypic with HLA-C*04:01 since the two alleles are in strong linkage disequilibrium. No other HLA class I alleles were associated with increased risk of SJS/TEN. The six patients diagnosed with nevirapine DRESS did not share carriage of any known risk alleles for nevirapine hypersensitivity. However, 5/6 of the nevirapine DRESS patients carried either HLA-B*45:01 or HLA-B*44:03, compared to 9/46 of the nevirapine tolerant controls (p=0.004) (Tables 2.6 and 2.7). These two closely-related HLA-B alleles share peptide binding specificities.

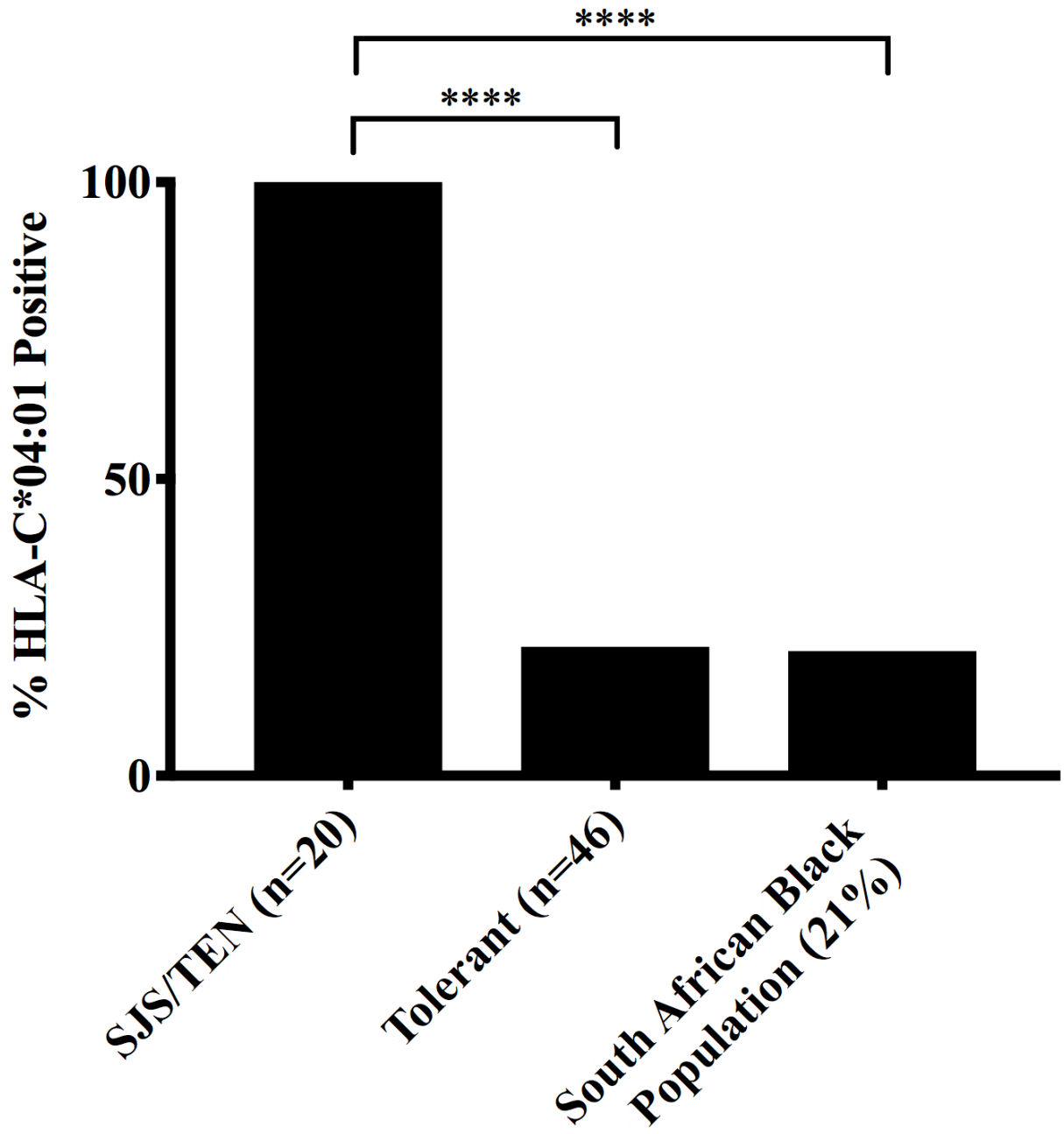

Figure 2.7. HLA-C*04:01 is strongly associated with nevirapine SJS/TEN. 20/20 (100%) of the nevirapine SJS/TEN cases carried HLA-C*04:01 compared with 10/46 (21.7%) of the nevirapine tolerant controls ($p=7.4x10^{-10}$, conditional logistic). HLA-C*04:01 carriage in the nevirapine tolerant cohort was representative of the South African Black Population[154]. **Legend:** HLA, human leukocyte antigen; SJS/TEN, Stevens-Johnson syndrome/toxic epidermal necrolysis.

ID	HLA-A Allele 1/2	HLA-B Allele 1/2	HLA-C Allele 1/2	HLA-DPB1 Allele 1/2	HLA-DQA1 Allele 1/2	HLA-DQB1 Allele 1/2	HLA-DRB1 Allele 1/2
1	29:02/68:02	15:03/53:01	**04:01**/06:02	02:01/04:02	01:01/01:02	05:01/06:09	12:01/13:02
2	34:02/68:02	15:10/44:03	03:04/**04:01**	01:01/04:02	01:03/05:01	02:01/06:03	03:01/13:01
3	30:01/33:03	42:01/53:01	**04:01**/17:01	01:01/01:01	01:02/04:01	03:01/06:09	08:04/13:02
4	36:01/74:01	49:01/53:01	**04:01**/07:01	02:01/18:01	01:01/04:01	04:02/05:01	01:02/08:08
5	23:01/34:02	44:03/45:01	**04:01**/06:02	01:01/01:01	01:01/05:01	02:01/05:01	01:02/03:01
6	68:02/74:01	15:10/35:01	03:04/**04:01**	01:01/02:01	01:01/05:01	02:01/05:01	01:02/03:01
7	03:01/74:01	35:01/58:02	**04:01**/06:02	02:01/04:02	03:01/04:01	03:02/04:02	03:02/04:05
8	01:01/30:01	15:03/42:01	**04:01**/17:01	01:01/04:02	01:01/05:01	02:01/05:01	03:01/10:01
9	30:04/68:02	15:03/44:03	03:04/**04:01**	01:01/01:01	01:01/05:01	03:01/05:01	03:01/12:01
10	68:02/80:01	18:01/53:01	02:02/**04:01**	02:01/04:02	01:01/02:01	02:02/05:01	07:01/12:01
11	74:01/74:01	15:10/35:01	03:04/**04:01**	01:01/02:01	01:01/01:02	05:01/06:02	01:02/15:03
12	01:01/34:02	44:03/47:01	**04:01**/06:02	04:02/13:01	01:03/05:01	03:01/06:03	11:01/13:01
13	34:01/43:01	15:10/57:01	**04:01**/06:02	NT	02:01/13:01	02:01/03:01	03:02/03:03
14	34:02/66:02	42:01/44:03	**04:01**/17:01	02:01/04:02	01:03/04:01	04:02/06:03	03:02/13:01
15	30:01/36:01	42:02/53:01	**04:01**/17:01	01:01/13:01	01:01/01:01	05:01/05:01	10:01/12:01
16	29:02/33:03	07:235/53:01	**04:01**/07:02	02:01/17:01	03:01/03:01	02:02/02:02	09:01/09:01
17	29:01/29:02	15:03/44:03	**04:01**/07:01	02:01/13:01	01:02/01:02	06:02/06:09	11:01/13:02
18	03:01/24:07	13:03/35:05	**04:01**/06:02	05:01/28:01	02:01/06:01	02:02/03:01	07:01/12:02
19	30:01/66:01	58:02/81:01	**04:01**/06:02	19:01/34:01	01:02/01:03	06:02/06:02	13:01/15:03
20	02:05/68:02	15:10/15:10	03:04/**04:01**	01:01/02:01	01:01/05:01	02:01/05:01	03:01/10:01

Table 2.5. Full HLA typing results of nevirapine SJS/TEN cases. Legend: ID, patient identification; HLA, human leukocyte antigen; NT, not typed.

ID	HLA-A Allele 1/2	HLA-B Allele 1/2	HLA-C Allele 1/2	HLA-DPB1 Allele 1/2	HLA-DQA1 Allele 1/2	HLA-DQB1 Allele 1/2	HLA-DRB1 Allele 1/2
C1	02:05/30:01	14:01/15:03	02:10/08:04	04:01/04:02	01:02/04:01	03:01/06:02	08:04/15:01
C2	11:01/68:02	15:02/53:01	04:01/08:01	03:01/04:02	01:02/01:02	06:01/06:04	13:02/15:01
C3	02:01/30:02	44:02/44:02	05:01/05:01	03:01/04:01	02:01/02:01	02:02/03:03	07:01/07:01
C4	03:01/68:02	15:03/58:02	02:10/06:02	04:01/13:01	01:03/02:01	02:02/06:04	07:01/13:01
C5	02:01/02:01	44:03/45:01	07:01/16:01	01:01/18:01	01:02/01:03	06:03/06:09	13:01/13:02
C6	30:01/43:01	15:10/58:02	03:04/06:02	01:01/55:01	01:01/05:01	02:01/06:02	03:01/14:01
C7	NT	13:02/52:01	06:02/12:02	01:02/NT	02:01/03:01	01:03/05:01	03:01/06:01
C8	29:02/30:02	44:03/45:01	07:01/16:01	18:01/18:01	01:01/05:01	03:01/05:01	01:02/11:01
C9	02:01/36:01	35:01/53:01	04:01/04:01	01:01/NT	02:01/04:02	01:02/05:01	02:01/06:02
C10	23:01/30:01	42:02/45:01	06:02/17:01	01:01/01:01	01:01/01:01	05:01/05:01	01:02/12:01
C11	26:01/29:02	38:01/45:01	06:02/12:03	NT	02:01/03:01	01:03/05:01	03:01/06:03
C12	30:01/34:02	42:01/44:03	04:01/17:01	NT	01:01/01:01	NT	04:02/06:03
C13	02:02/30:01	42:02/57:03	07:01/17:01	NT	03:01/04:02	01:01/01:03	05:01/06:03
C14	02:05/30:04	15:16/58:02	06:02/14:02	01:01/04:02	01:02/03:01	03:02/06:02	04:01/15:03
C15	02:01/03:01	15:10/49:01	04:01/07:01	NT	02:01/03:01	01:01/05:01	02:01/05:01
C16	68:01/74:01	15:10/35:01	04:01/04:01	NT	02:01/04:02	03:01/03:01	03:02/03:02
C17	02:01/74:01	15:13/58:02	06:02/08:01	01:01/13:01	03:01/06:01	02:02/03:01	07:01/12:02
C18	26:01/34:02	41:01/57:02	17:01/18:01	NT	01:01/01:01	01:02/05:01	03:01/06:09
C19	01:01/02:01	49:01/57:02	07:01/07:01	NT	13:01/18:01	01:01/05:02	03:03/05:03
C20	24:02/30:04	08:01/82:02	03:02/07:02	01:01/55:01	01:02/01:03	06:02/06:03	13:01/15:03
C21	29:01/68:02	15:03/18:01	02:10/07:04	04:01/13:01	01:02/02:01	02:02/06:02	07:01/15:03
C22	30:02/33:01	14:02/58:01	07:01/08:02	02:01/13:01	01:02/05:01	03:01/06:02	11:02/15:03
C23	02:01/23:01	15:10/51:01	03:02/16:01	01:01/29:01	02:01/05:01	02:01/02:02	03:01/07:01
C24	29:02/29:02	15:03/15:10	02:10/03:04	01:01/02:01	01:02/01:03	06:02/06:09	13:01/13:02
C25	43:01/68:02	15:03/58:02	02:10/06:02	13:01/13:01	01:03/02:01	02:02/06:02	07:01/13:01
C26	30:02/66:01	15:03/58:02	02:10/06:02	03:01/04:02	01:01/01:03	05:01/06:04	12:01/13:01
C27	02:01/30:01	35:01/58:02	03:04/06:02	02:01/11:01	01:02/01:02	06:02/06:02	15:03/15:03
C28	43:01/66:01	58:02/58:02	06:02/06:02	04:02/55:01	01:01/03:01	02:02/06:02	07:01/14:01
C29	30:02/68:02	08:01/53:01	04:01/07:01	01:01/01:01	01:02/02:01	02:02/06:04	07:01/13:02
C30	34:02/68:01	44:03/58:01	04:01/06:02	04:02/11:01	01:02/01:03	06:02/06:03	13:01/15:03
C31	24:02/29:11	07:02/13:02	06:02/07:02	01:01/04:02	01:02/01:03	06:02/06:03	13:01/15:03
C32	33:03/68:01	07:02/58:02	06:02/07:02	03:01/04:02	03:01/03:01	02:02/02:02	07:01/09:01
C33	03:01/24:02	52:01/56:01	04:01/12:02	04:02/04:02	01:01/05:01	03:01/05:03	11:01/14:04
C34	26:01/29:02	44:03/51:01	07:01/07:01	01:01/01:01	01:02/01:02	06:02/06:09	11:01/13:02
C35	11:01/43:01	15:32/27:05	02:02/12:03	04:02/93:01	01:02/03:01	03:02/05:02	04:01/12:02
C36	11:01/24:02	35:03/52:01	04:01/12:02	04:01/13:01	03:01/05:01	03:01/03:02	04:03/11:01
C37	03:01/30:04	08:01/82:02	03:02/07:02	01:01/04:02	01:02/04:01	04:02/06:02	03:02/15:03
C38	23:01/68:02	07:02/45:01	06:02/07:02	04:02/11:01	01:02/04:01	04:02/06:02	03:02/15:03
C39	03:01/43:01	15:03/81:01	04:01/18:01	04:01/04:02	01:01/05:01	03:01/06:02	03:01/14:01
C40	23:01/29:11	07:02/07:05	07:02/15:25	01:01/04:02	05:01/05:01	02:01/02:02	03:01/03:01
C41	68:02/68:02	14:02/57:02	08:02/18:01	01:01/34:01	01:02/01:02	06:02/06:09	13:02/15:03
C42	30:01/68:02	08:01/58:01	03:02/07:02	03:01/05:01	01:02/04:01	04:02/06:09	03:02/13:02
C43	30:01/30:01	42:01/58:02	06:02/17:01	04:02/04:02	01:03/04:01	04:02/06:03	03:02/13:01
C44	02:14/68:02	15:10/58:02	03:04/06:02	01:01/01:01	01:03/05:01	02:01/06:02	03:01/13:01
C45	02:01/80:01	18:01/45:01	02:02/16:01	01:01/03:01	02:01/03:01	02:02/02:02	07:01/09:01
C46	30:01/68:02	15:03/15:10	02:10/03:04	01:01/04:02	04:01/05:01	02:01/03:01	03:01/08:04

Table 2.6. Full HLA typing results of nevirapine tolerant controls. Legend: ID, patient identification; HLA, human leukocyte antigen; NT, not typed.

ID	HLA-A Allele 1/2	HLA-B Allele 1/2	HLA-C Allele 1/2	HLA-DPB1 Allele 1/2	HLA-DQA1 Allele 1/2	HLA-DQB1 Allele 1/2	HLA-DRB1 Allele 1/2
22	33:01/34:02	42:01/44:03	04:01/17:01	02:01/04:02	01:03/05:01	02:01/06:03	03:01/13:01
23	02:01/68:01	45:01/58:02	06:02/16:01	01:01/04:02	01:03/03:01	02:02/06:03	07:01/13:01
24	68:02/74:01	14:01/15:03	02:10/08:02	02:01/02:01	01:02/03:01	02:02/06:09	07:01/13:02
25	23:01/68:02	15:10/45:01	03:04/06:02	01:01/02:01	01:01/01:02	05:01/06:02	01:02/11:01
26	66:02/68:02	15:10/44:03	03:04/07:01	01:01/04:01	01:02/05:01	02:01/06:02	03:01/11:01
27	32:01/34:02	07:02/44:03	02:10/07:01	01:01/04:02	01:02/03:01	03:02/06:09	04:01/13:02

Table 2.7. Full HLA typing results of nevirapine DRESS cases. Legend: ID, patient identification; HLA, human leukocyte antigen.

CYP2B6 Genotyping Results

CYP2B6 genotyping revealed that patients with nevirapine hypersensitivities had slower nevirapine metabolizing phenotypes than nevirapine tolerant individuals. Of the three CYP2B6 SNPs genotyped (rs3745274 (516G→T), rs28399499 (983T→C), and rs4803419 (15582C→T)), both rs28399499 and rs4803419 were significantly associated with SJS/TEN development (Table 2.8). None of the SJS/TEN cases carried the minor rs4803419 (T) allele (p=0.048), while carriage of the rs28399499 minor allele (C) was associated with risk (p=0.014). In contrast, carriage of the minor rs3745274 (T) allele was associated with risk of nevirapine DRESS (p=0.005) (Table 2.9).

ERAP Genotyping Results

Of the 17 *ERAP* SNPs that were genotyped, rs78649652, rs111363347 and rs375081137 were completely conserved for the ancestral allele in this cohort and offered no discriminatory power. Very strong linkages exist among SNPs rs73148308 and rs73144471, among SNPs rs2287987, rs10050860 and rs17482078, among SNPs rs2248374 and rs2549782, and among SNPs rs26653, rs27434, rs27529, rs30187 and rs27044. Each SNP was tested separately for association with SJS/TEN and then again after adjustment for carriage of the ancestral allele (C) in SNP rs27044, which gave the strongest individual association ($p=3.2x10^{-6}$). While allele carriage of 10 *ERAP1* SNPs was independently significant between nevirapine SJS/TEN cases and tolerant individuals, only rs27044 remained significant after adjusting for carriage of rs27044(C) (Table 2.10). Furthermore, similar to the entire tolerant cohort, nevirapine tolerant individuals who carried HLA-C*04:01 were also less likely to carry the ancestral rs27044(C) allele compared to those who developed SJS/TEN (p=0.003) (Table 2.10 and Figure 2.8). *ERAP1* and *ERAP2* genotyping results for nevirapine DRESS cases are shown in Table 2.11.

Gene	SNP		SJS/TEN (n=20)	Tolerant (n=46)	Tolerant + C*04:01+ (n=10)	p-value (Case vs. Tolerant)	p-value (Case vs. Tolerant + HLA-C*04:01)
CYP2B6	rs3745274	G	50.0 (20/40)	69.6 (64/92)	65.0 (13/20)	0.059	0.34
		T	50.0 (20/40)	30.4 (28/92)	35.0 (7/20)		
		GG	35.0 (7/20)	52.2 (24/46)	40.0 (4/10)	0.12	0.31
		GT	30.0 (6/20)	34.8 (16/46)	50.0 (5/10)		
		TT	35.0 (7/20)	13.0 (6/46)	10.0 (1/10)		
	rs28399499	T	77.5 (31/40)	92.4 (85/92)	95.0 (19/20)	0.0090	0.058
		C	22.5 (9/40)	7.6 (7/92)	5.0 (1/20)		
		TT	55.0 (11/20)	84.8 (39/46)	90.0 (9/10)	0.014	0.10
		TC	45.0 (9/20)	15.2 (7/46)	10.0 (1/10)		
		CC	0.0 (0/20)	0.0 (0/46)	0.0 (0/10)		
	rs4803419	C	100.0 (40/40)	90.2 (83/92)	80.0 (16/20)	0.034	0.0015
		T	0.0 (0/40)	9.8 (9/92)	20.0 (4/20)		
		CC	100.0 (20/20)	80.4 (37/46)	60.0 (6/10)	0.048	0.0077
		CT	0.0 (0/20)	19.6 (9/46)	40.0 (4/10)		
		TT	0.0 (0/20)	0.0 (0/46)	0.0 (0/10)		

Table 2.8. *CYP2B6* genotyping of nevirapine SJS/TEN cases compared to nevirapine tolerant controls. The SNPs confer the following non-synonymous changes in the *CYP2B6* gene: rs3745274 (516G→T), rs28399499 (983T→C), and rs4803419 (15582C→T). Each allele is reported as % positive (positive/total). **Legend:** SNP, single nucleotide polymorphism; SJS/TEN, Stevens-Johnson syndrome/toxic epidermal necrolysis.

Gene	SNP		DRESS (n=6)	Tolerant (n=46)	p-value
CYP2B6	rs3745274	G	25.0 (3/12)	69.6 (64/92)	0.004
		T	75.0 (9/12)	30.4 (28/92)	
		GG	16.7 (1/6)	52.2 (24/46)	0.007
		GT	16.7 (1/6)	34.8 (16/46)	
		TT	66.7 (4/6)	13.0 (6/46)	
	rs28399499	T	100.0 (12/12)	92.4 (85/92)	>0.99
		C	0.0 (0/12)	7.6 (7/92)	
		TT	100.0 (6/6)	84.8 (39/46)	0.58
		TC	0.0 (0/6)	15.2 (7/46)	
		CC	0.0 (0/6)	0.0 (0/46)	
	rs4803419	C	100.0 (12/12)	90.2 (83/92)	0.59
		T	0.0 (0/12)	9.8 (9/92)	
		CC	100.0 (6/6)	80.4 (37/46)	0.57
		CT	0.0 (0/6)	19.6 (9/46)	
		TT	0.0 (0/6)	0.0 (0/46)	

Table 2.9. *CYP2B6* genotyping of nevirapine DRESS cases compared to nevirapine tolerant controls. The SNPs confer the following non-synonymous changes in the *CYP2B6* gene: rs3745274 (516G→T), rs28399499 (983T→C), and rs4803419 (15582C→T). Each allele is reported as % positive (positive/total). **Legend:** SNP, single nucleotide polymorphism; DRESS, drug reaction with eosinophilia and systemic symptoms.

Gene	SNP		SJS/TEN (n=20)	Tolerant (n=46)	Tolerant w/ C*04:01 (n=10)	BioVU (n=10,220)	BioVU w/ C*04:01 (n=3,527)	p-value (SJS vs. Tolerant)	p-value (SJS vs. Tolerant w/ C*04:01)
ERAP 1	rs3734016	G	40	87	20	19136	6596	0.13	>0.99
		A	0	5	0	1254	444		
		GG	20	41	10	8989	3100	0.31	>0.99
		GA	0	5	0	1158	396		
		AA	0	0	0	48	24		
	rs73148308	T	35	90	19			0.012	0.35
		C	5	2	1				
		TT	15	44	9			0.023	0.63
		TC	5	2	1				
		CC	0	0	0				
	rs26653	G	29	37	8	9631	3359	0.00083	0.018
		C	11	55	12	10801	3693		
		GG	10	8	2	2235	795	0.0043	0.059
		GC	9	21	4	5161	1769		
		CC	1	17	4	2820	962		
	rs27895	G	31	74	16	16578	5677	0.68	0.80
		A	9	18	4	3830	1365		
		GG	11	29	6	6744	2281	0.71	>0.99
		GA	9	16	4	3090	1115		
		AA	0	1	0	370	125		
	rs2287987	A	39	75	14	18187	6301	0.019	0.0030
		G	1	17	6	2101	701		
		AA	19	31	5	8166	2846	0.048	0.0088
		AG	1	13	4	1855	609		
		GG	0	2	1	123	46		
	rs27434	T	27	31	7	7867	2740	0.00023	0.019
		C	13	61	13	12539	4300		
		TT	8	5	2	1500	532	0.0011	0.024
		TC	11	21	3	4867	1676		
		CC	1	20	5	3836	1312		
	rs73144471	T	35	90	19			0.012	0.35
		A	5	2	1				
		TT	15	44	9			0.023	0.63
		TA	5	2	1				
		AA	0	0	0				
	rs27529	T	26	27	7	8058	2770	0.000076	0.027

	C	14	65	13	12368	4282		
	TT	7	4	2	1546	535	0.00026	0.021
	TC	12	19	3	4966	1700		
	CC	1	23	5	3701	1291		
rs78649652	G	40	92	20	20405	7039	>0.99	>0.99
	A	0	0	0	35	15		
	GG	20	46	10	10185	3512	>0.99	>0.99
	GA	0	0	0	35	15		
	AA	0	0	0	0	0		
rs30187	A	26	27	7	8065	2771	0.000076	0.027
	G	14	65	13	12367	4281		
	AA	7	4	2	1549	536	0.00026	0.021
	AG	12	19	3	4967	1699		
	GG	1	23	5	3700	1291		
rs10050860	G	39	76	14	18333	6351	0.018	0.0030
	A	1	16	6	2105	703		
	GG	19	31	5	8230	2867	0.033	0.0088
	GA	1	14	4	1873	617		
	AA	0	1	1	116	43		
rs111363347	G	40	92	20	20424	7050	>0.99	>0.99
	A	0	0	0	10	2		
	GG	20	46	10	10208	3524	>0.99	>0.99
	GA	0	0	0	8	2		
	AA	0	0	0	1	0		
rs17482078	G	40	82	16	18545	6411	0.024	0.0015
	A	0	10	4	1891	643		
	GG	20	36	6	8434	2925	0.026	0.0077
	GA	0	10	4	1677	561		
	AA	0	0	0	107	41		
rs27044	C	21	15	4	5975	2018	0.0000056	0.0071
	G	19	77	16	14455	5032		
	CC	3	2	1	854	300	0.0000070	0.0027
	CG	15	11	2	4267	1418		
	GG	2	33	7	5094	1807		
rs375081137	T	40	92	20			>0.99	>0.99
	TT	20	46	10			>0.99	>0.99

Gene	SNP		SJS/TEN (n=20)	Tolerant (n=46)	Tolerant w/ C*04:01 (n=10)	BioVU (n=10,220)	BioVU w/ C*04:01 (n=3,527)	p-value (SJS vs. Tolerant)	p-value (SJS vs. Tolerant w/ C*04:01)
ERAP 2	rs2248374	A	24	51	11			0.58	0.74
		G	16	41	9				
		AA	8	14	3			0.73	0.88
		AG	8	23	5				
		GG	4	9	2				
	rs2549782	G	24	48	11	8758	3037	0.64	0.74
		T	16	40	9	11674	4015		
		GG	8	13	3	1893	650	0.69	0.88
		GT	8	22	5	4972	1737		
		TT	4	9	2	3351	1139		

Table 2.10. *ERAP1* and *ERAP2* genotyping of nevirapine SJS/TEN cases compared to nevirapine tolerant controls. The number of individuals in each category carrying each allele or allele combination for the genotyped *ERAP1* and *ERAP2* SNPs is shown. **Legend:** SJS/TEN, Stevens-Johnson syndrome/toxic epidermal necrolysis.

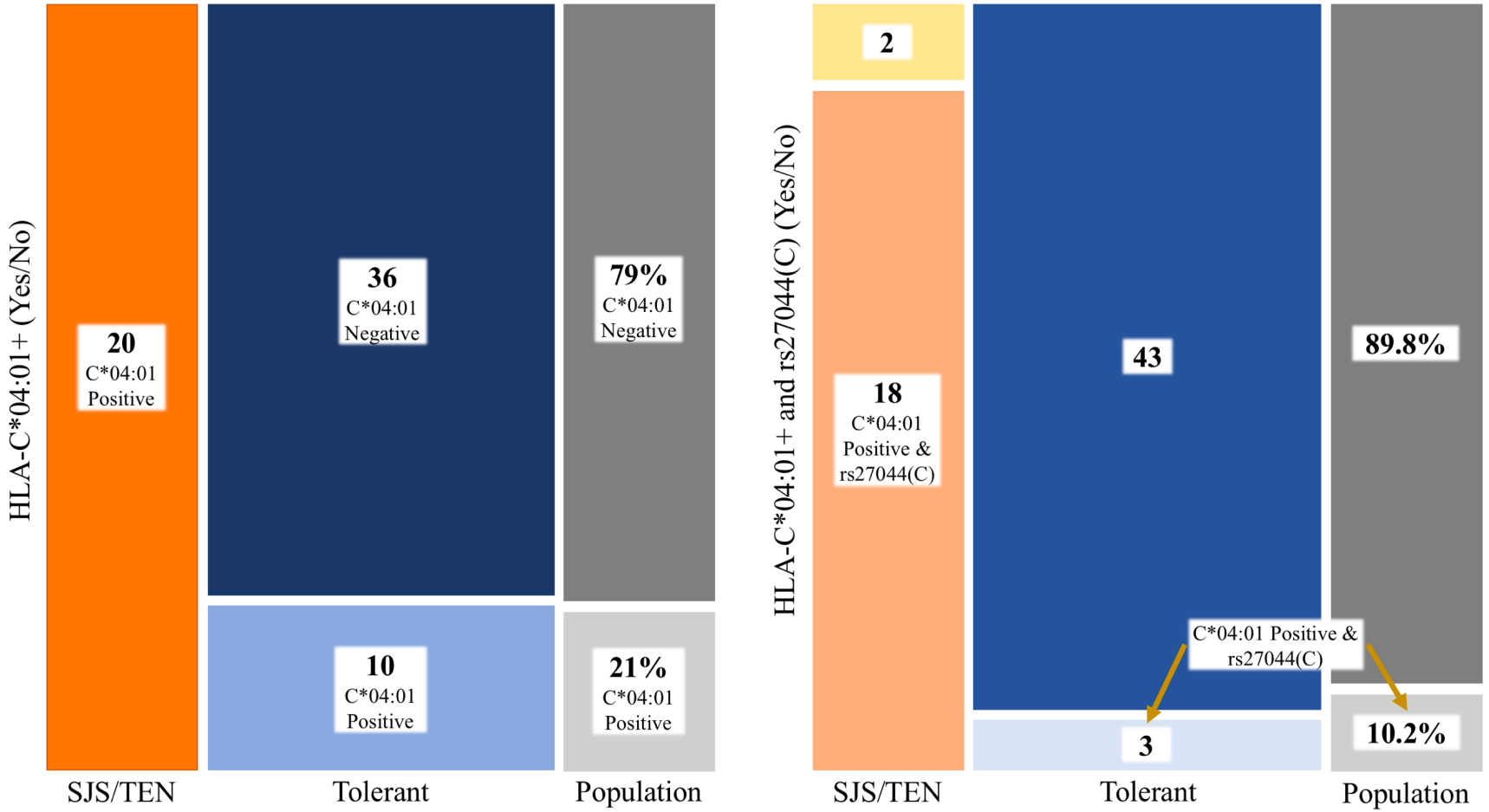

Figure 2.8 Absence of ancestral allele for ERAP1 SNP rs27044 may protect HLA-C*04:01 positive individuals from nevirapine SJS/TEN. The size of the boxes in the mosaic plot are proportional to the number of patients in each category, which is also denoted in the white boxes. All patients with nevirapine SJS/TEN carry HLA-C*04:01. When the HLA and ERAP genotyping data are combined, 2/20 patients with SJS/TEN and 43/46 tolerant individuals do not carry about HLA-C*04:01 and rs27044(C) compared to 89.8% of the population. **Legend:** SJS/TEN, Stevens-Johnson syndrome/toxic epidermal necrolysis.

Gene	SNP		DRESS (n=6)	Tolerant (n=46)	BioVU (n=10,220)	p-value
ERAP 1	rs3734016	G	12	87	19136	>0.99
		A	0	5	1254	
		GG	6	41	8989	>0.99
		GA	0	5	1158	
		AA	0	0	48	
	rs73148308	T	12	90		>0.99
		C	0	2		
		TT	6	44		>0.99
		TC	0	2		
		CC	0	0		
	rs26653	G	6	37	9631	0.55
		C	6	55	10801	
		GG	2	8	2235	0.64
		GC	2	21	5161	
		CC	2	17	2820	
	rs27895	G	9	74	16578	0.70
		A	3	18	3830	
		GG	4	29	6744	0.18
		GA	1	16	3090	
		AA	1	1	370	
	rs2287987	A	7	75	18187	0.12
		G	5	17	2101	
		AA	3	31	8166	0.04
		AG	1	13	1855	
		GG	2	2	123	
	rs27434	T	3	31	7867	0.75
		C	9	61	12539	
		TT	1	5	1500	0.40
		TC	1	21	4867	
		CC	4	20	3836	
	rs73144471	T	12	90		>0.99
		A	0	2		
		TT	6	44		>0.99
		TA	0	2		
		AA	0	0		
	rs27529	T	3	27	8058	>0.99
		C	9	65	12368	
		TT	1	4	1546	0.48
		TC	1	19	4966	

	CC	4	23	3701	
rs78649652	G	12	92	20405	>0.99
	A	0	0	35	
	GG	6	46	10185	>0.99
	GA	0	0	35	
	AA	0	0	0	
rs30187	A	3	27	8065	>0.99
	G	9	65	12367	
	AA	1	4	1549	0.48
	AG	1	19	4967	
	GG	4	23	3700	
rs10050860	G	7	76	18333	0.06
	A	5	16	2105	
	GG	3	31	8230	0.009
	GA	1	14	1873	
	AA	2	1	116	
rs111363347	G	12	92	20424	>0.99
	A	0	0	10	
	GG	6	46	10208	>0.99
	GA	0	0	8	
	AA	0	0	1	
rs17482078	G	12	82	18545	0.60
	A	0	10	1891	
	GG	6	36	8434	0.58
	GA	0	10	1677	
	AA	0	0	107	
rs27044	C	3	15	5975	0.43
	G	9	77	14455	
	CC	1	2	854	0.46
	CG	1	11	4267	
	GG	4	33	5094	
rs375081137	T	12	92		>0.99
	TT	6	46		>0.99

Gene	SNP		DRESS (n=6)	Tolerant (n=46)	BioVU (n=10,220)	p-value
ERAP 2	rs2248374	G	6	51		0.77
		T	6	41		
		GG	2	14		0.80
		GT	2	23		
		TT	2	9		
	rs2549782	A	6	48	8758	0.77
		G	6	40	11674	
		AA	2	13	1893	0.69
		AG	2	22	4972	
		GG	2	9	3351	

Table 2.11. *ERAP1* and *ERAP2* genotyping of nevirapine DRESS cases compared to nevirapine tolerant controls. The number of individuals in each category carrying each allele or allele combination for the genotyped *ERAP1* and *ERAP2* SNPs is shown. **Legend:** DRESS, drug reaction with eosinophilia and systemic symptoms.

In contrast to the nevirapine SJS/TEN ERAP typing, those with nevirapine DRESS were more likely to carry the ancestral alleles for rs2287987 and rs10050860 than nevirapine tolerant controls (p=0.04 and 0.009, respectively) (Table 2.11).

When considered jointly, carriage of HLA-C*04:01 and rs27044(C) were more significantly associated with nevirapine SJS/TEN development than either factor alone ($p=2.1x10^{-13}$). Compared to the African American patients with available genotyping in Vanderbilt's BioVU repository, the nevirapine SJS/TEN patients were more likely to carry rs27044(C) and the nevirapine tolerant controls were more likely to carry rs27044(G) (p=0.0006 and 0.013, respectively). There were no significant differences between any of the ERAP SNP distributions between the African American BioVU population as a whole and the subset of that population who also carried HLA-C*04:01 (Table 2.10). When the rs27044 SNP data for the nevirapine SJS/TEN cases and tolerant controls were combined, they did not differ in distribution from the BioVU population (p=0.91). Compared to the BioVU population, nevirapine SJS/TEN cases were also more likely to carry the ancestral alleles for rs26653, rs27434, rs27529 and rs30187, which are known to be in linkage disequilibrium with rs27044 (p=0.0052, 0.0004, 0.0016 and 0.0016, respectively).

KIR Genotyping Results

Carriage of specific KIR genes in nevirapine SJS/TEN and DRESS cases displayed as the presence or absence of a specific KIR gene was not significantly different than KIR gene carriage in tolerant controls. All three patient groups, SJS/TEN, DRESS and tolerant, reflected previously genotyped South African populations (Tables 2.12 and 2.13).

Haplotype	KIR	SJS/TEN	Tolerant	Tolerant w/ C*04:01	Xhosa (n=50)	San (n=91)	p-value (SJS/TEN vs. Tolerant)	p-value (SJS/TEN vs. Tolerant w/ C*04:01)
A	**2DL3**	68.4 (13/19)	76.1 (35/46)	88.9 (8/9)	64	60.4	0.53	0.37
A	**2DS4**	100 (19/19)	97.7 (42/43)	100 (9/9)	100	100	>0.99	>0.99
A	**3DL1**	100 (20/20)	100 (46/46)	100 (10/10)	100	98.9	>0.99	>0.99
AB	**2DL1**	100 (20/20)	100 (46/46)	100 (10/10)	96	95.6	>0.99	>0.99
AB	**2DL4**	100 (20/20)	100 (46/46)	100 (10/10)	100	100	>0.99	>0.99
AB	**2DP1**	100 (20/20)	100 (46/46)	100 (10/10)	98	92.3	>0.99	>0.99
N/A	**3DL2**	100 (15/15)	100 (22/22)	100 (4/4)	100	100	>0.99	>0.99
B	**2DL2**	65.0 (13/20)	67.4 (31/46)	60.0 (6/10)	72	73.6	>0.99	>0.99
B	**2DL5**	50.0 (10/20)	65.2 (30/46)	70.0 (7/10)	82	68.1	0.28	0.44
B	**2DS1**	20.0 (4/20)	22.0 (9/41)	37.5 (3/8)	10	14.3	>0.99	0.37
B	**2DS2**	65.0 (13/20)	56.5 (26/46)	50.0 (5/10)	64	72.5	0.59	0.46
B	**2DS3**	40.0 (8/20)	32.6 (15/46)	20.0 (2/10)	38	25.3	0.58	0.42
B	**2DS5**	40.0 (8/20)	46.5 (20/43)	66.7 (6/9)	62	63.7	0.79	0.25
B	**3DS1**	15.8 (3/19)	14.6 (6/41)	25.0 (2/8)	4	2.2	>0.99	0.62

Table 2.12. Killer-cell immunoglobulin-like receptor genotyping of nevirapine SJS/TEN cases compared to nevirapine tolerant controls and representative South African populations. Absence or presence of KIR genes is reported as % positive (positive/total). None of the KIR genotyping results differ significantly from what would be expected in the South African Black population. **Legend:** KIR, Killer-cell immunoglobulin-like receptor; SJS/TEN, Stevens-Johnson syndrome/toxic epidermal necrolysis.

Haplotype	KIR	DRESS	Tolerant	Xhosa (n=50)	San (n=91)	p-value
A	**2DL3**	66.7 (4/6)	75.5 (37/49)	64	60.4	0.64
A	**2DS4**	83.3 (5/6)	97.8 (45/46)	100	100	0.22
A	**3DL1**	83.3 (5/6)	100 (49/49)	100	98.9	0.11
AB	**2DL1**	100 (6/6)	100 (49/49)	96	95.6	>0.99
AB	**2DL4**	100 (6/6)	100 (49/49)	100	100	>0.99
AB	**2DP1**	83.3 (5/6)	100 (49/49)	98	92.3	0.11
N/A	**3DL2**	100 (4/4)	100 (25/25)	100	100	>0.99
B	**2DL2**	83.3 (5/6)	69.4 (34/49)	72	73.6	0.66
B	**2DL5**	66.7 (4/6)	71.4 (33/49)	82	68.1	>0.99
B	**2DS1**	33.3 (2/6)	20.5 (9/44)	10	14.3	0.60
B	**2DS2**	50.0 (3/6)	57.1 (28/49)	64	72.5	>0.99
B	**2DS3**	16.7 (1/6)	32.7 (16/49)	38	25.3	0.65
B	**2DS5**	66.7 (4/6)	47.8 (22/46)	62	63.7	0.41
B	**3DS1**	33.3 (2/6)	13.0 (6/44)	4	2.2	0.24

Table 2.13. Killer-cell immunoglobulin-like receptor genotyping of nevirapine DRESS cases compared to nevirapine tolerant controls and representative South African populations. Absence or presence of KIR genes is reported as % Positive (positive/total). None of the KIR genotyping results differ significantly from what would be expected in the South African Black population. **Legend:** KIR, Killer-cell immunoglobulin-like receptor; DRESS, drug reaction with eosinophilia and systemic symptoms.

Immunohistochemistry of Acute Nevirapine SJS Skin Biopsies

Immunohistochemistry staining of T-cell subsets on slides from a formalin-fixed, paraffin-embedded punch biopsy of affected skin taken during the acute reaction was done on nevirapine SJS patients 5, 7, 9 and 11. The staining revealed a dense lymphocytic infiltrate of predominantly CD3+ and CD8+ T cells with high CLA expression. Representative staining from patient 5 is shown in Figure 2.9, right panel. Healthy skin from a different individual is shown for comparison (Figure 2.9, left panel).

Granulysin Concentrations in Acute Nevirapine SJS Blister Fluid Supernatant and Plasma

Plasma samples were available from three patients with acute nevirapine SJS/TEN (Table 2.1). The plasma was collected and processed from patients 17, 18 and 19 (Table 2.1) on days 3, 8 and 4 of SJS/TEN symptoms, respectively, which corresponded to 2 days, 1 day and 1 day after nevirapine therapy was stopped. In addition to plasma, cryopreserved blister fluid supernatant was also available from nevirapine SJS patients 18 and 19. The blister fluid was collected and processed on the same day as the plasma. Plasma from a healthy donor and blister fluid supernatant from a patient with a thermal burn were used as controls. The granulysin concentrations in the samples from the nevirapine SJS/TEN patients were several-fold higher than healthy donor plasma and blister fluid supernatant from a patient with a thermal burn (Figure 2.10).

Skin and Blister Fluid Single-Cell Sorts

Cryopreserved skin biopsies were available from three patients with acute nevirapine SJS/TEN. The biopsies were taken from nevirapine SJS/TEN patients 17, 18 and 19 (Table 2.1) on days 3,

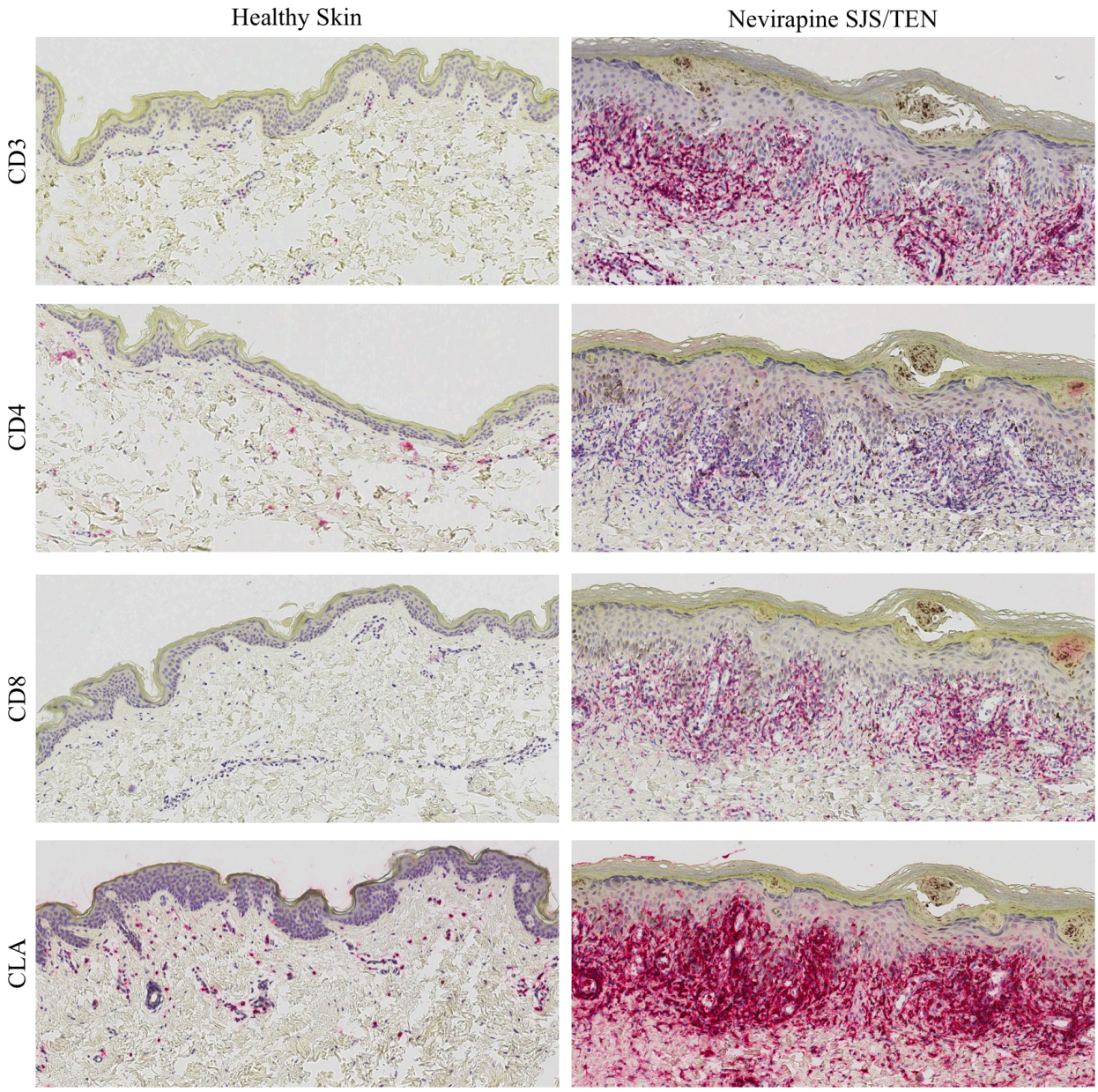

Figure 2.9. Immunohistochemistry of T-cell subsets in acute nevirapine SJS skin. Immunohistochemistry staining on a skin punch biopsy taken one day after initial rash development revealed a dense lymphocytic infiltrate (right panel). Healthy skin is shown for comparison (left panel). **Legend:** SJS/TEN, Stevens-Johnson syndrome/toxic epidermal necrolysis; CLA, cutaneous lymphocyte antigen.

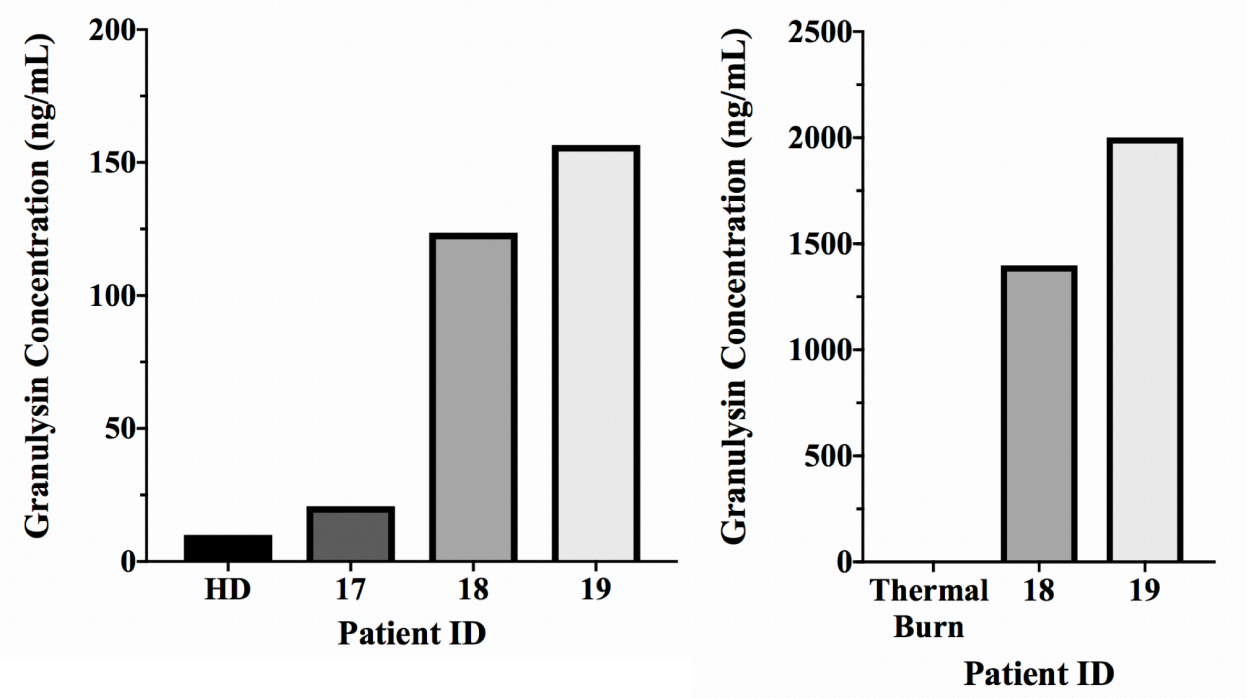

Figure 2.10. Granulysin levels are increased in plasma and blister fluid supernatant of patients with nevirapine SJS/TEN. Granulysin concentrations were measured by ELISA. Plasma from a healthy donor and blister fluid supernatant from a patient with a thermal burn were used as controls. **Legend:** HD, healthy donor; Patient ID, patient identification.

9 and 5 of SJS/TEN symptoms, respectively. Two biopsies were taken from each patient, one of skin affected by the disease and one of unaffected skin for comparison. One plate of CD3+ T cells was sorted from each skin punch biopsy. In the unaffected skin biopsy from nevirapine SJS patient 17, 25.4% of the total gated cells were live CD3+ T cells. Of the CD3+ T cells, 16.7% were CD8+ T cells and 50% were CD4+ T cells. In the biopsy of skin acutely SJS-affected from patient 17, 35.8% of the cells were live CD3+ T cells. Of the CD3+ T cells, 55.9% were CD8+ and 35.3% were CD4+. In the unaffected skin biopsy from patient 18, 59.8% of the total gated cells were live CD3+ T cells. Of the CD3+ T cells, 72.7% were CD8+ and 16.4% were CD4+. In the affected skin biopsy from patient 18, 51.9% of the cells were live CD3+ T cells. Of those, 85.1% were CD8+ and 4.5% were CD4+. In the unaffected skin biopsy from patient 19, 27.9% of the cells were live CD3+ T cells. Of the CD3+ T cells, 75.0% were CD8+ and 12.5% were CD4+. In the affected skin biopsy from patient 19, 69.0% of the affected cells were live CD3+ T cells. Of the CD3+ T cells, 87.7% were CD8+ and 4.1% were CD4+. The index sort data and memory T cell subsets from all six biopsies from the three nevirapine SJS patients are summarized in Tables 2.14 and 2.15.

In addition to skin, cryopreserved blister fluid cells were also available from nevirapine SJS/TEN patients 18 and 19 (Table 2.1). The blister fluid was collected from patient 18 on day 8 of SJS/TEN symptoms and from patient 19 on day 4 of SJS symptoms. Blister fluid cells from two different anatomical locations were sorted for both patients. In the single-cell sort of blister fluid collected from the top of SJS/TEN patient 18's right foot, 88.4% of the cells were CD3+ T cells. In the total CD3+ T cell population, 89.7% were CD3+CD8+ and 4.7% were CD3+CD4+ T cells. 4.0% of the CD3+CD8+ T cells were also CD137+. In the single-cell sort of blister fluid collected from the

Patient ID	Skin Type	CD3	CD8	CD4	CD69	CD137	CCR7	CD45RO	CD103	CCR10
17	**Unaffected**	100 (92/92)	38.0 (35/92)	38.0 (35/92)	15.2 (14/92)	6.5 (6/92)	47.8 (44/92)	35.9 (33/92)	21.7 (20/92)	22.8 (21/92)
17	**Affected**	100 (80/80)	47.5 (38/80)	51.3 (41/80)	36.3 (29/80)	12.5 (10/80)	32.5 (26/80)	63.8 (51/80)	30.0 (24/80)	38.8 (31/80)
18	**Unaffected**	100 (92/92)	75.0 (69/92)	20.7 (19/92)	52.2 (48/92)	13.0 (12/92)	35.9 (33/92)	70.7 (65/92)	70.7 (65/92)	23.9 (22/92)
18	**Affected**	100 (80/80)	92.5 (74/80)	5.0 (4/80)	40.0 (32/80)	3.8 (3/80)	46.3 (37/80)	73.8 (59/80)	23.8 (19/80)	11.3 (9/80)
19	**Unaffected**	100 (92/92)	82.6 (76/92)	6.5 (6/92)	28.3 (26/92)	4.3 (4/92)	13.0 (12/92)	42.4 (39/92)	16.3 (15/92)	23.9 (22/92)
19	**Affected**	100 (92/92)	88.0 (81/92)	9.8 (9/92)	27.2 (25/92)	4.3 (4/92)	23.9 (22/92)	63.0 (58/92)	17.4 (16/92)	13.0 (12/92)
Combined	**Unaffected**	100 (276/276)	65.2 (180/276)	21.7 (60//276)	31.9 (88/276)	8.0 (22/276)	32.2 (89/276)	49.6 (137/276)	36.2 (100/276)	23.6 (65/276)
Combined	**Affected**	100 (252/252)	76.6 (193/252)	21.4 (54/252)	34.1 (86/252)	6.7 (17/252)	33.7 (85/252)	66.7 (168/252)	23.4 (59/252)	20.6 (52/252)
Combined	**Total Cells**	100 (528/528)	70.6 (373/528)	21.6 (114/582)	33.0 (174/528)	7.4 (39/528)	33.0 (174/528)	57.8 (305/528)	30.1 (159/528)	22.2 (117/528)

Table 2.14. Summary index sort data from single-cell sorts of skin biopsies from patients 17, 18 and 19 with acute nevirapine SJS. Two biopsies were taken from each patient, one of skin affected by the disease and one of unaffected skin for comparison. One plate of CD3+ T cells was sorted from each skin punch biopsy. The number of cells that expressed each T-cell surface marker is reported as % positive (positive/total cells). Data were analyzed using FlowJo software (Tree Star).

Patient ID	Skin Type	Naïve (CCR7+CD45RO-)	TCM (CCR7+CD45RO+)	TEMRA (CCR7-CD45RO-)	TEM (CCR7-CD45RO+)
17	**Unaffected**	28.3 (26/92)	19.6 (18/92)	34.8 (32/92)	17.4 (16/92)
17	**Affected**	12.5 (10/80)	20.0 (16/80)	23.8 (19/80)	43.8 (35/80)
18	**Unaffected**	6.5 (6/92)	29.3 (27/92)	22.8 (21/92)	41.3 (38/92)
18	**Affected**	11.3 (9/80)	36.3 (29/80)	15.0 (12/80)	37.5 (30/80)
19	**Unaffected**	9.8 (9/92)	3.3 (3/92)	46.7 (43/92)	40.2 (37/92)
19	**Affected**	6.5 (6/92)	17.4 (16/92)	29.3 (27/92)	46.7 (43/92)
Combined	**Unaffected**	12.0 (33/276)	20.3 (56/276)	29.0 (80/276)	38.8 (107/276)
Combined	**Affected**	9.9 (25/252)	24.2 (61/252)	23.0 (58/252)	42.9 (108/252)
Combined	**Total Cells**	11.0 (58/582)	22.2 (117/528)	26.1 (138/528)	40.7 (215/528)

Table 2.15. Memory T-cell subsets from single-cell sorts of skin biopsies from patients 17, 18 and 19 with acute nevirapine SJS. Two biopsies were taken from each patient, one of skin affected by the disease and one of unaffected skin for comparison. One plate of CD3+ T cells was sorted from each skin punch biopsy. The number of cells in each memory subset is reported as % positive (positive/total cells). Data were analyzed using FlowJo software (Tree Star). **Legend:** TCM, T central memory cell; TEMRA, T effector memory re-expressing CD45RA cell; TEM, T effector memory cell.

top of SJS patient 18's left foot, 79.3% of the cells were CD3+ T cells. In the total CD3+ T cell population, 91.0% were CD3+CD8+ and 2.9% were CD3+CD4+ T cells. 3.8% of the CD3+CD8+ T cells were also CD137+. In the single-cell sort of blister fluid collected from the neck of patient 19, 76.2% of the cells were CD3+ T cells. In the total CD3+ T cell population, 88.7% were CD3+CD8+ and 6.7% were CD3+CD4+ T cells. 3.0% of the CD3+CD8+ T cells were also CD137+. In the single-cell sort of blister fluid collected from the left cheek of patient 19, 81.6% of the cells were CD3+ T cells. In the total CD3+ T cell population, 88.8% were CD3+CD8+ and 6.4% were CD3+CD4+ T cells. 3.4% of the CD3+CD8+ T cells were also CD137+. The index sort data and memory T cell subsets from the nevirapine SJS/TEN blister fluid single-cell sorts are summarized in Tables 2.16, 2.17, 2.18 and 2.19. Overall, the majority of the blister fluid T cells were memory cells. Specifically, 87.9% (384/437) of the sorted blister fluid cells from patient 18 and 92.5 (500/541) of the sorted blister fluid cells from patient 19 were CD45RO+.

Single-cell TCR Sequencing in Acute Nevirapine SJS Blister Fluid and Skin

Single-cell TCR sequencing of the sorted CD3+ T cells from the cryopreserved skin biopsies from nevirapine SJS patients 17, 18 and 19 revealed a polyclonal T-cell repertoire in the skin (Figure 2.11). The sorted CD8+ blister fluid T cells from patient 18 that were collected eight days after initial SJS symptom onset were also polyclonal (Figure 2.12). In contrast, in the sorted CD8+ blister fluid T cells from patient 19 that were collected four days after SJS symptoms onset, 45% of the activated (CD137+) CD8+ T cells shared a dominant TCR Vβ chain (TRBV28). The dominant TCR Vβ was predominately paired with a dominant TCR Vα chain (TRAV35) (Figure 2.13). In the other sorted samples from patient 19, one CD3+/CD8+/CD69+/CCR10+/CD103+ T

Blister Location	Gated Cells	CD3	CD8	CD4	CD56	CD69	CD137	CCR7	CD45RO	CLA
Right Foot	**CD8+CD137-**	100 (92/92)	100 (92/92)	7.6 (7/92)	42.4 (39/92)	43.5 (40/92)	0.0 (0/92)	65.2 (60/92)	91.3 (84/92)	75.0 (69/92)
Right Foot	**CD8+CD137+**	100 (92/92)	100 (92/92)	9.8 (9/92)	58.7 (54/92)	80.4 (74/92)	100 (92/92)	72.8 (67/92)	87.0 (80/92)	82.6 (76/92)
Right Foot	**CD3+CD56+**	100 (87/87)	100 (87/87)	3.4 (3/87)	100 (87/87)	86.2 (75/87)	11.5 (10/87)	18.4 (16/87)	92.0 (80/87)	82.8 (72/87)
Left Foot	**CD8+CD137-**	100 (92/92)	100 (92/92)	2.1 (2/92)	23.9 (22/92)	64.1 (59/92)	0.0 (0/92)	37.0 (34/92)	84.8 (78/92)	82.6 (76/92)
Left Foot	**CD8+CD137+**	100 (74/74)	100 (74/74)	4.1 (3/74)	44.6 (33/74)	87.8 (65/74)	100 (74/74)	35.1 (26/74)	83.8 (62/74)	93.2 (69/74)
Combined	**CD8+CD137-**	100 (184/184)	100 (184/184)	4.9 (9/184)	33.2 (61/184)	53.8 (99/184)	0.0 (0/184)	51.1 (94/184)	88.0 (162/184)	78.8 (145/184)
Combined	**CD8+CD137+**	100 (166/166)	100 (166/166)	7.2 (12/166)	52.4 (87/166)	83.7 (139/166)	100 (166/166)	56.0 (93/166)	85.5 (142/166)	87.3 (145/166)
Combined	**Total Cells**	100 (437/437)	100 (437/437)	5.5 (24/437)	53.8 (235/437)	71.6 (313/437)	40.3 (176/437)	46.5 (203/437)	87.9 (384/437)	82.8 (362/437)

Table 2.16. Summary index sort data from single-cell sorts of blister fluid from acute nevirapine SJS patient 18. Blister fluid cells collected on Day 8 of SJS symptoms from two different anatomical locations were sorted. The number of cells that expressed each T-cell surface marker is reported as % positive (positive/total cells). Data were analyzed using FlowJo software (Tree Star).

Blister Location	Gated Cells	Naïve (CCR7+CD45RO-)	TCM (CCR7+CD45RO+)	TEMRA (CCR7-CD45RO-)	TEM (CCR7-CD45RO+)
Right Foot	**CD8+CD137-**	5.4 (5/92)	59.8 (55/92)	3.3 (3/92)	31.5 (29/92)
Right Foot	**CD8+CD137+**	10.9 (10/92)	63.0 (58/92)	2.2 (2/92)	23.9 (22/92)
Right Foot	**CD3+CD56+**	3.4 (3/87)	14.9 (13/87)	4.6 (4/87)	77.0 (67/87)
Left Foot	**CD8+CD137-**	6.5 (6/92)	30.4 (28/92)	8.7 (8/92)	54.3 (50/92)
Left Foot	**CD8+CD137+**	2.7 (2/74)	32.4 (24/74)	13.5 (10/74)	51.4 (38/74)
Combined	**CD8+CD137-**	6.0 (11/184)	45.1 (83/184)	6.0 (11/184)	42.9 (79/184)
Combined	**CD8+CD137+**	7.2 (12/166)	49.4 (82/166)	7.2 (12/166)	36.1 (60/166)
Combined	**Total Cells**	5.9 (26/437)	40.7 (178/437)	6.2 (27/437)	47.1 (206/437)

Table 2.17. Memory T-cell subsets from single-cell sorts of blister fluid from acute nevirapine SJS patient 18. Blister fluid cells collected on Day 8 of SJS symptoms from two different anatomical locations were sorted. The number of cells in each memory subset is reported as % positive (positive/total cells). Data were analyzed using FlowJo software (Tree Star). **Legend:** TCM, T central memory cell; TEMRA, T effector memory re-expressing CD45RA cell; TEM, T effector memory cell.

Blister Location	Gated Cells	CD3	CD8	CD4	CD56	CD69	CD137	CCR7	CD45RO	CLA
Neck	**CD8+CD137-**	100 (91/91)	100 (91/91)	2.2 (2/91)	29.7 (27/91)	20.9 (19/91)	0.0 (0/91)	59.3 (54/91)	84.6 (77/91)	59.3 (54/91)
Neck	**CD8+CD137+**	100 (178/178)	100 (178/178)	5.1 (9/178)	14.0 (25/178)	49.4 (88/178)	100 (178/178)	42.7 (76/178)	97.2 (173/178)	57.3 (102/178)
Left Cheek	**CD8+CD137-**	100 (91/91)	100 (91/91)	2.2 (2/91)	29.7 (27/91)	17.6 (16/91)	0.0 (0/91)	42.9 (39/91)	83.5 (76/91)	52.7 (48/91)
Left Cheek	**CD8+CD137+**	100 (90/90)	100 (90/90)	3.3 (3/90)	20.0 (18/90)	46.7 (42/90)	100 (90/90)	53.3 (48/90)	100 (90/90)	52.2 (47/90)
Left Cheek	**CD3+CD56+**	100 (91/91)	100 (91/91)	5.5 (5/91)	100 (91/91)	35.2 (32/91)	4.4 (4/91)	19.8 (18/91)	92.3 (84/91)	68.1 (62/91)
Combined	**CD8+CD137-**	100 (182/182)	100 (182/182)	2.2 (4/182)	29.7 (54/182)	19.2 (35/182)	0.0 (0/182)	51.1 (93/182)	84.1 (153/182)	56.0 (102/182)
Combined	**CD8+CD137+**	100 (268/268)	100 (268/268)	4.5 (12/268)	16.0 (43/268)	48.5 (130/268)	100 (268/268)	46.3 (124/268)	98.1 (263/268)	55.6 (149/268)
Combined	**Total Cells**	100 (541/541)	100 (541/541)	3.9 (21/541)	34.8 (188/541)	36.4 (197/541)	50.3 (272/541)	43.4 (235/541)	92.4 (500/541)	57.9 (313/541)
Dominant TCRαβ	**Total Cells**	100 (45/45)	100 (45/45)	4.4 (2/45)	24.4 (11/45)	42.2 (19/45)	91.1 (41/45)	42.2 (19/45)	95.6 (43/45)	55.6 (25/45)

Table 2.18. Summary index sort data from single-cell sorts of blister fluid from acute nevirapine SJS patient 19. Blister fluid cells collected on Day 4 of SJS symptoms from two different anatomical locations were sorted. The number of cells that expressed each T-cell surface marker is reported as % positive (positive/total cells). Data were analyzed using FlowJo software (Tree Star).

Blister Location	Gated Cells	Naïve (CCR7+CD45RO-)	TCM (CCR7+CD45RO+)	TEMRA (CCR7-CD45RO-)	TEM (CCR7-CD45RO+)
Neck	**CD8+CD137-**	8.8 (8/91)	50.5 (46/91)	6.6 (6/91)	34.1 (31/91)
Neck	**CD8+CD137+**	1.1 (2/178)	41.6 (74/178)	1.7 (3/178)	55.6 (99/178)
Left Cheek	**CD8+CD137-**	6.6 (6/91)	36.3 (33/91)	9.9 (9/91)	47.3 (43/91)
Left Cheek	**CD8+CD137+**	0 (0/90)	53.3 (48/90)	0 (0/90)	46.7 (42/90)
Left Cheek	**CD3+CD56+**	2.2 (2/91)	17.6 (16/91)	5.5 (5/91)	74.7 (68/91)
Combined	**CD8+CD137-**	7.7 (14/182)	43.4 (79/182)	8.2 (15/182)	40.7 (74/182)
Combined	**CD8+CD137+**	0.7 (2/268)	45.5 (122/268)	1.1 (3/268)	52.6 (141/268)
Combined	**Total Cells**	3.3 (18/541)	40.1 (217/541)	4.3 (23/541)	52.3 (283/541)
Dominant TCRαβ	**Total Cells**	4.4 (2/45)	37.8 (17.45)	0 (0/45)	57.8 (26/45)

Table 2.19. Memory T-cell subsets from single-cell sorts of blister fluid from acute nevirapine SJS patient 19. Blister fluid cells collected on Day 4 of SJS symptoms from two different anatomical locations were sorted. The number of cells in each memory subset is reported as % positive (positive/total cells). Data were analyzed using FlowJo software (Tree Star). **Legend:** TCM, T central memory cell; TEMRA, T effector memory re-expressing CD45RA cell; TEM, T effector memory cell.

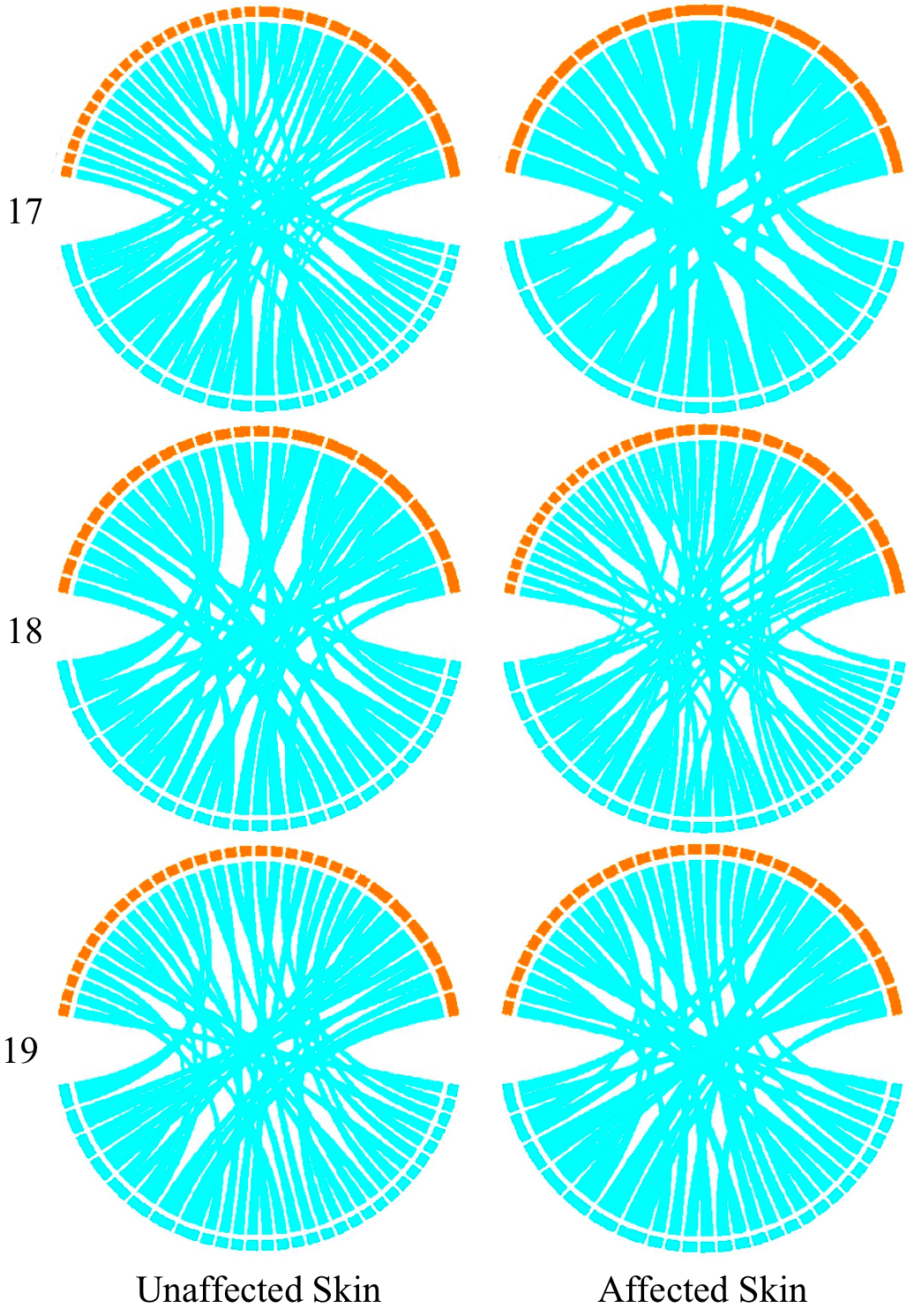

Figure 2.11. T-cell receptor sequencing results of acute skin biopsies from nevirapine SJS/TEN patients. CD3+ T cells from patients 17, 18 and 19 were single-cell sorted and subjected to paired TCRαβ sequencing. The TCRαβ sequencing results were polyclonal. TCRβ CDR3 sequences in blue are paired with TCRα CDR3 sequences in orange. The patient study numbers are labelled on the left.

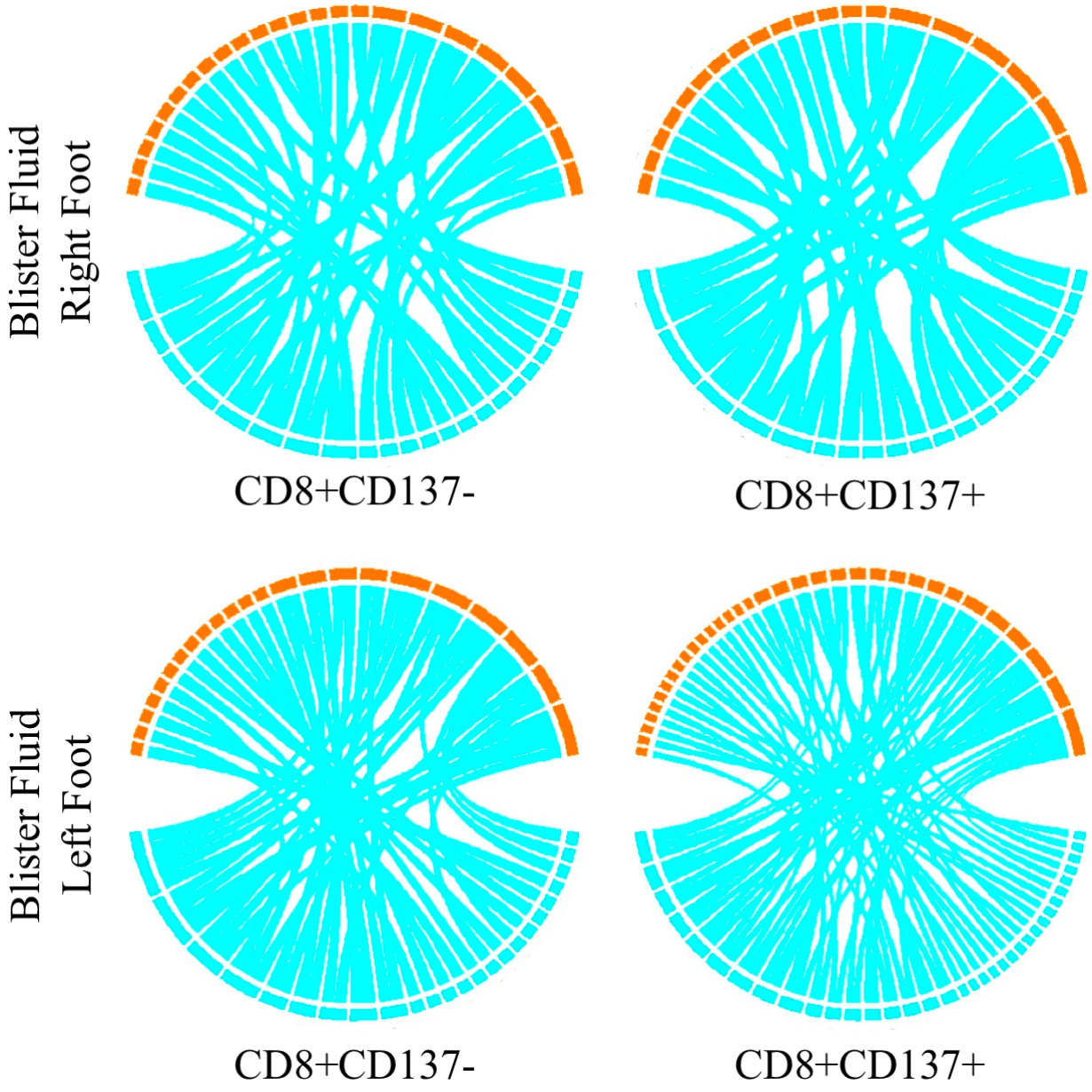

Figure 2.12. T-cell receptor sequencing results of nevirapine SJS/TEN patient 18 single-cell blister fluid sort. The blister fluid was collected 8 days after SJS symptom onset. All sorted cells were CD3+CD8+ T cells. The TCRαβ sequencing results were polyclonal. TCRβ CDR3 sequences in blue are paired with TCRα CDR3 sequences in orange.

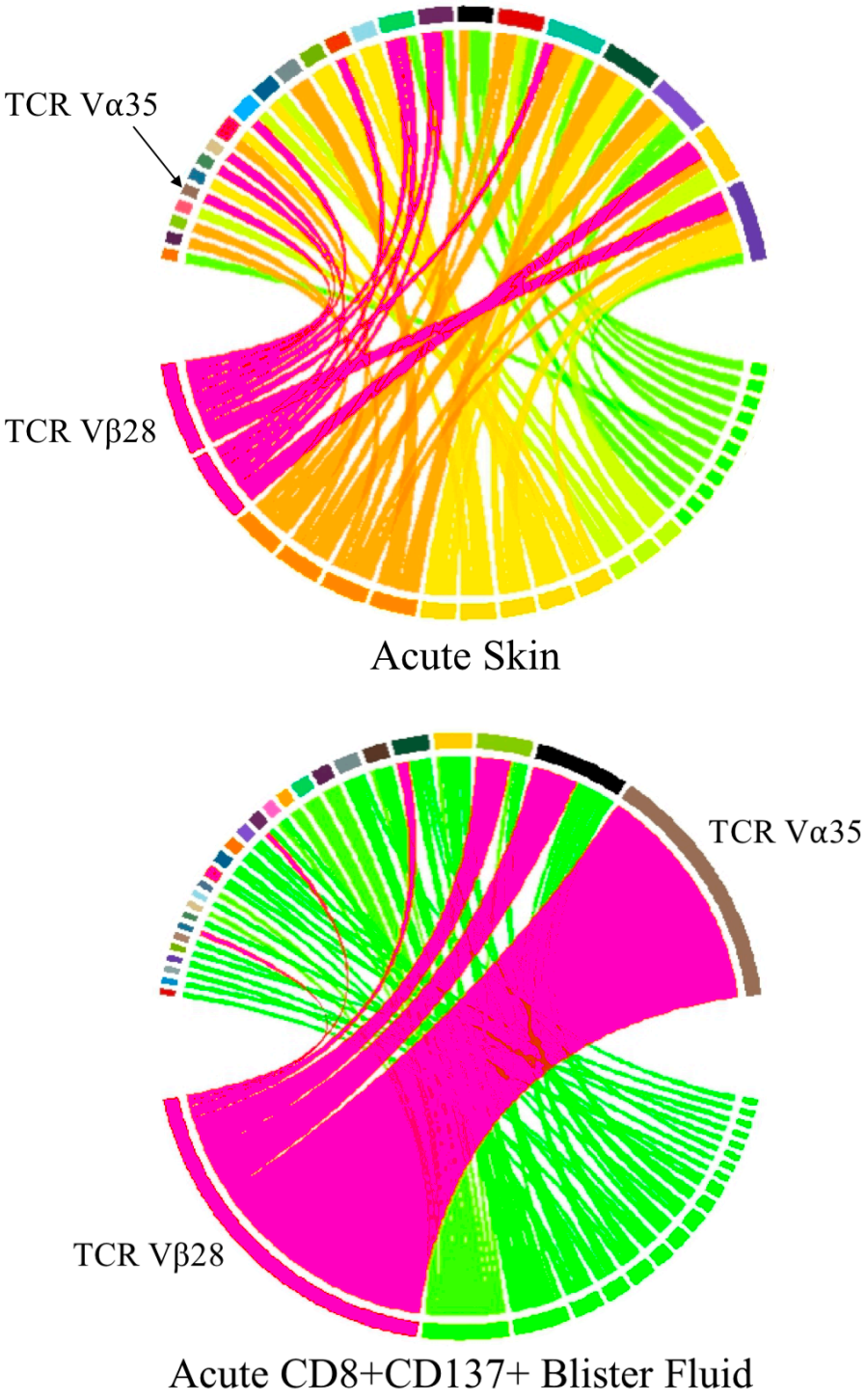

Figure 2.13. Single-cell T-cell receptor sequencing revealed a dominant Vα and Vβ rearrangement in activated CD8+ T cells in acute blister fluid from nevirapine SJS/TEN patient 19. The blister fluid was collected 4 days after SJS symptoms onset. The same TCR Vα Vβ pairing was found in one T cell in the acutely affected skin of the same patient taken on day 5 of SJS symptoms. TCR Vβ rearrangements on the bottom are paired with TCR Vα rearrangements on the top. **Legend:** TCR, T-cell receptor.

central memory (CCR7+/CD45RO+) cell from the affected skin and four CD8+CD137- blister fluid cells also shared this TCR Vα Vβ rearrangement.

Single-cell RNA Sequencing in Acute Nevirapine SJS Blister Fluid and Skin

Analyses of single-cell RNA sequencing results comparing total blister fluid cells (904 cells) to total skin cells (310 cells) from patients 18 and 19 revealed significantly higher levels of several immune-related genes in the blister fluid cells (Figures 2.14 and 2.15 and Table 2.20). Notably, genes encoding several cytotoxic proteins including granulysin (*GNLY*), granzyme B (*GZMB*) and perforin (*PRF1*) were expressed at very significantly higher levels in the blister fluid compared to the skin ($p=1.1x10^{-57}$, $7.3x10^{-24}$ and $5.9x10^{-9}$, respectively). Known co-receptors for HIV cell entry, *CXCR6* and *CCR5*, were also more highly expressed in the blister fluid ($p=8.5x10^{-11}$ and $7.4x10^{-7}$, respectively) as well as *TIGIT,* (T cell immunoreceptor with Ig and ITIM domains), which has been associated with clinical markers of HIV disease progression[159-161]. As expected, the dominant TCR Vβ chain (TRBV28) was also more highly expressed in the blister fluid cells ($p=3.0x10^{-7}$).

I then used the single-cell TCR sequencing results to distinguish the blister fluid cells from SJS patient 19 that carried the dominant TRBV28 chain (128 total cells) from the patient's other blister fluid T cells (408 total cells) and compared the single-cell RNA sequencing results from these two groups (Figures 2.16 and 2.17 and Table 2.21). As expected, the cells that carried the dominant TCR Vβ chain by TCR sequencing expressed significantly more of the *TRBV28* gene than the other blister fluid cells ($p=1.7x10^{-17}$). The T cells with TRBV28 expressed higher levels of cytotoxic proteins (GNLY, GZMB, PRF1) compared to the other blister fluid cells ($p=2.2x10^{-23}$,

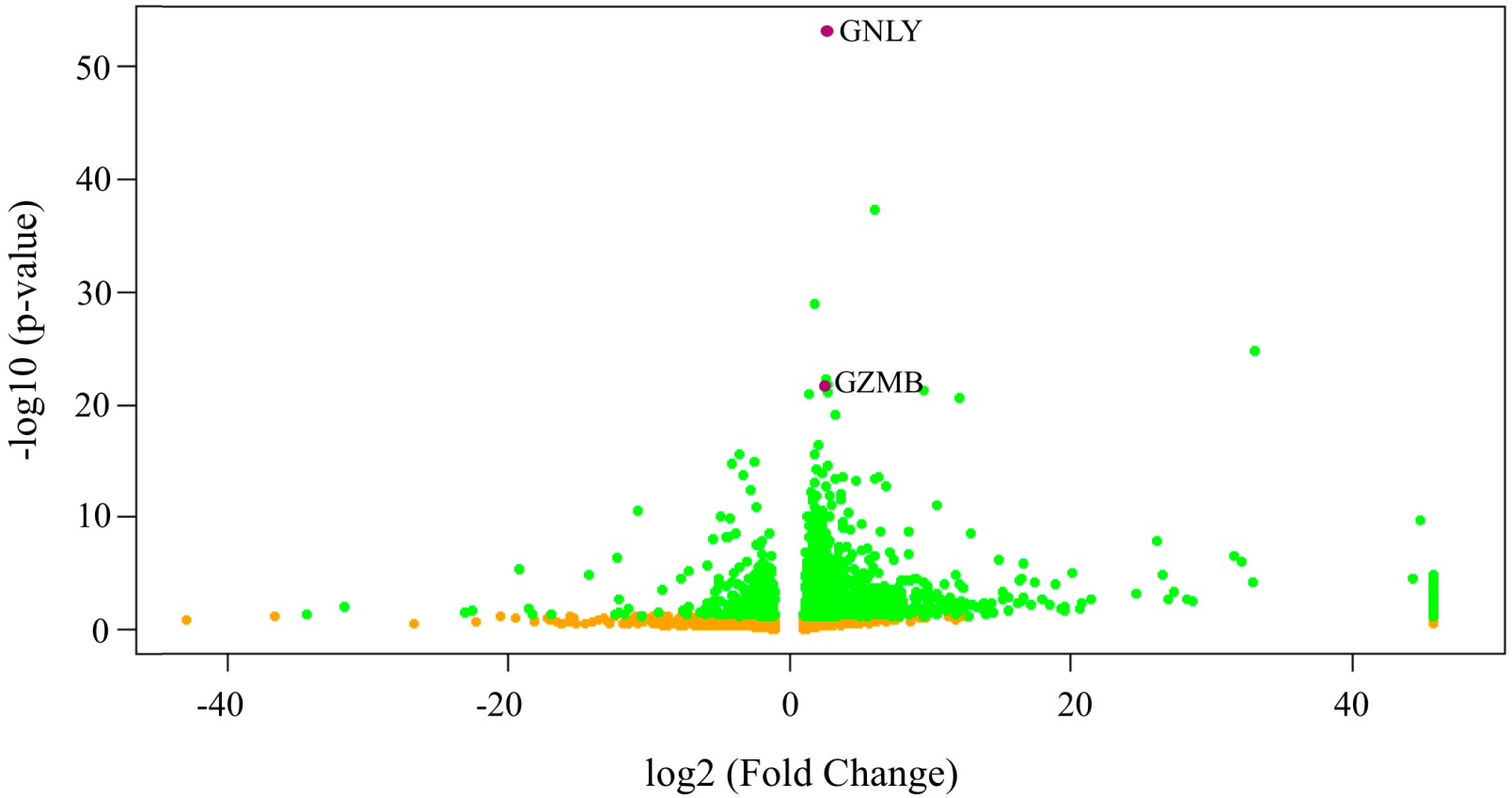

Figure 2.14. Single-cell RNA sequencing revealed that acute nevirapine SJS/TEN cells in the blister fluid were phenotypically more cytotoxic than cells in the skin. The volcano plot compares single-cell RNA sequencing results between total blister fluid cells (904 cells) and total skin cells (310 cells) from acute nevirapine SJS/TEN patients 18 and 19. Each dot represents an expressed gene. Genes represented with green and magenta dots are significantly differentially expressed between the two groups ($p<0.05$). Genes represented with orange dots are not differentially expressed. The x-axis depicts the fold change difference in gene expression between the two groups. Genes more highly expressed in the blister fluid are on the right and genes more highly expressed in the skin are on the left. The blister fluid cells expressed significantly higher levels of cytotoxic genes including granulysin (*GNLY*) and granzyme B (*GZMB*) (represented with magenta dots) compared to the skin ($p=1.1\times10^{-57}$, 7.3×10^{-24}, respectively).

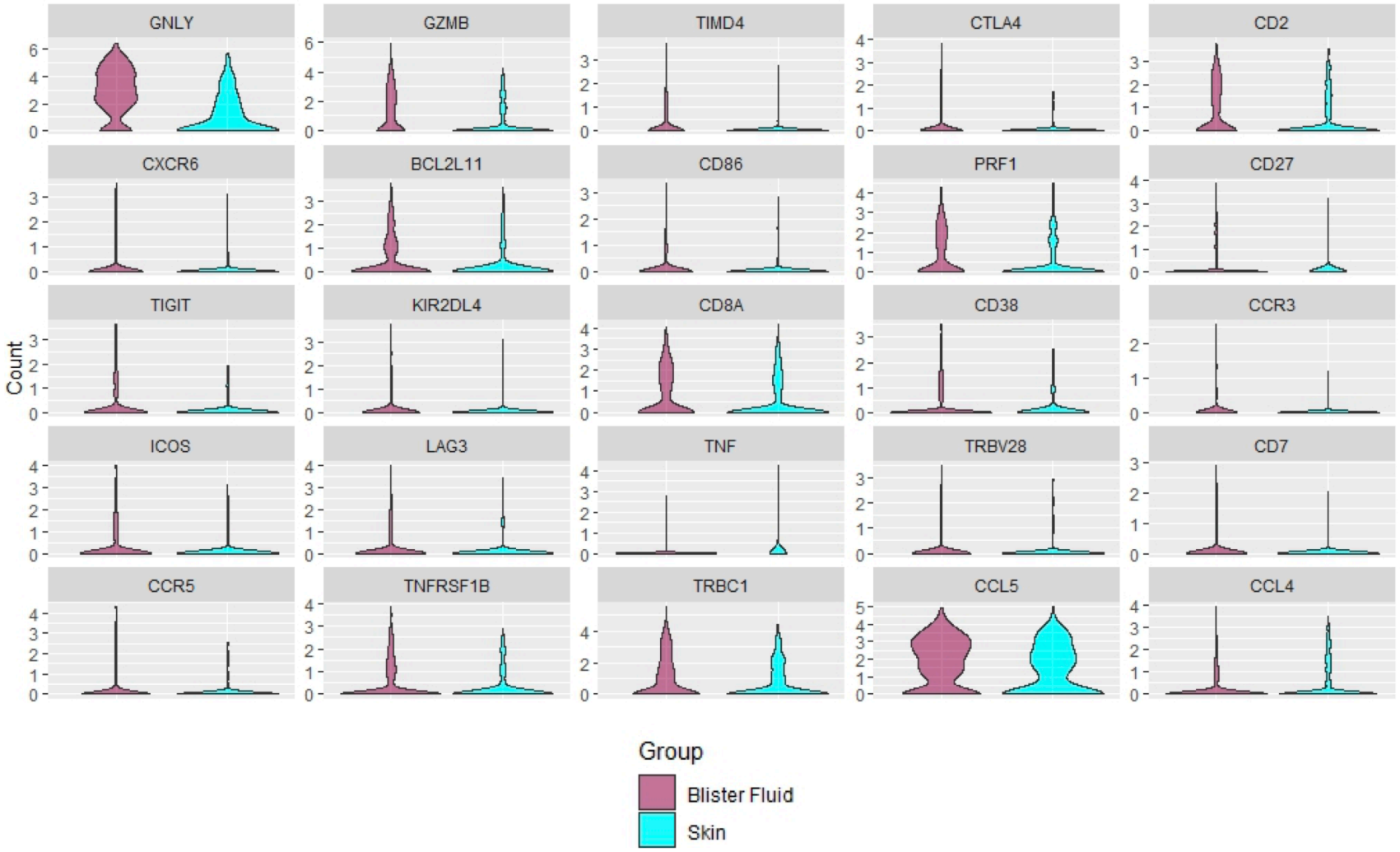

Figure 2.15. Violin plots of the top differentially expressed immune-related genes between acute nevirapine SJS/TEN blister fluid and skin. The plots compare single-cell RNA sequencing results between total blister fluid cells (904 cells) and total skin cells (310 cells) from acute nevirapine SJS/TEN patients 18 and 19. All genes shown except *TNF* and *CCL4* were more highly expressed in blister fluid than skin.

	Blister Fluid			Skin			
Gene	**Average Expression**	**Expressed**	**Not Expressed**	**Average Expression**	**Expressed**	**Not Expressed**	**p-value**
GNLY	2.88	729	134	1.11	153	157	1.1×10^{-57}
GZMB	1.36	507	356	0.57	88	222	7.3×10^{-24}
TIMD4	0.30	194	669	0.03	8	302	1.9×10^{-23}
CTLA4	0.23	143	720	0.04	9	301	5.2×10^{-15}
CD2	0.89	422	441	0.46	86	224	6.5×10^{-12}
CXCR6	0.20	127	736	0.04	10	300	8.5×10^{-11}
BCL2L11	0.56	319	544	0.25	49	261	9.1×10^{-11}
CD86	0.20	126	737	0.05	14	296	3.2×10^{-10}
PRF1	0.90	412	451	0.52	87	223	5.9×10^{-9}
CD27	0.39	221	642	0.16	31	279	8.6×10^{-9}
TIGIT	0.27	175	688	0.10	26	284	1.0×10^{-8}
KIR2DL4	0.20	116	747	0.05	11	299	1.5×10^{-8}
CD8A	0.88	411	452	0.52	89	221	1.7×10^{-8}
CD38	0.35	233	630	0.16	43	267	2.5×10^{-8}
CCR3	0.10	81	782	0.02	9	301	3.7×10^{-8}
ICOS	0.30	182	681	0.11	24	286	5.1×10^{-8}
LAG3	0.27	164	699	0.10	22	288	1.4×10^{-7}
TNF	0.02	17	846	0.26	43	267	1.4×10^{-7}
TRBV28	0.16	89	774	0.04	7	303	3.0×10^{-7}
CD7	0.16	106	757	0.04	11	299	3.7×10^{-7}
CCR5	0.23	137	726	0.08	18	292	7.4×10^{-7}
TNFRSF1B	0.48	276	587	0.26	57	253	8.0×10^{-7}
TRBC1	1.04	438	425	0.67	116	194	9.0×10^{-7}
CCL5	1.79	630	233	1.35	177	133	1.5×10^{-6}
CCL4	0.21	148	715	0.47	89	221	1.5×10^{-6}

Table 2.20. Average expression of the top differentially expressed immune-related genes between acute nevirapine SJS/TEN blister fluid and skin. The table compares single-cell RNA sequencing results between total blister fluid cells (904 cells) and total skin cells (310 cells) from acute nevirapine SJS/TEN patients 18 and 19. The "expressed" and "not expressed" columns depict the total number of cells in each category that either do or do not express each gene. All genes shown except *TNF* and *CCL4* were more highly expressed in blister fluid than skin.

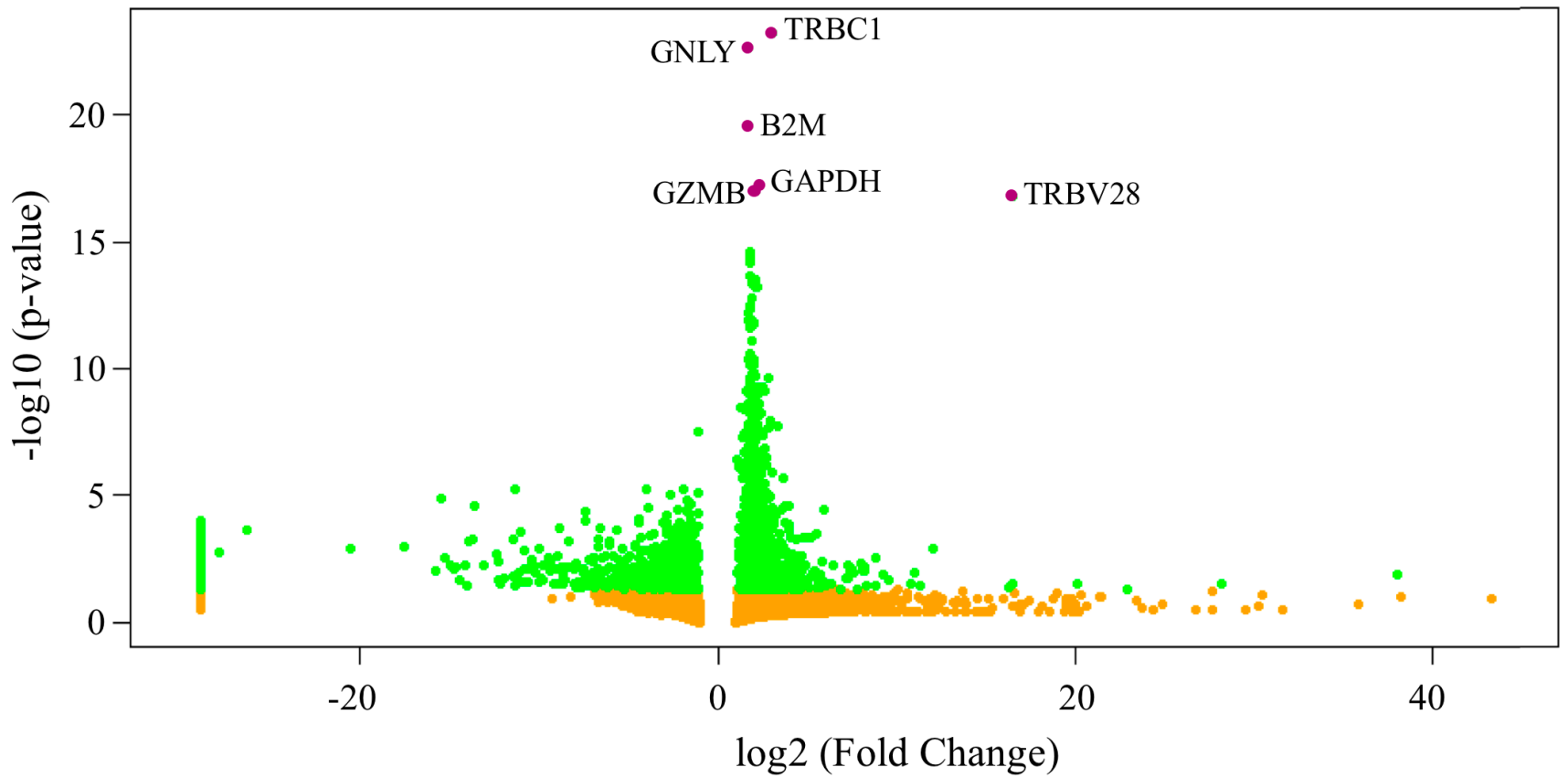

Figure 2.16. Single-cell RNA sequencing revealed that blister fluid with the dominant TCR Vβ were phenotypically more cytotoxic than the other blister fluid cells. The volcano plot compares single-cell RNA sequencing results between the blister fluid cells expressing TRBV28 on TCR sequencing (128 cells) and the other blister fluid cells (408 cells) from acute nevirapine SJS/TEN patient 19. Each dot represents an expressed gene. Genes represented with green and magenta dots are significantly differentially expressed between the two groups ($p<0.05$). Genes represented with orange dots are not differentially expressed. The x-axis depicts the fold change difference in gene expression between the two groups. Genes more highly expressed in the blister fluid cells with TRBV28 are on the right and more highly expressed in the other blister fluid cells are on the left. The top differentially expressed genes were *TRBC1* ($p=5.8\times10^{-24}$), *GNLY* ($p=2.2\times10^{-23}$), *B2M* ($p=2.4\times10^{-20}$), *GAPDH* ($p=5.4\times10^{-18}$), *GZMB* ($p=1.0\times10^{-17}$) and *TRBV28* ($p=1.7\times10^{-17}$) (represented with magenta dots). Expression of all of these genes was higher in the blister fluid cells with TRBV28.

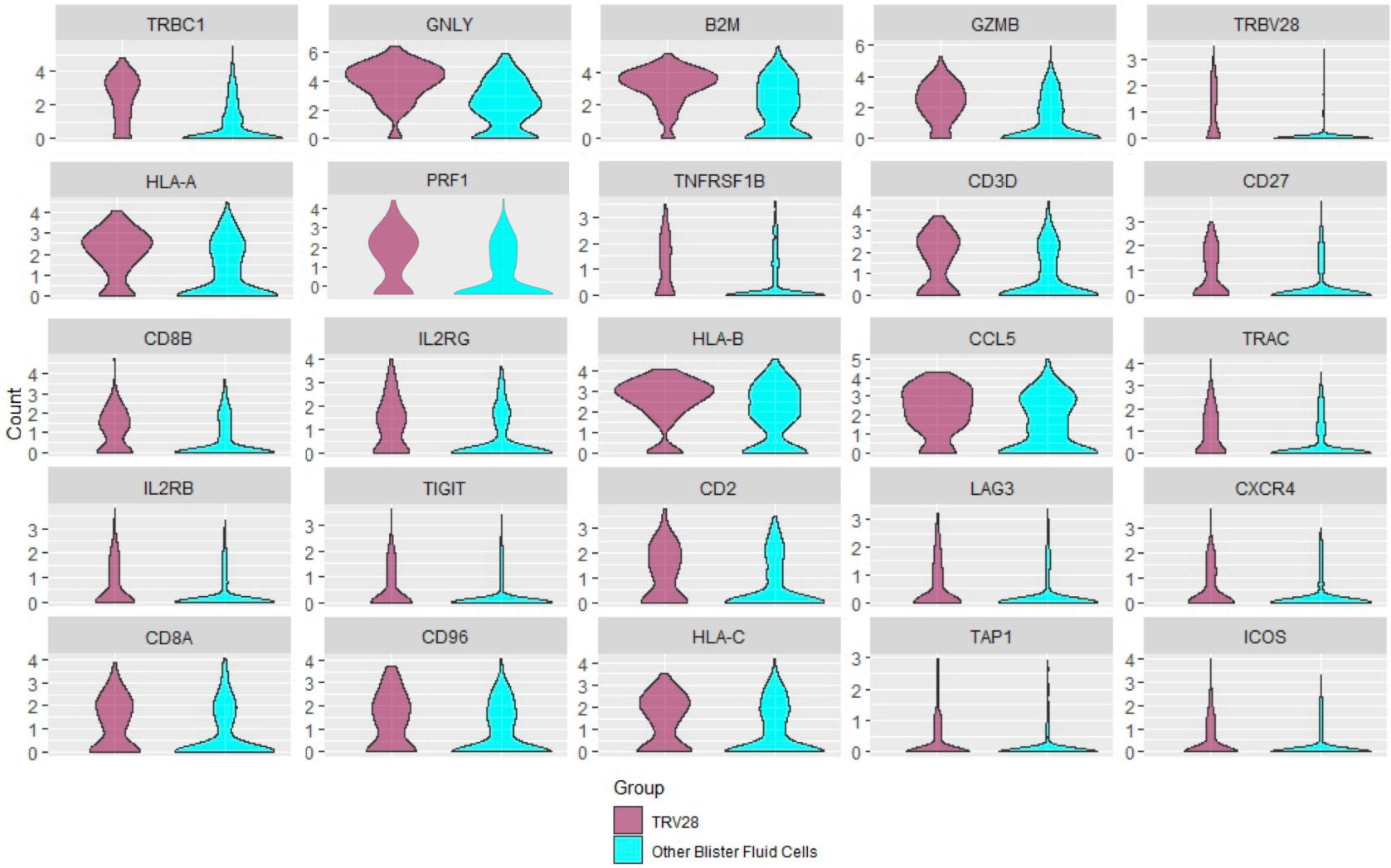

Figure 2.17. Violin plots of the top differentially expressed immune-related genes between blister fluid with the dominant TCR Vβ and blister fluid cells with other TCR Vβ chains. The plots compare single-cell RNA sequencing results between the blister fluid cells expressing TRBV28 on TCR sequencing (128 cells) and the other blister fluid cells (408 cells) from acute nevirapine SJS/TEN patient 19. All genes shown were more highly expressed in the blister fluid cells with TRBV28.

	Blister Fluid with Dominant TCR Vβ			Other Blister Fluid Cells			
Gene	Average Expression	Expressed	Not Expressed	Average Expression	Expressed	Not Expressed	p-value
TRBC1	2.36	108	20	0.78	171	237	$5.8x10^{-24}$
GNLY	3.89	122	6	2.28	314	94	$2.2x10^{-23}$
B2M	3.12	122	6	1.86	281	127	$2.4x10^{-20}$
GZMB	2.28	112	16	1.07	200	208	$1.0x10^{-17}$
TRBV28	0.91	70	58	0.06	19	389	$1.7x10^{-17}$
HLA-A	1.98	105	23	1.14	219	189	$2.4x10^{-11}$
PRF1	1.66	93	35	0.83	183	225	$4.4x10^{-11}$
TNFRSF1B	1.09	79	49	0.43	117	291	$5.0x10^{-10}$
CD3D	1.55	88	40	0.83	177	231	$1.7x10^{-8}$
CD27	0.84	65	63	0.30	78	330	$2.1x10^{-8}$
CD8B	1.15	85	43	0.58	149	259	$3.8x10^{-8}$
IL2RG	1.21	85	43	0.60	145	263	$4.8x10^{-8}$
HLA-B	2.46	111	17	1.78	288	120	$5.4x10^{-8}$
CCL5	2.20	109	19	1.51	262	146	$1.9x10^{-7}$
TRAC	0.90	74	54	0.46	126	282	$5.3x10^{-6}$
IL2RB	0.65	54	74	0.26	79	329	$6.2x10^{-6}$
TIGIT	0.54	49	79	0.19	55	353	$8.6x10^{-6}$
CD2	1.19	82	46	0.72	162	246	$1.6x10^{-5}$
LAG3	0.56	49	79	0.23	68	340	$6.8x10^{-5}$
CXCR4	0.57	50	78	0.24	68	340	$7.3x10^{-5}$
CD8A	1.22	81	47	0.78	172	236	$1.1x10^{-4}$
CD96	1.32	85	43	0.88	203	205	$1.4x10^{-4}$
HLA-C	1.35	85	43	0.94	203	205	$4.2x10^{-4}$
TAP1	0.36	38	90	0.14	50	358	$5.7x10^{-4}$
ICOS	0.46	43	85	0.21	61	347	$8.3x10^{-4}$
CCR5	0.39	31	97	0.14	45	363	0.001

Table 2.21. Average expression of the top differentially expressed immune-related genes between blister fluid with the dominant TCR Vβ and blister fluid cells with other TCR Vβ chains. The table compares single-cell RNA sequencing results between the blister fluid cells expressing TRBV28 on TCR sequencing (128 cells) and the other blister fluid cells (408 cells) from acute nevirapine SJS/TEN patient 19. The "expressed" and "not expressed" columns depict the total number of cells in each category that either do or do not express each gene. All genes shown were more highly expressed in the blister fluid cells with TRBV28.

$1.0x10^{-17}$ and $4.4x10^{-11}$, respectively). Known co-receptors for HIV cell entry, *CXCR6* and *CCR5*, were also more highly expressed in the blister fluid cells with TRBV28 ($p=8.5x10^{-11}$ and $7.4x10^{-7}$, respectively) as well as *TIGIT* ($p=8.6x10^{-6}$). All HLA class I receptors (HLA-A, HLA-B and HLA-C) were more highly expressed in the blister fluid cells with TRBV28 ($p=2.4x10^{-11}$, $5.4x10^{-8}$ and $4.2x10^{-4}$, respectively).

DISCUSSION

Nevirapine use in antiretroviral therapy is limited by severe cutaneous adverse reactions including SJS/TEN and DRESS. Strategies to predict the development of nevirapine IM-ADRs would hence facilitate first-line global use of this drug. With this goal in mind, we put together a well-phenotyped cohort of South African patients with nevirapine hypersensitivity and nevirapine tolerant controls.

Overall, the nevirapine hypersensitive patients and tolerant controls were relatively similar patient cohorts. All individuals were infected with HIV, there was no discrepancy in age between hypersensitive and tolerant individuals, and the majority of both groups were of African ancestry with some mixed ancestry. The median latency between drug initiation and reaction of 19 days for SJS/TEN and 28.5 days for DRESS matched the expected latency periods for these reactions. While many of these patients were on other medications including trimethoprim-sulfamethoxazole and anti-tuberculous agents known to be associated with IM-ADRs, drug causality assessments determined nevirapine to be the most likely cause of the reaction in all cases. Patients developed SJS/TEN with a wide range of CD4+ T cell counts. In contrast to SJS/TEN, all patients who developed DRESS, had a CD4+ T cell count over 200 cells/μL suggesting that lower CD4+ T cell

counts may be protective against nevirapine DRESS development. This supports that hypothesis that SJS/TEN is an HLA Class I restricted disease that does not require the need for CD4+ T cell help while nevirapine DRESS is thought to be dependent on both CD4+ and CD8+ T cells[77,106].

In this cohort, women were more likely to have a severe reaction than men. While women have more reported side effects to medications and early studies in HIV-coinfected individuals suggested that women may develop more nevirapine rash, sex overall is not thought to influence the likelihood of developing a severe hypersensitivity[162]. In addition, in contemporary practice in South Africa, men and women tend to be given nevirapine for different reasons. HIV-positive women of childbearing age are frequently prescribed nevirapine because it is safe in pregnancy. Nevirapine is also increasingly being used in patients co-infected with HIV and multi-drug resistant tuberculosis, and this is the setting in which men are commonly prescribed the drug. Therefore, the women in this cohort tended to have higher CD4+ T cell counts and fewer opportunistic infections when prescribed nevirapine. Because many of the nevirapine tolerant patients were recruited from tuberculosis treatment facilities, more men were enrolled as tolerant controls. However, the differences in reaction frequency are notable and warrant further study.

In this South African population, I identified a strong association between HLA-C*04:01 and nevirapine SJS/TEN. All nevirapine SJS/TEN patients in this cohort carried this allele resulting in a 100% negative predictive value for HLA-C*04:01 in this population and suggesting that this allele is necessary but not sufficient for SJS/TEN development (Figure 2.7 and Table 2.5). While HLA-C*04:01 has previously been associated with nevirapine SJS/TEN in African populations, to my knowledge, this is the first time this association has been studied specifically in a South

African cohort and found to be present in all individuals with SJS/TEN. The 100% negative predictive value for HLA-C*04:01 in this cohort is likely due to the careful phenotyping of the SJS/TEN cases.

Similar to nevirapine, a drug hypersensitivity syndrome that was easily confused with other AIDS-related morbidities was the major treatment-limiting short-term toxicity of abacavir. As a result, safe use of abacavir-based regimens to treat HIV was limited. Following the discovery of the association between abacavir hypersensitivity syndrome and HLA-B*57:01, a guideline-based strategy for HLA-B*57:01 screening has been implemented in the developed world. Now, following negative HLA-B*57:01 screening, abacavir is widely prescribed as part of single tablet once-daily combination antiretroviral treatment regimen. Similarly, based on the results described here, HLA-C*04:01 screening could be used before nevirapine prescription to prevent SJS/TEN. With an estimated positive predictive value of 2.4%, this would translate into a number needed to test for HLA-C*04:01 to prevent one case of SJS/TEN of roughly 200 individuals.

The nevirapine DRESS cases suggest that HLA-B*44:03 and HLA-B*45:01 may represent novel HLA-B risk alleles associated with nevirapine DRESS in South African Black populations (Table 2.7). However, further research with more cases of nevirapine DRESS will be needed to confirm this finding.

Based on CYP2B6 genotyping results, patients with nevirapine hypersensitivity had slower nevirapine metabolizing phenotypes than drug tolerant controls (Tables 2.8 and 2.9). Therefore, accumulation of the parent drug appears to be a factor in risk of severe hypersensitivity

development. Rapid metabolism could be protective since this would result in less drug available for presentation by HLA-C*04:01. This may help explain why some HLA-C*04:01 positive individuals tolerate nevirapine. This observation is in line with current literature which recognizes that most immune-mediated adverse reactions are dose-related as opposed to historical classifications which categorized off-target reactions as dose-independent[163]. Notably, the DRESS patients had significantly slower nevirapine metabolizing genotypes than the tolerant controls based on their *CYP2B6* rs3745274 minor allele carriage. Interestingly, 4/6 of these patients were on additional medications known to be metabolized in part through CYP enzymes which are known to play a role in nevirapine metabolism including olanzapine (metabolized in part through CYP2D6), risperidone (metabolized in part through CYP2D6), trimethoprim-sulfamethoxazole (metabolized in part through CYP2C9) and citalopram (metabolized in part through CYP3A4 and CYP2D6) (Figure 2.1). One possibility is that the addition of these medications in the setting of already slow nevirapine metabolism has the potential to further increase nevirapine plasma levels or levels of specific metabolites, and therefore increase the risk of a serious adverse drug reaction.

The significant association of nevirapine SJS/TEN with *ERAP1* SNP rs27044 suggests that the repertoire of peptides available to be presented to T cells in the presence of the drug may contribute to the development of hypersensitivity (Table 2.10). *ERAP1* SNP rs27044 leads to amino acid change Q730E in the ERAP1 enzyme, which is thought to decrease aminopeptidase activity[164]. Additionally, rs27044 is known to be important in HLA-restricted diseases as this SNP has been previously associated with the autoimmune disease ankylosing spondylitis in HLA-B*27 positive individuals[165,166]. Other factors such as ERAP allotype and carriage of other HLA class I alleles could impact TCR repertoire. However, in this cohort, no other HLA class I alleles were associated

with increased risk of SJS/TEN in this population and no other ERAP SNPs remained significant after adjustment of rs27044(C) carriage. The addition of rs27044(C) genotyping could be added to HLA-C*04:01 testing to increase to positive predictive value of genetic testing for nevirapine SJS/TEN (Figure 2.18). Compared to HLA-C*04:01 testing alone which has a positive predictive value of 2.4% and a negative predictive value of 100%, the addition of rs27044(C) genotyping would increase the positive predictive value to 4.4% with only a small reduction in negative predictive value to 99.94%. While a 100% negative predictive value is obviously ideal, in a patient who is known to be HLA-C*04:01 positive, but for whom nevirapine is the best treatment option, such as a pregnant woman initiating antiretroviral therapy or a patient co-infected with HIV and multi-drug resistant tuberculous on bedaquiline-based therapy, rs27044(C) genotyping could be used in a risk stratification algorithm to determine the best treatment options. HLA-C*04:01 testing with rs27044(C) genotyping could also be used as a diagnostic test after a patient develops SJS/TEN in the setting multiple concurrently dosed drugs to determine how likely nevirapine is to be the causative agent.

Although HLA-C is a known ligand for KIRs on NK cells, the nevirapine hypersensitive patients did not differ in their carriage of specific KIRs from nevirapine tolerant controls or other South African populations with known KIR genotyping (Tables 2.12 and 2.13). While presence or absence of specific KIRs did not affect risk of severe nevirapine hypersensitivity development in this cohort, these data do not rule out the possibility that specific SNPs within KIRs may influence reaction risk. Relevant to this observation, specific mutations in KIR genes have recently been found to affect KIR and HLA-C interaction in populations from Southern Africa[167].

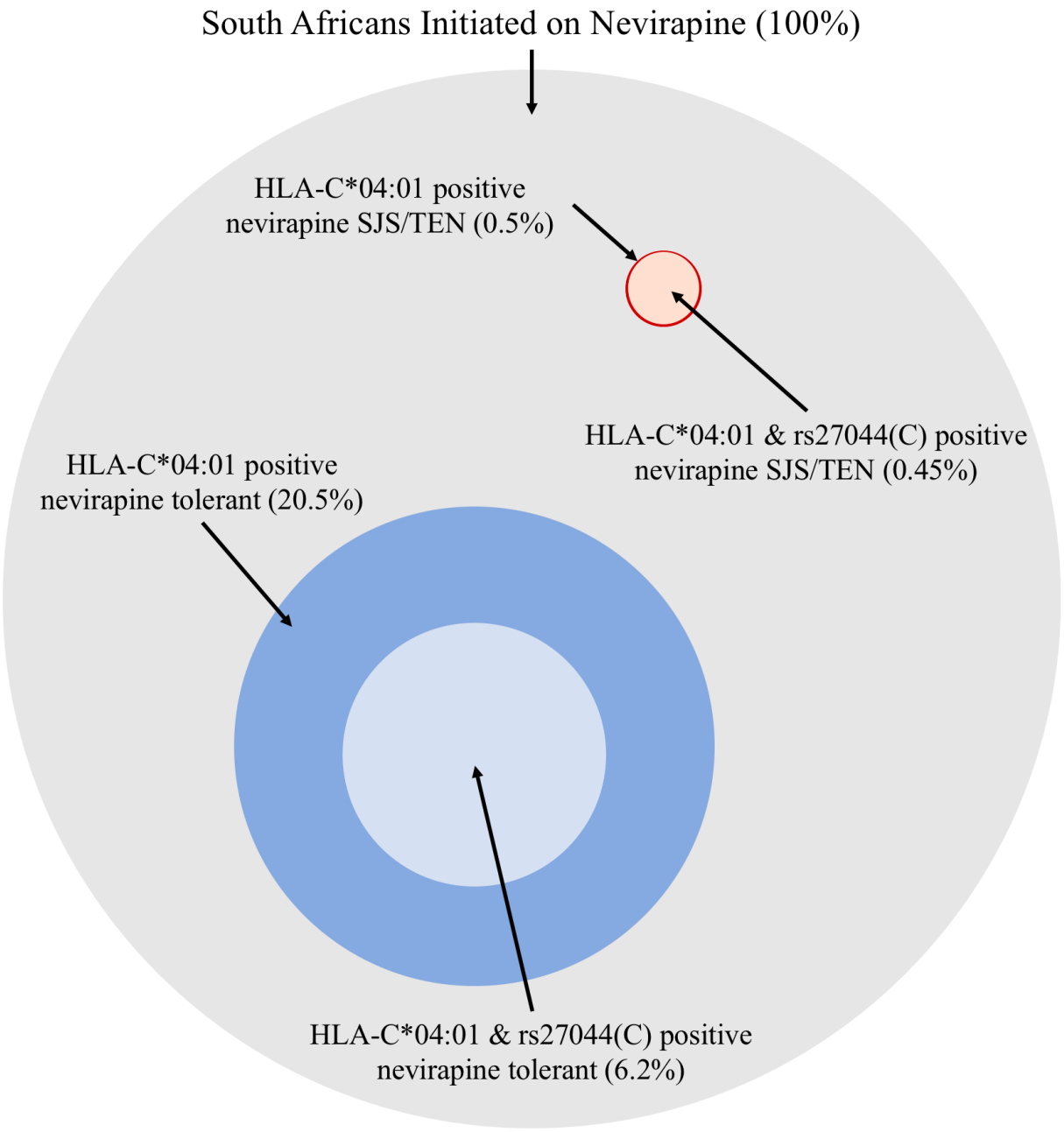

Figure 2.18. Relationship between HLA-C*04:01 and rs27044(C) carriage and nevirapine SJS/TEN development in our South African patient cohort. 100% (20/20) of the nevirapine SJS/TEN patients carried HLA-C*04:01. 90% (18/20) also carried rs27044(C).

In addition to strong genetic associations with nevirapine severe hypersensitivity reactions, this study specifically highlights the importance of studying the cells at the sites of disease. In the immunohistochemistry and cell sorting experiments, CD8+ T cells were a dominant population in acute nevirapine SJS/TEN skin and blister fluid supporting the conclusion that this is an HLA Class I restricted disease (Figure 2.9 and Tables 2.14, 2.16 and 2.18). However, the especially low numbers of CD4+ T cells in the skin and blister fluid from patients with acute nevirapine SJS/TEN may be due in part to the low overall CD4+ T cells counts in these HIV-infected patients. Loss of protective CD4+ regulatory T cells in the skin has previously been postulated as a risk factor for SJS/TEN in HIV-infected patients[168]. In addition, an HLA-B*57:01 transgenic mouse model of abacavir hypersensitivity supported that CD4+ depletion was necessary for dendritic cell maturation and provided a mechanism by which CD4+ T cells may mediate tolerance to the altered endogenous peptide repertoire induced by abacavir in this context[169,170]. Furthermore, the high granulysin concentrations in the acute plasma and blister fluid supernatant are biologically congruent with previous studies which demonstrated elevated granulysin levels as the key SJS/TEN biomarker mediating epidermal necrosis[35].

While the single cell studies are limited by the number of patient samples included, the difference in TCR clonality between the blister fluid samples from nevirapine SJS/TEN patients 18 and 19 highlights the importance of the timing of the samples. While the samples were both collected the day after the patient was transferred to the Groote Schuur Hospital dermatology ward, the sample from patient 18 was collected 8 days after initial SJS/TEN symptom development and contained polyclonal population of T cells based on TCR sequencing. In contrast, the blister fluid cells from patient 19, collected at the more acute time point of only 4 days after symptom development,

expressed a dominant TCR Vβ chain in 45% of the activated (CD137) CD8+ T cells. More patient samples will be needed to verify these findings, but this could suggest that the population of cells in the blister fluid becomes more polyclonal as the reaction progresses and more cells are recruited to the sites of disease.

The finding of a dominant population of highly cytotoxic TRBV28+ CD8+ T cells in the blister fluid of an acute nevirapine SJS/TEN patient is an important step in identifying the most likely candidate drug-specific T cells. The high levels of granulysin expression in the blister fluid cells support the granulysin ELISA data from the blister fluid supernatant. The fact that >90% of the blister fluid CD8+ T cells sorted were CD45RO+ memory cells supports the heterologous immunity model of drug hypersensitivity, which predicts that a substantial proportion of drug-specific responses stem from activation of pathogen-specific T cells sensitized much earlier that subsequently recognize a neoantigen created by drug exposure[9].

A few obvious viruses come to mind when considering potential pathogens to which these T cells have been sensitized. Since nevirapine in an antiretroviral medication, all individuals in this study are known to be infected with HIV. Additionally, the majority of individuals with HIV are co-infected with herpes simplex virus type 1 (HSV1) and cytomegalovirus (CMV). The potential importance of HIV infection in nevirapine hypersensitivities is particularly difficult to study in this cohort in part because very few patients had viral load measurements around the time of nevirapine exposure. Furthermore, nevirapine is no longer used in adult populations for exposure prophylaxis because of the risk of life-threatening, non-immune-mediated liver toxicities in individuals with higher CD4+ T cell counts[171,172]. The possibility that viruses play a role in severe nevirapine

hypersensitivity development is especially intriguing when one considers the high expression of HIV co-receptors in the blister fluid T cells. One potential hypothesis for virus involvement is that since HIV's negative regulatory factor (Nef) protein is known to selectively down-regulate HLA-A and HLA-B to minimize cytotoxic lymphocyte surveillance while maintaining HLA-C expression to maintain NK cell inhibition, HIV infection would increase the likelihood of a patient developing an HLA-C-restricted disease such as nevirapine SJS/TEN[173,174].

This work has provided several insights into the immunopathogenesis of nevirapine hypersensitivities, and specifically nevirapine-induced SJS/TEN. Overall, the results support the model that SJS/TEN develops when nevirapine interacts with peptide-bound HLA-C*04:01 on antigen-presenting cells, which activate drug-specific CD8+ cytotoxic T cells (Figure 2.19). These drug-specific T cells produce high levels of granulysin, which are capable of causing keratinocyte death. Future research should focus on further elucidating the specificities of the cytotoxic T cells mediating the adverse reaction and the implementation of genetic screening tests to improve the safety of nevirapine therapy.

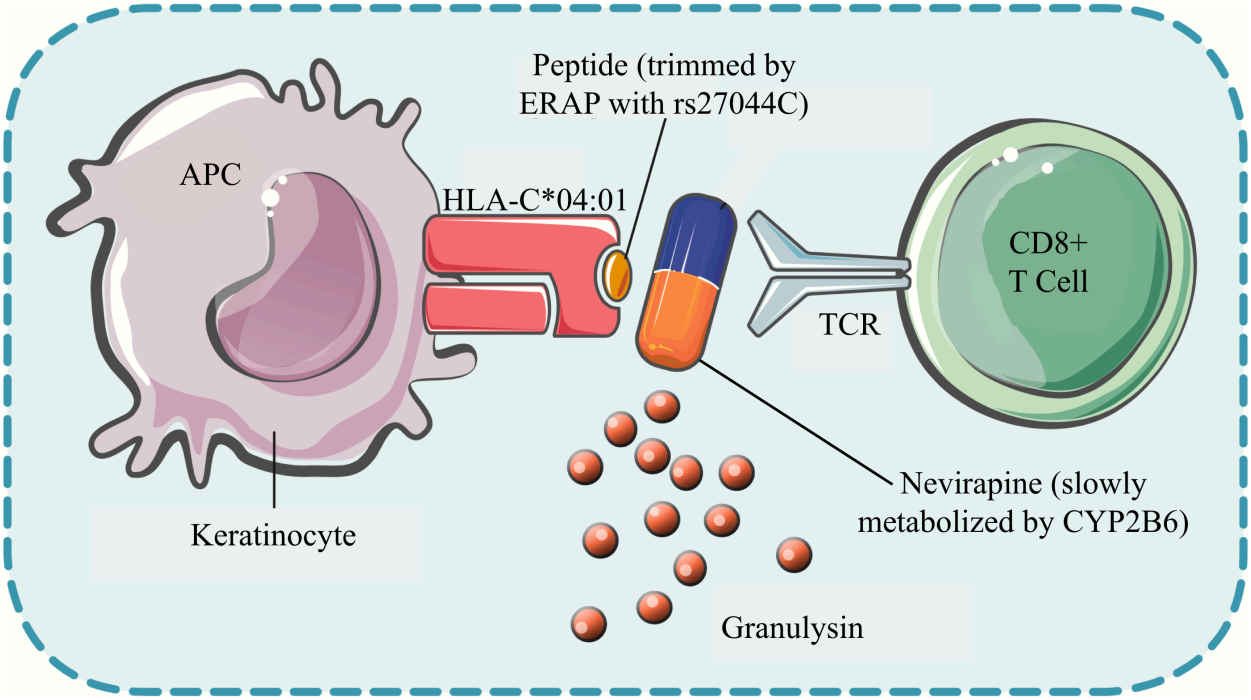

Figure 2.19. Model of proposed pathogenic mechanisms in nevirapine-induced SJS/TEN. Nevirapine likely interacts with peptide-bound HLA-C*04:01 on keratinocytes that act as antigen-presenting cells to activate drug-specific CD8+ cytotoxic T cells. **Legend:** APC, antigen-presenting cell; HLA, human leukocyte antigen; ERAP, endoplasmic reticulum aminopeptidase; CYP2B6, cytochrome P450 2B6; TCR, T-cell receptor. Adapted from Peter, Lehloenya, Dlamini, Risma, White, Konvinse, *et al*, *JACI: In Practice* (2017).

CHAPTER III

HLA-A*32:01 IS STRONGLY ASSOCIATED WITH VANCOMYCIN-INDUCED DRUG REACTION WITH EOSINOPHILIA AND SYSTEMIC SYMPTOMS

INTRODUCTION

Vancomycin is a widely used antibiotic of global importance for the treatment of serious, deep-seated, antibiotic-resistant Gram-positive infections which frequently require prolonged treatment courses. Worldwide the use of vancomycin is increasing because of the increasing incidence of methicillin-resistant *Staphylococcus aureus* infections. Vancomycin is associated with infusional pruritus and rash ("red man syndrome") which is managed by decreasing the infusion rate and anti-histamines. However, vancomycin is also a very common cause of a life-threatening delayed T-cell-mediated reaction known as drug reaction with eosinophilia and systemic symptoms (DRESS) and has been implicated in up to 40% of antibiotic-related cases[64,175]. DRESS, otherwise known as drug-induced hypersensitivity syndrome, typically develops 2-8 weeks after drug initiation and presents with features including fever, a widespread rash, facial edema, white cell abnormalities, and involvement of internal organs such as the liver, kidneys, heart and lungs[77]. The mortality of DRESS is 1-10% and long-term morbidity such as autoimmune disease has been described up to 4 years following acute disease[176,177]. When DRESS develops in the setting of combination antibiotics and other co-administered drugs, all treatment is stopped and future exposure to all concurrently-dosed drugs is contraindicated due to the associated risks of morbidity and mortality if DRESS reoccurs and the inability to implicate any one drug on clinical grounds

alone. The ability to more definitively diagnose DRESS associated with vancomycin may allow patients not only to avoid the current and future risk of vancomycin exposure but also to continue or resume therapy, particularly with other falsely implicated antibiotics.

METHODS

Vancomycin DRESS Cases

Retrospective patients were detected using Vanderbilt's BioVU repository, a deidentified electronic health record (EHR) database linked to a DNA biobank in operation since February 7, 2007. Prospective patients with potential vancomycin DRESS were enrolled to confirm genetic findings from the BioVU analysis using vancomycin-specific immunological studies to support clinical diagnoses. Patients were prospectively recruited between 2010 and 2018 through drug allergy clinics and inpatient facilities at participating institutions (Vanderbilt University Medical Center in Nashville (Tennessee, USA), Austin Health, Peter MacCallum Cancer Centre, and Alfred Health in Melbourne (Victoria, Australia), Fiona Stanley Hospital and Royal Perth Hospital in Perth (Western Australia, Australia)). Institutional review board (IRB) approvals were in place for the BioVU study and for all sites contributing to the prospective study. All aspects of the study including the collection and storage of DNA, plasma, peripheral blood mononuclear cells (PBMCs) and skin were IRB-approved and all patients provided written or electronic informed consent. Saliva and blood were routinely collected from prospective patients, processed and stored as repositories of DNA, PBMCs and plasma. Patients >17 years of age who were diagnosed with DRESS with vancomycin identified as a primary implicated drug, a corresponding Naranjo adverse drug reaction score of ≥5 (probable adverse drug reaction), a RegiSCAR score of ≥4 (probable DRESS) and available DNA or genotyping were included in the study[144,178]. The

RegiSCAR diagnostic score for DRESS determines the likelihood that the patient's symptoms are due to DRESS. The algorithm considers the signs and symptoms of DRESS including fever, enlarged lymph nodes, atypical lymphocytes, eosinophilia, extensive skin rash, internal organ involvement as well as the length of time until symptom resolution and whether investigations were done to rule out other causes. Any potential duplicate cases between the prospective patients and the BioVU cohort were eliminated by an observer blinded to identifiable patient information.

Vancomycin Tolerant Controls

Controls from the BioVU genotyped cohort (n=54,249) were defined as individuals who tolerated intravenous vancomycin for greater than 5 weeks and had at least five vancomycin therapeutic trough levels over the treatment period recorded in the Vanderbilt EHR. 297/54,249 individuals were prescribed at least 5 weeks of vancomycin treatment. Using this subset, controls were matched 2:1 with cases on sex, race and age within five years. Vancomycin tolerance and length of treatment was verified by manual review of the EHR by a reviewer blinded to the HLA results. Additional controls for vancomycin Enzyme-Linked ImmunoSpot (ELISpot) assays were recruited from our Vanderbilt IRB-approved studies to investigate drug responses in individuals with a broad range of immune-mediated adverse drug reactions and healthy volunteers.

Human Leukocyte Antigen (HLA) Typing

High resolution four-digit HLA A B C DP DR DQ typing was performed using either sequence-based typing on 454FLX or Illumina Miseq[75,146] or imputed from SNP data from HumanExome BeadChip and GWAS platforms by Expanded Multi-Ethnic Genotyping Array (MEGA^{EX}, Illumina), HumanOmni-Quad, HumanOmni5-Quad and Human660W-Quad using SNP2HLA as

previously described[179]. Imputation for HLA-A*32:01 using SNP2HLA has a reported accuracy of 99.46%[9]. Associations between DRESS and carriage of Class I HLA-A/B/C and Class II HLA-DRB1/DQA1/DQB1/DPB1 alleles at the 4-digit level were assessed by conditional logistic regression to accommodate the matching. Analyses were carried out in R version 3.4.3. (R Core Team (2017)). R: A language and environment for statistical computing. R Foundation for Statistical Computing, Vienna, Austria. URL https://www.R-project.org/).

Enzyme-Linked ImmunoSpot (ELISpot) Assays

Overnight IFN-γ ELISpot assays were performed in triplicate (Mabtech Kit 3420-2H) as previously described[106,180,181] and included negative (unstimulated) and positive (anti-CD3 Mabtech antibody and/or Staphylococcal enterotoxin B (SEB)) controls. PBMCs plated at 200,000 cells per well were incubated with pharmacy stock vancomycin and other implicated drugs at concentrations representative of peak serum concentrations (Cmax) as well as 10-fold higher and 10-fold lower than Cmax. As supported by consensus in the literature, a positive response was defined as >50 spot forming units (SFU)/million cells after background removal[106,180,181]. Figures representing ELISpot results were generated using GraphPad Prism 7.0a Macintosh Version, GraphPad Software, La Jolla California USA, www.graphpad.com.

Time-to-Event Analysis of Vancomycin-Exposed BioVU Cohort

In the BioVU cohort of 54,249 patients with available genotyping, we identified 137 patients that were HLA-A*32:01 positive and 1,672 who did not carry HLA-A*32:01 and for whom at least two weeks of intravenous vancomycin treatment was intended. 137 of the 1,672 HLA-A*32:01 negative individuals were randomly selected to serve as an equal-sized control group. The

deidentified EHRs of the 274 patients in both sub-cohorts were reviewed during the period of vancomycin exposure to determine the patients' sex, race, age, longest treatment period, development of an adverse drug reaction (ADR) and specifically, the development of possible DRESS. Since DRESS is an immune-mediated reaction and vancomycin is renally cleared, patient immunosuppression, chronic renal failure and end stage renal failure with dialysis were documented as potential covariates. ADR latency, defined as the length of time from initiation of vancomycin to symptom onset, as well as any concurrent antimicrobials were documented. Analyses were carried out by Fisher's exact tests, logistic and Cox regression as appropriate in R version 3.4.3.

Skin Testing and Histopathology

Intradermal skin testing (IDT) with 0.05, 0.5, 5 and 50 mg/mL of sterile pharmacy grade vancomycin was performed with readings at 20 minutes, 24 and 48 hours on two subjects: patient 18, a prospectively enrolled patient who had experienced probable vancomycin DRESS 6.5 months earlier and C50, an HLA-A*32:01 positive, vancomycin-naïve healthy control. For patient 18, histopathology was examined from the acute DRESS reaction and from a biopsy of the positive 5 mg/ml vancomycin delayed IDT. Formalin-fixed, paraffin-embedded skin biopsies were sectioned at 5 μm intervals. Slides were deparaffinized and stained with hematoxylin and eosin (H&E). For the immunohistochemistry (IHC), slides were placed on the Leica Bond Max IHC stainer and deparaffinized. Slides were incubated with anti-FOXP3 (Cat.14-4777-82, eBioscience, Inc.) for one hour at a 1:100 dilution, Ready-To-Use anti-CD4 (PA0427, Leica) for one hour, or Ready-To-Use anti-CD8 (MM39-10, StatLab) for 15 minutes. The Bond Polymer Refine detection system was used for visualization. Dermatopathologist Jeff Zwerner, MD, PhD scored all slides.

*Molecular Docking of Vancomycin with HLA-A*32:01*

Sequences of HLA-A*32:01 and HLA-A*29:02 were obtained from the HLA/IGMT database (http://www.ebi.ac.uk/ipd/imgt/hla/allele.html). An atomic homology model for HLA-A*32:01 was generated with SWISS-MODELLER[182] based on the most closely related crystal structure, PDB 6EI2, which is 92% identical. To generate a peptide/HLA-A*32:01 complex model, the peptide from the crystal structure of 6EI2 was positioned into the antigen binding cleft of the HLA-A*32:01 model using SSM in the COOT program package, then mutated to RLYGKSLYSF, a peptide eluted from HLA-A*32:01[183]. The peptide/HLA-A*32:01 complex model was then geometry minimized using PHENIX[93].

Vancomycin was docked into the HLA-A*32:01 model with AutoDock Vina[184]. The scoring grid dimensions were 40 × 40 × 40 Å, centered on a site corresponding to the Cα of the fifth peptide amino acid (P5). Vancomycin was docked with exhaustiveness set to 40. The top nine scoring orientations were output and compared. PyMol was used to generate molecular graphics (The PyMOL Molecular Graphics System, Version 1.8 Schrödinger, LLC.).

RESULTS

Baseline Demographics

Twenty-three individuals were identified that met inclusion criteria for clinically diagnosed vancomycin-associated DRESS in our study (Tables 3.1 and 3.2). The cohort included 15 prospectively recruited patients (7 from Vanderbilt University Medical Center in Nashville, 5 from Melbourne, and 3 from Perth) and 8 retrospectively ascertained individuals from Vanderbilt's

ID	Age	Sex	Race	Latency	RegiSCAR	Naranjo	HLA-A*32:01	Trough	Indication for vancomycin	Other potentially implicated medications
1	56	F	W	18	5	8	Positive	27	*MRSA* cervical spine post-operative wound infection	rifampin
2	52	M	W	26	6	8	Positive	9	Culture negative post-operative soft tissue infection of right foot	ceftriaxone, ciprofloxacin
3	59	M	W	19	4	8	Positive	14	Gram-positive cocci right chronic calcaneal osteomyelitis	ciprofloxacin
4	66	M	W	21	4	8	Positive	3	*MRSA* osteomyelitis	rifampin
5	27	M	W/H	29	5	8	Positive	21	Lumbar spine osteomyelitis	isoniazid, rifampin, ethambutol, pyrazinamide
6	33	M	W	28	5	8	Positive	14	*MRSE*-infected mesh post bariatric surgery abdominal repair	None
7	52	M	W	17	6	8	Positive	16	Epidural abscess and osteomyelitis with Gram-positive bacteremia	ceftriaxone
8	48	M	B	21	5	8	Negative	12	Cellulitis post exploratory laparotomy and inguinal hernia repair	piperacillin-tazobactam
9	53	F	W	23	7	8	Positive	7	Culture negative soft tissue infection with underlying rib osteomyelitis	levofloxacin, fluconazole
10	29	M	W	26	5	8	Positive	19	Traumatic arm injury and possible osteomyelitis	trimethoprim/sulfamethoxazole, piperacillin-tazobactam, ciprofloxacin
11	58	M	W	36	6	8	Positive	22	Culture negative osteomyelitis	ciprofloxacin
12	62	M	W	21	4	8	Negative	21	Implantable cardioverter defibrillator pocket infection	None
13	17	M	W	29	4	8	Positive	10	*MRSA* bacteremia secondary to right pelvic myositis and phlebitis	ibuprofen, hydroxyzine
14	51	F	W	14	6	8	Positive	23	*Enterococcus faecium* bacteremia	ceftazidime
15	57	M	W	15	5	8	Negative	24	Culture negative febrile neutropenia and neutropenic colitis during AML treatment	meropenem
16	24	F	W	14	6	10	Positive	16	*MRSE* and *Bacteroides fragilis* post-operative wound infection following caesarean section and supracervical hysterectomy for uterine necrosis	azithromycin, clindamycin, gentamicin, piperacillin-tazobactam, amoxicillin, meropenem, metronidazole

17	38	M	W	18	5	8	Positive	14	*MRSA* right chest phlegmon, deep soft tissue infection, underlying osteomyelitis of 2nd rib with fracture	rifampin
18	47	F	W	17	6	8	Positive	13	*MRSA* and *E. coli* bacteremia w/ chest infiltrate	levofloxacin
19	76	M	W	27	6	8	Positive	12	*Enterococcus* bacteremia and endocarditis	gentamicin, benzylpenicillin
20	61	F	W	50	5	8	Positive	N/A	*MRSA* wound infection leading to hip prosthesis removal and placement of vancomycin spacer	ciprofloxacin
21	71	F	W	28	5	8	Negative	16	*MRSA* and *E. coli* hardware infection post knee replacement	ceftriaxone, rifampin
22	40	F	W	15	4	8	Positive	17	*E. coli* and *Enterococcus faecalis* urosepsis during pregnancy	ceftriaxone
23	47	F	W	15	5	8	Positive	22	*Staphylococcus epidermis* ventriculitis	ceftriaxone

Table 3.1. Summary of case basic demographics, clinical characteristics, HLA risk allele carriage and DRESS history. Legend: ID, patient identification; Age, age at time of vancomycin treatment; Latency, days between vancomycin initiation and symptoms development; HLA, human leukocyte antigen; Trough, last vancomycin trough level before development of hypersensitivity symptoms in μg/mL. F, female; M, male; W, Caucasian; W/H, Caucasian/Hispanic; B, African American; N/A, not available; *MRSA*, Methicillin-resistant *Staphylococcus aureus*; *MRSE*, Methicillin-resistant *Staphylococcus epidermidis*; AML, acute myeloid leukemia; *E. coli, Escherichia coli.*

ID	Fever (Y/N)	Rash >50% BSA (Y/N)	Facial Edema (Y/N)	LAD (Y/N)	Peak Liver Enzymes >2x Normal (Y/N)	Peak Creatinine (mg/dL)	Absolute Eosinophil Count (Cells/μL)	Resolution >15 days (Y/N)	Biopsy Supporting DRESS (Y/N)	Prior Exposure to Vanc >7 Days (Y/N)	Steroid Treatment Course
1	Y	Y	Y	N	Y	1.10	17.4% (no absolute)	Y	Y	N	"1 dose of high dose steroids"
2	Y	Y	Y	Y	Y	2.19	2450	Y	Y	N	Slow taper starting at 60mg/day of prednisone
3	Y	Y	N	N	N	1.10	680	Y	Y	N	Slow taper starting at 80mg/day of prednisone
4	Y	Y	U	U	Y	1.38	990	Y		N	None
5	Y	Y	Y	N	Y	0.98	5480	Y	Y	N	Slow taper starting at 60mg/day of prednisone
6	Y	Y	N	N	Y	1.69	3610	Y	Y	N	1mg/kg methylprednisolone, then slow taper starting at 80mg/day of prednisone
7	Y	Y	Y	N	Y	1.67	2770	Y	Y	N	Slow taper starting at 40mg/day of prednisone
8	Y	Y	Y	N	Y	6.98	2400	Y	N	N	None
9	Y	Y	Y	N	Y	1.44	5290	Y	Y	N	Slow taper starting at 60mg/day of prednisone; 60 mg/day restarted 11 months after reaction for DRESS colitis
10	Y	Y	Y	U	Y	2.24	2280	Y	Y	U	None
11	Y	Y	Y	U	Y	2.10	5100	Y	Y	N	Slow taper starting at 60mg/day of prednisone
12	Y	Y	N	N	N	2.12	1840	N	N	N	None
13	Y	Y	Y	N	N	2.12	1030	Y	Y	N	Slow taper starting at 40mg/day of prednisone

14	Y	Y	Y	U	Y	1.35	1950	Y	Y	N	250 mg methylprednisolone, then slow taper starting at 50mg/day of prednisone
15	Y	Y	Y	N	Y	1.65	2150	Y	Y	N	None
16	Y	Y	Y	N	Y	2.22	3810	Y	Y	N	Slow taper starting at 60mg/day of prednisone
17	Y	Y	Y	Y	N	1.12	710	Y	Y	N	Slow taper starting at 30mg/day of prednisone
18	Y	Y	Y	U	Y	0.71	1470	Y	Y	N	Slow taper starting at 80mg/day of prednisone
19	Y	Y	Y	U	Y	6.19	3180	Y	N	U	“High dose steroids"
20	Y	Y	N	N	Y	5.12	6550	Y	N	N	Slow taper starting at 80mg/day of prednisone
21	Y	Y	N	N	Y	3.77	1230	Y	Y	N	Slow taper starting at 12mg/day of dexamethasone
22	Y	Y	Y	U	Y	1.39	1200	N	Y	N	None
23	Y	Y	Y	U	Y	"Normal"	6000	Y	Y	N	100mg/day hydrocortisone, then slow taper starting at 75mg/day of prednisolone

Table 3.2. Additional hypersensitivity syndrome characteristics for vancomycin DRESS cases. The length of the steroid tapers ranged from 4 weeks to >6 months. Data in quotes were taken directly from the electronic health records when laboratory values or medication records were not available. Where relevant creatinine values have been converted from μmol/L to mg/dL. **Legend:** Y, yes; N, No; BSA, body surface area; LAD, lymphadenopathy; vanc, vancomycin; U, Unknown.

BioVU repository. The patient cohort was primarily of European ancestry and included 9 women and 14 men from 17 to 76 years of age who developed DRESS between 2004 and 2018. Using a blinded observer, only one patient was identified that overlapped between the Vanderbilt retrospectively identified BioVU cohort and the prospectively collected patients. The duplicate was eliminated from the BioVU cohort. All patients had Naranjo adverse drug reaction scores of 8 to 10 (probable or definite adverse drug reaction) and RegiSCAR scores of 4 to 7 (probable or definite DRESS). 21/23 (91%) patients were being treated with other antibiotics concurrently with vancomycin. The median latency period from vancomycin initiation to the first symptoms of DRESS was 21 days (mean, 22.9 days; range, 14 – 50 days) (Table 3.1). Age, race and sex matching was successful (Table 3.3) and indications for vancomycin treatment were similar between cases and controls (Tables 3.1 and 3.4). Similar to the DRESS cases who had a median vancomycin trough of 16 μg/mL (mean, 17.2 μg/mL; range, 3 – 44 μg/mL; n = 116), the tolerant controls had a median vancomycin trough of 18 μg/mL (mean, 19.6 μg/mL; range, 2 – 86 μg/mL; n = 644).

HLA Associations with DRESS

The HLA-A*32:01 allele was carried by 19/23 (86%) DRESS cases compared with 0/46 (0%) of the matched vancomycin tolerant controls ($p=1x10^{-8}$, conditional logistic with Bonferroni multiple comparisons correction) (Tables 3.1, 3.4, 3.5 and 3.6 and Figure 3.1). After adjusting for HLA-A*32:01 carriage, no other alleles were significant (p=0.13). In a larger BioVU cohort of DNA samples from 54,249 Vanderbilt patients, the HLA-A*32:01 allele carriage rate was 6.30% which matches the carriage rate in other cohorts of predominant European ancestry[158,185]. Carriage of

Vancomycin DRESS Cases				Vancomycin Tolerant Controls			
ID	**Age**	**Sex**	**Race**	**ID**	**Age**	**Sex**	**Race**
1	56	F	W	C1	57	F	W
				C2	56	F	W
2	52	M	W	C3	53	M	W
				C4	51	M	W
3	59	M	W	C5	57	M	W
				C6	60	M	W
4	66	M	W	C7	66	M	W
				C8	65	M	W
5	27	M	W/H	C9	22	M	W
				C10	28	M	W
6	33	M	W	C11	33	M	W
				C12	37	M	W
7	52	M	W	C13	50	M	W
				C14	50	M	W
8	48	M	B	C15	52	M	B
				C16	43	M	B
9	53	F	W	C17	54	F	W
				C18	57	F	W
10	29	M	W	C19	32	M	W
				C20	26	M	W
11	58	M	W	C21	59	M	W
				C22	56	M	W
12	62	M	W	C23	62	M	W
				C24	62	M	W
13	17	M	W	C25	18	M	W
				C26	17	M	W
14	51	F	W	C27	51	F	W
				C28	51	F	W
15	57	M	W	C29	57	M	W
				C30	56	M	W
16	24	F	W	C31	22	F	W
				C32	25	F	W
17	38	M	W	C33	37	M	W
				C34	40	M	W
18	47	F	W	C35	49	F	W
				C36	48	F	W
19	76	M	W	C37	78	M	W
				C38	80	M	W
20	61	F	W	C39	62	F	W
				C40	60	F	W
21	71	F	W	C41	66	F	W
				C42	74	F	W
22	47	F	W	C43	47	F	W
				C44	49	F	W
23	47	F	W	C45	49	F	W
				C46	45	F	W

Table 3.3. Results of the 1:2 case to control match. Controls were identified using Vanderbilt's BioVU, a deidentified electronic medical record database linked to a DNA biobank. Patients were matched on sex, race and age within five years. **Legend:** DRESS, drug reaction with eosinophilia and systemic symptoms; ID, patient identification; F, Female; M, Male; W, Caucasian; W/H, Caucasian/Hispanic; B, African American.

ID	Age	Sex	Race	HLA-A*32:01	Indication for vancomycin treatment
C1	57	F	W	Negative	Right orbital cellulitis with interconal and extraconal abscess
C2	56	F	W	Negative	*MRSA*-infected failed aortobifemoral bypass graft
C3	53	M	W	Negative	Tongue and pulmonary lesions concerning for infection in setting of AML
C4	51	M	W	Negative	*Saccharomyces cerevisiae* pneumonia post bone marrow transplant
C5	57	M	W	Negative	Scrotal abscess and probable rectus sheath hematoma infection
C6	60	M	W	Negative	Osteomyelitis with abscess right heel
C7	66	M	W	Negative	Osteomyelitis and sepsis secondary to diabetic foot infection
C8	65	M	W	Negative	Mediastinal infection status post coronary artery bypass grafting
C9	22	M	W	Negative	Pneumonia and neutropenic with persistent fevers in the setting of AML
C10	28	M	W	Negative	Prosthetic aortic valve endocarditis with perivalvular abscess
C11	33	M	W	Negative	Pneumonia and skin lesion in setting of neutropenia and CLL
C12	37	M	W	Negative	Coagulase negative *Staphylococcus* native aortic valve endocarditis and septicemia
C13	50	M	W	Negative	Native valve *MSSA* endocarditis with embolization to skin, brain and kidney and enterococcus in blood culture
C14	50	M	W	Negative	Sepsis secondary to contaminated decubiti
C15	52	M	B	Negative	Fever and altered mental status in the setting of HIV/AIDS
C16	43	M	B	Negative	*MRSA* pneumonia in the setting of AIDS and end stage renal disease
C17	54	F	W	Negative	*MRSE* infection of right total knee arthroplasty after liner exchange
C18	57	F	W	Negative	*MRSE*-infected left chest port in setting of AML
C19	32	M	W	Negative	Persistent fevers in the setting of Ewing's sarcoma on chemotherapy
C20	26	M	W	Negative	Pneumonia in the setting of relapsed AML
C21	59	M	W	Negative	*MRSA* bacteremia in the setting of chronic renal failure
C22	56	M	W	Negative	Empiric vancomycin for cellulitis of foot with chronic non-healing wound following nail puncture
C23	62	M	W	Negative	*MRSE* empyema in the setting of a single lung transplant
C24	62	M	W	Negative	Donor-derived surgical culture growing *Staphylococcus aureus* after double lung transplant
C25	18	M	W	Negative	Empiric therapy in patient with cystic fibrosis exacerbation and history of growing *MSSA* and Pseudomonas
C26	17	M	W	Negative	Coagulase-negative staphylococcal bacteremia in the setting of hypoplastic left heart syndrome status post failed Fontan
C27	51	F	W	Negative	Inferior ischiopubic ramus osteomyelitis
C28	51	F	W	Negative	*MRSA* bacteremia and endocarditis of the atrioventricular valves with evidence of septic embolization
C29	57	M	W	Negative	Coagulase-negative staphylococcal bacteremia status post autologous peripheral blood stem cell transplant
C30	56	M	W	Negative	*MRSA* bacteremia in the setting of cellulitis of lower abdomen and possible endocarditis

C31	22	F	W	Negative	Poly-Gram negative rod septicemia in the setting of orthotopic liver transplantation complicated
C32	25	F	W	Negative	*MRSA* pneumonia in the setting of severe end stage cystic fibrosis
C33	37	M	W	Negative	Left femur osteomyelitis and surrounding soft tissue infection at stump site of above knee amputation
C34	40	M	W	Negative	Supracystic abscess communicating with the sigmoid colon after failed kidney/pancreas transplant status post explant of failed grafts
C35	49	F	W	Negative	Probable pneumonia in the setting of splenic rupture and AML
C36	48	F	W	Negative	Right toe osteomyelitis with overlying abscess positive for *MRSA, Enterococcus faecalis, and Providencia* status post amputation
C37	78	M	W	Negative	*MRSA*-infected graft and right iliac region
C38	80	M	W	Negative	Enterococcal septicemia
C39	62	F	W	Negative	*Enterococcus faecalis* positive sacral decubitus ulcer with associated osteomyelitis
C40	60	F	W	Negative	Fever and altered mental status in the setting of AML
C41	66	F	W	Negative	Tibial osteomyelitis and hardware infection
C42	74	F	W	Negative	*MRSA*-positive right shoulder prosthetic septic arthritis and sepsis
C43	47	F	W	Negative	Necrotic anal mass with associated draining abscess
C44	49	F	W	Negative	*Staphylococcal aureus* positive post-surgical meningitis and sepsis
C45	49	F	W	Negative	Parapharyngeal abscess and cervical spine osteomyelitis with epidural abscess
C46	45	F	W	Negative	*MRSA* osteomyelitis of the spine

Table 3.4. Demographics, HLA risk allele carriage and indication for vancomycin treatment for case-matched vancomycin tolerant individuals. Legend: ID, patient identification; Age, age at time of vancomycin treatment; HLA, human leukocyte antigen; F, female; M, male; W, Caucasian; B, African American; *MRSA*, Methicillin-resistant *Staphylococcus aureus*; AML, acute myeloid leukemia; ALL, acute lymphoblastic leukemia; CLL, chronic lymphoblastic leukemia; *MSSA*, Methicillin-sensitive *Staphylococcus aureus*; HIV/AIDS, human immunodeficiency virus/acquired immune deficiency syndrome; *MRSE*, Methicillin-resistant *Staphylococcus epidermidis.*

ID	HLA-A Allele 1/2	HLA-B Allele 1/2	HLA-C Allele 1/2	HLA-DPB1 Allele 1/2	HLA-DQA1 Allele 1/2	HLA-DQB1 Allele 1/2	HLA-DRB1 Allele 1/2
1	02:01/**32:01**	07:02/44:02	05:01/07:02	04:02/04:02	NT	03:01/06:02	04:08/15:01
2	02:01/**32:01**	51:01/51:01	02:02/16:02	04:02/06:01	01:01/03:01	03:02/05:01	01:01/04:04
3	**32:01**	40:01	02:02/03:04				
4	01:01/**32:01**	08:01/44:02	05:01/07:01	04:01/19:01	NT	05:03/06:02	14/15
5	02:06/**32:01**	39:05/40:02	02:02/07:02	04:02/04:02	01:03/03:01	03:02/06:03	04:07/13:01
6	02:01/**32:01**	44:02/44:02	05:01/05:01	03:01/04:02	03:01/05:01	03:01/03:01	04:01/11:04
7	01:01/**32:01**	08:01/27:05	02:02/07:01	01:01/15:01	03:01/05:01	02:01/03:02	03:01/04:01
8	23:01/23:01	08:01/15:16	07:02/14:02	01:01/85:01	01:02/05:01	02:03/05:02	03:02/16:02
9	03:01/**32:01**	07:02/18:01	07:02/07:41	03:01/04:01	NT	02:01/06:02	03:01/15:01
10	23:01/**32:01**	44:02/49:01	05:01/07:01	02:01/04:02	05:01/05:01	03:01/03:01	11:01/12:01
11	**32:01/32:01**	15:01/35:01	03:03/04:01	04:02/10:01	01:01/01:01	05:01/05:03	01:01/11:13
12	02:01/26:01	14:01/45:01	06:02/08:02	02:01/04:01	02:01/04:01	02:02/04:02	07:01/08:01
13	01:01/**32:01**	44:02/44:03	04:01/05:01	04:01/04:01	02:01/03:01	02:02/03:01	04:01/07:01
14	24:02/**32:01**	35:03/35:08	04:01/04:01	04:01/14:01	01:02/01:02	05:02/05:02	16:01/16:02
15	01:01/02:01	08:01/44:02	05:01/07:01	01:01/04:02	03:01/05:01	02:01/03:01	03:01/04:01
16	03:01/**32:01**	07:02/35:01	04:01/07:02	04:01/04:01	05:01/05:01	03:01/03:01	11:04/12:01
17	03:01/**32:01**	07:02/07:02	07:02/07:02	03:01/04:01	01:02/03:01	03:01/06:02	04:07/15:01
18	03:01/**32:01**	07:02/14:01	07:02/08:02	02:01/05:01	03:01/03:01	03:02/03:02	04:04/04:04
19	01:01/**32:01**	13:02/51:01	06:02/14:02	01:01/04:01	02:01/02:01	02:02/02:02	07:01/07:01
20	68:01/**32:01**	13:02/51:01	02:02/06:02	02:01/04:01	02:01/03:01	02:02/03:03	07:01/09:01
21	01:01/03:01	07:02/08:01	07:01/07:02	03:01/04:01	01:02/05:01	03:01/06:02	11:01/15:01
22	03:01/**32:01**	15:01/44:02	03:04/05:01	02:01/11:01	01:01/02:01	02:02/05:02	01:01/11:01
23	24:02/**32:01**	08:01/40:01	03:04/07:01	02:01/04:02	03:01/05:01	02:01/03:02	03:01/04:04

Table 3.5. Full HLA typing results of potential vancomycin DRESS cases. Empty wells could not be imputed. **Legend:** ID, patient identification; HLA, human leukocyte antigen; NT, not typed.

ID	HLA-A Allele 1/2	HLA-B Allele 1/2	HLA-C Allele 1/2	HLA-DPB1 Allele 1/2	HLA-DQA1 Allele 1/2	HLA-DQB1 Allele 1/2	HLA-DRB1 Allele 1/2
C1	01:01/24:02	08:01/08:01	07:01/07:01	01:01/13:01	01:02/05:01	02:01/06:02	03:01/15:01
C2	01:01/02:01	08:01/44:02	07:01/07:04	04:01/11:01	02:01/05:01	02:02/03:01	07:01/11:01
C3	03:01/11:01	07:02/07:02	07:02/07:02	03:01/04:01	03:01/03:01	03:01/03:02	04:01/04:04
C4	02:01/29:02	07:02/44:03	07:02/16:01	04:01/04:02	01:01/02:01	02:02/05:01	07:01/10:01
C5	03:01/26:01	35:01/45:01	04:01/06:02	04:01/09:01	01:01/01:01	05:01/05:01	01:01/01:01
C6	01:01/02:01	18:01/57:01	06:02/07:01	04:01/04:01	01:02/02:01	03:03/06:02	07:01/15:01
C7	01:01/03:01	07:02/57:01	06:02/07:02	04:01/04:01	01:02/02:01	03:03/06:02	07:01/15:01
C8	01:01/02:01	18:01/50:01	06:02/07:01	03:01/14:01	01:01/02:01	02:02/05:01	01:01/07:01
C9	02:01/03:01	15:18/40:01	03:04/07:04	02:01/04:01	01:01/01:02	05:01/06:02	01:02/15:01
C10	01:01/24:02	37:01/55:01	03:03/06:02	02:01/02:01	01:02/05:01	03:01/06:04	12:01/13:02
C11	25:01/29:02	15:01/44:02	03:04/05:01	02:01/03:01	03:01/03:01	03:02/03:02	04:01/04:01
C12	02:01/11:01	44:02/50:01	05:01/06:02	04:01/04:01	01:02/03:01	03:01/06:02	04:08/15:01
C13	01:01/03:01	18:01/40:02	02:02/07:01	04:01/04:01	01:01/05:01	03:01/05:01	01:01/11:04
C14	02:01/03:01	44:02/51:01	01:02/07:04	03:01/03:01	01:01/05:01	03:01/05:01	01:01/11:01
C15	30:02/66:02	07:02/07:02	07:01/15:05	02:01/17:01	01:01/01:02	05:01/05:01	10:01/11:01
C16	23:01/30:01	07:02/18:01	02:10/07:02	01:01/18:01	01:02/01:02	06:02/06:02	11:01/15:03
C17	01:01/02:01	08:01/08:01	07:01/07:01	01:01/01:01	05:01/05:01	02:01/02:01	03:01/03:01
C18	26:01/68:02	15:01/15:07	03:03/05:01	04:01/11:01	01:02/01:03	06:02/06:03	13:01/15:01
C19	02:01/02:01	15:82/44:02	03:03/05:01	04:01/04:02	03:01/05:01	03:02/03:02	04:01/11:01
C20	01:01/68:01	08:01/39:01	07:01/07:02	03:01/04:01	01:02/03:01	03:02/06:02	04:07/15:01
C21	01:01/11:01	40:02/51:01	01:02/02:02	04:01/04:01	01:01/05:01	03:01/05:03	11:01/14:01
C22	03:01/03:01	07:02/15:01	03:03/07:02	03:01/04:01	01:01/03:01	03:02/05:01	01:03/04:01
C23	02:01/68:01	40:01/55:01	03:03/03:04	03:01/05:01	01:01/03:01	03:01/05:03	04:01/14:01
C24	02:01/11:01	44:02/52:01	05:01/12:02	04:01/04:01	01:01/01:02	05:03/06:02	14:04/15:01
C25	01:01/01:01	15:01/44:02	03:03/05:01	04:01/19:01	01:03/01:03	06:03/06:03	13:01/13:02
C26	02:01/24:02	40:02/44:02	01:02/02:02	02:01/04:01	01:01/05:01	03:01/05:01	01:03/11:01
C27	03:01/03:01	07:02/51:01	01:02/07:02	03:01/04:01	01:01/01:02	05:01/06:02	01:01/15:01
C28	23:01/24:02	49:01/NT	03:03/07:01	01:01/04:01	02:01/05:01	02:02/03:01	07:01/11:01
C29	25:01/29:02	18:01/44:02	05:01/12:03	03:01/04:01	01:02/03:01	03:01/06:02	04:01/15:01
C30	02:01/02:01	15:01/44:02	03:04/05:01	04:01/20:01	01:01/03:01	03:02/05:03	04:01/14:01
C31	02:01/02:01	15:01/44:02	03:04/05:01	03:01/04:01	01:02/01:03	06:02/06:03	13:01/15:01
C32	03:01/11:01	35:01/56:01	04:01/04:01	04:01/04:02	01:02/01:02	06:02/06:02	15:01/15:01
C33	02:01/02:01	27:02/44:02	02:02/05:01	04:02/04:02	03:01/03:01	03:02/03:02	04:01/04:04
C34	01:01/23:01	08:01/49:01	07:01/07:01	01:01/01:01	03:01/05:01	02:01/03:02	03:01/04:05
C35	01:01/01:01	14:01/57:01	06:02/06:02	05:01/13:01	02:01/02:01	02:02/03:03	07:01/07:01
C36	01:01/02:01	08:01/57:01	06:02/07:01	03:01/04:01	02:01/05:01	02:01/03:03	03:01/07:01
C37	02:01/29:02	44:03/44:03	16:01/16:01	01:01/03:01	02:01/02:01	02:02/02:02	07:01/07:01
C38	02:01/11:01	08:01/55:01	03:03/07:01	02:01/04:01	03:01/05:01	02:01/03:01	03:01/04:07
C39	03:01/25:01	07:02/18:01	07:02/12:03	04:01/04:01	01:02/01:02	06:02/06:02	15:01/15:01
C40	01:01/02:01	08:01/08:01	07:01/07:01	01:01/03:01	05:01/05:01	02:01/02:01	03:01/03:01
C41	02:01/02:02	15:01/44:02	03:03/05:01	02:01/04:01	03:01/05:01	03:01/03:01	04:01/12:01
C42	02:01/03:01	07:02/07:02	07:02/07:02	01:01/04:01	05:01/05:01	02:01/02:01	03:01/03:01
C43	03:01/30:01	07:02/40:02	02:02/07:02	04:01/04:01	01:02/05:01	03:01/06:02	11:01/15:01
C44	01:01/26:01	08:01/38:01	07:01/12:03	01:01/04:01	01:02/05:01	02:01/06:04	03:01/13:02
C45	01:01/31:01	08:01/40:01	03:04/07:01	03:01/04:01	01:02/05:01	02:01/06:02	03:01/15:01
C46	29:02/31:01	07:02/49:01	07:01/07:02	03:01/03:01	01:02/03:01	03:02/06:02	04:05/15:01

Table 3.6. Full HLA typing results of vancomycin tolerant controls. Legend: ID, patient identification; HLA, human leukocyte antigen; NT, not typed.

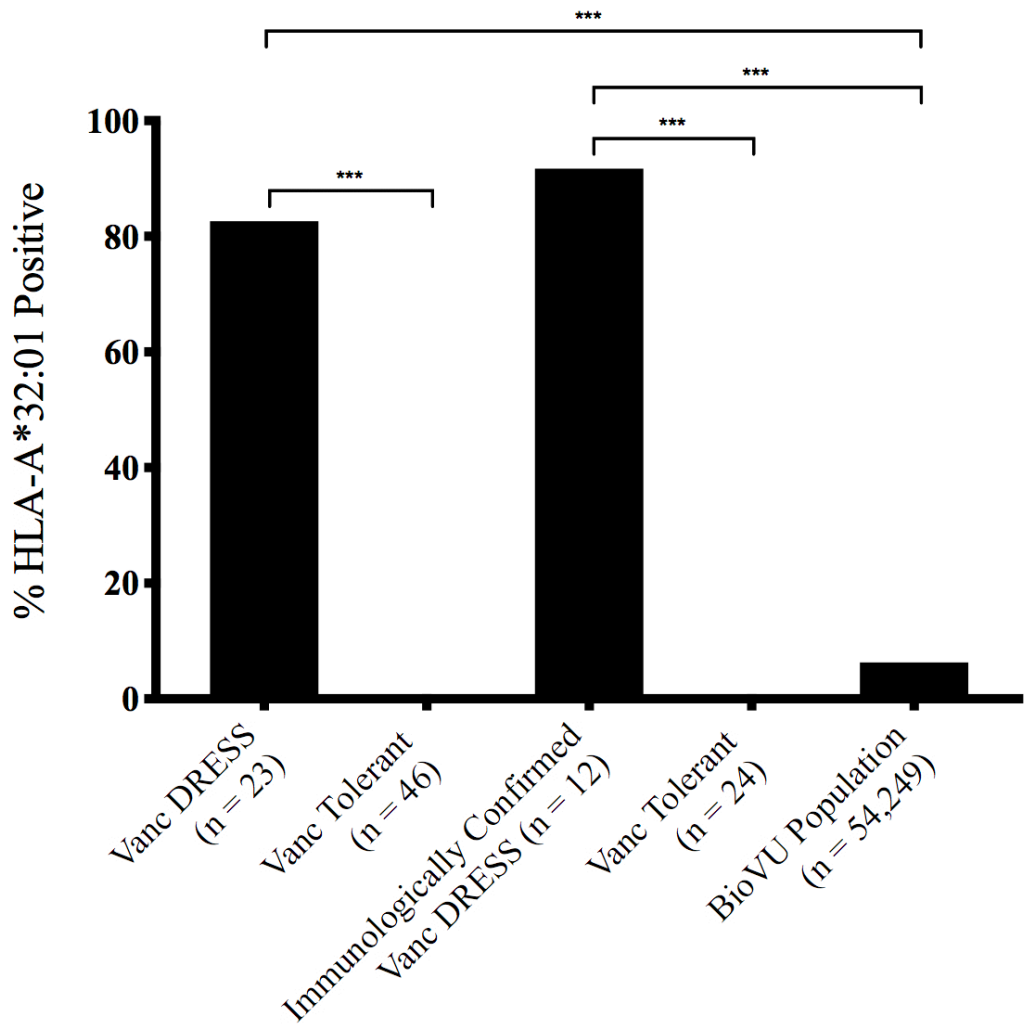

Figure 3.1. HLA-A*32:01 is strongly associated with vancomycin DRESS. 19/23 (83%) DRESS cases carried HLA-A*32:01 compared with 0/46 (0%) of the matched vancomycin tolerant controls ($p=1x10^{-8}$, conditional logistic). If analyses are restricted to immunologically confirmed cases, then 11/12 (92%) vancomycin ELISpot positive patients carried HLA-A*32:01 compared with 0/24 (0%) of the BioVU matched controls ($p=9x10^{-7}$, conditional logistic). HLA-A*32:01 carriage in all identified vancomycin DRESS cases and immunologically confirmed cases was also very significantly overrepresented compared to HLA-A*32:01 carriage in the entire BioVU cohort (6.3%) ($p=2x10^{-16}$ and $p=2=7x10^{-13}$ respectively, exact binomial tests). There was no significant difference in HLA-A*32:01 carriage between the vancomycin tolerant populations and the BioVU cohort (p=0.12 for all controls, p=0.40 for controls matched to immunologically confirmed cases, exact binomial tests). Additionally, there was no significant difference in HLA-A*32:01 carriage between the immunologically confirmed vancomycin DRESS cases and those that were not immunologically confirmed (p=0.32, Fisher's exact test). All analyses shown included Bonferroni correction for multiple comparisons. **indicates p<0.01 and *** indicates p<0.001. **Legend:** HLA, human leukocyte antigen; Vanc, vancomycin; DRESS, drug reaction with eosinophilia and systemic symptoms.

HLA-A*32:01 in our BioVU cohort (n=54,249) was more prevalent in European Americans (6.78%) than African American populations (2.78%).

IFN-γ ELISpot Responses in DRESS

IFN-γ ELISpot assays were performed on all prospectively enrolled cases for which cryopreserved PBMCs were available (14/15). PBMCs from 12/14 (86%) DRESS cases had a positive IFN-γ ELISpot response to vancomycin (Figure 3.2). Analyses restricted to immunologically confirmed cases and matched controls, revealed that 11/12 (92%) IFN-γ ELISpot positive patients carried HLA-A*32:01 compared with 0/24 (0%) of the matched controls ($p=9x10^{-7}$, conditional logistic) (Figure 3.1). Three IFN-γ ELISpot positive patients had multiple blood draws at time points distant from the initial reaction with repeat positive results (Figure 3.3). In Patient 4, a positive IFN-γ ELISpot to vancomycin was demonstrated 9 years after the initial DRESS reaction. In samples with sufficient cell numbers, PBMCs were routinely tested against all other concurrently administered medications potentially implicated in DRESS development (Figure 3.4). Notably, patient 21, one of the two patients with a negative vancomycin IFN-γ ELISpot, is HLA-A*32:01 negative and demonstrated a reproducible positive IFN-γ ELISpot to rifampin stimulation leading us to conclude that her DRESS syndrome was associated with rifampin rather than vancomycin. Thirteen controls were tested concurrently with cases and none demonstrated a positive vancomycin IFN-γ ELISpot (Figure 3.2 and Table 3.7).

Time to DRESS Analysis of the Vancomycin-Exposed BioVU Cohort

While at least two weeks of vancomycin was intended in all patients, 22/137 (16%) HLA-A*32:01 positive and 18/137 (13%) HLA-A*32:01 negative patients completed <1 week of vancomycin

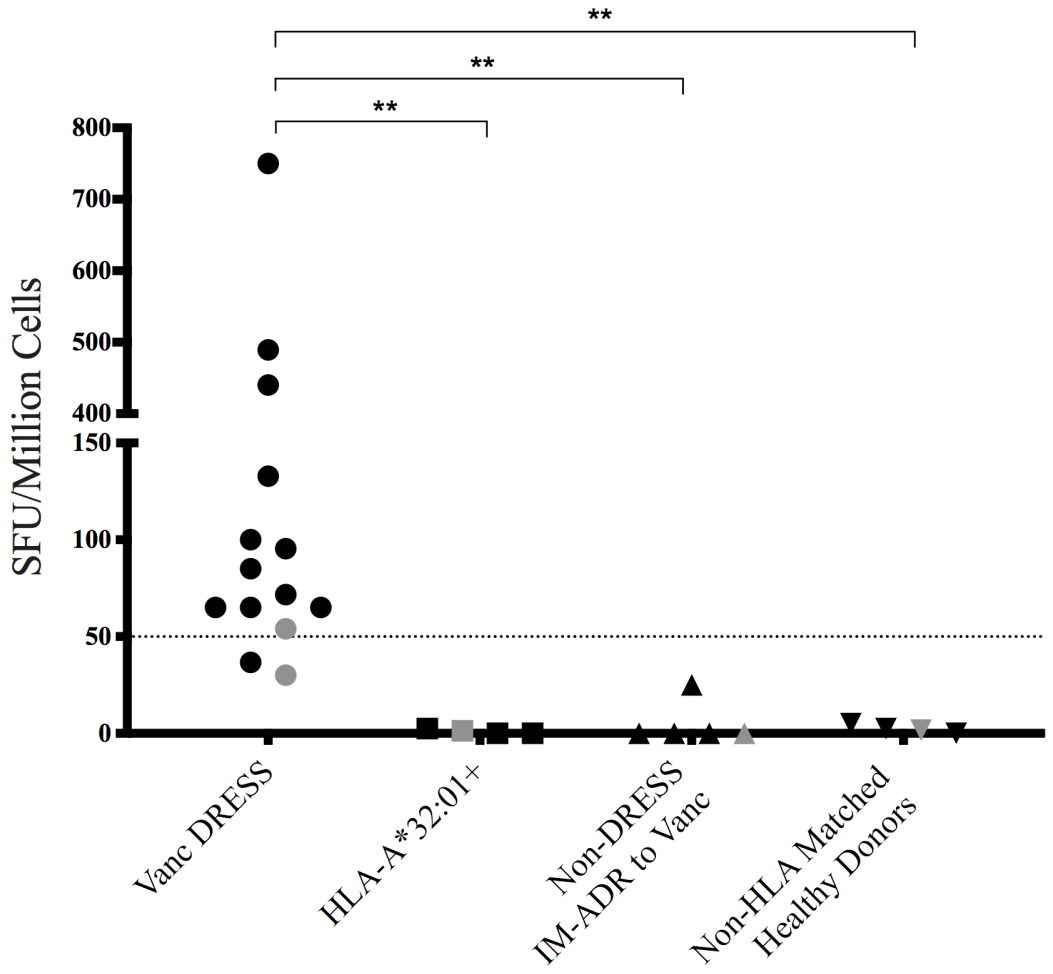

Figure 3.2. Peripheral blood mononuclear cells from vancomycin DRESS patients release IFN-γ in response to vancomycin stimulation. Enzyme-Linked ImmunoSpot (ELISpot) assays were used to measure IFN-γ release after 18-hour incubation with vancomycin at concentrations of 250 μg/mL (grey) or 500 μg/mL (black). Controls included cells from vancomycin-naïve, HLA-A*32:01 positive healthy donors (n = 3) including the son of case patient 18 and the vancomycin skin test negative control C50, an HLA-A*32:01 positive individual tolerant of 4 weeks of vancomycin (n = 1), patients who had developed a non-DRESS immune-mediated adverse reaction to vancomycin (n = 5) and non-HLA matched healthy donors (n = 4). Means of the replicates are plotted. In patients with multiple blood draws at time points distant from the reaction, ELISpot results from the first blood draw are plotted. 12/14 (85.7%) DRESS cases had a positive vancomycin ELISpot compared to none of the controls (p=0.005 (DRESS vs. HLA-A-32:01 positive controls), p=0.002 (DRESS vs. non-DRESS ADRs), p=0.005 (DRESS vs. non-HLA matched healthy donors)). Positive results are those above the dotted line intersecting the y-axis at 50 SFU/million cells. Differences in proportion of positive responses between groups were assessed using Fisher's exact tests. Patient and control PBMCs were also stimulated with vancomycin at concentrations of 5 μg/mL and 50 μg/mL and exhibited a dose-dependent response (data not shown). **indicates $p<0.01$. **Legend:** Vanc, vancomycin; HLA, human leukocyte antigen; DRESS, drug reaction with eosinophilia and systemic symptoms; SFU, spot-forming units; IM-ADR, immune-mediated adverse drug reaction.

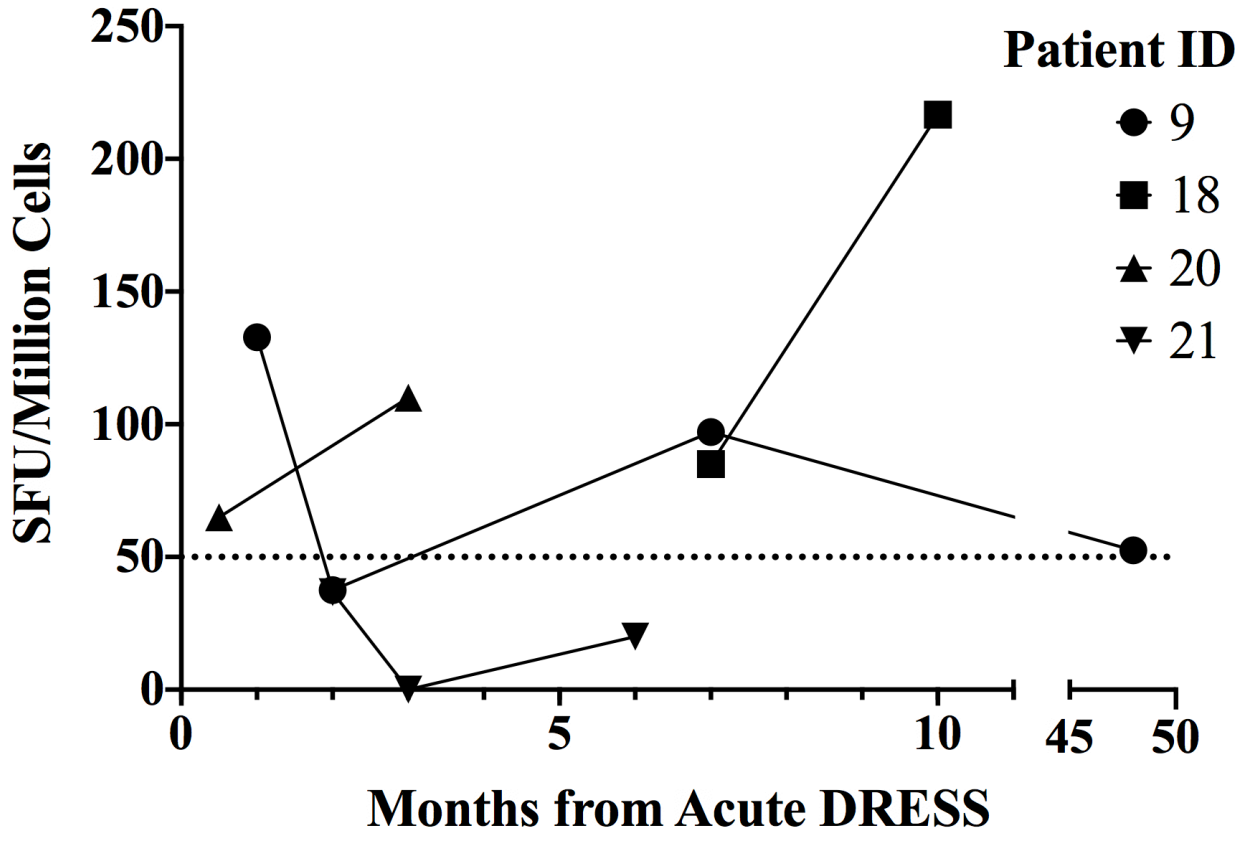

Figure 3.3. T-cell Responses to Vancomycin Appear Persistent Months to Years after Acute Reaction. IFN-γ release ELISpot results after overnight stimulation at a vancomycin concentration of 500 μg/mL using peripheral blood mononuclear cells (PBMCs) from vancomycin DRESS patients. Vancomycin DRESS patients 9, 18 and 20 had multiple blood draws at time points distant from the initial reaction with repeat positive results. Counting from the start of DRESS symptoms, sample time points were at one month, two months, seven months and four years for patient 9, seven months and ten months for patient 18, twelve days and three months for patient 20, and two months, three months and six months for patient 21. Blood from time point 2 on patient 9 was drawn during steroid treatment, which likely dampened the ELISpot response. Patient 21 does not carry HLA-A*32:01 and had a persistently negative vancomycin ELISpot. Means of the replicates are plotted. Positive results are those above the dotted line intersecting the y-axis at 50 SFU/million cells. **Legend:** Patient ID, patient identification; SFU, spot-forming units; DRESS, drug reaction with eosinophilia and systemic symptoms.

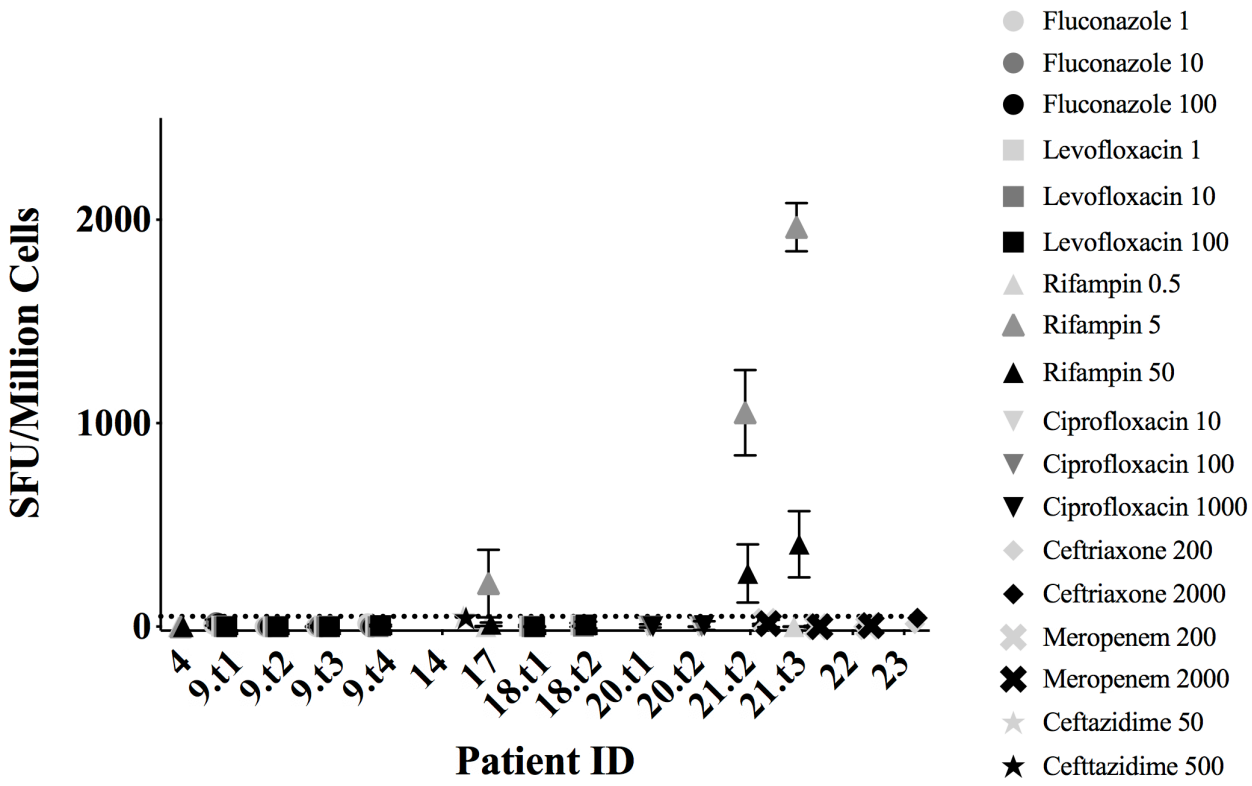

Figure 3.4. IFN-γ release ELISpot results using peripheral blood mononuclear cells from DRESS patients after overnight stimulation with all medications taken concurrently with vancomycin. All drugs were tested at μg/mL concentrations. Counting from the start of DRESS symptoms, sample time points were at one month, two months, seven months and four years for patient 9, seven months and ten months for patient 18, twelve days and three months for patient 20, and three months and six months for patient 21. Cells from Patient 21 who did not respond to vancomycin stimulation and does not carry the HLA-A*32:01 risk allele had a strong response to rifampin stimulation. Cells from Patient 17 who does carry the risk allele and did respond to *ex vivo* vancomycin stimulation also had a positive response to rifampin. However, cells from Patient 4 and other healthy donors did not respond to rifampin stimulation. No other patient samples tested released IFN-γ in response to stimulation from any other medication. Means of the replicates are plotted. Error bars indicate standard deviations of the mean after background subtraction. Positive results are those above the dotted line intersecting the y-axis at 50 SFU/million cells. **Legend:** Patient ID, patient identification; SFU, spot-forming units.

ID	Age	Sex	Race	Adverse Reaction	HLA-A*32:01
C51	57	F	W	Delayed rash	Negative
C52	51	M	W	Linear IgA Bullous Dermatosis	Negative
C53	47	M	W	Linear IgA Bullous Dermatosis	Negative
C54	28	F	W	Fixed Drug Eruption	Negative
C55	64	F	W	Acute Generalized Exanthematous Pustulosis	Positive

Table 3.7. Demographics and HLA risk allele carriage for vancomycin ELISpot negative patients who developed non-DRESS adverse reactions to vancomycin. Legend: ID, patient identification; Age, age at time of vancomycin treatment; HLA, human leukocyte antigen; F, female; M, male; W, Caucasian.

therapy. Possible and definitive DRESS cases in the HLA-A*32:01 carriers occurred after one week to four weeks of vancomycin therapy and the estimated probability of developing DRESS was 19.2% at four weeks (Figures 3.5 and 3.6). The median time to DRESS symptoms after vancomycin initiation was 18 days in this cohort. In comparison, none of the 119 HLA-A*32:01 negative individuals who were exposed to at least one week of uninterrupted vancomycin treatment developed DRESS or symptoms suggestive of DRESS ($p=6x10^{-5}$). Development of non-DRESS ADRs did not differ between risk allele positive and negative groups (p=0.35). Within the HLA-A*32:01 positive group, when considered jointly by logistic regression with DRESS as outcome, hemodialysis (p=0.03) and immunosuppression (p=0.04) were both protective factors against DRESS development. Among the DRESS cases, 2/13 (15%) had either hemodialysis or immunosuppression compared with 64/124 (52%) carrying HLA-A*32:01 who tolerated vancomycin (p=0.02). Notably, 18 HLA-A*32:01 positive individuals tolerated vancomycin for $\geq$5 weeks. This demonstrates that not all HLA-A*32:01 positive individuals will develop DRESS after prolonged vancomycin treatment.

Skin Testing, Oral Rechallenge, and Skin Histology Results

Vancomycin intradermal testing (IDT) produced strong immediate histamine responses at 20 minutes in both HLA-A*32:01 positive individuals who were tested, but only the patient with a history of DRESS developed a delayed positive IDT with dermal induration and erythema at vancomycin concentrations of 0.5, 5 and 50 mg/mL recorded 24 and 48 hours after drug placement (Figure 3.7A and 3.7B). In addition, DRESS patient 18 had negative immediate testing, delayed IDT and oral challenge to levofloxacin which had been co-administered with vancomycin. H&E staining from skin biopsies obtained from patient 18 from the acute DRESS reaction and the 5

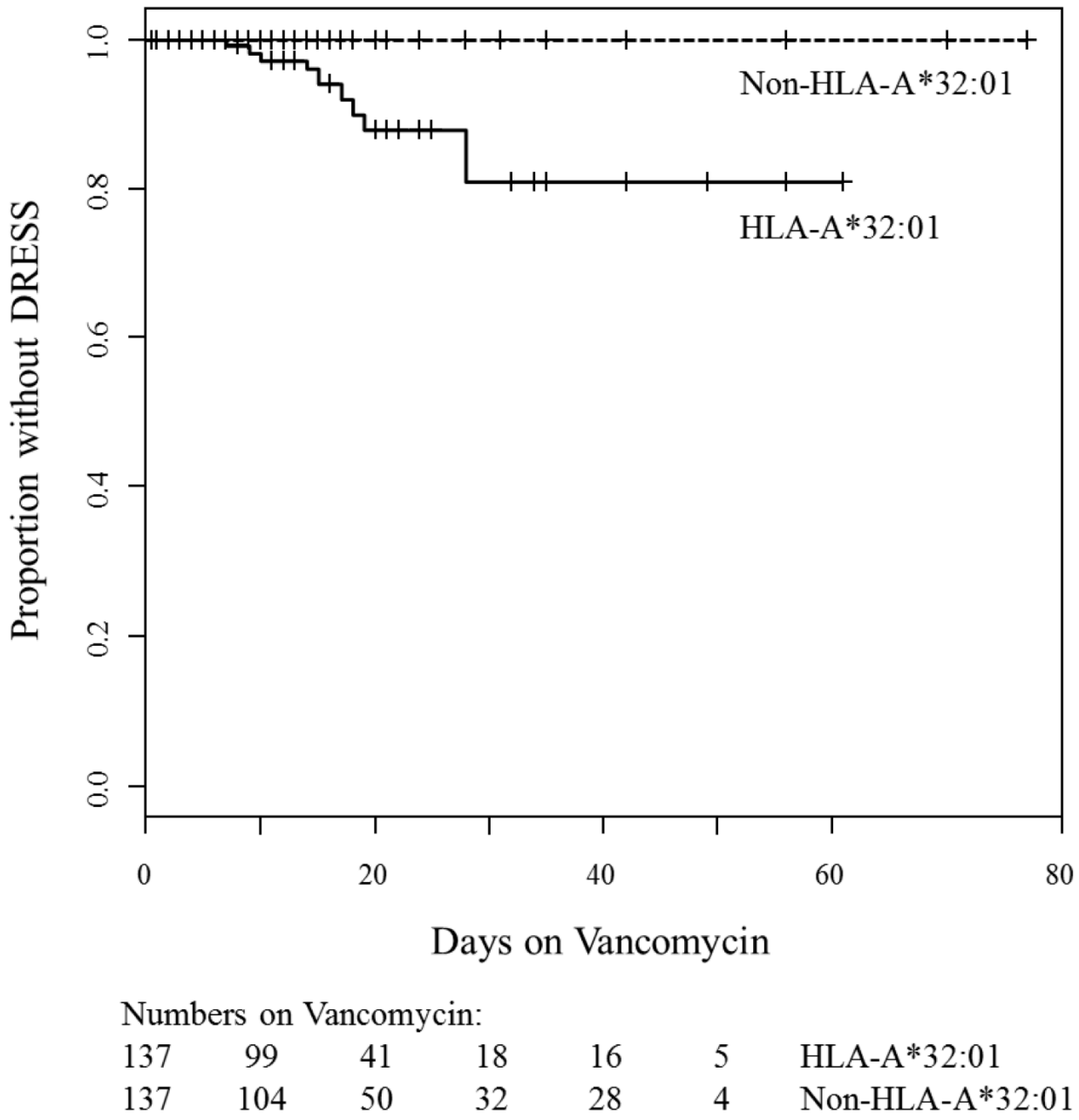

Figure 3.5. Time-to-event analysis demonstrating that only HLA-A*32:01 positive patients developed DRESS. Kaplan-Meier estimates were used to determine time to DRESS or possible DRESS development during vancomycin treatment stratified by carriage of HLA-A*32:01. Cases of DRESS occurred in HLA-A*32:01 positive subjects between 1 and 4 weeks of vancomycin therapy but not in HLA-A*32:01 negative subjects. The estimated risk of DRESS prior to 4 weeks of treatment was 19.2% in those carrying the HLA-A*32:01 allele. **Legend:** DRESS, drug reaction with eosinophilia and systemic symptoms.

A	HLA-A*32:01 Positive (n=137)	HLA-A*32:01 Negative (n=137)	p-value
Age (years) Mean (SD)	52.6 (21.0)	47.7 (22.3)	0.061
Longest treatment length (days) Mean (SD)	17.3 (13.5)	20.0 (15.0)	0.12
Sex n (%)			
Female	50 (36.5%)	61 (44.5%)	
Male	87 (63.5%)	76 (55.5%)	0.22
Race n (%)			
European American	125 (91.2%)	120 (87.6%)	
Other	12 (8.8%)	17 (12.4%)	0.43
Adverse Reaction n (%)			
Yes	20 (14.6%)	12 (8.8%)	
No	117 (85.4%)	125 (91.2%)	0.19
Possible or definite DRESS n (%)			
Yes	13 (9.5%)	0 (0%)	
No	124 (90.5%)	137 (100%)	0.00018

B

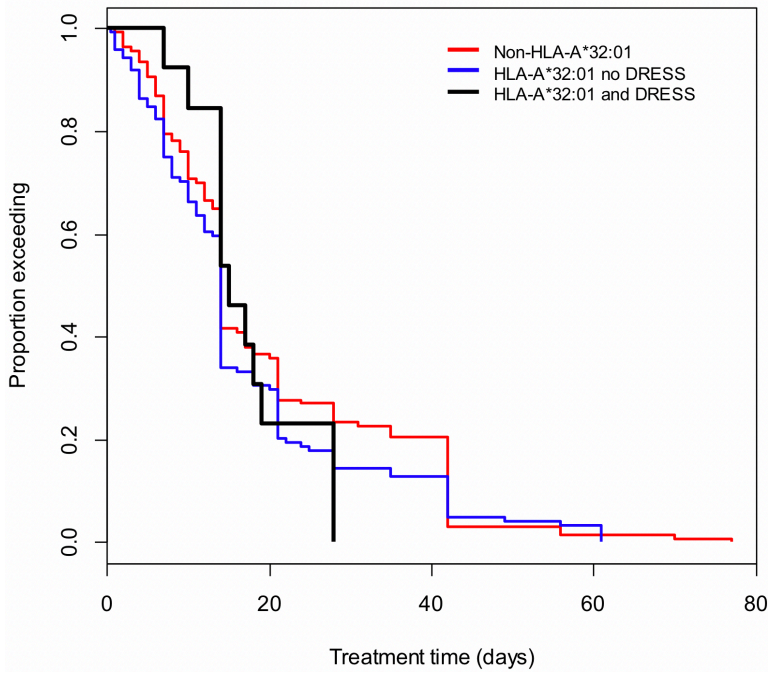

Figure 3.6. Summary of vancomycin-exposed BioVU Cohort. A. None of the factors including age, longest treatment length, sex, race and overall adverse drug reaction rate differed significantly between the HLA-A*32:01 positive and HLA-A*32:01 negative groups (t-tests or Fisher exact tests as appropriate). In a joint logistic regression with vancomycin DRESS as response, none of the other factors including age, treatment length, sex and race were significant individually ($p>0.4$) or jointly ($p=0.95$) after adjusting for HLA-A*32:01, nor did they abrogate the significance of HLA-A*32:01 ($p=0.00014$, all based on likelihood ratio tests). 3/13 vancomycin DRESS cases overlapped with the previously identified BioVU cases (Patients 1, 6 and 7 from Table 1). **B.** The maximal treatment periods were similar for HLA-A*32:01 negative patients and HLA-A*32:01 positive patients who did not develop DRESS. **Legend:** DRESS, drug reaction with eosinophilia and systemic symptoms; SD, standard deviation.

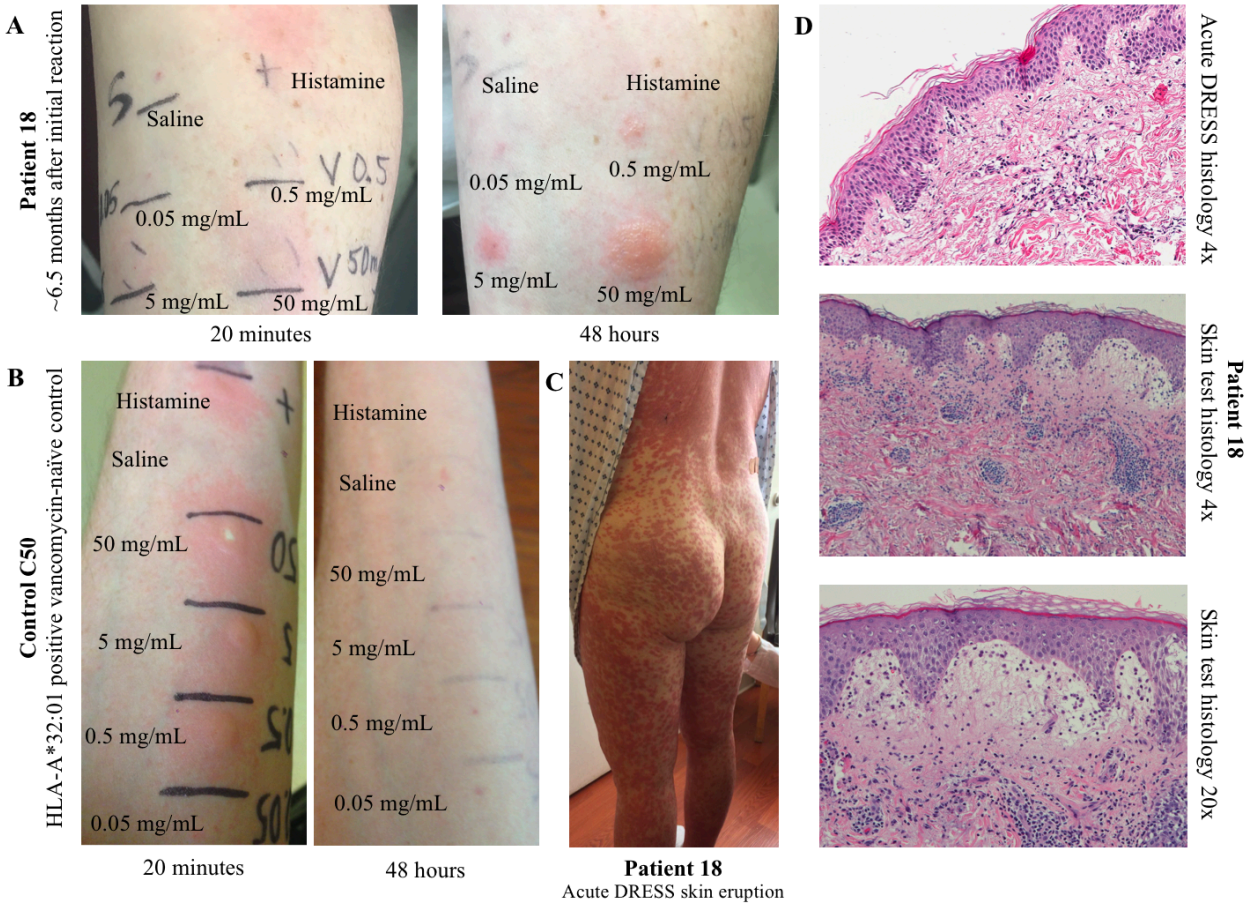

Figure 3.7. Vancomycin skin testing, acute DRESS skin eruption and skin biopsy histology. **A** and **B**. Vancomycin intradermal testing (IDT) results in patient 18 approximately 6.5 months after developing vancomycin DRESS and control C50, an HLA-A*32:01 positive, vancomycin-naïve healthy donor. IDT was performed on the volar forearm of the skin with 0.02 mL of vancomycin at concentrations of 0.05, 0.5, 5 and 50 mg/mL. The positive histamine and negative saline controls worked as expected. Vancomycin produced a strong immediate histamine response at 20 minutes in both control C50 and patient 18, but only patient 18 with a history of HLA-A*32:01 positive DRESS developed a concentration dependent induration of the skin at 48 hours at the 0.5, 5 and 50 mg/ml concentrations. Additionally, patient 18 had negative IDT to levofloxacin (not shown) and was successfully rechallenged with levofloxacin, a drug that, at the time of reaction, was administered with vancomycin. **C**. A representative example of the skin eruption from patient 18 during acute vancomycin DRESS. She had a diffuse morbilliform exanthema with facial involvement and facial edema (not shown). **D**. Hematoxylin and eosin staining of punch biopsies of skin from patient 18. Acute DRESS histology from a skin biopsy taken three days following onset of symptoms (upper panel) and skin test histology from the 5 mg/ml vancomycin positive intradermal skin test at 48 hours (lower panels) demonstrate papillary dermal edema, epidermal spongiosis and a dense lymphocytic infiltrate. Rare eosinophils are present on both biopsies. The skin test histology mirrors the results from the acute biopsy. **Legend:** DRESS, drug reaction with eosinophilia and systemic symptoms.

mg/ml vancomycin positive IDT skin test showed the papillary dermal edema, epidermal spongiosis and dense lymphocytic infiltrate classically seen in DRESS histology (Figure 3.7C and 3.7D). Immunohistochemistry of these same biopsies showed no appreciable difference in the distribution of CD4 and CD8 positive cells in the dermal infiltrate between the acute and skin test biopsies. The acute biopsy did, however, demonstrate a substantially higher number of intraepidermal CD8+ T cells when compared to the skin test biopsy. Conversely, dermal FOXP3+ T regulatory cells were present in the skin test biopsy but absent in the acute biopsy (Figure 3.8).

*Molecular Docking of Vancomycin with HLA-A*32:01*

We used molecular docking to estimate potential interactions between vancomycin and HLA-A*32:01. We generated a homology model of peptide/HLA-A*32:01 complex based on the most similar solved structure (PDB 6EI2, HLA-A68, 92 % identical) and used AutoDock Vina to predict binding orientations and scores. Vancomycin was not predicted to bind HLA-A*32:01 with high affinity when peptide occupied the antigen binding cleft (ΔG=-7.3 kcal/mole) (RLYGKSLYSF, corresponding to a peptide eluted from HLA-A*32:01). However, vancomycin was predicted to bind the antigen binding cleft of HLA-A*32:01 with higher affinity in the absence of peptide, ΔG=-7.7 kcal/mole (Figure 3.9). These data suggest that vancomycin has the potential to bind within the antigen binding cleft of HLA-A*32:01 in the absence of peptides that conform to the canonical HLA-A*32:01 binding motif (9mer P1 K or R, PΩ F, I or L)[186]. Vancomycin was predicted to bind antigen binding cleft residues in HLA-A*32:01 that differ between closely related alleles not associated with vancomycin induced DRESS, such as HLA-A*29:02 (polymorphic differences shown in magenta in Figure 3.9). Since the on-target mechanism of action for vancomycin is binding D-Ala-D-Ala in the bacterial cell wall, we asked if vancomycin

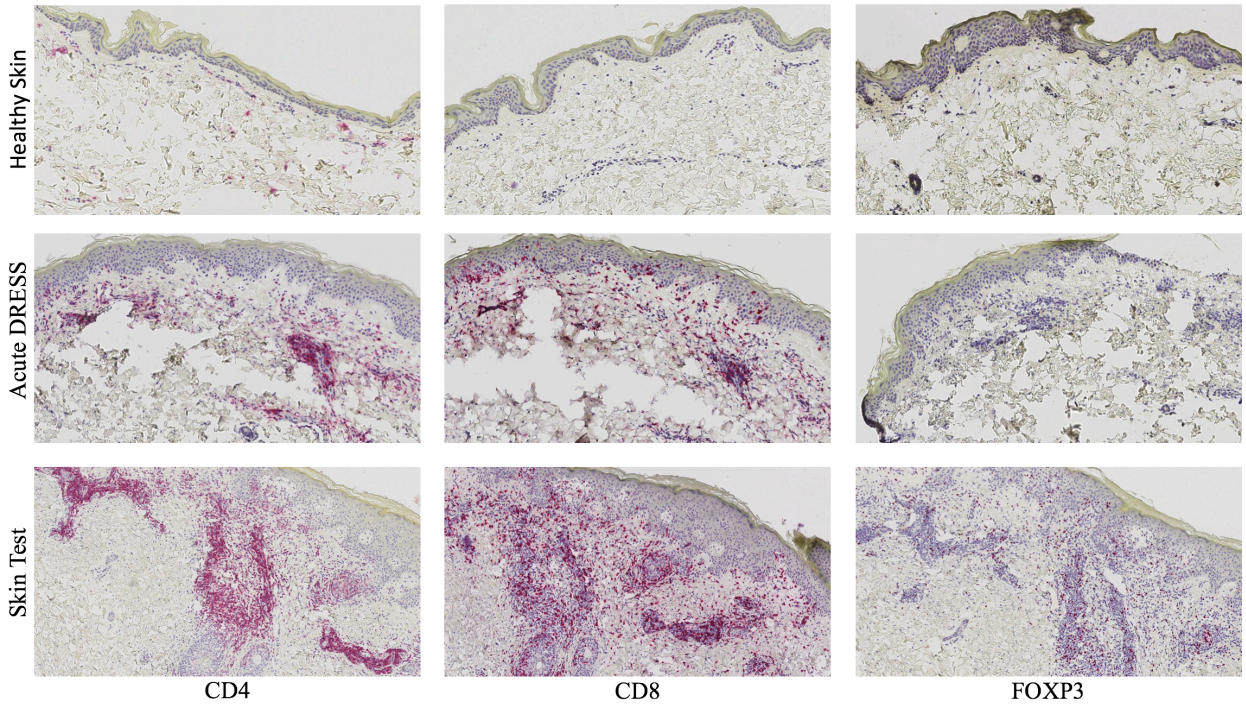

Figure 3.8. Immunohistochemistry of T-cell subsets from acute DRESS and positive skin test biopsies from patient 18. Healthy skin is shown for comparison (upper panel). There was no discernable difference in the distribution of CD4 and CD8 positive cells in the dermal infiltrate between the acute (middle panel) and skin test (lower panel) biopsies. The number of intraepidermal CD8 positive cells was substantially higher in the acute biopsy. There was no appreciable exocytosis of CD4 T cells in the acute biopsy or CD4 or CD8 T cells in the biopsy from vancomycin IDT. Notably, dermal FOXP3+, regulatory T cells were present in the skin test biopsy, but absent in the acute biopsy. **Legend:** DRESS, drug reaction with eosinophilia and systemic symptoms.

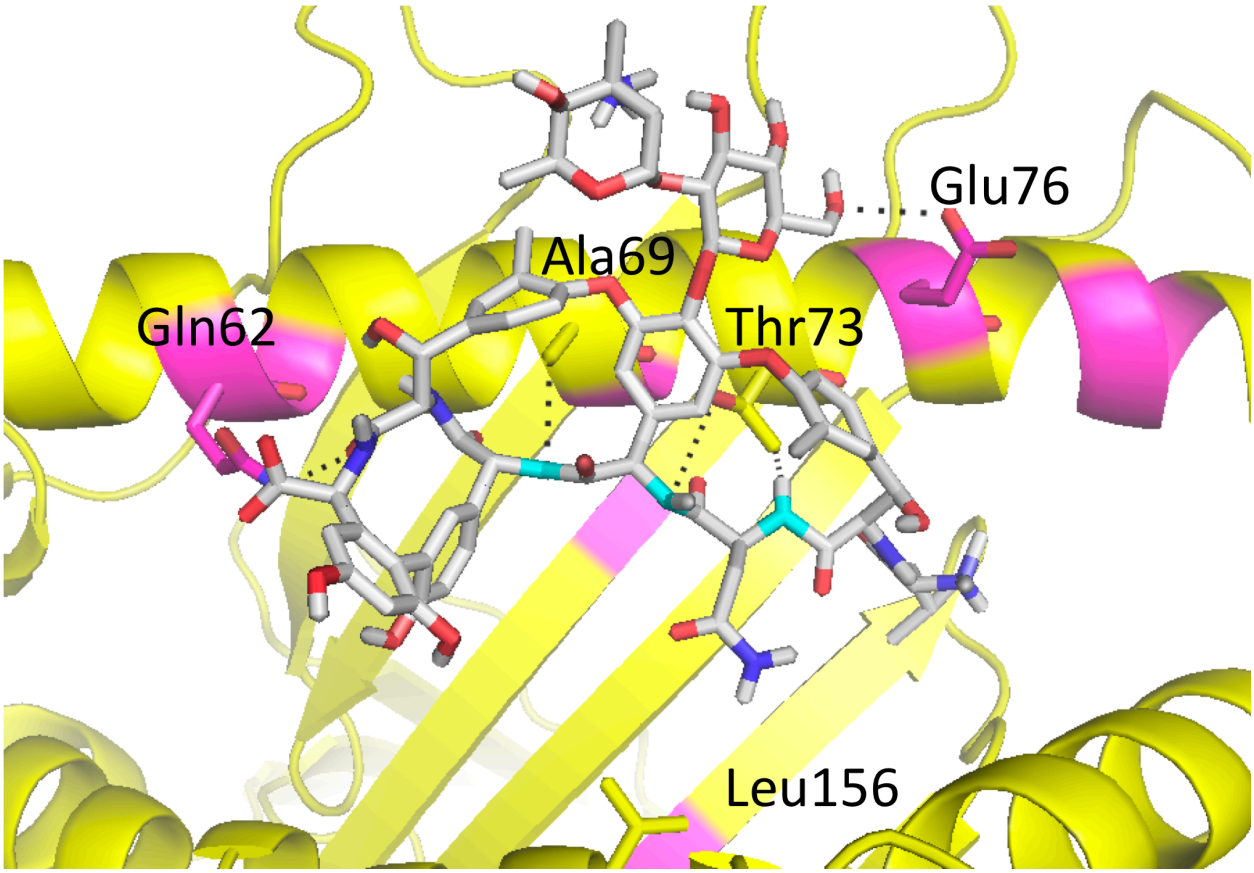

Figure 3.9. Molecular docking prediction of vancomycin binding HLA-A*32:01. Vancomycin is shown as sticks, white for carbon, blue for nitrogen, red for oxygen. Vancomycin atoms that mediate intermolecular contacts with D-Ala-D-Ala (in PDB 1FVM) are shown in cyan. A homology model of HLA-A*32:01 is shown in yellow as a ribbon diagram. Polymorphic positions that distinguish the associated HLA-A*32:01 allele from the closely related HLA-A*29:02 allele are shown in magenta. Intermolecular contacts between vancomycin and HLA-A*32:01 predicted by molecular docking are shown as black dashes.

has the potential to bind consecutive alanine residues in HLA-A*32:01. Molecular docking suggests that vancomycin is not likely to bind consecutive alanine residues (L isomers) in HLA-A*32:01. The top scoring molecular docking orientation shows that the vancomycin atoms contacting D-Ala-D-Ala were predicted to bind HLA-A*32:01 in the central region of the cleft normally occupied by the central positions in peptide backbone (shown in cyan in Figure 3.9).

DISCUSSION

In a population of predominantly European ancestry, we showed that carriage of the HLA-A*32:01 allele was strongly associated with the development of vancomycin DRESS. HLA-A*32:01 testing could increase the safety of vancomycin treatment. A similar finding involving an association between HLA-B*57:01 and abacavir hypersensitivity led to the international implementation of routine pre-prescription screening for HLA-B*57:01, which has eliminated abacavir hypersensitivity as a clinical entity and has paved the way for the translation of other HLA screening strategies for the prevention of drug hypersensitivity reactions into clinical practice[75,76,146,187]. Similar to the discovery of abacavir and HLA-B*57:01, our study highlights the utility of using large clinical databases and prospectively defined cases in combination with adjunctive immunological information to define genetic associations with a specific clinical phenotype[75,146,188]. Since vancomycin is frequently prescribed empirically in an urgent manner for acute life-threatening infections, and since DRESS typically takes 2 weeks to occur, unlike previous models that suggest HLA screening prior to intended prescription of a drug, use of HLA-A*32:01 typing may be more appropriate following initiation of vancomycin, at which time bacterial culture information is available, and in patients destined to receive longer or multiple treatment courses to identify those that could be at risk for vancomycin DRESS. This would be

facilitated through the development of a single allele assay for HLA-A*32:01, similar to approaches developed for HLA-B*57:01 and HLA-B*15:02, which are now widely available through commercial laboratories with short turnaround times. Since certain HLA alleles are known to influence the natural history of some infections, one potential limitation of this study is that we were not able to match controls based on indication for vancomycin treatment. However, given that HLA-A*32:01 was not represented at all in our matched tolerant controls despite the good distribution of almost identical Gram positive and mixed infections and similar host risk factors and co-morbidities that led to the intent for prolonged vancomycin treatment in both vancomycin DRESS cases and tolerant controls, we feel confident that this finding is not a disease association.

Our time-to-event analysis suggests that the risk of DRESS approaches 20% at four weeks of therapy in those carrying HLA-A*32:01 (Figures 3.5 and 3.6). Based on this analysis and the prevalence of HLA-A*32:01 of approximately 6.8% in individuals of European ancestry, we can estimate that approximately 75 patients started on vancomycin would need to undergo HLA-A*32:01 testing to prevent or preempt one case of vancomycin DRESS, which is a favorable ratio compared with other well-defined HLA-drug associations where HLA testing is used in clinical practice (Figure 3.10 and Table 3.8)[77].

Ex vivo and *in vivo* diagnostic approaches such as IFNγ ELISpot assays and IDT warrant further study for their sensitivity, specificity and safety for vancomycin and concurrently administered medications[189]. Additionally, if these techniques were to become routine in the diagnosis of vancomycin DRESS, standardized IFNγ ELISpot assays would need to be commercially available for clinical laboratories. In patient 18, evidence of a localized DRESS reaction on histopathology

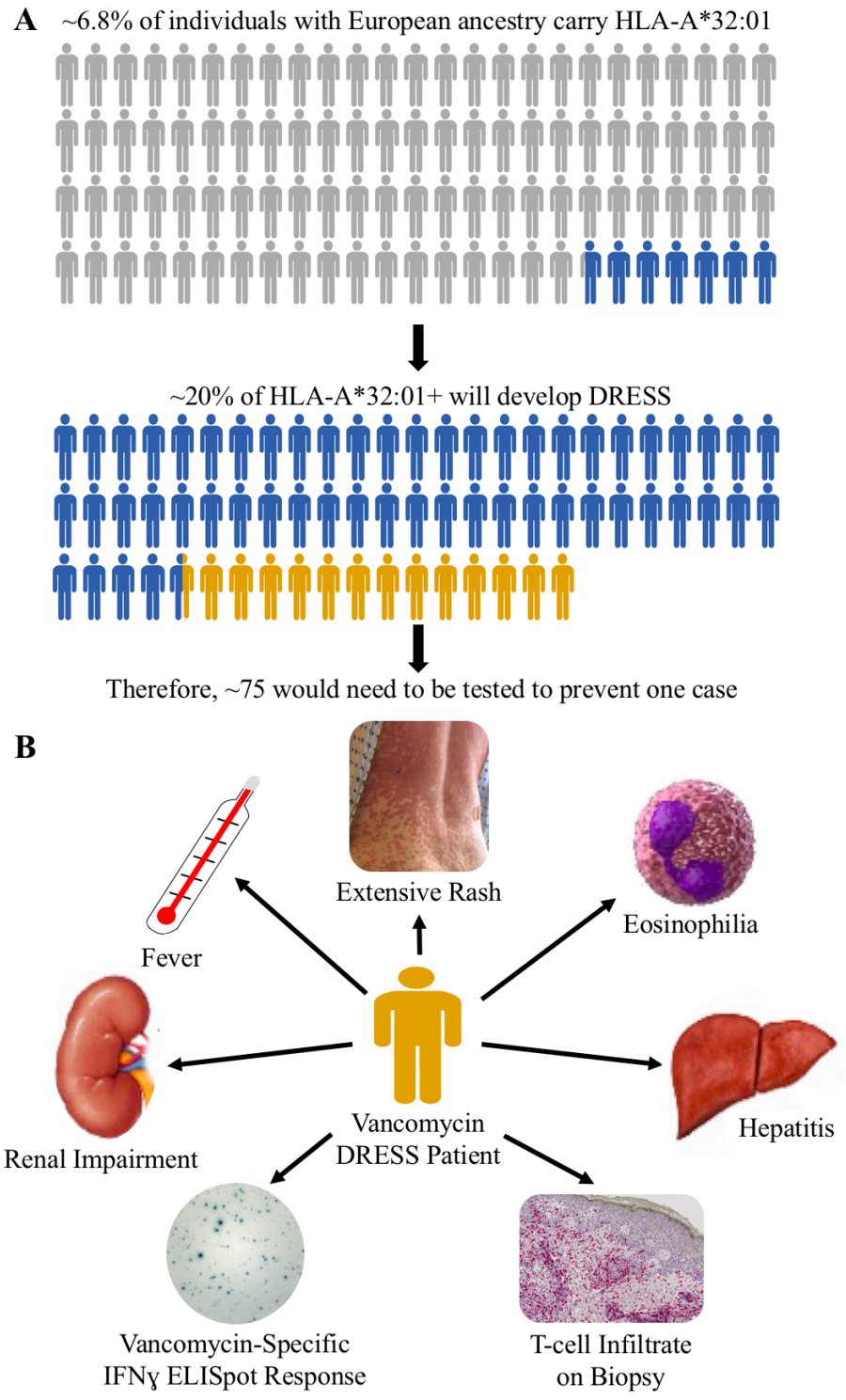

Figure 3.10. HLA-A*32:01 testing to prevent and diagnose vancomycin DRESS. A. Estimate of the number of patients of European ancestry needed to test for HLA-A*32:01 carriage to prevent on case of vancomycin DRESS. **B.** Clinical symptoms and laboratory findings of a patient with vancomycin DRESS. **Legend:** HLA, human leukocyte antigen; DRESS, drug reaction with eosinophilia and systemic symptoms; ELISpot, Enzyme-Linked ImmunoSpot.

Drug	Disease	HLA Risk Allele	Population	Number Needed to Test to Prevent 1 Case	Use in Routine Clinical Practice
Abacavir	Hypersensitivity	HLA-B*57:01	European African	13	YES
Allopurinol	DRESS/ SJS-TEN	HLA-B*58:01	South East Asian African	250	NO
Carbamazepine	SJS-TEN	HLA-B*15:02	South East Asian	1000	SELECTIVE
Dapsone	Hypersensitivity	HLA-B*13:01	South East Asian	84	UNDER STUDY
Flucloxacillin	DILI	HLA-B*57:01	European	13,819	NO
Vancomycin	**DRESS**	**HLA-A*32:01**	**European**	**70**	

Table 3.8. Clinical applications of HLA-associated T-cell mediated adverse drug reactions. Legend: SJS/TEN, Stevens-Johnson Syndrome/toxic epidermal necrolysis; DILI, drug-induced liver injury.

from a positive IDT biopsy demonstrates that the immunopathology of the acute reaction can be recapitulated in the skin following disease recovery. Consistent with previous studies showing that the ratio of FOXP3+ T cells to overall CD3+ T cells in acute DRESS skin positively correlates with longer times from start of symptoms to skin biopsy, we observed an increase is FOXP3+ regulatory T cells in the dermis of recovery phase skin following intradermal vancomycin administration (Figure 3.8)[190]. This also suggests that regulatory T cells may reside in the skin weeks to months following acute DRESS. While these immunohistopathologic results are compelling, they are from a single patient and require further study in additional patients with vancomycin DRESS.

Vancomycin has been associated with other ADRs including linear IgA bullous dermatosis, fixed drug eruption, acute generalized exanthematous pustulosis, and Stevens-Johnson syndrome/toxic epidermal necrolysis[64,191]. We have enrolled 10 individuals with non-DRESS vancomycin immune-mediated adverse drug reactions in our broader drug hypersensitivity studies. While the heterogeneity and small number of patients limits our ability to rule out other HLA associations with non-DRESS vancomycin-induced reactions, only 1/10 is HLA-A*32:01 positive. These HLA typing results suggest that this association is specific for vancomycin DRESS and that HLA screening would not prevent other vancomycin-induced delayed hypersensitivity reactions. Our study was powered to identify a strong association between HLA-A*32:01 and vancomycin DRESS in a population of primary European ancestry and we cannot generalize at this point to non-European ancestries where HLA associations with vancomycin DRESS will need to be independently studied.

Although the specific mechanism of vancomycin DRESS is unknown, our data may provide clues to the immunopathogenesis of this syndrome. The strong association with HLA-A*32:01 supports that vancomycin DRESS is an HLA Class I-restricted, CD8+ T-cell mediated process. For the HLA-B*57:01-restricted abacavir hypersensitivity reaction, immunologically-confirmed hypersensitivity can occur as early as 1.5 days of first dosing suggesting that a pre-existing memory T-cell response may be mechanistic[146]. In contrast, vancomycin DRESS in ours and other studies is characterized by a long latency period (median 21 days)[192]. Further, HLA-A*32:01 positive individuals who have not been exposed to vancomycin were observed to have negative responses to vancomycin by both *in vivo* (intradermal challenge) (n=1) and *ex vivo* (IFNγ ELISpot) assessments (n=4). These data might suggest that vancomycin DRESS pathogenesis is dependent upon a naïve T-cell response requiring CD4+ T-cell help. Vancomycin is a large glycopeptide and is excreted unchanged in the urine. Unlike abacavir which has been shown to alter the repertoire of self-peptides presented to T cells in HLA-B*57:01 positive individuals[56,58], our model suggests that vancomycin may bind within the antigen binding cleft of HLA-A*32:01 in the absence of peptides that conform to the canonical HLA-A*32:01 binding motif (Figure 3.9).

Currently, the use of HLA testing in clinical practice has been limited to pre-prescription screening strategies. This discovery of a strong association between HLA-A*32:01 and one of the most serious immunologically-mediated reactions associated with a commonly used antibiotic, vancomycin, raises the possibility that HLA testing could be used as a diagnostic risk stratification tool after initiation of vancomycin treatment but prior to development of vancomycin DRESS. Patients with complex and life-threatening infections commonly receive vancomycin dosed concurrently with beta-lactams or fluoroquinolone antibiotics as was noted in 21/23 (91%) of our

cases. This often leads to patients with DRESS being labeled as allergic to all of these antibiotic classes, which significantly restricts current and future treatment options. In those found to be HLA-A*32:01 positive, vancomycin treatment could either be rationalized where therapeutically appropriate or continued under close clinical observation and laboratory monitoring with discontinuation of vancomycin at the first sign of early DRESS symptoms. Alternatively, for those who develop possible vancomycin-induced DRESS or who have a known history suggestive of vancomycin DRESS, HLA-A*32:01 testing could be combined with adjunctive testing such as IFNγ ELISpot to vancomycin and other co-administered drugs to improve drug causality assessment. These strategies have the immediate potential to improve patient care by improving drug safety, increasing short-term drug efficacy and reducing future constriction of antibiotic choices.

CHAPTER IV

CHARACTERIZATION OF T-CELL RESPONSE IN A PATIENT WITH ACUTE RECHALLENGE VANCOMYCIN-INDUCED STEVENS-JOHNSON SYNDROME/TOXIC EPIDERMAL NECROLYSIS

OVERVIEW

In this chapter, I describe the clinical course and acute immune response of an individual of pacific-islander ancestry with rechallenge vancomycin-induced Stevens-Johnson syndrome. Notably, we found a dominant TCRαβ clonotype in the activated CD8+ T cells from multiple blister fluid samples from this patient collected at days 3 and 4 after symptoms onset.

INTRODUCTION

In addition to Drug Reaction with Eosinophilia and Systemic Symptoms (DRESS), vancomycin has also been associated with other adverse drug reactions (ADRs) including rarely Stevens-Johnson syndrome/toxic epidermal necrolysis (SJS/TEN)[64]. Unlike allopurinol-induced SJS/TEN and DRESS where both hypersensitivity syndromes are associated with the HLA-B*58:01 risk allele, in European populations, HLA-A*32:01 is specifically associated with vancomycin DRESS, not other vancomycin-induced immune-mediated ADRs (Chapter 3)[54,77]. No genetic risk factors have been identified for vancomycin-induced SJS/TEN. Due to the rare occurrence of vancomycin SJS/TEN and the common occurrence of combination antibiotic treatment, definitive cases are unusual and the thorough investigation of one case has the potential to provide important insights into the immunopathogenesis of this disease. In this chapter, I describe the clinical course,

human leukocyte antigen (HLA) typing results and T-cell repertoire of an Australian patient of Pacific Islander ancestry with acute rechallenge vancomycin-induced SJS.

METHODS

Vancomycin SJS Patient Identification and Enrollment

This patient with vancomycin SJS was identified by our collaborator, Jason Trubiano, MBBS, PhD, at Austin Health in Melbourne, Victoria, Australia. She was enrolled in our research study while hospitalized for her acute ADR in February 2017. All patients in our Vanderbilt drug hypersensitivities studies require a Naranjo adverse drug reaction score of ≥5 (probable adverse drug reaction and all SJS patients require an ALDEN score of ≥4 (probable that the implicated drug caused the reaction)[144,145]. All aspects of the study including the collection and storage of DNA, plasma, peripheral blood mononuclear cells (PBMCs), blister fluid and skin were IRB-approved and the patient signed informed consent.

Vancomycin-Naïve Control

A 62-year-old, vancomycin-naïve woman of European ancestry who shared carriage of one HLA Class I allele (HLA-B*56:01) with the vancomycin SJS patient was used as an experimental control. This individual has no known drug allergies and signed informed consent.

Peripheral Blood Mononuclear Cells (PBMCs) and Blister Fluid Preparation

Heparinized blood was drawn for the preservation of PBMCs on Day 2 of SJS Symptoms. PBMCs were isolated by Ficoll separation and stored at 10 million cells/vial. Blister fluid was collected from intact, fluid-filled bullae by an 18-gauge needle attached to a syringe on Days 3 and 4 of SJS

Symptoms. The needle was inserted in the base of each bulla, fluid contents were aspirated and inserted into ethylenediaminetetraacetic acid (EDTA) tubes for processing. Similar to standard PBMC processing, blister fluid cells and supernatant were separated by centrifugation. Vials of blister fluid supernatant were frozen in 500μL aliquots and cells were stored at 4 million cells/vial in standard freezing media (90% FBS, 10% DMSO). Cryopreserved PBMCs and blister fluid were shipped frozen from Australia to Vanderbilt on dry ice.

Human Leukocyte Antigen (HLA) Typing

High resolution four-digit HLA A B C DP DR DQ typing was performed using sequence-based typing on the Illumina Miseq (Chapter 2)[75,146].

Enzyme-Linked ImmunoSpot (ELISpot) Assays

Overnight IFN-γ ELISpot assays were performed in triplicate (Mabtech Kit 3420-2H) as previously described[106,180,181] using negative (unstimulated) and positive (anti-CD3 Mabtech antibody) controls. PBMCs plated at 200,000 cells per well were incubated with pharmacy stock vancomycin diluted in distilled water at concentrations of 5, 50, and 500 μg/mL. As supported by consensus in the literature, a positive response was defined as >50 spot forming units (SFU)/million cells after background removal[106,180,181]. The ELISpot results figure was generated using GraphPad Prism 7.0a Macintosh Version, GraphPad Software, La Jolla California USA, www.graphpad.com.

Immunohistochemistry of Skin Biopsy

A formalin-fixed, paraffin-embedded punch biopsy of acutely affected skin collected one day after the first appearance of rash was sectioned at 5 μm intervals. Slides were placed on the Leica Bond Max IHC stainer. All steps besides dehydration, clearing and coverslipping were performed on the Bond Max. Slides were deparaffinized. Heat induced antigen retrieval was performed on the Bond Max using their Epitope Retrieval 2 solution for 20 minutes. Slides were incubated with anti-CD3 (Cat# NCL-CD3-PS1, Leica, Newcastle, United Kingdom) for one hour at 1:100 dilution, Ready-To-Use anti-CD4 (PA0427, Leica, Buffalo Grove, IL) for one hour or Ready-To-Use anti-CD8 (MM39-10, McKinney, TX) for 15mins. For the anti-CLA stained sections, slides were placed in a Protein Block (Ref# x0909, DAKO, Carpinteria, CA) for 10 minutes and then incubated with anti-CLA (Cat.NB100-78039, Novus, Littleton, CO) for 1 hour at a 1:100 dilution followed by a biotinylated anti-rat (Cat. BA-5000, Vector Laboratories, Inc.) for 15 minutes at a 1:200 dilution. The Bond Polymer Refine detection system was used for visualization. Slides were the dehydrated, cleared and coverslipped. Sections of formalin-fixed, paraffin-embedded normal skin were stained as controls. Vanderbilt dermatopathologist Jeffrey Zwerner, MD, PhD scored all slides.

Flow Cytometry Staining

Cryopreserved blister fluid cells and PBMCs were thawed and washed with PBS. Cells were incubated with Live/DEAD Fixable Aqua (ThermoFisher). Cells were surface stained with antibodies at room temperature except for the CCR7 marker, which was stained separately at 37°C. Total blister fluid cells were stained with a targeted T-cell antibody panel including basic T cell markers (CD3, CD4, CD8), activation markers (CD69, CD137), memory markers (CCR7, CD45RO), an NK cell marker (CD56), and a marker of skin homing (CLA). PBMCs were stained

with a similar panel, which included antibodies for all of the same markers except for CD56. Antibodies for fluorescence cytometry included CD3-A700 (UCHT1, BD Pharmingen), CD4-PerCPCy5.5 (RPA-T4, BD Pharmingen), CD8-APC-AF750 (Invitrogen), CD137-PE (BD Pharmingen), CD69-APC (FN50, BD Pharmingen), CD14-V500 (M5E2, BD Horizon), CD19-V500 (H1B19, BD Horizon), CLA-PE/Cy7 (HECA-452, Biolegend), CD45RO-CF594 (UCHL1, Invitrogen), CD56-BV421 (HCD56, Biolegend) (blister fluid only), CCR7-BB515 (3D12, BD Horizon) (blister fluid only) and CCR7 BB421 (150503, BD Pharmingen) (PBMCs only).

Cell Sorting

All fluorescence-activated cell sorting (FACS) experiments were perform on an ARIA III flow cytometer (Becton Dickinson) at the Vanderbilt University Medical Center Flow Cytometry Shared Resource. The gating strategies for single-cell sorting of blister fluid cells and bulk sorting of memory populations of PBMCs are shown in Figures 4.1 and 4.2, respectively. PBMCs from healthy donors were used as biological controls for gating. Data were analyzed using FACSDiva (BD Biosciences) and FlowJo software (Tree Star).

Bulk TCR Sequencing

Genomic DNA from sorted CD8+ T-cells memory populations was isolated using the QIAamp DNA Blood Mini Kit (QIAGEN). Isolated DNA was used for bulk TCRβ CDR3 region amplification and sequencing using the ImmunoSEQ assay (Adaptive Biotechnologies, Seattle, WA). In this method, bias-controlled V and J gene primers are used to amplify rearranged V(D)J segments for sequencing[193].

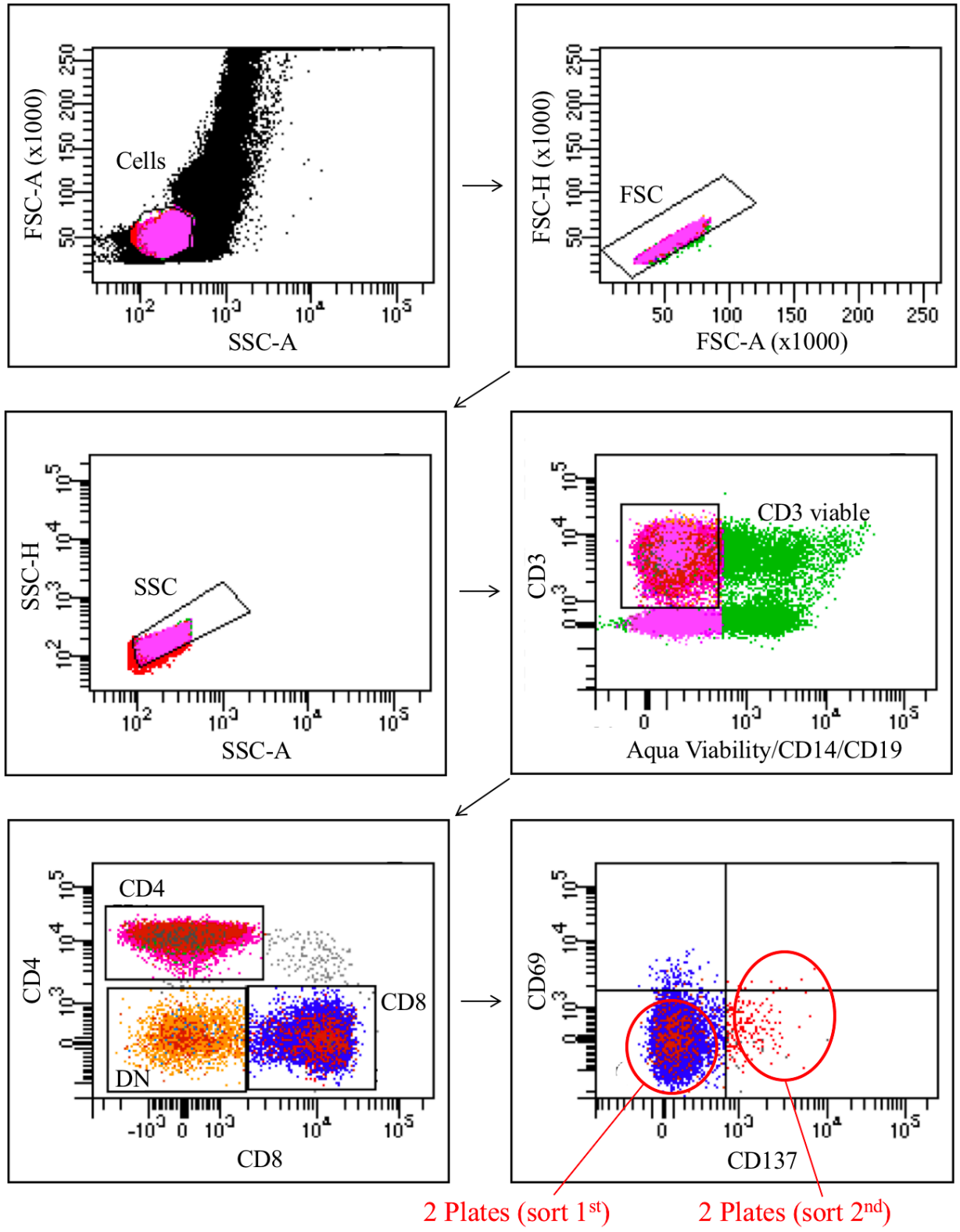

Figure 4.1. Gating strategy for single-cell blister fluid sort. Gating shown on peripheral blood mononuclear cells from a healthy donor. **Legend:** FSC, forward scatter; SSC, side scatter; H, height; A, area; DN, double negative.

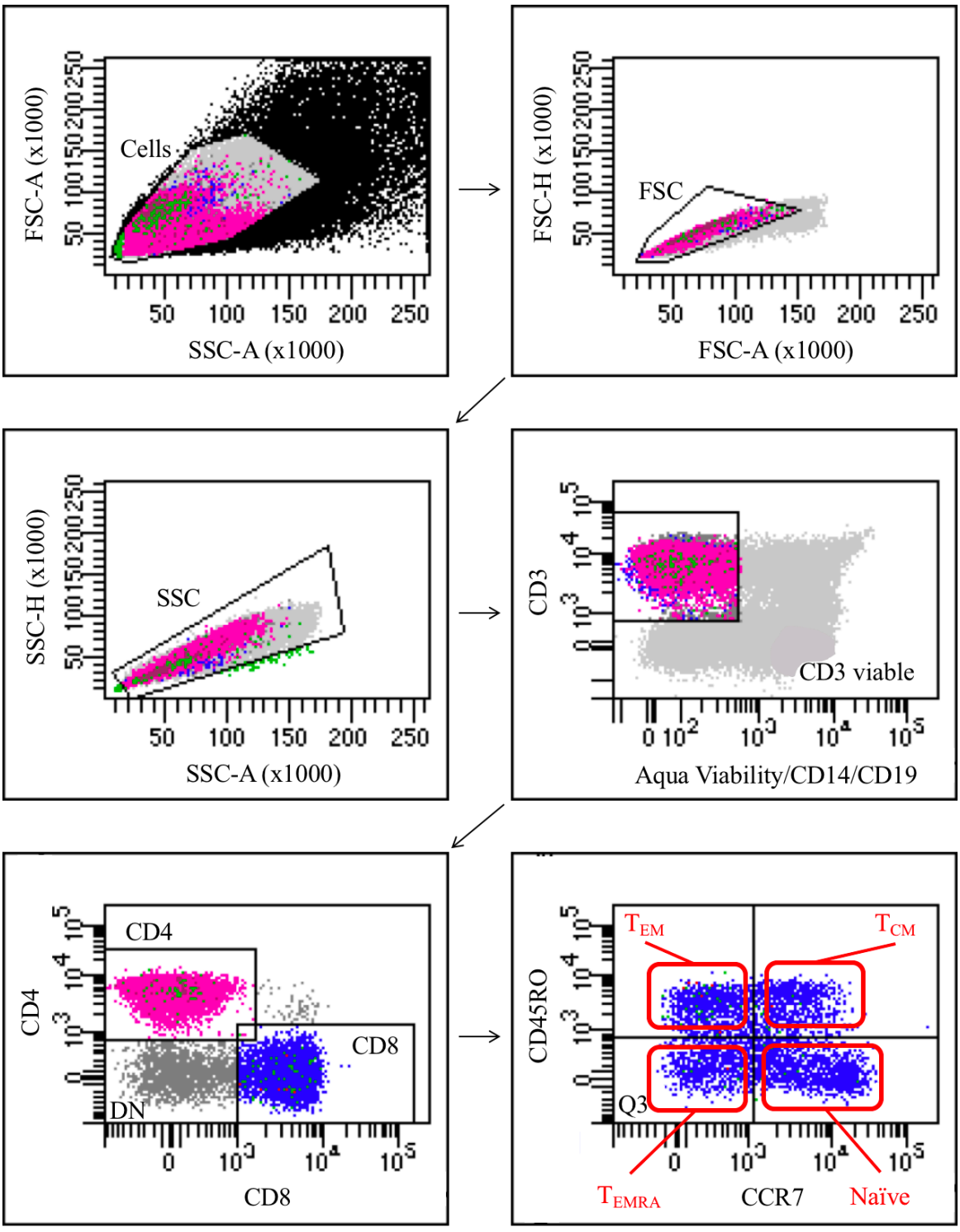

Figure 4.2. Gating strategy for bulk sort on acute vancomycin SJS peripheral blood mononuclear cells. Gating shown on peripheral blood mononuclear cells from a healthy donor. **Legend:** FSC, forward scatter; SSC, side scatter; H, height; A, area; DN, double negative; TEM, T effector memory cells; TCM, T central memory cells; TEMRA, T effector memory re-expressing CD45RA cells.

Single-cell TCR Sequencing

The single-cell TCR sequencing was done by our scientific partners at the Institute for Immunology and Infectious Diseases (IIID). Using our novel TCR/RNA sequencing platform, single blister fluid cells were sorted directly into 4μL of a cDNA-conversion compatible buffer, centrifuged and then stored on dry ice prior to transfer to -80C for temporary storage. The single cells then underwent oligo (dT)-primed reverse transcription during which the cDNA products of individual wells are barcoded and generically tagged with both 3' oligo (dT) and 5' biotin labelled template switching oligonucleotides (TSO). Subsequent amplification of the cDNA derived from a single cell was amplified using the generic tags. Specific transcripts were targeted with a combination of nested generic tags and gene specific primers including TCRα and TCRβ conserved regions. The transcriptome was analyzed using a modified Nextera transposon-mediated tagging-and-fragmentation ("tagmentation") assay with subsequent amplification of the 5' and 3' ends of the transcripts between the introduced Nextera-tag and the generic tags from cDNA conversion. Samples were multiplexed for next generation library preparation and sequencing. Single cell sequences were bioinformatically separated.

TCR Sequencing Analyses

The TCR sequencing data were analyzed using IIID's Visual Genome Analysis Studio (VGAS), which was designed for high performance next generation sequencing analysis[148].

RESULTS

Relevant Patient Medical History and Disease Course

In February 2017, a 55-year-old woman of Pacific Islander Ancestry with a past medical history significant for short gut syndrome on long-term total parental nutrition developed central intravenous line sepsis. She had multiple positive blood cultures, which grew Gram positive bacilli, but a definitive identification of the bacteria causing her sepsis was not acquired. According to the adverse reactions listed in her medical records, she had a previous history of vancomycin-induced "red man syndrome" two years prior to this infection. Red man syndrome is not a contraindication for vancomycin treatment because the infusional pruritis and rash can typically be managed by a slower infusion rate and anti-histamines. Accordingly, she was started on intravenous vancomycin therapy. Within 48 hours, she developed a blistering rash and the vancomycin therapy was stopped. The skin was positive for Nikolsky's sign, meaning that slight rubbing of the skin caused separation of the outermost epidermal skin layer, a strong diagnostic indicator for SJS. <10% of her body surface area was involved and there was no clear mucosal or internal organ involvement. Other pertinent laboratory tests including autoimmune antibodies (ANA/ANCA) and mycoplasma testing were negative. She had no eosinophilia. A biopsy of the affected skin was taken one day after rash developed. The biopsy supported a diagnosis of SJS, distinguishing the reaction from generalized fixed drug eruption. She received supportive care for the adverse reaction to vancomycin, treatment for sepsis was reinitiated with another antibiotic, and the patient recovered. Review of the clinical notes from her prior vancomycin exposure revealed that her previous vancomycin-induced rash lasted for over two weeks, which is inconsistent with a diagnosis of red man syndrome.

Based on the pertinent clinical information above, I calculated this patient's Naranjo score, or probability that this event was an adverse drug reaction, to be a **9**. A Naranjo score ≥9 is categorized as a definite adverse drug reaction. Her score was calculated as follows: **+1** – previous conclusive reports of vancomycin being associated with SJS development, **+2** – the adverse event appeared after the suspected drug was administered, **+1** – adverse reaction improved when drug was discontinued, **+2** – there were no alternative causes that could have caused this reaction on their own (e.g. testing for mycoplasma, which is known to be a cause of SJS, especially in children, was negative), **+1** – the reaction did not reappear when other drugs were given, **+1** – the patient had a similar reaction to the same drug in the past, and **+1** – the adverse event was confirmed by objective evidence (i.e. biopsy). Vancomycin was not readministered during the acute reaction. It is unknown whether the drug concentrations were at toxic levels. Vancomycin was stopped when blistering occurred so dosage effects could not be assessed. Therefore, no additional criteria factored into the scoring of her reaction.

I similarly used the ALDEN algorithm to determine the likelihood that vancomycin was causal drug. Her ALDEN score was a **9**. A score ≥6 signifies that the implicated drug was "very probably" the cause of the reaction. Her score was calculated as follows: **+3** – delay from initial drug intake to onset of reaction was 1-4 days in case of previous reaction to the same drug, **0** – drug was present in the body on index day, **+4** – previous SJS/TEN after use of same drug, **+2** – the drug has been associated with definite cases, but is not a common cause of SJS/TEN, **0** – no other potential cause for the reaction was identified. Vancomycin was stopped when symptoms appeared so harm done based on drug continuation could not be determined.

HLA Typing

The patient's high resolution, four-digit HLA Class 1 and II typing results were HLA-A*02:06, HLA-A*03:01, HLA-B*07:02, HLA-B*56:01, HLA-C*07:02, HLA-C*07:02, HLA-DPB1*04:01, HLA-DBP1*05:01, HLA-DQA1*01:03, HLA-DQA1*05:01, HLA-DQB1*03:01, HLA-DQB1*06:01, HLA-DRB1*08:03 and HLA-DRB1*12:01. The allele frequencies of these HLA Class 1 alleles in representative populations is shown in Table 4.1.

ELISpot Assay

PBMCs from the patient with vancomycin SJS released IFN-γ after overnight incubation with vancomycin in a drug dose-dependent pattern (Figure 4.3). Based on the >50 SFU/million cell cutoff, the ELISpot was positive at vancomycin concentration of both 50 and 500 μg/mL. PBMCs from the HLA-B*56:01 matched vancomycin-naïve control did not release IFN-γ in response to vancomycin stimulation at any of the tested concentrations. Positive (anti-CD3) and negative (media) controls worked as expected.

Immunohistochemistry of Skin Biopsy

Immunohistochemistry of T-cell subsets on a skin punch biopsy taken one day after initial rash development revealed a dense lymphocytic infiltrate. The CD4+ T cell infiltrate was largely restricted to the dermis. In contrast, CD8+ and CLA+ T cells infiltrated both the dermis and epidermis. Healthy skin is shown for comparison (Figure 4.4).

	Population Allele Frequency (%)		
Vancomycin SJS Patient (n=1)	**America Samoa (n=51)**	**New Zealand Maori (n=46)**	**Australia New South Wales Caucasian (n=134)**
HLA-A*02:06	13.0	29.4	0.0
HLA-A*03:01	2.0	2.9*	13.8
HLA-B*07:02	1.0	1.1	12.0
HLA-B*56:01	2.0	1.1	0.0
HLA-C*07:02	8.0	10.9	15.8
HLA-C*07:02	8.0	10.9	15.8

Table 4.1. Vancomycin SJS patient HLA Class I typing compared to allele frequency in representative populations. Populations represented were chosen based on patient's ancestry and availability of public HLA typing data. Population allele frequencies are from allelefrequencies.net[158]. *HLA-A*03:01 allele frequency is from a New Zealand Maori admixed population (n=105). **Legend:** SJS, Stevens-Johnson syndrome.

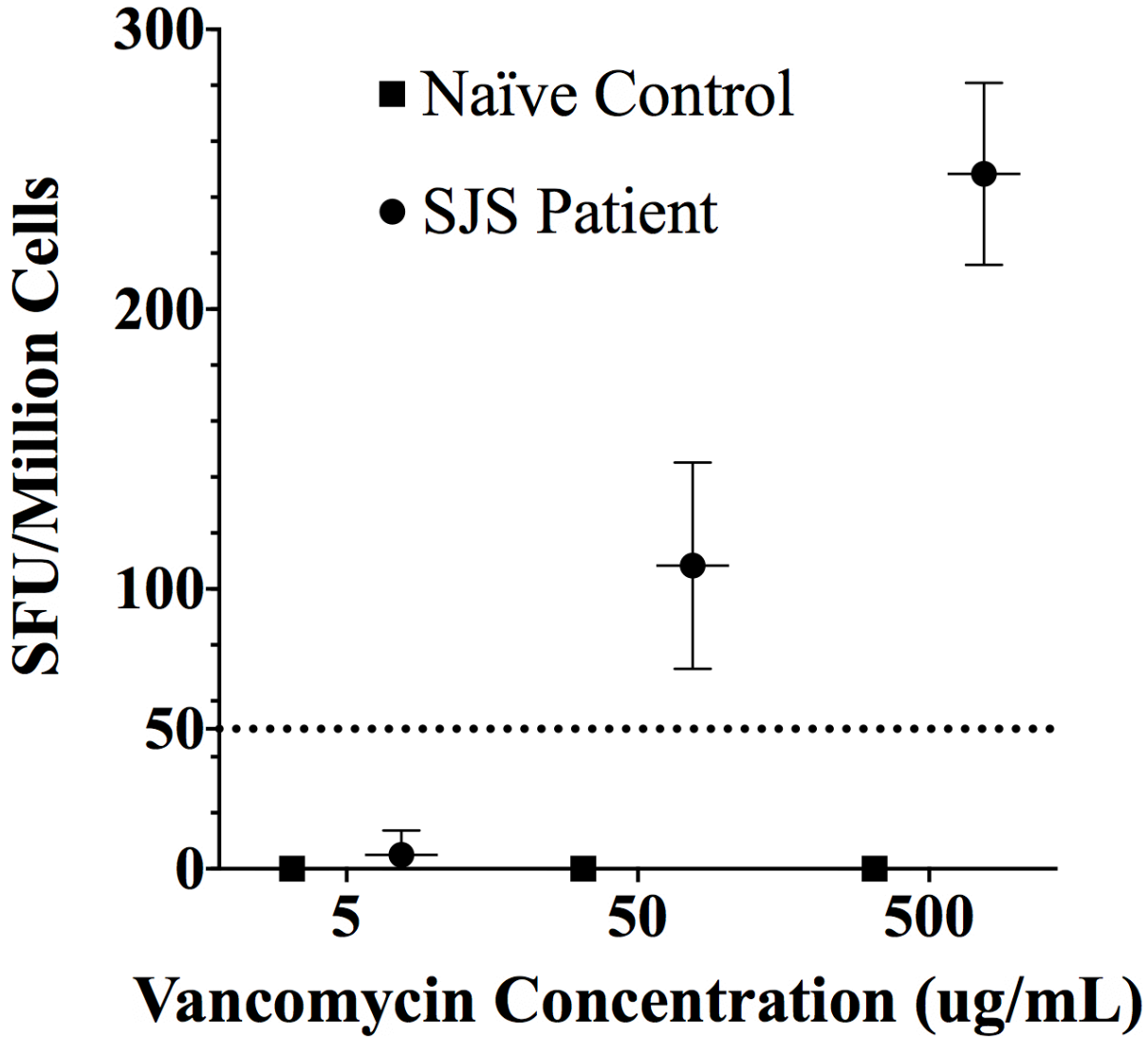

Figure 4.3. Peripheral blood mononuclear cells from vancomycin SJS patient release IFN-γ in response to vancomycin stimulation. Enzyme-Linked ImmunoSpot (ELISpot) assays were used to measure IFN-γ release after 18-hour incubation with vancomycin at concentrations of 5, 50 and 500 μg/mL. Cells from a vancomycin-naïve woman of European ancestry who also carried HLA-B*56:01 was used as a control. Means of the replicates are plotted. Positive results are those above the dotted line intersecting the y-axis at 50 SFU/million cells. **Legend:** SJS, Stevens-Johnson syndrome; SFU, spot-forming units.

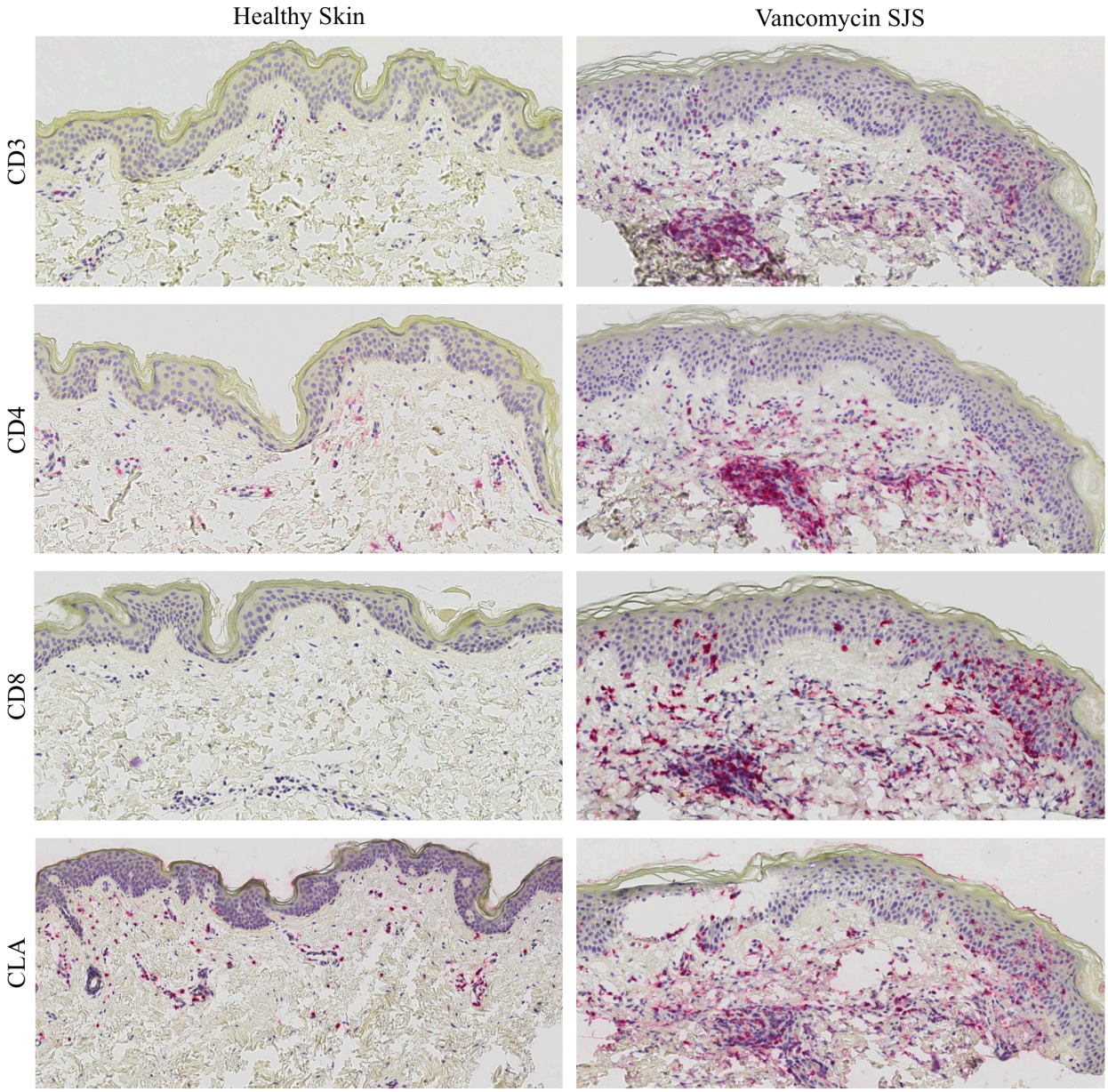

Figure 4.4. Immunohistochemistry of T-cell subsets in acute SJS skin. Immunohistochemistry staining on a skin punch biopsy taken one day after initial rash development revealed a dense lymphocytic infiltrate (right panel). The CD4+ T cell infiltrate was largely restricted to the dermis. In contrast, CD8+ and CLA+ T cells infiltrated both the dermis and epidermis. Healthy skin is shown for comparison (left panel). **Legend:** SJS, Stevens-Johnson syndrome; CLA, cutaneous lymphocyte antigen.

Cell Sorting

Blister fluid cells collected on Days 3 and 4 of SJS symptoms were single-cell sorted in separate experiments. One 96-well plate of CD8+CD137- and one 96-well plate of activated CD8+CD137+ T cells were sorted for each experiment. In the single-cell sort of blister fluid collected on Day 3 of symptoms, 77.8% of the cells were CD3+ T cells. In the total CD3+ T cell population, 50.9% were CD3+CD8+ and 6.6% were CD3+CD4+ T cells. 1.3% of the CD3+CD8+ T cells were also CD137+ (Figure 4.5). In the single-cell sort of blister fluid collected on Day 4 of symptoms, 75.7% of the cells were CD3+ T cells. In the total CD3+ T cell population, 66.1% were CD3+CD8+ and 10.4% were CD3+CD4+ T cells. 1.4% of the CD3+CD8+ T cells were also CD137+. CD8+ T cells from PBMCs collected and processed on Day 2 of SJS symptoms were bulk sorted into memory T cell populations. In total, 314,146 naïve T cells (CCR7+CD45RO-), 18,768 T central memory cells (TCM) (CCR7+CD45RO+), 80,429 T effector memory re-expressing CD45RA cells (TEMRA) (CCR7-CD45RO-) and 65,376 T effector memory cells (TEM) (CCR7-CD45RO+) were bulk sorted for DNA extraction and TCR sequencing.

TCR Sequencing

The index-sorted, single, live CD8+CD137- and CD8+CD137+ cells were subjected to paired TCRαβ sequencing. A dominant CD8+ T-cell clonotype comprised of the TCRα chain rearrangement TRAV19/J28 with the TCRα complementary determining region 3 (CDR3) sequence CALSEGPGAGSYQLTF and the TCRβ chain rearrangement TRBV9/D1/J2-3 with the TCRβ CDR3 sequence CASSLSGAEDTQYF was identified in the CD8+ blister fluid T cells (Figure 4.6). If the results from the two blister fluid sorts are combined, this clonotype represented 79.4% of total paired TCRαβ sequences identified in the blister fluid. Strikingly, this clonotype

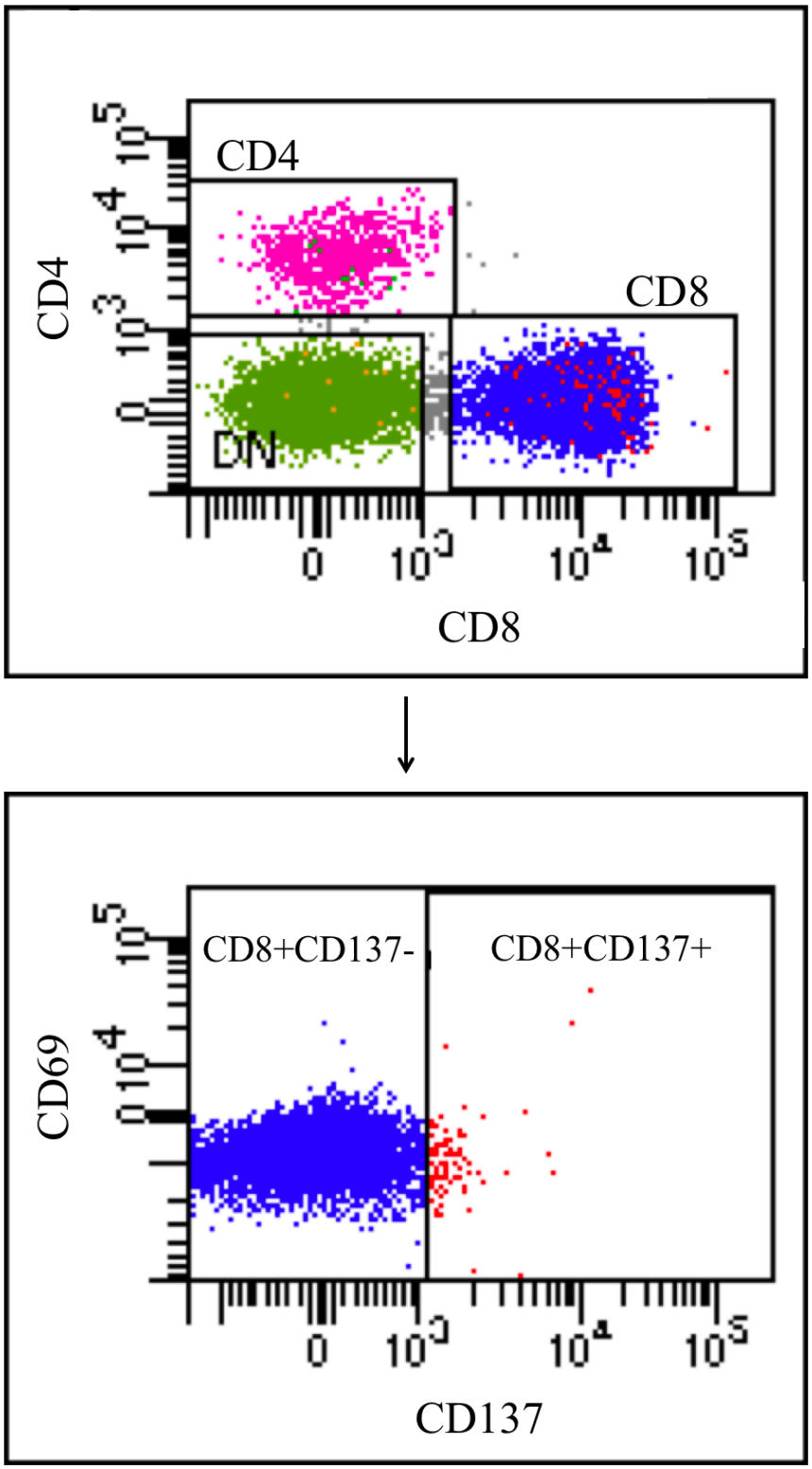

Figure 4.5. Vancomycin SJS single-cell blister fluid sort. Single cells from the CD8+CD137- and CD8+CD137+ T cell populations were index sorted into 96-well plates. Gates were set based on peripheral blood mononuclear cells. **Legend:** DN, double negative.

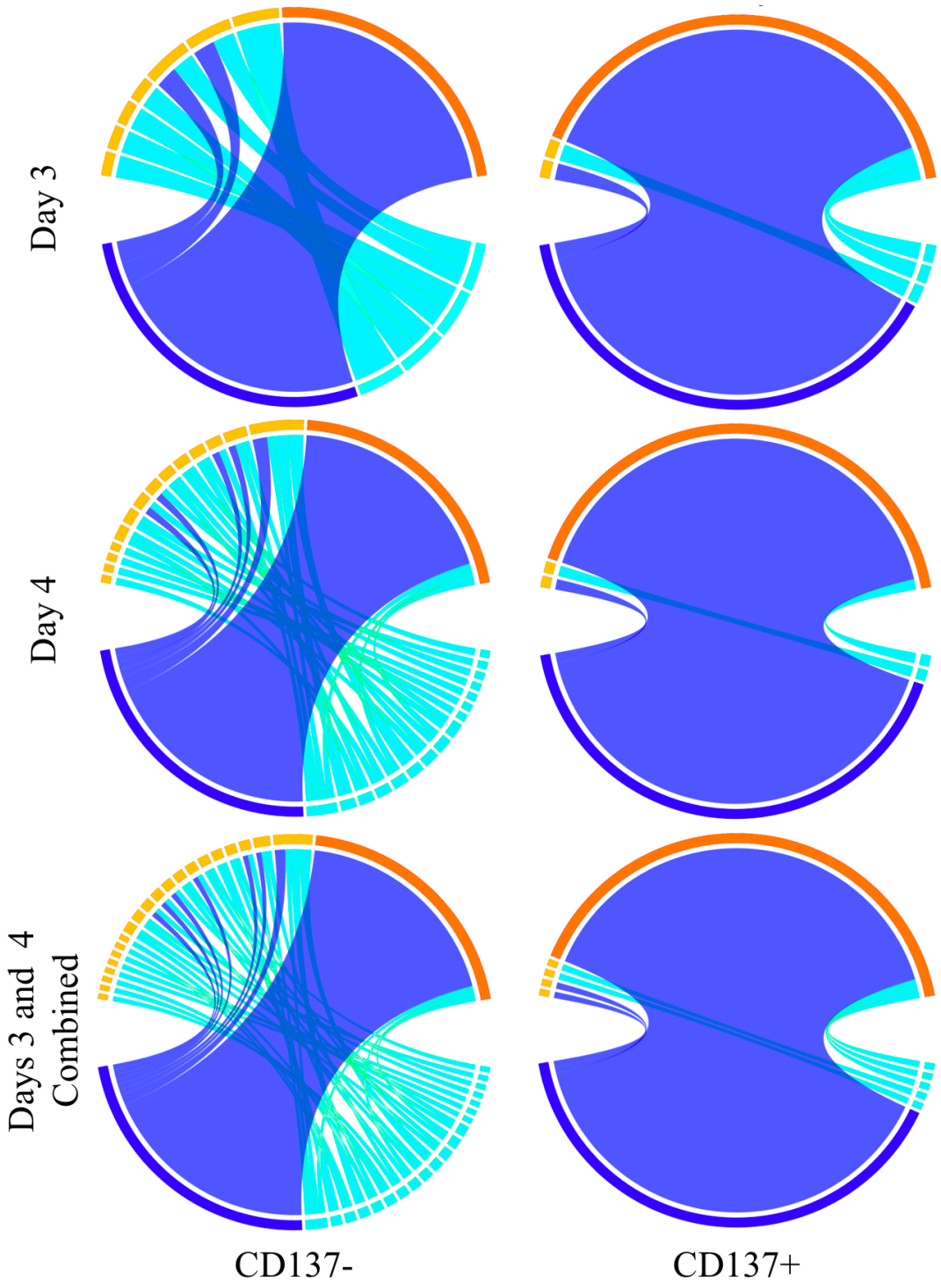

Figure 4.6. T-cell receptor sequencing results of vancomycin SJS single-cell blister fluid sort. A dominant TCRαβ clonotype CALSEGPGAGSYQLTF/CASSLSGAEDTQYF was found in 79.4% of the paired TCRαβ sequences recovered from the blister fluid and made up 92.1% of the activated (CD8+CD137+) T cell population. All sorted cells were CD3+CD8+ T cells. TCRβ sequences in blue are paired with TCRα sequences in orange. The dominant TCRαβ pair is shown in dark blue and dark orange.

represented 92.1% (70/76) of total paired TCRαβ sequences identified in the activated CD8+CD137+ T cells compared to 65.6% (42/64) of the CD8+CD137- blister fluid T cells, demonstrating marked clonality among activated CD8+ T cells present in the blister fluid from this subject (p=0.001). The results from the two blister fluid sorts analyzed separately are similar. Of total paired TCRαβ sequences identified in the activated CD8+CD137+ T cells, the dominant clonotype represented 92.9% (26/28) in blister fluid collected on Day 3 of symptoms and 91.7% (44/48) in blister fluid collected on Day 4 of symptoms. Comparatively, of the total paired TCRαβ sequences identified in the CD8+CD137- T cells, the dominant clonotype represented 70.6% (12/17) in blister fluid collected on Day 3 of symptoms and 63.8% (30/47) in blister fluid collected on Day 4 of symptoms.

TCRβ sequencing of PBMCs collected on Day 2 of SJS symptoms revealed a polyclonal population of T cells. The specific TCRβ CDR3 clonotype CASSLSGAEDTQYF that was dominant in the blister fluid was not present in any of the 67,186 TCRβ sequences recovered from the bulk sort of PBMCs including TCRβ sequences from 59,504 Naïve T cells, 2,553 TCM cells, 2,871 TEMRA cells, and 2,258 TEM cells. The TRBV9/D1/J2-3 TCRβ chain rearrangement that was dominant in the blister fluid was present in 0.06% (40/67,186) of the sorted PBMCs including 0.06% (35/59,504) of Naïve T cells, 0.12% (3/2,553) of TCM cells, 0.03% (1/2,871) of TEMRA cells and 0.04% (1/2,258) of TEM cells.

DISCUSSION

In this chapter, I described a clinical case of vancomycin SJS and document the patient's acute immune response to the ADR. Similar to the cases of vancomycin DRESS described in Chapter 3,

this patient's PBMCs had a positive vancomycin-specific, dose-dependent overnight IFNγ ELISpot, supporting vancomycin as the causative drug. More cases will be needed to speculate about a putative HLA risk allele for vancomycin SJS development, but similar to the other non-DRESS vancomycin IM-ADR cases discussed in Chapter 3, this patient was HLA-A*32:01 negative. This may suggest that HLA-A*32:01 is not a risk factor for vancomycin SJS/TEN. However, given the rarity of this phenotype and this patient's Pacific Islander ancestry, it cannot be ruled out that she carries an HLA risk factor that would both be a risk factor for vancomycin DRESS and SJS/TEN in this population. Notably, HLA-B*56 has been associated with other severe cutaneous adverse drug reactions in this population[194]. The CLA+, CD8+ and CD3+ lymphocytic infiltrate in the epidermis of acutely affected vancomycin SJS skin demonstrated with immunohistochemistry supports the hypothesis that cytotoxic CD8+ T cells are mediating the keratinocyte death and epidermal sloughing in SJS.

This patient carried a previous diagnosis of vancomycin-induced red man syndrome. However, upon review of her medical records, which documented a prior vancomycin-associated rash that lasted >2 weeks two vancomycin which did not respond to treatment with antihistamines or slowed antibiotic infusion, it became clear that the February 2017 reaction was more likely her second episode of vancomycin-induced SJS. The finding of a dominant TCRαβ clonotype in both the activated CD8+CD137+ T cells and the CD8+CD137- T cells in blister fluid drawn at two separate time points is consistent with other data from our lab from a rechallenge allopurinol TEN patient who also exhibited a dominant TCR clonotype in both the activated and non-activated blister fluid cells (White et al, unpublished data). The fact that the dominant TCRβ CDR3 from the blister fluid

was not found in any of the 67,186 TCRβ sequences identified in the peripheral blood, highlights the importance of studying T cells at the sites of disease during the acute reaction.

Multiple future studies are evident based on the preliminary data described in this chapter. Full-transcriptome single-cell RNA sequencing data will soon be available for all of the blister fluid cells with single-cell TCR sequencing. The additional data will provide key insights into the immune phenotype(s) of the blister fluid T-cells including information on their expression of transcripts for cytotoxic proteins such as granulysin, the only previously reported biomarker of SJS. This finding would be consistent with previously presented data, as granulysin was highly expressed in the activated CD8+ T cells in the nevirapine SJS blister fluid (Chapter 2)[35]. The single-cell RNA sequencing data will be analyzed with a particular focus on the blister fluid T cells expressing the dominant TCRαβ clonotype.

Additionally, the identification of a dominant TCR in the blister fluid of a patient with acute vancomycin SJS provides important insights into the pathogenesis of this disease and identifies a potential drug-specific TCR for functional studies in a Jurkat cell reporter assay. In this assay, a Jurkat T cell line will be transfected with plasmids encoding the specific TCR α and β genes, CD8 α and an NFAT-luciferase reporter vector. I have developed a lymphoblastoid cell line (LCL) derived from the PBMCs of this vancomycin SJS patient. This LCL will be incubated with and without vancomycin with the candidate TCR transfectoma. We hypothesize that co-culture will trigger antigen-specific, TCR-dependent calcium flux in the Jurkat cells resulting in quantifiable NFAT-driven luciferase. If the TCR transfectomas expresses luciferase in response to LCL with vancomycin but not LCL alone, this will provide strong evidence that we have identified a drug-

reactive and potentially pathogenic T cell. Obviously, the observations in this study are limited by the fact that only a single patient with this specific drug-induced phenotype has been studied thus far. While the data in this chapter are derived from a single patient, the experimental approach described can be used as a roadmap for investigating future cases of vancomycin SJS or other vancomycin-induced blistering diseases such as fixed drug eruption and linear IgA bullous dermatosis.

CHAPTER V

CONCLUSIONS, CLINICAL IMPLICATIONS AND FUTURE DIRECTIONS

Conclusions and Clinical Implications from the Nevirapine Hypersensitivity Patient Cohort

The 100% negative predictive value of HLA-C*04:01 in the South African patients with nevirapine SJS/TEN suggests that this allele could be used as a screening test to identify patients at risk for developing a reaction before nevirapine is prescribed. Several other antiretroviral therapy treatment options exist for patients found to carry the HLA risk allele so nevirapine can be safely avoided in HLA-C*04:01 positive patients. However, for the other ~80% of South Africans without HLA-C*04:01, nevirapine therapy has a favorable long-term safety profile. The addition of *ERAP1* genotyping for rs27044(C) could be added to HLA-C*04:01 testing to increase to positive predictive value of genetic testing for nevirapine SJS/TEN. While the addition of this test would lower the negative predictive value, in a patient who is known to be HLA-C*04:01 positive, but for whom nevirapine is the best treatment option, such as a pregnant woman initiating antiretroviral therapy or a patient co-infected with HIV and multi-drug resistant tuberculous on bedaquiline-based therapy, rs27044(C) genotyping could be used in a risk stratification algorithm to determine the best treatment options.

Future Directions for Research on Severe Nevirapine Hypersensitivities

The high prevalence of HIV in the South African population provides a unique opportunity to study nevirapine-exposed relatives of nevirapine hypersensitive patients. In addition to the 46 unrelated nevirapine tolerant controls that I discussed in Chapter 2, I have also recruited three

nevirapine tolerant relatives of nevirapine SJS/TEN patients (Figure 5.1). All three relatives carry HLA-C*04:01 and have similar KIR distributions as their hypersensitive relatives. Nevirapine tolerant relative 1, daughter of nevirapine SJS/TEN patient 1 and first cousin of nevirapine SJS/TEN patient 10, carries rs27044(C), which is associated with a higher risk for nevirapine SJS/TEN. However, based on CYP2B6 genotyping, she metabolizes nevirapine faster than her hypersensitive relatives. In contrast, nevirapine tolerant relative 2, first cousin of nevirapine SJS/TEN patient 1 and first cousin once removed of nevirapine SJS/TEN patient 10, is a slow metabolizer of nevirapine based on CYP2B6 genotyping, putting him at an increased risk of hypersensitivity. However, he does not carry the ancestral allele for rs27044, but is instead homozygous for the non-ancestral allele, rs27044(GG), which may have protected him from developing nevirapine SJS/TEN. Nevirapine tolerant relative 3, mother of nevirapine SJS/TEN patient 12, has a slow metabolizing phenotype for nevirapine based on CYP2B6 genotyping and carries the ancestral allele for *ERAP1* SNP rs27044(C). Based on my overall results, the genetic findings of nevirapine tolerant relative 3 should have put her at a higher risk of nevirapine SJS/TEN, but she did not develop a reaction.

The tolerant relatives particularly highlight the fact that not everyone with known genetic risk alleles will develop a reaction to nevirapine. Samples from these three relatives may provide valuable insight into the risk factors that are important for nevirapine SJS/TEN beyond the targeted gene approach I have used thus far in this cohort. Future work will focus on whole genome sequencing of these three individuals and their three nevirapine hypersensitive relatives to see if we can uncover additional genetic factors that may increase an individual's risk of developing nevirapine SJS/TEN. If additional genetic risk factors are found, they can then be studied in a

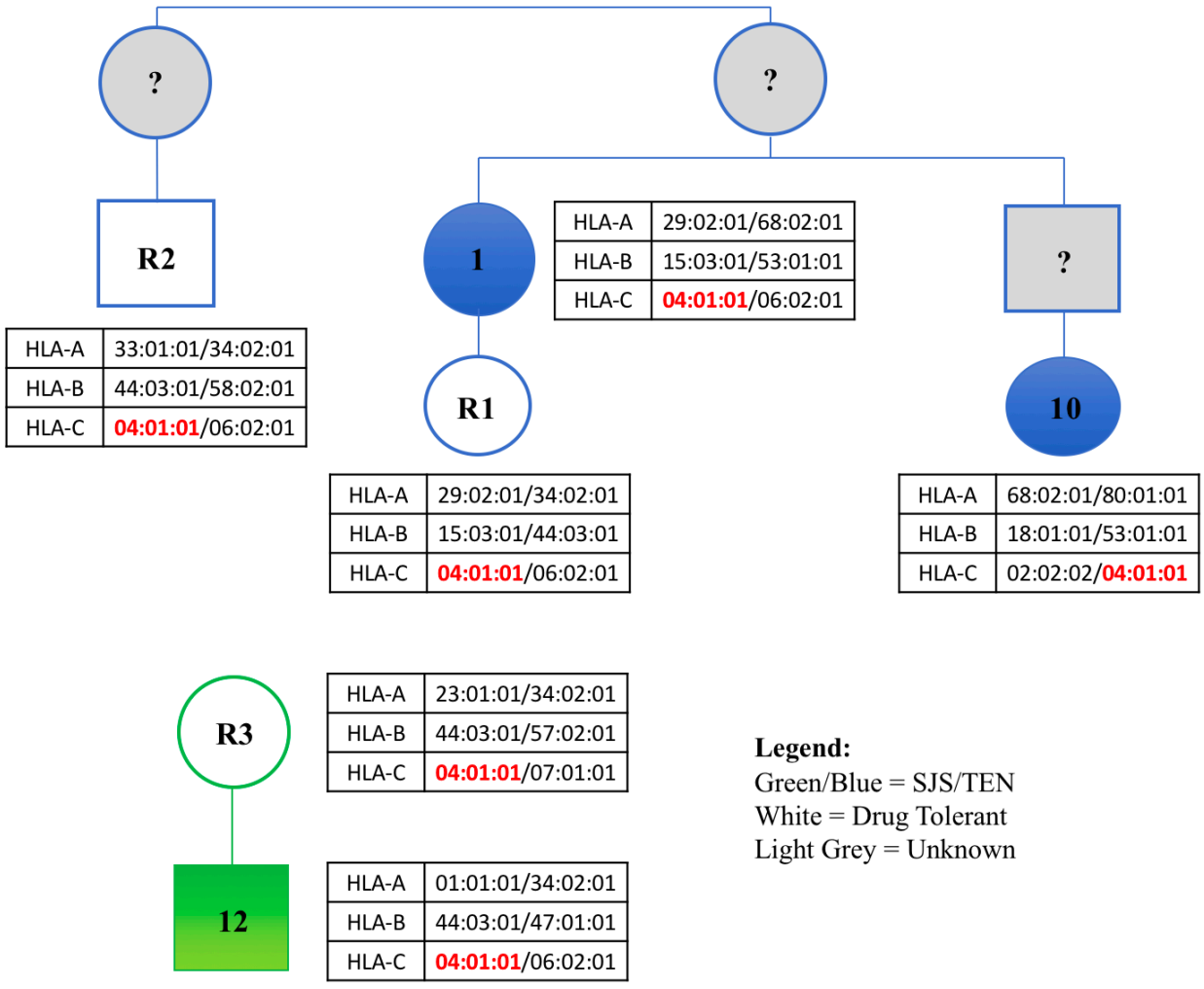

Figure 5.1. Pedigrees of nevirapine SJS/TEN patients and their nevirapine tolerant relatives. The SJS/TEN patient numbers correspond to those in Chapter 2, Table 2.2. **Legend:** R1, nevirapine tolerant relative 1; R2, nevirapine tolerant relative 2; R3, nevirapine tolerant relative 3.

larger cohort of nevirapine hypersensitive patients.

The single cell TCR sequencing and RNA sequencing of acutely-affected skin and blister fluid from nevirapine SJS/TEN patients highlighted the cytotoxicity of the blister fluid T cells. We are currently pursuing this work further with additional analyses of the single cell RNA sequencing data and 10x Genomics experiments to look at the entire repertoire of cells present in the blister fluid, as opposed to focusing solely on the T cells. However, the conclusions from this work will still be limited by the number of patient samples. Additional blister fluid samples from patients with acute nevirapine SJS/TEN will be needed to determine whether the majority of patients have an oligoclonal T-cell response. Ideally, blister fluid should be collected as early as possible in the disease process and then, if available, additional samples should be collected over time. This will help elucidate how the population of cells in the blister fluid changes over the natural history of the disease. If strong candidate TCRs are identified with these approaches, their specificity to nevirapine should be tested in a Jurkat cell reporter assay as described in Chapter 4.

Conclusions and Clinical Implications from the Vancomycin DRESS Patient Cohort

In a population of predominantly European ancestry, I showed that carriage of the HLA-A*32:01 allele is strongly associated with the development of vancomycin DRESS. Accordingly, HLA-A*32:01 testing to help preempt and implicate vancomycin as the causal drug for DRESS could improve the safety and efficacy of antibiotic treatment. Conventional HLA typing is done by serological or sequence-specific typing methods. Serologic approaches to HLA typing that have been traditionally used in the selection of donors for organ transplantation lack specificity since commercially available monoclonal antibodies cross-react with different HLA alleles[195]. In

contrast, sequence-based typing, which was used to for the great majority of the patient samples discussed in this dissertation, is comparatively expensive and requires specialized DNA sequencing equipment and highly-trained analysts. In order for HLA-A*32:01 testing to have diagnostic utility for vancomycin DRESS in a clinical setting, the genetic test should be accurate, timely and cost-effective. With this goal in mind, with the help of our colleagues at IIID in Perth, Western Australia, we have developed a single allele assay for HLA-A*32:01 with a turnaround time of less than two days (Rwandamuriye, Chopra, Konvinse, *et al*., Accepted). This test uses an allele-specific polymerase chain reaction (AS-PCR) assay with melt curve analysis for typing of the HLA-A*32:01 allele. The assay was validated using a cohort of 458 DNA samples from patients with known sequence-based typing. The AS-PCR correctly identified the 30/458 patients who were positive for HLA-A*32:01 with no false positive from the other 428 patients, many of whom carried related HLA-A alleles. Due to the rapid turnaround time of this test, it is now feasible to use this HLA-A*32:01 AS-PCR assay in a clinical setting either after starting vancomycin but before the patient is at risk for vancomycin DRESS or as an ancillary diagnostic test in patients who have developed DRESS on multiple antibiotics.

Future Directions for Research on Vancomycin DRESS

The vancomycin DRESS cohort described in Chapter 3 was recruited from patients who were seen at either the Vanderbilt University Medical Center in Nashville, Tennessee or by our collaborators in Australia. Consequently, the patients enrolled in this study were predominantly of European ancestry. Future research should focus on associations between HLA alleles and vancomycin DRESS in those of non-European ancestry. Notably, the one African American patient with vancomycin DRESS that was identified retrospectively in BioVU did not carry HLA-A*32:01, but

was positive for the closely-related HLA-A*23:01 allele. Along with HLA-A*24:02, HLA-A*32:01 and HLA-A*23:01 are the only three HLA-A ligands known to interact with KIR3DL1, suggesting that genetic variation in KIR may also be relevant for vancomycin DRESS development[196]. Similar to the nevirapine SJS/TEN cohort, initial presence/absence KIR genotyping does not differ between the vancomycin DRESS cases and the expected carriage of KIRs at the population level (Table 5.1). Future work should focus on the possibility that specific SNPs within KIRs may influence reaction risk.

Unlike risk of nevirapine SJS/TEN development in South Africans who carry HLA-C*04:01, preliminary analyses suggest that carriage of key *ERAP1* and *ERAP2* alleles does not differ between individuals of European ancestry with HLA-A*32:01 who developed vancomycin-associated DRESS and the overall Caucasian population. Of the 17 ERAP SNPs genotyped, individuals with vancomycin DRESS had similar carriage rates of all alleles compared with HLA-A*32:01 negative vancomycin tolerant controls and the BioVU Caucasian population with and without the HLA risk allele (Table 5.2). Interestingly, HLA-A*32:01 vancomycin tolerant patients were more likely to carry the non-ancestral alleles for SNPs rs2287987, rs10050860 and rs17482078 than the HLA-A*32:01 BioVU population as a whole (p=0.0016, 0.0023 and 0.029, respectively). These three SNPs are in linkage disequilibrium with each other. These preliminary data suggest that absence of the ancestral allele for these SNPs may protect patients with HLA-A*32:01 against developing vancomycin DRESS.

Haplotype	KIR	Vancomycin DRESS	US Caucasian Population	p-value
A	**2DL3**	87.0 (20/23)	86.7 (221/255)	>0.99
A	**2DS4**	91.3 (21/23)	94.9 (242/255)	0.36
A	**3DL1**	91.3 (21/23)	94.9 (242/255)	0.36
AB	**2DL1**	95.7 (22/23)	95.3 (243/255)	>0.99
AB	**2DL4**	100 (23/23)	100 (255/255)	>0.99
AB	**2DP1**	95.7 (22/23)	95.3 (243/255)	>0.99
N/A	**3DL2**	100 (13/13)	100 (255/255)	>0.99
N/A	**3DL3**	100 (10/10)	100 (255/255)	>0.99
B	**2DL2**	56.5 (13/23)	52.9 (135/255)	0.83
B	**2DL5**	34.8 (8/23)	54.9 (140/255)	0.081
B	**2DS1**	17.4 (4/23)	41.2 (105/255)	0.026
B	**2DS2**	56.5 (13/23)	53.3 (136/255)	0.83
B	**2DS3**	30.4 (7/23)	29.4 (75/255)	>0.99
B	**2DS5**	17.4 (4/23)	34.5 (88/255)	0.11
B	**3DS1**	21.7 (5/23)	38.8 (99/255)	0.12

Table 5.1. Killer-cell immunoglobulin-like receptor genotyping of vancomycin DRESS cases compared to the United States Caucasian Population. Absence or presence of KIR genes is reported as % Positive (positive/total). None of the KIR genotyping results differ significantly from what would be expected in the population[158]. **Legend:** KIR, Killer-cell immunoglobulin-like receptor; DRESS, drug reaction with eosinophilia and systemic symptoms; US, United States.

Gene	SNP		DRESS (n=25)	A*32- Tolerant (n=29)	A*32+ Tolerant (n=16)	BioVU (n=53,142)	A*32+ BioVU (n=3,693)	p-value (DRESS vs. A*32+ BioVU)
ERAP 1	rs3734016	G	46	55	31	101772	7086	0.16
		A	4	3	1	4312	294	
		GG	21	26	15	48822	3403	
		GA	4	3	1	4128	280	
		AA	0	0	0	92	7	
	rs73148308	T	48					
		C	0					
		TT	24					
		TC	0					
		CC	0					
	rs26653	G	15	12	4	30055	2119	0.67
		C	35	46	28	76157	5263	
		GG	1	1	0	4286	284	
		GC	13	10	4	21483	1551	
		CC	11	18	12	27337	1856	
	rs27895	G	47	53	31	99118	6878	>0.99
		A	3	5	1	6960	492	
		GG	22	24	15	46298	3210	
		GA	3	5	1	6522	458	
		AA	0	0	0	219	17	
	rs2287987	A	39	46	18	82756	5724	0.94
		G	11	10	14	22660	1620	
		AA	15	20	3	32509	2243	
		AG	9	6	12	17738	1238	
		GG	1	2	1	2461	191	
	rs27434	T	12	7	4	22842	1605	0.27
		C	38	51	28	83208	5759	
		TT	0	1	0	2487	180	
		TC	12	5	4	17868	1245	
		CC	13	23	12	32670	2257	
	rs73144471	T	50					
		A	0					
		TT	25					
		TA	0					
		AA	0					
	rs27529	T	16	14	7	36689	2555	0.89
		C	34	44	25	69539	4827	
		TT	2	2	0	6324	469	
		TC	12	10	7	24041	1617	
		CC	11	17	9	22749	1605	
	rs78649652	G	50	57	32	105156	7312	>0.99
		A	0	1	0	1104	72	
		GG	25	28	16	52030	3621	
		GA	0	1	0	1096	70	
		AA	0	0	0	4	1	
	rs30187	A	16	14	7	36688	2557	0.89
		G	34	44	25	69510	4827	
		AA	2	2	0	6320	469	
		AG	12	10	7	24048	1619	
		GG	11	17	9	22731	1604	
	rs10050860	G	39	47	18	83076	5737	>0.99
		A	11	11	14	23186	1649	

		GG	15	20	3	32443	2235	
		GA	9	7	12	18190	1267	
		AA	1	2	1	2498	191	
	rs111363347	G	50	58	32	106078	7364	>0.99
		A	0	0	0	206	22	
		GG	25	29	16	52937	3671	
		GA	0	0	0	204	22	
		AA	0	0	0	1	0	
	rs17482078	G	39	48	20	83832	5790	0.94
		A	11	10	12	22396	1590	
		GG	15	21	5	33032	2279	
		GA	9	6	10	17768	1232	
		AA	1	2	1	2314	179	
	rs27044	C	11	14	9	29688	2080	0.50
		G	39	44	23	76484	5290	
		CC	2	2	1	4162	313	
		CG	7	10	7	21344	1454	
		GG	16	17	8	27570	1918	
	rs375081137	T	48					
			0					
		TT	24					
			0					
			0					
ERAP 2	rs2248374	A	26					
		G	22					
		AA	6					
		AG	14					
		GG	4					
	rs2549782	G	27	31	15	51870	3595	0.065
		T	23	27	17	54366	3791	
		GG	6	8	6	12711	875	
		GT	15	15	3	26448	1845	
		TT	4	6	7	13959	973	

Table 5.2. *ERAP1* and *ERAP2* genotyping of vancomycin DRESS cases compared to BioVU populations of European ancestry. Legend: DRESS, drug reaction with eosinophilia and systemic symptoms; A*32, HLA-A*32:01.

It is likely that other genetic factors outside of HLA, ERAP and KIR genes contribute to risk of vancomycin DRESS development. Future research may benefit from a more unbiased approach of determining genetic risk. With the help of the VANTAGE genetics core, our lab is planning to approach this hypothesis by performing Multi-Ethnic Global Array (MEGA) genotyping (Illumina) on the vancomycin DRESS cohort. MEGA microarrays allow detection of both common and rare variants to allow for a better genetic understanding of complex disease in diverse human populations.

In addition to populations of different ethnic backgrounds, special patient populations at risk of developing vancomycin DRESS also warrant further research. The time-to-event analyses suggested that patients who were immunosuppressed or had end-stage renal disease on hemodialysis were protected against DRESS suggesting that an intact immune response and timely clearance of the drug may be relevant to reaction development. Additional work should focus on patient populations known to be at higher risk for ADRs such as individuals living with cystic fibrosis and HIV.

Similar to the single-cell SJS/TEN research, further work focused on the T cells in the skin might provide important insights into the immunopathogenesis of vancomycin DRESS. The immunohistochemistry staining from the acute and skin test positive skin of vancomycin DRESS patient 18 in Chapter 3 revealed a dense lymphocytic infiltrate characterized by both CD4+ and CD8+ T cells. However, FoxP3+ regulatory cells were only present in the biopsy from the vancomycin skin test that was done 6.5 months after the initial reaction. Single-cell TCR sequencing and single-cell RNA sequencing of the T cells in the acutely affected and skin test

positive skin may help identify vancomycin-specific T cells for future study. This would also provide insights into the evolution of the skin T-cell repertoire from the time of acute disease to many months into the recovery phase. Additionally, less biased techniques such as those performed by 10x Genomics that provide single cell transcriptomic data without cell sorting may prove to be a useful approach to looking at all cells in the affected skin, not just the T cells. Finding the specific population of cells that react to vancomycin may elucidate why not all patients with HLA-A*32:01 who receive a prolonged course of vancomycin therapy develop disease.

Conclusions and Future Directions for Research on Vancomycin-induced Blistering Diseases

The most obvious and immediate clinical implication from the case of vancomycin SJS described in Chapter 4 is the importance of always verifying the information in a patient's allergy box. Most commonly patients' medical records overstate their allergies or list all adverse reactions such as gastrointestinal discomfort as true allergies. However, occasionally severe allergies are recorded incorrectly or missed entirely. The fact that the patient's previous vancomycin-induced rash lasted for >2 weeks should have been a red flag to avoid future vancomycin therapy.

As discussed in Chapter 4, forthcoming single-cell RNA sequencing data will further characterize the gene expression patterns of the T cells expressing the dominant TCRαβ clonotype in the blister fluid of the patient with vancomycin SJS. Due to the overwhelming dominance of that TCRαβ clonotype in the blister fluid, it is also a good candidate for our Jurkat cell reporter assay to test if the TCR reacts specifically with vancomycin. While only a single case of vancomycin SJS was described in this dissertation, the same experimental approach can be used to study additional cases of vancomycin SJS or other vancomycin-induced blistering diseases such as fixed drug eruption

and linear IgA bullous dermatosis. Our lab already has samples from several patients with these conditions for study.

Conclusion

In summary, this dissertation describes the use of cutting-edge experimental techniques to study severe cutaneous adverse reactions to antimicrobial medications. The validation and discovery of specific HLA risk alleles for nevirapine SJS/TEN in a South African population and for vancomycin DRESS in a population of predominantly European ancestry have direct clinical translations. Additionally, this experimental approach can be used as a roadmap for future research on a range of immune-mediated adverse reactions induced by other drugs and in other patient populations. In the 21st century, safely prescribing medications will increasingly involve considering the immunogenetics and pharmacogenomics of every patient and every aspect of their treatment. As scientists and medical providers, we have a responsibility to provide the safest care possible to patients.

LIST OF PUBLISHED MANUSCRIPTS AND BOOK CHAPTERS

1. **Konvinse, K.C.**, Trubiano, J.A., Pavlos, R.K., James, I., Shaffer, C.M., Bejan, C.A., Schutte, R.J., Ostrov, D.A., Pilkinton, M.A., Rosenbach, M.A., Zwerner, J.P., Williams, K.B., Bourke, J., Martinez, P., Rwandamuriye, F., Chopra, A., Watson, M., Redwood, A.J., White, K.D., Mallal, S.A. & Phillips, E.J. HLA-A*32:01 is strongly associated with vancomycin-induced drug reaction with eosinophilia and systemic symptoms. *J Allergy Clin Immunol* (2019).
2. Karnes, J.H., Miller, M.A., White, K.D., **Konvinse, K.C.**, Pavlos, R.K., Redwood, A.J., Peter, J.G., Lehloenya, R., Mallal, S.A. & Phillips, E.J. Applications of Immunopharmacogenomics: Predicting, Preventing, and Understanding Immune-Mediated Adverse Drug Reactions. *Annu Rev of Pharmacol and Toxicol* (2019).
3. Norton, A.E., **Konvinse, K.C.,** Phillips, E.J. & Broyles, A.D. Antibiotic Allergy in Pediatrics. *Pediatrics* **141** (2018).
4. Trubiano, J.A., Strautins, K., Redwood, A.J., Pavlos, R.K., **Konvinse, K.C.**, Aung, A.K., Slavin, M.A., Thursky, K.A., Grayson, M.L. & Phillips, E.J. The Combined Utility of *Ex vivo* IFN-gamma Release Enzyme-Linked ImmunoSpot Assay and *In vivo* Skin Testing in Patients with Antibiotic-Associated Severe Cutaneous Adverse Reactions. *J Allergy Clin Immunol Pract* **6**, 1287-1296 e1281 (2018).
5. White, K.D., **Konvinse, K.C.,** Redwood, A.J. & Phillips, E.J. Immune Mechanisms of Drug Allergy. Chapter 4. David Khan and Aleena Banerji (Eds). *Drug Allergy Testing* Elsevier, Inc. (2017).
6. Peter, J.G., Lehloenya, R., Dlamini, S., Risma, K., White, K.D., **Konvinse, K.C.** & Phillips, E.J. Severe Delayed Cutaneous and Systemic Reactions to Drugs: A Global Perspective on the Science and Art of Current Practice. *J Allergy Clin Immunol Pract* **5**, 547-563 (2017).
7. **Konvinse, K.C.,** Phillips, E.J., White, K.D. & Trubiano, J.A. Old dog begging for new tricks: current practices and future directions in the diagnosis of delayed antimicrobial hypersensitivity. *Curr Opin Infect Dis* **29**, 561-576 (2016).

REFERENCES

1. Hakkarainen, K.M., Hedna, K., Petzold, M. & Hagg, S. Percentage of patients with preventable adverse drug reactions and preventability of adverse drug reactions--a meta-analysis. *PLoS One* **7**, e33236 (2012).
2. Kongkaew, C., Noyce, P.R. & Ashcroft, D.M. Hospital admissions associated with adverse drug reactions: a systematic review of prospective observational studies. *Ann Pharmacother* **42**, 1017-1025 (2008).
3. Lazarou, J., Pomeranz, B.H. & Corey, P.N. Incidence of adverse drug reactions in hospitalized patients: a meta-analysis of prospective studies. *JAMA* **279**, 1200-1205 (1998).
4. Weiss, A.J., Freeman, W.J., Heslin, K.C. & Barrett, M.L. Adverse Drug Events in U.S. Hospitals, 2010 Versus 2014. *Agency for Healthcare Research and Quality* (2018).
5. Peter, J.G.*, et al.* Severe Delayed Cutaneous and Systemic Reactions to Drugs: A Global Perspective on the Science and Art of Current Practice. *J Allergy Clin Immunol Pract* **5**, 547-563 (2017).
6. Pichler, W.J. Delayed drug hypersensitivity reactions. *Ann Intern Med* **139**, 683-693 (2003).
7. Dioun, A. Management of Multiple Drug Allergies in Children. *Current Allergy and Asthma Reports* **12**, 79-84 (2012).
8. Garon, S.L.*, et al.* Pharmacogenomics of off-target adverse drug reactions. *Br J Clin Pharmacol* (2017).
9. White, K.D., Chung, W.H., Hung, S.I., Mallal, S. & Phillips, E.J. Evolving models of the immunopathogenesis of T cell-mediated drug allergy: The role of host, pathogens, and drug response. *J Allergy Clin Immunol* **136**, 219-234; quiz 235 (2015).
10. Thong, B. & Tan, T.C. Epidemiology and risk factors for drug allergy. *British Journal of Clinical Pharmacology* **71**, 684-700 (2011).
11. Gomes, E.R. & Demoly, P. Epidemiology of hypersensitivity drug reactions. *Current opinion in allergy and clinical immunology* **5**, 309-316 (2005).
12. Caubet, J.C. & Eigenmann, P.A. Diagnostic issues in pediatric drug allergy. *Curr Opin Allergy Clin Immunol* **12**, 341-347 (2012).
13. Gell, P.G.H. & Coombs, R.R.A. *Clincal Aspects of Immunology*, (Blackwell, Oxford, 1963).
14. McNeil, B.D.*, et al.* Identification of a mast-cell-specific receptor crucial for pseudo-allergic drug reactions. *Nature* **519**, 237-241 (2015).
15. Pichler, W., Yawalkar, N., Schmid, S. & Helbling, A. Pathogenesis of drug-induced exanthems. *Allergy* **57**, 884-893 (2002).
16. Padovan, E., Mauri-Hellweg, D., Pichler, W.J. & Weltzien, H.U. T cell recognition of penicillin G: structural features determining antigenic specificity. *Eur J Immunol* **26**, 42-48 (1996).
17. Lee, J.H., Cho, D.H. & Park, H.J. IL-18 and Cutaneous Inflammatory Diseases. *Int J Mol Sci* **16**, 29357-29369 (2015).
18. Guarneri, F.*, et al.* IL-31 and IL-33 circulating levels in allergic contact dermatitis. *Eur Ann Allergy Clin Immunol* **47**, 156-158 (2015).
19. Liu, J.*, et al.* IL-9 regulates allergen-specific Th1 responses in allergic contact dermatitis. *J Invest Dermatol* **134**, 1903-1911 (2014).

20. Taniguchi, K.*, et al.* Interleukin 33 is induced by tumor necrosis factor alpha and interferon gamma in keratinocytes and contributes to allergic contact dermatitis. *J Investig Allergol Clin Immunol* **23**, 428-434 (2013).
21. Lee, H.Y., Stieger, M., Yawalkar, N. & Kakeda, M. Cytokines and chemokines in irritant contact dermatitis. *Mediators Inflamm* **2013**, 916497 (2013).
22. Mockenhaupt, M. Epidemiology of cutaneous adverse drug reactions. *Chem Immunol Allergy* **97**, 1-17 (2012).
23. Gomez, E., Torres, M.J., Mayorga, C. & Blanca, M. Immunologic evaluation of drug allergy. *Allergy Asthma Immunol Res* **4**, 251-263 (2012).
24. Fernandez, T.D.*, et al.* Cytokine and chemokine expression in the skin from patients with maculopapular exanthema to drugs. *Allergy* **63**, 712-719 (2008).
25. Tapia, B.*, et al.* Up-regulation of CCL17, CCL22 and CCR4 in drug-induced maculopapular exanthema. *Clin Exp Allergy* **37**, 704-713 (2007).
26. Fujiyama, T.*, et al.* Increased frequencies of Th17 cells in drug eruptions. *J Dermatol Sci* **73**, 85-88 (2014).
27. Wang, F., He, D., Tang, X. & Zhang, X. Chemokine expression in diverse nonimmediate drug hypersensitivity reactions: focus on thymus activation-regulated chemokine, cutaneous T-cell-attracting chemokine, and interleukin-10. *Ann Allergy Asthma Immunol* **113**, 204-208 (2014).
28. Niu, J.*, et al.* Association of CD8(+) T lymphocyte repertoire spreading with the severity of DRESS syndrome. *Sci Rep* **5**, 9913 (2015).
29. Ogawa, K.*, et al.* Elevated serum thymus and activation-regulated chemokine (TARC/CCL17) relates to reactivation of human herpesvirus 6 in drug reaction with eosinophilia and systemic symptoms (DRESS)/drug-induced hypersensitivity syndrome (DIHS). *Br J Dermatol* **171**, 425-427 (2014).
30. Ortonne, N.*, et al.* Histopathology of drug rash with eosinophilia and systemic symptoms syndrome: a morphological and phenotypical study. *Br J Dermatol* **173**, 50-58 (2015).
31. Wei, C.Y., Chung, W.H., Huang, H.W., Chen, Y.T. & Hung, S.I. Direct interaction between HLA-B and carbamazepine activates T cells in patients with Stevens-Johnson syndrome. *J Allergy Clin Immunol* **129**, 1562-1569 e1565 (2012).
32. Teraki, Y., Kawabe, M. & Izaki, S. Possible role of TH17 cells in the pathogenesis of Stevens-Johnson syndrome and toxic epidermal necrolysis. *J Allergy Clin Immunol* **131**, 907-909 (2013).
33. Takahashi, R.*, et al.* Defective regulatory T cells in patients with severe drug eruptions: timing of the dysfunction is associated with the pathological phenotype and outcome. *J Immunol* **182**, 8071-8079 (2009).
34. Lee, H.Y. & Chung, W.H. Toxic epidermal necrolysis: the year in review. *Curr Opin Allergy Clin Immunol* **13**, 330-336 (2013).
35. Chung, W.H.*, et al.* Granulysin is a key mediator for disseminated keratinocyte death in Stevens-Johnson syndrome and toxic epidermal necrolysis. *Nat Med* **14**, 1343-1350 (2008).
36. Murata, J., Abe, R. & Shimizu, H. Increased soluble Fas ligand levels in patients with Stevens-Johnson syndrome and toxic epidermal necrolysis preceding skin detachment. *J Allergy Clin Immunol* **122**, 992-1000 (2008).
37. Chung, W.H. & Hung, S.I. Recent advances in the genetics and immunology of Stevens-Johnson syndrome and toxic epidermal necrosis. *J Dermatol Sci* **66**, 190-196 (2012).

38. Hakuta, A.*, et al.* Reduction of interleukin-10 production by B cells in intractable toxic epidermal necrolysis. *J Dermatol* **42**, 804-808 (2015).
39. Kakar, R., Paugh, H. & Jaworsky, C. Linear IgA bullous disease presenting as toxic epidermal necrolysis: a case report and review of the literature. *Dermatology* **227**, 209-213 (2013).
40. Khan, I., Hughes, R., Curran, S. & Marren, P. Drug-associated linear IgA disease mimicking toxic epidermal necrolysis. *Clin Exp Dermatol* **34**, 715-717 (2009).
41. Cummings, J.E., Snyder, R.R., Kelly, E.B. & Raimer, S.S. Drug-induced linear immunoglobulin A bullous dermatosis mimicking Stevens-Johnson syndrome: a case report. *Cutis* **79**, 203-207 (2007).
42. Coelho, S., Tellechea, O., Reis, J.P., Mariano, A. & Figueiredo, A. Vancomycin-associated linear IgA bullous dermatosis mimicking toxic epidermal necrolysis. *Int J Dermatol* **45**, 995-996 (2006).
43. Tranvan, A.*, et al.* Interleukin-2 associated linear IgA bullous dermatosis. *J Am Acad Dermatol* **35**, 865-867 (1996).
44. Lin, M.S.*, et al.* Autoimmune responses in patients with linear IgA bullous dermatosis: both autoantibodies and T lymphocytes recognize the NC16A domain of the BP180 molecule. *Clin Immunol* **102**, 310-319 (2002).
45. Mizukawa, Y., Yamazaki, Y. & Shiohara, T. In vivo dynamics of intraepidermal CD8+ T cells and CD4+ T cells during the evolution of fixed drug eruption. *Br J Dermatol* **158**, 1230-1238 (2008).
46. Shiohara, T. Fixed drug eruption: pathogenesis and diagnostic tests. *Curr Opin Allergy Clin Immunol* **9**, 316-321 (2009).
47. Akkurt, Z.M.*, et al.* Expression of interleukin-17 in lesions of erythema multiforme may indicate a role for T helper 17 cells. *Cent Eur J Immunol* **39**, 370-376 (2014).
48. Chodorowska, G., Czelej, D. & Niewiedziol, M. Interleukin-2 and its soluble receptor in selected drug-induced cutaneous reactions. *Ann Univ Mariae Curie Sklodowska Med* **58**, 7-13 (2003).
49. Kokuba, H., Aurelian, L. & Burnett, J. Herpes simplex virus associated erythema multiforme (HAEM) is mechanistically distinct from drug-induced erythema multiforme: interferon-gamma is expressed in HAEM lesions and tumor necrosis factor-alpha in drug-induced erythema multiforme lesions. *J Invest Dermatol* **113**, 808-815 (1999).
50. Ueda, T.*, et al.* Acute generalized exanthematous pustulosis due to allylisopropylacetylurea: role of IL-17-producing T cells. *Eur J Dermatol* **21**, 140-141 (2011).
51. Smith, K., Norwood, C. & Skelton, H. Do the physical and histologic features and time course in acute generalized exanthematous pustulosis reflect a pattern of cytokine dysregulation? *J Cutan Med Surg* **7**, 7-12 (2003).
52. Britschgi, M. & Pichler, W.J. Acute generalized exanthematous pustulosis, a clue to neutrophil-mediated inflammatory processes orchestrated by T cells. *Curr Opin Allergy Clin Immunol* **2**, 325-331 (2002).
53. Halevy, S. Acute generalized exanthematous pustulosis. *Curr Opin Allergy Clin Immunol* **9**, 322-328 (2009).
54. Konvinse, K.C., Phillips, E.J., White, K.D. & Trubiano, J.A. Old dog begging for new tricks: current practices and future directions in the diagnosis of delayed antimicrobial hypersensitivity. *Curr Opin Infect Dis* **29**, 561-576 (2016).

55. Zanni, M.P.*, et al.* HLA-restricted, processing- and metabolism-independent pathway of drug recognition by human alpha beta T lymphocytes. *J Clin Invest* **102**, 1591-1598 (1998).
56. Ostrov, D.A.*, et al.* Drug hypersensitivity caused by alteration of the MHC-presented self-peptide repertoire. *Proc Natl Acad Sci U S A* **109**, 9959-9964 (2012).
57. Pichler, W.J.*, et al.* Pharmacological interaction of drugs with immune receptors: the p-i concept. *Allergol Int* **55**, 17-25 (2006).
58. Illing, P.T.*, et al.* Immune self-reactivity triggered by drug-modified HLA-peptide repertoire. *Nature* **486**, 554-558 (2012).
59. Norcross, M.A.*, et al.* Abacavir induces loading of novel self-peptides into HLA-B*57: 01: an autoimmune model for HLA-associated drug hypersensitivity. *AIDS* **26**, F21-29 (2012).
60. Pavlos, R.*, et al.* T cell-mediated hypersensitivity reactions to drugs. *Annu Rev Med* **66**, 439-454 (2015).
61. Norton, A.E., Konvinse, K., Phillips, E.J. & Broyles, A.D. Antibiotic Allergy in Pediatrics. *Pediatrics* **141** (2018).
62. Phillips, E.J.*, et al.* Controversies in drug allergy: Testing for delayed reactions. *J Allergy Clin Immunol* **143**, 66-73 (2019).
63. Blumenthal, K.G., Wickner, P.G., Lau, J.J. & Zhou, L. Stevens-Johnson syndrome and toxic epidermal necrolysis: a cross-sectional analysis of patients in an integrated allergy repository of a large health care system. *The journal of allergy and clinical immunology. In practice* **3**, 277-280 e271 (2015).
64. Lin, Y.F.*, et al.* Severe cutaneous adverse reactions related to systemic antibiotics. *Clin Infect Dis* **58**, 1377-1385 (2014).
65. Trubiano, J.A.*, et al.* A Comparative Analysis Between Antibiotic- and Nonantibiotic-Associated Delayed Cutaneous Adverse Drug Reactions. *The journal of allergy and clinical immunology. In practice* (2016).
66. Goodman, M.H. & Levy, C.S. The development of a cutaneous eruption (toxicodermatosis): During administration of sulfanilamide; report of two cases. *Journal of the American Medical Association* **109**, 1009-1011 (1937).
67. Jaslowitz, H. Reaction to penicillin. *British medical journal* **2**, 767 (1945).
68. Kolodny, M.H. & Denhoff, E. Reactions in penicillin therapy. *Journal of the American Medical Association* **130**, 1058-1061 (1946).
69. Trubiano, J.A., Adkinson, N.F. & Phillips, E.J. Penicillin Allergy Is Not Necessarily Forever. *JAMA* **318**, 82-83 (2017).
70. Macy, E. & Contreras, R. Health care use and serious infection prevalence associated with penicillin "allergy" in hospitalized patients: A cohort study. *J Allergy Clin Immunol* **133**, 790-796 (2014).
71. Caimmi, S.*, et al.* Comprehensive allergy work-up is mandatory in cystic fibrosis patients who report a history suggestive of drug allergy to beta-lactam antibiotics. *Clin Transl Allergy* **2**, 10 (2012).
72. Lin, D., Tucker, M.J. & Rieder, M.J. Increased adverse drug reactions to antimicrobials and anticonvulsants in patients with HIV infection. *Ann Pharmacother* **40**, 1594-1601 (2006).
73. Petroni, D.H.*, et al.* Approach to the evaluation of adverse antibiotic reactions in patients with cystic fibrosis. *Ann Allergy Asthma Immunol* **117**, 378-381 (2016).
74. Phillips, E. & Mallal, S. Drug hypersensitivity in HIV. *Curr Opin Allergy Clin Immunol* **7**, 324-330 (2007).

75. Mallal, S.*, et al.* Association between presence of HLA-B*5701, HLA-DR7, and HLA-DQ3 and hypersensitivity to HIV-1 reverse-transcriptase inhibitor abacavir. *Lancet* **359**, 727-732 (2002).
76. Hetherington, S.*, et al.* Genetic variations in HLA-B region and hypersensitivity reactions to abacavir. *Lancet* **359**, 1121-1122 (2002).
77. Pavlos, R., Mallal, S. & Phillips, E. HLA and pharmacogenetics of drug hypersensitivity. *Pharmacogenomics* **13**, 1285-1306 (2012).
78. Vitezica, Z.G.*, et al.* HLA-DRB1*01 associated with cutaneous hypersensitivity induced by nevirapine and efavirenz. *AIDS* **22**, 540-541 (2008).
79. Chantarangsu, S.*, et al.* HLA-B*3505 allele is a strong predictor for nevirapine-induced skin adverse drug reactions in HIV-infected Thai patients. *Pharmacogenet Genomics* **19**, 139-146 (2009).
80. Chantarangsu, S.*, et al.* Genome-wide association study identifies variations in 6p21.3 associated with nevirapine-induced rash. *Clin Infect Dis* **53**, 341-348 (2011).
81. Gao, S.*, et al.* HLA-dependent hypersensitivity reaction to nevirapine in Chinese Han HIV-infected patients. *AIDS Res Hum Retroviruses* **28**, 540-543 (2012).
82. Gatanaga, H.*, et al.* HLA-Cw8 primarily associated with hypersensitivity to nevirapine. *AIDS* **21**, 264-265 (2007).
83. Likanonsakul, S.*, et al.* HLA-Cw*04 allele associated with nevirapine-induced rash in HIV-infected Thai patients. *AIDS Res Ther* **6**, 22 (2009).
84. Littera, R.*, et al.* HLA-dependent hypersensitivity to nevirapine in Sardinian HIV patients. *AIDS* **20**, 1621-1626 (2006).
85. Martin, A.M.*, et al.* Predisposition to nevirapine hypersensitivity associated with HLA-DRB1*0101 and abrogated by low CD4 T-cell counts. *AIDS* **19**, 97-99 (2005).
86. Phillips, E.*, et al.* Associations between HLA-DRB1*0102, HLA-B*5801, and hepatotoxicity during initiation of nevirapine-containing regimens in South Africa. *J Acquir Immune Defic Syndr* **62**, e55-57 (2013).
87. Yuan, J.*, et al.* Toxicogenomics of nevirapine-associated cutaneous and hepatic adverse events among populations of African, Asian, and European descent. *AIDS* **25**, 1271-1280 (2011).
88. Thomas, M.*, et al.* Association of the HLA-B*53:01 Allele With Drug Reaction With Eosinophilia and Systemic Symptoms (DRESS) Syndrome During Treatment of HIV Infection With Raltegravir. *Clin Infect Dis* **64**, 1198-1203 (2017).
89. Daly, A.K.*, et al.* HLA-B*5701 genotype is a major determinant of drug-induced liver injury due to flucloxacillin. *Nat Genet* **41**, 816-819 (2009).
90. Nicoletti, P.*, et al.* Drug-Induced Liver Injury due to Flucloxacillin: Relevance of Multiple Human Leukocyte Antigen Alleles. *Clin Pharmacol Ther* (2019).
91. Daly, A.K. & Day, C.P. Genetic association studies in drug-induced liver injury. *Semin Liver Dis* **29**, 400-411 (2009).
92. Zhang, F.R.*, et al.* HLA-B*13:01 and the dapsone hypersensitivity syndrome. *N Engl J Med* **369**, 1620-1628 (2013).
93. Adams, P.D.*, et al.* PHENIX: a comprehensive Python-based system for macromolecular structure solution. *Acta Crystallogr D Biol Crystallogr* **66**, 213-221 (2010).
94. Hautekeete, M.L.*, et al.* HLA association of amoxicillin-clavulanate--induced hepatitis. *Gastroenterology* **117**, 1181-1186 (1999).

95. Lucena, M.I., *et al.* Susceptibility to amoxicillin-clavulanate-induced liver injury is influenced by multiple HLA class I and II alleles. *Gastroenterology* **141**, 338-347 (2011).
96. O'Donohue, J., *et al.* Co-amoxiclav jaundice: clinical and histological features and HLA class II association. *Gut* **47**, 717-720 (2000).
97. Ozkaya-Bayazit, E. & Akar, U. Fixed drug eruption induced by trimethoprim-sulfamethoxazole: evidence for a link to HLA-A30 B13 Cw6 haplotype. *J Am Acad Dermatol* **45**, 712-717 (2001).
98. Lonjou, C., *et al.* A European study of HLA-B in Stevens-Johnson syndrome and toxic epidermal necrolysis related to five high-risk drugs. *Pharmacogenet Genomics* **18**, 99-107 (2008).
99. Romano, A., *et al.* Delayed hypersensitivity to aminopenicillins is related to major histocompatibility complex genes. *Ann Allergy Asthma Immunol* **80**, 433-437 (1998).
100. Roujeau, J.C., *et al.* Genetic susceptibility to toxic epidermal necrolysis. *Arch Dermatol* **123**, 1171-1173 (1987).
101. Vedove, C.D., Del Giglio, M., Schena, D. & Girolomoni, G. Drug-induced lupus erythematosus. *Arch Dermatol Res* **301**, 99-105 (2009).
102. Daly, A.K. & Day, C.P. Genetic association studies in drug-induced liver injury. *Drug Metab Rev* **44**, 116-126 (2012).
103. Diez, R.A. HLA-B27 and agranulocytosis by levamisole. *Immunol Today* **11**, 270 (1990).
104. Urban, T.J., *et al.* Minocycline hepatotoxicity: Clinical characterization and identification of HLA-B *35:02 as a risk factor. *J Hepatol* **67**, 137-144 (2017).
105. Nicoletti, P., *et al.* Association of Liver Injury From Specific Drugs, or Groups of Drugs, With Polymorphisms in HLA and Other Genes in a Genome-Wide Association Study. *Gastroenterology* **152**, 1078-1089 (2017).
106. Keane, N.M., *et al.* HLA Class I restricted CD8+ and Class II restricted CD4+ T cells are implicated in the pathogenesis of nevirapine hypersensitivity. *AIDS* **28**, 1891-1901 (2014).
107. Haw, W.Y., Polak, M.E., McGuire, C., Erlewyn-Lajeunesse, M. & Ardern-Jones, M.R. In vitro rapid diagnostic tests for severe drug hypersensitivity reactions in children. *Ann Allergy Asthma Immunol* **117**, 61-66 (2016).
108. Hausmann, O.V., Gentinetta, T., Bridts, C.H. & Ebo, D.G. The basophil activation test in immediate-type drug allergy. *Immunol Allergy Clin North Am* **29**, 555-566 (2009).
109. Romano, A., Torres, M.J., Castells, M., Sanz, M.L. & Blanca, M. Diagnosis and management of drug hypersensitivity reactions. *J Allergy Clin Immunol* **127**, S67-73 (2011).
110. Aranda, A., *et al.* In vitro evaluation of IgE-mediated hypersensitivity reactions to quinolones. *Allergy* **66**, 247-254 (2011).
111. Gamboa, P.M., *et al.* Basophil activation and sulfidoleukotriene production in patients with immediate allergy to betalactam antibiotics and negative skin tests. *J Investig Allergol Clin Immunol* **14**, 278-283 (2004).
112. Torres, M.J., *et al.* The diagnostic interpretation of basophil activation test in immediate allergic reactions to betalactams. *Clin Exp Allergy* **34**, 1768-1775 (2004).
113. Dias de Castro, E., Leblanc, A., Sarmento, A. & Cernadas, J.R. An unusual case of delayed-type hypersensitivity to ceftriaxone and meropenem. *Eur Ann Allergy Clin Immunol* **47**, 225-227 (2015).

114. Kim, J.Y., Sohn, K.H., Song, W.J. & Kang, H.R. A case of drug reaction with eosinophilia and systemic symptoms induced by ethambutol with early features resembling Stevens-Johnson syndrome. *Acta Derm Venereol* **93**, 753-754 (2013).
115. Schnyder, B. & Pichler, W.J. Skin and laboratory tests in amoxicillin- and penicillin-induced morbilliform skin eruption. *Clin Exp Allergy* **30**, 590-595 (2000).
116. Tomida, E.*, et al.* Causative drug detection by drug-induced lymphocyte stimulation test in drug-induced linear IgA bullous dermatosis. *Br J Dermatol* **175**, 1106-1108 (2016).
117. Yawalkar, N.*, et al.* Drug-induced linear IgA bullous dermatosis associated with ceftriaxone- and metronidazole-specific T cells. *Dermatology* **199**, 25-30 (1999).
118. Porebski, G.*, et al.* In vitro drug causality assessment in Stevens-Johnson syndrome - alternatives for lymphocyte transformation test. *Clin Exp Allergy* **43**, 1027-1037 (2013).
119. Rive, C.M., Bourke, J. & Phillips, E.J. Testing for drug hypersensitivity syndromes. *Clin Biochem Rev* **34**, 15-38 (2013).
120. Romano, A.*, et al.* Diagnosis of nonimmediate reactions to beta-lactam antibiotics. *Allergy* **59**, 1153-1160 (2004).
121. Trautmann, A., Seitz, C.S., Stoevesandt, J. & Kerstan, A. Aminopenicillin-associated exanthem: lymphocyte transformation testing revisited. *Clin Exp Allergy* **44**, 1531-1538 (2014).
122. Bensaid, B., Rozieres, A., Nosbaum, A., Nicolas, J.F. & Berard, F. Amikacin-induced drug reaction with eosinophilia and systemic symptoms syndrome: delayed skin test and ELISPOT assay results allow the identification of the culprit drug. *J Allergy Clin Immunol* **130**, 1413-1414 (2012).
123. El-Ghaiesh, S.*, et al.* Characterization of the antigen specificity of T-cell clones from piperacillin-hypersensitive patients with cystic fibrosis. *J Pharmacol Exp Ther* **341**, 597-610 (2012).
124. Jenkins, R.E.*, et al.* beta-Lactam antibiotics form distinct haptenic structures on albumin and activate drug-specific T-lymphocyte responses in multiallergic patients with cystic fibrosis. *Chem Res Toxicol* **26**, 963-975 (2013).
125. Khalil, G.*, et al.* Cytokine expression profile of sensitized human T lymphocytes following in vitro stimulation with amoxicillin. *Eur Cytokine Netw* **19**, 131-141 (2008).
126. Phatharacharukul, P. & Klaewsongkram, J. A case of sulfasalazine-induced hypersensitivity syndrome confirmed by enzyme-linked immunospot assay. *Allergy Asthma Immunol Res* **5**, 415-417 (2013).
127. Rozieres, A.*, et al.* Detection and quantification of drug-specific T cells in penicillin allergy. *Allergy* **64**, 534-542 (2009).
128. Tanvarasethee, B., Buranapraditkun, S. & Klaewsongkram, J. The potential of using enzyme-linked immunospot to diagnose cephalosporin-induced maculopapular exanthems. *Acta Derm Venereol* **93**, 66-69 (2013).
129. Tassignon, J.*, et al.* Monitoring of cellular responses after vaccination against tetanus toxoid: comparison of the measurement of IFN-gamma production by ELISA, ELISPOT, flow cytometry and real-time PCR. *J Immunol Methods* **305**, 188-198 (2005).
130. Garcia-Doval, I., LeCleach, L., Bocquet, H., Otero, X.L. & Roujeau, J.C. Toxic epidermal necrolysis and Stevens-Johnson syndrome: does early withdrawal of causative drugs decrease the risk of death? *Arch Dermatol* **136**, 323-327 (2000).
131. McGee, T. & Munster, A. Toxic epidermal necrolysis syndrome: mortality rate reduced with early referral to regional burn center. *Plast Reconstr Surg* **102**, 1018-1022 (1998).

132. Carr, D.F., *et al.* Association of human leukocyte antigen alleles and nevirapine hypersensitivity in a Malawian HIV-infected population. *Clin Infect Dis* **56**, 1330-1339 (2013).
133. Haas, D.W., *et al.* Associations between CYP2B6 polymorphisms and pharmacokinetics after a single dose of nevirapine or efavirenz in African americans. *J Infect Dis* **199**, 872-880 (2009).
134. Penzak, S.R., *et al.* Cytochrome P450 2B6 (CYP2B6) G516T influences nevirapine plasma concentrations in HIV-infected patients in Uganda. *HIV Med* **8**, 86-91 (2007).
135. Evans, D.M., *et al.* Interaction between ERAP1 and HLA-B27 in ankylosing spondylitis implicates peptide handling in the mechanism for HLA-B27 in disease susceptibility. *Nat Genet* **43**, 761-767 (2011).
136. Genetic Analysis of Psoriasis, C., *et al.* A genome-wide association study identifies new psoriasis susceptibility loci and an interaction between HLA-C and ERAP1. *Nat Genet* **42**, 985-990 (2010).
137. International Genetics of Ankylosing Spondylitis, C., *et al.* Identification of multiple risk variants for ankylosing spondylitis through high-density genotyping of immune-related loci. *Nat Genet* **45**, 730-738 (2013).
138. Kirino, Y., *et al.* Genome-wide association analysis identifies new susceptibility loci for Behcet's disease and epistasis between HLA-B*51 and ERAP1. *Nat Genet* **45**, 202-207 (2013).
139. Tang, H., *et al.* A large-scale screen for coding variants predisposing to psoriasis. *Nat Genet* **46**, 45-50 (2014).
140. Carr, D.F., *et al.* Genome-wide association study of nevirapine hypersensitivity in a sub-Saharan African HIV-infected population. *J Antimicrob Chemother* **72**, 1152-1162 (2017).
141. Whirl-Carrillo, M., *et al.* Pharmacogenomics knowledge for personalized medicine. *Clin Pharmacol Ther* **92**, 414-417 (2012).
142. Falk, K. & Rotzschke, O. The final cut: how ERAP1 trims MHC ligands to size. *Nat Immunol* **3**, 1121-1122 (2002).
143. Tran, T.M. & Colbert, R.A. Endoplasmic reticulum aminopeptidase 1 and rheumatic disease: functional variation. *Curr Opin Rheumatol* **27**, 357-363 (2015).
144. Naranjo, C.A., *et al.* A method for estimating the probability of adverse drug reactions. *Clin Pharmacol Ther* **30**, 239-245 (1981).
145. Sassolas, B., *et al.* ALDEN, an algorithm for assessment of drug causality in Stevens-Johnson Syndrome and toxic epidermal necrolysis: comparison with case-control analysis. *Clin Pharmacol Ther* **88**, 60-68 (2010).
146. Mallal, S., *et al.* HLA-B*5701 screening for hypersensitivity to abacavir. *N Engl J Med* **358**, 568-579 (2008).
147. Holzinger, E.R., *et al.* Genome-wide association study of plasma efavirenz pharmacokinetics in AIDS Clinical Trials Group protocols implicates several CYP2B6 variants. *Pharmacogenet Genomics* **22**, 858-867 (2012).
148. Leary, S., Cooper, D., Chopra, A. & Watson, M. IIID VGAS - A Visual Genome Analyses Studio incorporating high performance next generation sequence analysis (Poster). in *Great Lakes Bioinformatics Conference (GLBIO)* (Pittsburgh, Pennsylvania, 2013).
149. Alves, L.G., Rajalingam, R. & Canavez, F. A novel real-time PCR method for KIR genotyping. *Tissue Antigens* **73**, 188-191 (2009).

150. Koehler, R.N., *et al.* High-throughput genotyping of KIR2DL2/L3, KIR3DL1/S1, and their HLA class I ligands using real-time PCR. *Tissue Antigens* **74**, 73-80 (2009).
151. Langmead, B. & Salzberg, S.L. Fast gapped-read alignment with Bowtie 2. *Nat Methods* **9**, 357-359 (2012).
152. Li, B. & Dewey, C.N. RSEM: accurate transcript quantification from RNA-Seq data with or without a reference genome. *BMC Bioinformatics* **12**, 323 (2011).
153. Cole, M.B., *et al.* Performance Assessment and Selection of Normalization Procedures for Single-Cell RNA-seq. *bioRxiv* (2018).
154. DeTomaso, D. & Yosef, N. FastProject: a tool for low-dimensional analysis of single-cell RNA-Seq data. *BMC Bioinformatics* **17**, 315 (2016).
155. Butler, A., Hoffman, P., Smibert, P., Papalexi, E. & Satija, R. Integrating single-cell transcriptomic data across different conditions, technologies, and species. *Nat Biotechnol* **36**, 411-420 (2018).
156. Afik, S., *et al.* Targeted reconstruction of T cell receptor sequence from single cell RNA-seq links CDR3 length to T cell differentiation state. *Nucleic Acids Res* **45**, e148 (2017).
157. Kim, D., *et al.* TopHat2: accurate alignment of transcriptomes in the presence of insertions, deletions and gene fusions. *Genome Biol* **14**, R36 (2013).
158. Gonzalez-Galarza, F.F., *et al.* Allele frequency net 2015 update: new features for HLA epitopes, KIR and disease and HLA adverse drug reaction associations. *Nucleic Acids Res* **43**, D784-788 (2015).
159. Chew, G.M., *et al.* TIGIT Marks Exhausted T Cells, Correlates with Disease Progression, and Serves as a Target for Immune Restoration in HIV and SIV Infection. *PLoS Pathog* **12**, e1005349 (2016).
160. Deng, H.K., Unutmaz, D., KewalRamani, V.N. & Littman, D.R. Expression cloning of new receptors used by simian and human immunodeficiency viruses. *Nature* **388**, 296-300 (1997).
161. Liao, F., *et al.* STRL33, A novel chemokine receptor-like protein, functions as a fusion cofactor for both macrophage-tropic and T cell line-tropic HIV-1. *J Exp Med* **185**, 2015-2023 (1997).
162. Bersoff-Matcha, S.J., *et al.* Sex differences in nevirapine rash. *Clin Infect Dis* **32**, 124-129 (2001).
163. Phillips, E.J. Classifying ADRs--does dose matter? *Br J Clin Pharmacol* **81**, 10-12 (2016).
164. Evnouchidou, I., *et al.* Cutting Edge: Coding single nucleotide polymorphisms of endoplasmic reticulum aminopeptidase 1 can affect antigenic peptide generation in vitro by influencing basic enzymatic properties of the enzyme. *J Immunol* **186**, 1909-1913 (2011).
165. Fierabracci, A., Milillo, A., Locatelli, F. & Fruci, D. The putative role of endoplasmic reticulum aminopeptidases in autoimmunity: insights from genomic-wide association studies. *Autoimmun Rev* **12**, 281-288 (2012).
166. Lee, Y.H., Choi, S.J., Ji, J.D. & Song, G.G. Associations between ERAP1 polymorphisms and ankylosing spondylitis susceptibility: a meta-analysis. *Inflamm Res* **60**, 999-1003 (2011).
167. Nemat-Gorgani, N., *et al.* Different Selected Mechanisms Attenuated the Inhibitory Interaction of KIR2DL1 with C2(+) HLA-C in Two Indigenous Human Populations in Southern Africa. *J Immunol* **200**, 2640-2655 (2018).

168. Yang, C., Mosam, A., Mankahla, A., Dlova, N. & Saavedra, A. HIV infection predisposes skin to toxic epidermal necrolysis via depletion of skin-directed CD4(+) T cells. *J Am Acad Dermatol* **70**, 1096-1102 (2014).
169. Cardone, M.*, et al.* A transgenic mouse model for HLA-B*57:01-linked abacavir drug tolerance and reactivity. *J Clin Invest* **128**, 2819-2832 (2018).
170. Phillips, E.J. & Mallal, S.A. Active suppression rather than ignorance: tolerance to abacavir-induced HLA-B*57:01 peptide repertoire alteration. *J Clin Invest* **128**, 2746-2749 (2018).
171. Stern, J.O.*, et al.* A comprehensive hepatic safety analysis of nevirapine in different populations of HIV infected patients. *J Acquir Immune Defic Syndr* **34 Suppl 1**, S21-33 (2003).
172. van Leth, F.*, et al.* The effect of baseline CD4 cell count and HIV-1 viral load on the efficacy and safety of nevirapine or efavirenz-based first-line HAART. *AIDS* **19**, 463-471 (2005).
173. Cohen, G.B.*, et al.* The selective downregulation of class I major histocompatibility complex proteins by HIV-1 protects HIV-infected cells from NK cells. *Immunity* **10**, 661-671 (1999).
174. Collins, K.L., Chen, B.K., Kalams, S.A., Walker, B.D. & Baltimore, D. HIV-1 Nef protein protects infected primary cells against killing by cytotoxic T lymphocytes. *Nature* **391**, 397-401 (1998).
175. Blumenthal, K.G., Peter, J.G., Trubiano, J.A. & Phillips, E.J. Antibiotic allergy. *Lancet* (2018).
176. Aota, N. & Shiohara, T. Viral connection between drug rashes and autoimmune diseases: how autoimmune responses are generated after resolution of drug rashes. *Autoimmun Rev* **8**, 488-494 (2009).
177. Ghislain, P.D. & Roujeau, J.C. Treatment of severe drug reactions: Stevens-Johnson syndrome, toxic epidermal necrolysis and hypersensitivity syndrome. *Dermatol Online J* **8**, 5 (2002).
178. Kardaun, S.H.*, et al.* Drug reaction with eosinophilia and systemic symptoms (DRESS): an original multisystem adverse drug reaction. Results from the prospective RegiSCAR study. *Br J Dermatol* **169**, 1071-1080 (2013).
179. Karnes, J.H.*, et al.* Comparison of HLA allelic imputation programs. *PLoS One* **12**, e0172444 (2017).
180. Keane, N.M.*, et al.* High-avidity, high-IFNgamma-producing CD8 T-cell responses following immune selection during HIV-1 infection. *Immunol Cell Biol* **90**, 224-234 (2012).
181. Trubiano, J.A.*, et al.* The Combined Utility of Ex Vivo IFN-gamma Release Enzyme-Linked ImmunoSpot Assay and In Vivo Skin Testing in Patients with Antibiotic-Associated Severe Cutaneous Adverse Reactions. *J Allergy Clin Immunol Pract* **6**, 1287-1296 e1281 (2018).
182. Bordoli, L.*, et al.* Protein structure homology modeling using SWISS-MODEL workspace. *Nat Protoc* **4**, 1-13 (2009).
183. Emsley, P., Lohkamp, B., Scott, W.G. & Cowtan, K. Features and development of Coot. *Acta Crystallogr D Biol Crystallogr* **66**, 486-501 (2010).

184. Trott, O. & Olson, A.J. AutoDock Vina: improving the speed and accuracy of docking with a new scoring function, efficient optimization, and multithreading. *J Comput Chem* **31**, 455-461 (2010).
185. Gragert, L., Madbouly, A., Freeman, J. & Maiers, M. Six-locus high resolution HLA haplotype frequencies derived from mixed-resolution DNA typing for the entire US donor registry. *Hum Immunol* **74**, 1313-1320 (2013).
186. Rapin, N., Hoof, I., Lund, O. & Nielsen, M. MHC motif viewer. *Immunogenetics* **60**, 759-765 (2008).
187. Chung, W.H.*, et al.* Medical genetics: a marker for Stevens-Johnson syndrome. *Nature* **428**, 486 (2004).
188. Martin, A.M.*, et al.* Predisposition to abacavir hypersensitivity conferred by HLA-B*5701 and a haplotypic Hsp70-Hom variant. *Proc Natl Acad Sci U S A* **101**, 4180-4185 (2004).
189. Empedrad, R., Darter, A.L., Earl, H.S. & Gruchalla, R.S. Nonirritating intradermal skin test concentrations for commonly prescribed antibiotics. *J Allergy Clin Immunol* **112**, 629-630 (2003).
190. Morito, H.*, et al.* Increased ratio of FoxP3+ regulatory T cells/CD3+ T cells in skin lesions in drug-induced hypersensitivity syndrome/drug rash with eosinophilia and systemic symptoms. *Clin Exp Dermatol* **39**, 284-291 (2014).
191. Baden, L.A., Apovian, C., Imber, M.J. & Dover, J.S. Vancomycin-induced linear IgA bullous dermatosis. *Arch Dermatol* **124**, 1186-1188 (1988).
192. Minhas, J.S., Wickner, P.G., Long, A.A., Banerji, A. & Blumenthal, K.G. Immune-mediated reactions to vancomycin: A systematic case review and analysis. *Ann Allergy Asthma Immunol* **116**, 544-553 (2016).
193. Robins, H.*, et al.* Ultra-sensitive detection of rare T cell clones. *J Immunol Methods* **375**, 14-19 (2012).
194. Harding, D.J., Subramaniam, K., MacQuillan, G., Davis, J. & Nolan, D. Severe drug-induced hypersensitivity syndrome with a shared HLA-B allele. *Med J Aust* **197**, 411-413 (2012).
195. Bozon, M.V.*, et al.* Comparison of HLA-A antigen typing by serology with two polymerase chain reaction based DNA typing methods: implications for proficiency testing. *Tissue Antigens* **47**, 512-518 (1996).
196. Stern, M., Ruggeri, L., Capanni, M., Mancusi, A. & Velardi, A. Human leukocyte antigens A23, A24, and A32 but not A25 are ligands for KIR3DL1. *Blood* **112**, 708-710 (2008).